University of Huddersfield Repository

Fish, Michael Anderson

Transmission errors in precision worm gear drives

Original Citation

Fish, Michael Anderson (1998) Transmission errors in precision worm gear drives. Doctoral thesis, University of Huddersfield.

This version is available at http://eprints.hud.ac.uk/id/eprint/4851/

TRANSMISSION ERRORS IN PRECISION WORM GEAR DRIVES

MICHAEL ANDERSON FISH

A thesis submitted to the University of Huddersfield in partial fulfilment of the requirements for the degree of Doctor of Philosophy

School of Engineering
University of Huddersfield

November 1998

DEDICATION

To my parents Mary and Geoff for their infinite patience and understanding.

You have taught me so much.

ABSTRACT

Transmission error is a measure of the positioning accuracy of a gear system. This has been widely documented in gearing for many years as the source of problems in noise and vibration. It is a result of errors in the contact conditions which affect the driven gear with respect to the rotation of the driver gear. This research aims to present a better understanding of the basic kinematics of worm gear systems by identifying the significant influences which determine the contact conditions.

A literature review of existing theory is described which determines the major areas considered in worm gear contact analysis. Formulae are derived which quantify the effect of component parameter variation on contact. An investigation of the design, manufacture, and operating processes is recorded which identifies error sources relative to the theoretical contact condition. A computer program is developed which calculates contact characteristics such as worm and wheel component form, transmission error and contact marking pattern for a given design including any contact error sources. Computer calculations are validated by comparing direct measurements of these characteristics from several manufactured gear sets with synthesised results produced using the design information, machine settings and error sources detected during production. The behaviour of these gear sets during operation under a torque load has been investigated experimentally. Measured transmission error data from a test rig is used to develop a basic model of worm gear deformation under load. This model has been added to the computer program to improve and extend the analysis capability. The test rig has also been used to investigate the effect of initial wear on contact characteristics.

The good correlation between calculated and experimental results shows that the characteristics of a worm gear set can be predicted once all elements of the design and manufacture are known. The results also validate the software as a useful design tool for academic and industrial applications. Important conclusions are drawn on design techniques, the manufacturing process, and the effects of operating under load. Further areas of investigation are identified which offer future research an opportunity to expand upon these conclusions.

DECLARATION

This thesis consists of the original work of the author except where specific reference is made to the work of others, and has not been previously submitted for any other degree or qualification.

ACKNOWLEDGEMENTS

NOTATION

MAIN CHARACTER SYMBOL

a - Centre distance.

b - Tooth facewidth.

c - Arbitrary linear constant.

d - Diameter.

e - Transmission error.

f - Tooth stiffness function.

h - Tooth height.

k - Linear constant of tooth stiffness.

l - Lead.

m - Module.

p - Pitch.

q - Quotient.

r - Radius.

s - Tooth thickness.

u - Axial displacement.

z - Tooth number.

B - Backlash.

E - Young's modulus.

F - Force.

M - Torque load.

P - Profile point.

R - Electrical resistance.

α - Pressure angle.

β - Angular displacement.

ε - Arbitrary angle of rotation.

γ - Angle of generatrix relative to transverse plane.

λ - Lead angle.

σ - Principal stress.

ξ - Principal strain.

ψ - Helix angle.

ϑ - Vector angle.

Δ - Small increment.

Σ - Angle formed by the worm and wheel cutter axes.

SUBSCRIPTS

0 - Wheel cutter.

1 - Worm.

2 - Wheel.

a - Relative to the worm axis.

b - Base Cylinder.

n - Direction normal to profile.

p - Pitch Cylinder.

r - Relative to a rack section plane.

CONTENTS

6. TEST RIG DEVELOPMENT 118

1. INTRODUCTION

1.1. THE NEED FOR WORM GEAR RESEARCH

Worm gears are widely used in a range of industries in numerous applications. They are chosen for accuracy in machine tools, rotary tables and robotics, low maintenance and durability becomes an advantage for installation in centrifuges and elevators, while their compact nature for high ratio variations and relatively high load capacity makes them useful for heavy duty automotive transmissions and steam turbines.

Lack of accuracy (known as *transmission error*) represents a direct source of error in any precision application, but has also been widely documented for many years as causing problems in noise and vibration. Industrial sources quote normal positioning accuracy of worm gear sets as 10-15 arc seconds, however this value is influenced by the contact conditions established during production and operation.

Contact conditions are difficult to predict or control for three main reasons. The first is that a large number of calculations are needed to investigate changes in design parameters due to the relatively complex geometry. The second is the unpredictability of additional effects from machining errors during production. The third has been the limited accuracy of the measurement equipment used to inspect components during their manufacture. As a consequence worm gear development has mainly been empirical using trial and error methods.

Increases in computing speed within the last decade have made it possible to complete fast and accurate calculations. Developments in data acquisition technology and measuring systems can produce measurement of linear surfaces in the 1-2 μm range, and rotary accuracy to 0.3 arc seconds[1]. This has permitted a controlled and accurate investigation of worm gear kinematics to be carried out. Several British worm gearing companies have taken the opportunity to collaborate in a program of research established at the University of Huddersfield. The aim of this has been to improve the understanding of the contact process and apply this knowledge to the operation of industrial worm gear systems.

1.2. REVIEW OF GEAR RESEARCH AND DEVELOPMENT

1.2.1. Early use of worm gears

Walker[2] gives a short summary of the origins and the initial development of worm gears. Archimedes is credited with introducing the worm gear concept by interlocking a screw thread and toothed wheel. An improvement made by cutting a radius into the tip of the wheel tooth to allow for the worm thread root diameter was termed a *single enveloping gear set*. The clearance allowed a smaller centre distance as the wheel begins to envelop the worm. Loveless[3] reports that Leonardo DaVinci developed the *double enveloping gear set* concept in the 15th century by varying the worm thread height relative to a radius about the wheel axis. However, in the same paper Henry Hindley is largely credited as the first to manufacture gear sets of this type in the 18th century. The reduction in centre distances provided a more compact system and increased the length of worm thread flank making contact with the wheel teeth. This combination resulted in a smaller unit being able to transmit a higher torque load theoretically. The effect of this development on centre distance and engagement is demonstrated in the diagrams in Figure 1.1.

Vos[4] identifies the *CAVEX* form as originally developed by Flender in the early 1950's. This type of worm drive derives its name from the concave flanks of the worm thread which differed from conventional convex forms as shown in Figure 1.2. This improved the theoretical efficiency and the potential load capacity relative to an equivalent single enveloping system by directing more of the force parallel to the worm axis, and consequently tangential to the wheel rotation.

Worm Outside Diameter ——————— Wheel Outside Diameter

Worm Inside Diameter ·················· Wheel Inside Diameter

View along the worm axis.

View along the wheel axis.
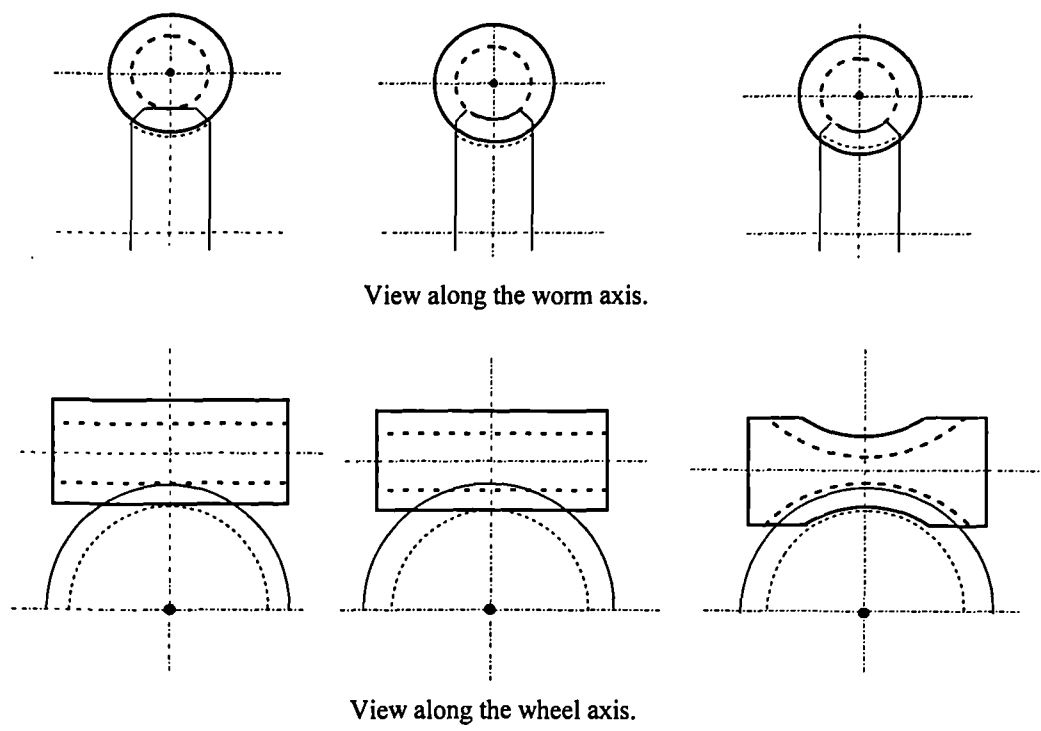
PROTOTYPE   SINGLE
ENVELOPING   DOUBLE
ENVELOPING

Figure 1.1 : A diagram showing the reduction in centre distance due to the development of worm gear drive engagement.

Worm Axis

CONVENTIONAL   CAVEX
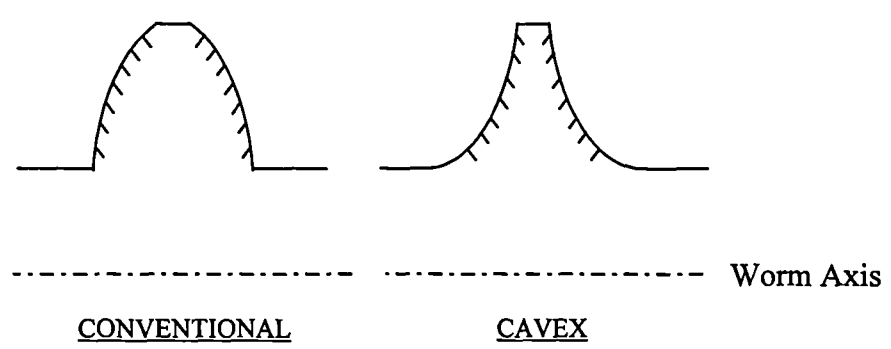
Figure 1.2 : The thread profiles for the conventional helicoid and CAVEX forms.

The theoretical operation of a gear set is affected by the design parameters, lubrication, load cycle, and axis deflections. These factors vary widely due to manufacturing preference and the intended application. Initial claims of operating advantages were therefore often driven by commercial rather than scientific reasoning. An example of this principle is given by Walker[5] in a review of results from a source in Russia making a direct comparison in performance between the Arcuate gear (a parallel axis gear form which determines tooth profile from sections in the circumference of a circle) and the involute gear form. These were criticised on the basis that even basic definitions of size and operating capability in gear specification were not given relative to any standard. This made direct comparison difficult and nullified many of the conclusions.

1.2.2.   Basic mathematics of worm gear systems

No scientific basis was defined for worm gear development until approximately the 1920's. At this point, research into various design principles for cylindrical worm gear sets was recorded by Tuplin[6] and Merritt[7][8]. Work by Merritt and Walker led to the standardisation of gear production through the initial development of BS721[9] in the 1930's. This standard had a latest revision in 1983 and is still used by industrial gear designers today to determine the worm and wheel tooth dimensions.

Analysis of worm gear contact initially involved modelling worm thread flanks as a series of helices about an axis. These helices passed through a profile which was determined by the worm gear type. A detailed analysis for cylindrical gear forms soon followed from Buckingham[10] in which standard equations were defined. This derived equations for the geometry of involute, screw, chased, and milled helicoid worm forms. The analysis goes on to calculate the 3-dimensional co-ordinates of theoretical contact lines for the engaging flanks, and pressure angles relating to the curvature of the thread profiles which determine the line of acting force. Authors such as Dudley and Poritsky[11] also made considerable contributions in this area. From these basic equations it has been possible to develop formulae for the load capacity, stress limits, and efficiency of a gear set.

A recent paper from Octrue[12][13] showed that calculations of load capacity using these fundamental equations gave a good correlation with experimental results. This demonstrates the importance and applicability of such equations to the operating performance of worm gears.

1.2.3. Manufacturing developments

Most of the analysis up to the 1940's had been based on the worm profile and had assumed a perfect or ideal contact (often termed *conjugate*) with the wheel tooth. A paper by Wildhaber[14] explained that industrial gear sets were produced using wheel cutters which were slightly modified relative to the worm thread. This process is known as *ease-off*, or *mismatch*, The mismatch is a combination of changes in profile, lead, and axis alignment in the gear cutter. The process reduces the contact area but induces clearance between the flanks allowing oil entrainment for the lubrication of contacting surfaces as in Figure 1.3. Oil is entrained into the contact region by the motion of the worm against the *entry* side of the tooth flank and expelled on the *exit* side. Variation of the parameters creates different conditions of entry and exit clearance and indicated contact.

CONJUGATE
CONTACT
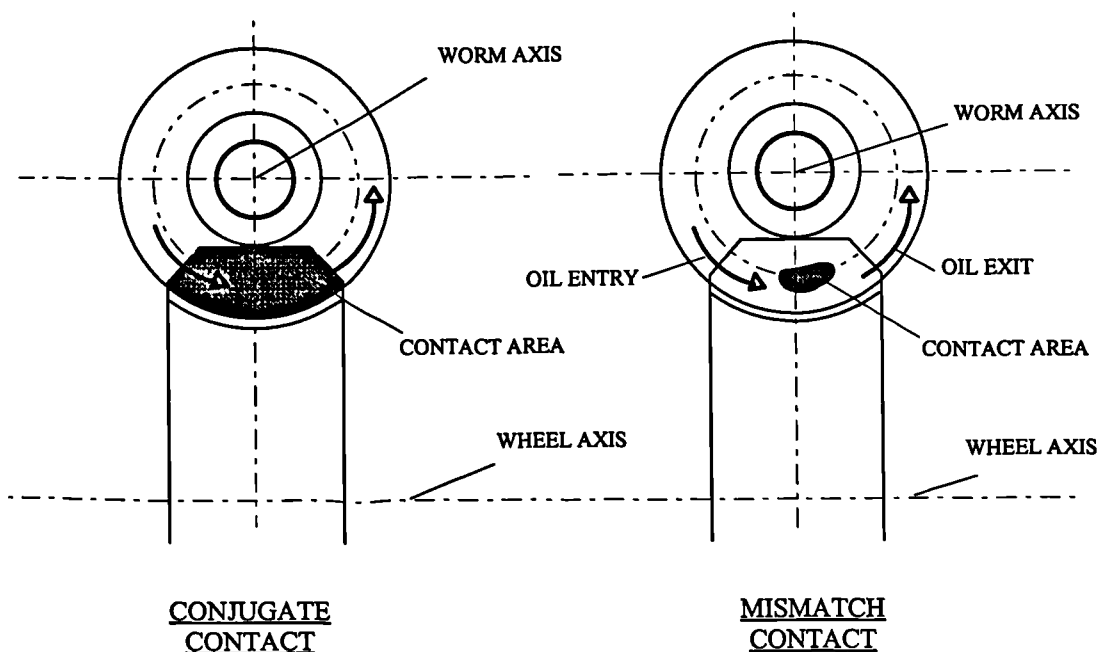
MISMATCH
CONTACT

Figure 1.3 :   The effect of 'ease-off', or 'mismatch', on worm gear contact area.

A manufactured set is assessed by the contact area generated by indicator ink paste transfer between contacting flanks during the meshing cycle. Industrial sources state that mismatch criteria are often defined on an empirical basis using trial and error results. The suitability of specific contact conditions to a given application and the knowledge necessary to achieve them is therefore largely held by industry and not stated in any formal literature as part of an accepted design theory.

South[15] stated that the manufacturing process and contact conditions of double enveloping gear set was improved by Samuel L. Cone to such an extent that this gear form is often termed a 'Cone' drive. The same paper also states that Niemann and Flender completed similar work on the CAVEX form. Investigations of the performance and production methods of double enveloping gears relative to that of cylindrical gears has been performed in papers by Qin, Zhang, Kato, & Zhang[16], and Chen[17].

1.2.4. Improvements in mismatch analysis

The clearance can be estimated by calculating the relative loci of the helical paths of points on the worm thread and wheel cutter profile. This determines the quantity of metal, known as the *relief*, which would be removed by the wheel cutting tool from a conjugate gear tooth form. This technique was used by Janninck[18] to investigate the changes in contact conditions due to variation in values of mismatch parameters. The results indicate a specific contact can be induced by the appropriate choice of mismatch parameter values.

Recent analysis of gear systems by Colbourne[19][20] has used a mathematical vector approach to determine tooth contact. Zang & Hu[21] developed a method which applies a transformation matrix to co-ordinate points on the worm or wheel cutter to establish contact positions on the wheel. A mathematical design method using matrix transformation which allowed misalignment of a gear system and profile modification of cutting tools has been developed by Litvin & Kin[22][23]. Similar methods have been applied to double enveloping gears by Hu, Zhang & Bin[24].

1.2.5. Transmission error

The relief in the wheel tooth produced by mismatch creates small modifications in rotary contact position during engagement. This represents an error in the positioning accuracy and is known as *transmission error*. Transmission error is defined by Munro[25] as : *the error in position of a gear output shaft relative to the position of the input shaft for a given angular rotation and velocity ratio*. The value varies at each displacement during a tooth engagement due to varying contact conditions. The compilation of all the transmission error values at a series of wheel displacements during the meshing cycle creates a wave form as in Figure 1.4.

Transmission Error
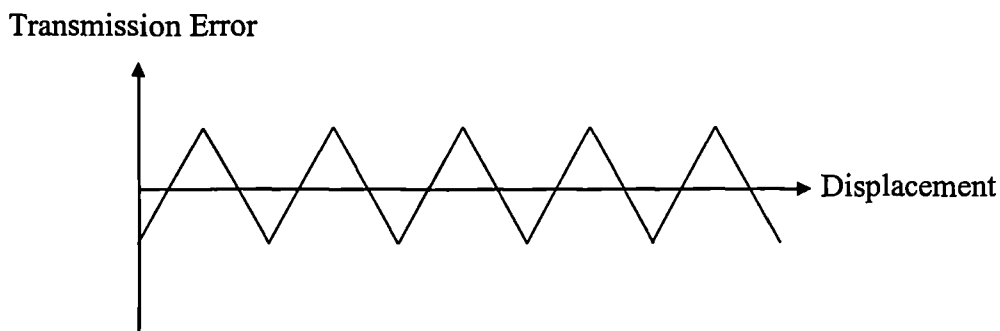
Figure 1.4 :   A transmission error wave over 5 tooth engagements.

It was the work by Harris[26] that first looked at the dynamic load effect of design on the operation of spur gear systems. This led to the concept and measurement of transmission error in a gear system being developed by Gregory, Harris and Munro[27] for spur gears. Transmission error was found by Kohler[28] to be a direct factor in determining the overall accuracy, noise and vibration characteristics of a gear set during operation. Smith[29] also identified the distinct link between transmission error tests and gear set noise. This effect was recently confirmed experimentally by Palmer and Munro[30]. Though the transmission error concept has been developed using research on spur gears, the principles can be applied to any form of gearing.

1.2.6. Tooth load bending effects

A transmitted load can cause tooth deformation, shaft bending, and axis deflections due to movement in the bearings in any gear system. Walker[31] states that the contact area of a worm gear set will change under load due to modification of the alignment by axis deflections. By considering this during the cutter design process, it is possible to define mismatch parameters such that the contact area while under no load compensates for the conditions expected at the operating load.

The principle of tooth deformation in worm gears has been recognised since the 1940's at which point Weber[32] attempted to assess and quantify the effect. The mathematical techniques and experimental equipment were not available to validate any detailed study.

Munro & Yildirim[33] have shown that the transmission error wave form and magnitude for spur gears is influenced by changes in the tooth profile and applied load. Further experimental results have shown that by controlling the generated tooth form the magnitude of the transmission error can be minimised at a specific load. This has direct consequences for worm gear operation as mismatch induces inherent profile relief, and hence transmission error, in the gear set.

A paper by Bagci[34] implies that the calculation of relief is essential when determining loaded contact conditions. It states that the compression of the contacting surfaces contributes significantly to the transmission error value. It is therefore important to know the clearances between the contacting surfaces as this establishes which points on the worm thread and wheel tooth should be included in this calculation.

Experimental work on point loaded spur and helical gear systems has been performed by Oda et al[35][36], and Umezawa et al[37] in order to develop a stiffness model predicting gear tooth deflection as a function of the wheel tooth form. Smith[38][39] uses the simple technique of relating relief in helical gear sets to the total tooth deformation using a constant tooth stiffness value. Work investigating load deformation effects on transmission error in spur and helical gears using a variable stiffness model has been performed by Barnett & Yildirim[40]. This allows for a reduction in stiffness toward the edges of the tooth. Calculations have been confirmed by experiment and associated software has been developed.

Load analysis using a finite element technique is favoured by many researchers. An example of this is given by Li et al[41] which uses the analysis to model the effects of profile modification during the gear meshing cycle. Papers by Hiltcher & Guingand[42] and Tang[43] have applied a finite element technique and stress analysis to determining the load distribution of double enveloping worm gears.

1.2.7. Worm gear metrology

Industrial collaborators have found that measurement of the worm helix and profile accuracy is a simple operation while wheel tooth form measurement has proved difficult and is largely ignored once the wheel has been cut. Small changes in contact conditions necessary for precision work are often achieved by the iterative procedure of modifying the machine settings used to manufacture the worm and inspecting the effect on the contact conditions of the gear set. This process reduces production efficiency and leads to a matched set. Pennell & Hu[44] have shown that improvements in machine tooling and control systems allow the possibility of measuring the wheel tooth form. This can confirm the accuracy of the wheel tooth profiles and therefore be used as part of the development process. Further work on the standardisation of gear metrology by Frazer, Myers and Hu[45][46][47][48][49] of the Design Unit at the University of Newcastle-upon-Tyne has ensured that constancy and accuracy have been introduced to the inspection process. This has helped considerably toward improving the reliability of the measurements and the achievable machining quality.

1.3. CONCLUSIONS FROM THE LITERATURE REVIEW

Design methods based on conjugate contact are well established. Empirical manufacturing techniques exist to allow variations in gear tooth form to improve contact conditions and ensure correct operation of the gear set. These are often derived by experience rather than any scientific reasoning and follow no unique procedure.

Some work has been completed which demonstrates the influence of mismatch parameter variation on worm gear contact marking pattern. Published literature provides little description of the model used in these calculations or validation of the predicted results using measured results. Further, no work has established the influence of mismatch on transmission error in a worm gear system.

No manufacturing error sources have been identified or quantified during previous research on worm gears. These have therefore never been considered when calculating contact conditions. As a result, appropriate contact conditions for a specific application are often still obtained by trial and error variations of machine settings when manufacturing the components rather than using purely theoretical values defined by a preferred design method.

Previous worm gear research for an operating system has concentrated on load capacity. This has often involved comparing different gear forms rather than investigating the effect of changes in individual design parameters on gear set contact conditions for a single worm form.

The effect of an applied load on transmission error has been largely ignored for worm gear systems despite experimentally validated results for spur and helical gear systems which indicate that this is a considerable influence.

Research has shown that transmission error resulting in spur and helical gears can be linked directly to noise and vibration. Profile modification allows designs to minimise transmission error at a specified load. Noise and vibration effects can be reduced by 10dB through profile changes of a few microns using this technique. No work has been carried out to investigate this principle when applied to worm gear systems.

1.4.   RESEARCH PROGRAM OBJECTIVES

The conclusions from the literature survey identified several aspects of worm gearing which required research in order to better understand the kinematics of worm gear systems under various operating conditions. Five main objectives have been defined for the research program :

- SURVEY AND ANALYSE DESIGN AND MANUFACTURING PRACTICE.

- IDENTIFY AND QUANTIFY ERRORS IN THE DESIGN AND MANUFACTURE PROCESS.

- DEVELOP A NEW MODEL TO SIMULATE TOOTH LOAD EFFECTS.

- PRODUCE SOFTWARE TO PREDICT WORM GEAR CONTACT CHARACTERISTICS.

- VALIDATE RESULTS USING A NEW TEST RIG.

- APPLY THE CONCLUSIONS TO WORM GEAR DESIGN AND MANUFACTURE.

These objectives were defined to assess current design and manufacturing techniques and identify the important factors to consider when optimising worm gear accuracy for a given set of operating parameters.

1.5. RESEARCH PROGRAM OUTLINE

The work in Chapter 2 describes the geometric relations established in previous literature to define conjugate and mismatch gear forms. It further describes how these have been applied in the development of a new model to calculate contact characteristics such as marking pattern and full transmission error curves.

Chapter 3 identifies sources of manufacturing error which influence contact conditions by monitoring the production of two gear sets. The error sources are quantified and their impact on contact conditions is examined. Additional sources of contact error occurring during worm gear operation such as axis deflection and tooth deformation are identified and described. This chapter also demonstrates how the model developed in Chapter 2 has been expanded to include these influences and thus improve the contact analysis.

Chapter 4 demonstrates the software developed to perform the calculations based on the contact analysis model, and identifies the improvements over existing software. Validation of the software is presented in Chapter 5 including comparisons of calculated results with measurements of contact characteristics recorded from manufactured gear sets.

Chapter 6 documents the design and testing of a test rig used to record transmission error under an operating load. Chapter 7 presents the results of transmission error tests recorded using this test rig. Variations induced by design parameters, alignment, running speed, and temperature change at a range of loads are recorded. This chapter also contains validation of the contact analysis model transmission error under load. Chapter 8 identifies and quantifies initial wear development in the components of a system operating under continuous load. It also illustrates the effect of the change in contact conditions on transmission error characteristics at a range of loads.

Chapter 9 states the conclusions derived from the results of the work in this thesis. It goes on to discuss how these conclusions can be applied to worm gear development and outlines potential areas for further research.

1.6. RELATED STUDIES

During the course of the research the work at Huddersfield University was supplemented by a continuing program of related studies. Close contacts were maintained with the collaborating companies with a continued exchange of advice and suggestions, as well as quarterly progress review meetings. Several courses and events were also attended :

- 'Gear Design' , Dr. Kohler at Sheffield University.
- 'Gear Loading Workshop' , Newcastle University.
- 'Practical Data Acquisition' , Instrument Data Communications (IDC).
- '1994 International Gearing Conference' Newcastle University
- A paper was written and presented at a conference of the British Gear Association (BGA) [50].
- A paper was produced for the Lamdamap '97 conference held at the University of Huddersfield[51].

2. CALCULATION OF THEORETICAL WORM GEAR CONTACT CHARACTERISTICS

2.1. INTRODUCTION

The review of existing theory carried out in Chapter 1 found several different methods for calculating worm gear form and contact position. Some analytical techniques, such as that used by Buckingham[10], have been established for many decades. More mathematically complex techniques from Colbourne[20] using vector analysis, and Zhang & Hu[21] using matrix transformation of co-ordinate systems have been developed within the last few years. This chapter states the design principles and equations derived in literature from such authors for the definition of worm and wheel geometry. It then describes the contact analysis model for the work in this thesis established by applying existing design knowledge, and the further development undertaken in order to calculate the resulting worm gear characteristics. This also represents the model used by the associated computer software. The development of the basic equations has been limited to the case of cylindrical involute and screw helicoid forms, which represent the majority of industrial specifications, and identifies the basic convolute form from which these are derived.

2.2. ANALYSIS OF WORM GEAR GEOMETRY

2.2.1. Development of the convolute, screw and involute helicoid

To analyse the convolute geometry a base cylinder of radius r_b is defined about an axis as shown in Figure 2.1. A helix is formed around this base cylinder which completes one revolution over each fixed length along the axis, defined as the lead l. The generatrix is a tangent to the base cylinder. This is set at an angle γ to a plane transverse to the axis of the base cylinder. The convolute curve is the locus of intersection points of the generatrix with the transverse plane for each point on the base cylinder helix, as shown in Figure 2.1.
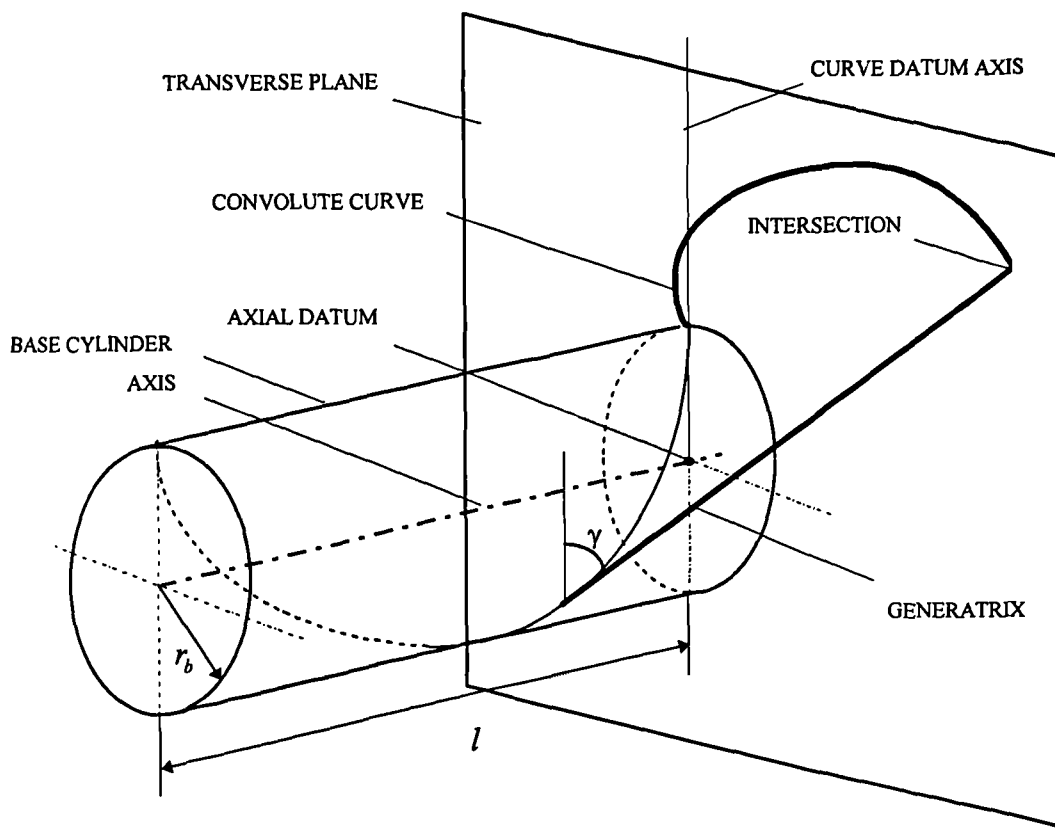
Figure 2.1 :   The intersection of the generatrix in the transverse plane at a single point on the base cylinder helix, and the convolute curve development.

Values of r and ϑ represent the polar co-ordinates, vector radius and angle respectively, of an intersection point of the generatrix in the transverse plane. The curve datum is the vector at which $\vartheta = 0$ and $r = r_b$. The diagram in Figure 2.2 (A) shows this as the convolute development in the transverse plane viewed along the base cylinder axis. The rotation about the base cylinder axis, ε, relative to the datum vector is proportional to the axial displacement. The relationship of the generatrix with the axial displacement from the transverse plane is shown in Figure 2.2 (B). In these diagrams, G' represents the length of the generatrix projection in the transverse plane.
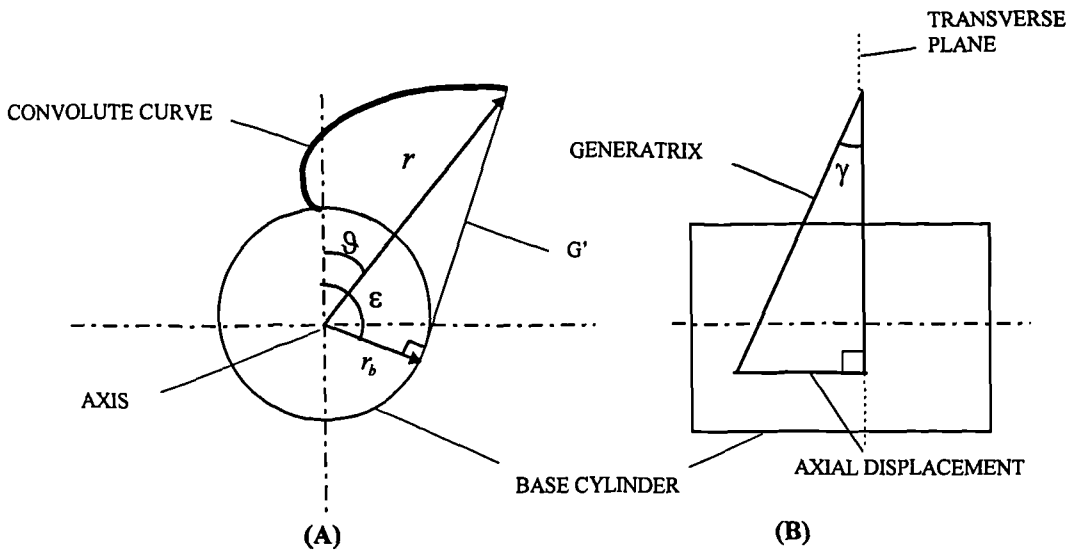
Figure 2.2 : The convolute curve development relative to axial displacement of the generatrix along a base cylinder helix.

Using these diagrams a relation between the generatrix position along the base cylinder helix and the intersection point in the transverse plane can be established. Using simple geometric relationships such as those derived by Buckingham[10], the convolute curve has the following relation in the transverse plane :

$$\vartheta = \left(\frac{2.\pi.\tan(\gamma)}{l}\right)\sqrt{r^2 - r_b^2} - \tan^{-1}\left(\frac{\sqrt{r^2 - r_b^2}}{r_b}\right) \qquad (1)$$

Special cases of the convolute curve are defined by fixing a single parameter in the equations. The *screw helicoid* case development is defined as a convolute in which the base radius is reduced to zero. Substituting this value into equation (1) gives :

$$\vartheta = \left(\frac{2.\pi.\tan(\gamma)}{l}\right)r - \tan^{-1}\infty$$

The inverse tan function is a constant which can be considered optional as the original transverse plane of generation is in an arbitrary axial datum position.

The *involute helicoid* case development is defined as a convolute in which γ is equal to the base cylinder lead angle value.

The lead angle at any radius 'r' is defined as :
$$\lambda = \tan^{-1}\left(\frac{l}{2.\pi.r}\right)$$

The base lead angle is then :
$$\lambda_b = \tan^{-1}\left(\frac{l}{2.\pi.r_b}\right)$$

When substituted for γ in equation (1) this gives:

$$\vartheta = \frac{\sqrt{r^2 - r_b^2}}{r_b} - \tan^{-1}\left(\frac{\sqrt{r^2 - r_b^2}}{r_b}\right)$$

Equations for the involute are used extensively throughout the gearing industry to generate tooth profiles. The analysis of spur and helical gear forms by Dudley[52] and Litvin[53] are examples which demonstrate this.

2.2.2. Worm thread profile defined in an axial section

An axial section is a plane which contains the axis and which divides the base cylinder symmetrically in two. A point on the axial profile of a thread represents the intersection of a helicoid generated in a transverse plane with the axial plane. The axial profile is a series of such intersections formed when the curve datum is rotated in successive transverse planes along a helical path around the base cylinder helix as shown in Figure 2.3.

For a radial distance in the profile of length r, the associated ϑ can be calculated using the relationship established in section 2.2.1. This represents the rotation of the curve datum. In following a base cylinder helix, the rotation of the curve is proportional to the displacement 'z_a' along the axis. Because of this, it is possible to calculate the transverse plane at z_a for each r using the relation :

$$z_a = \frac{\vartheta\, l}{2\pi} \tag{2}$$
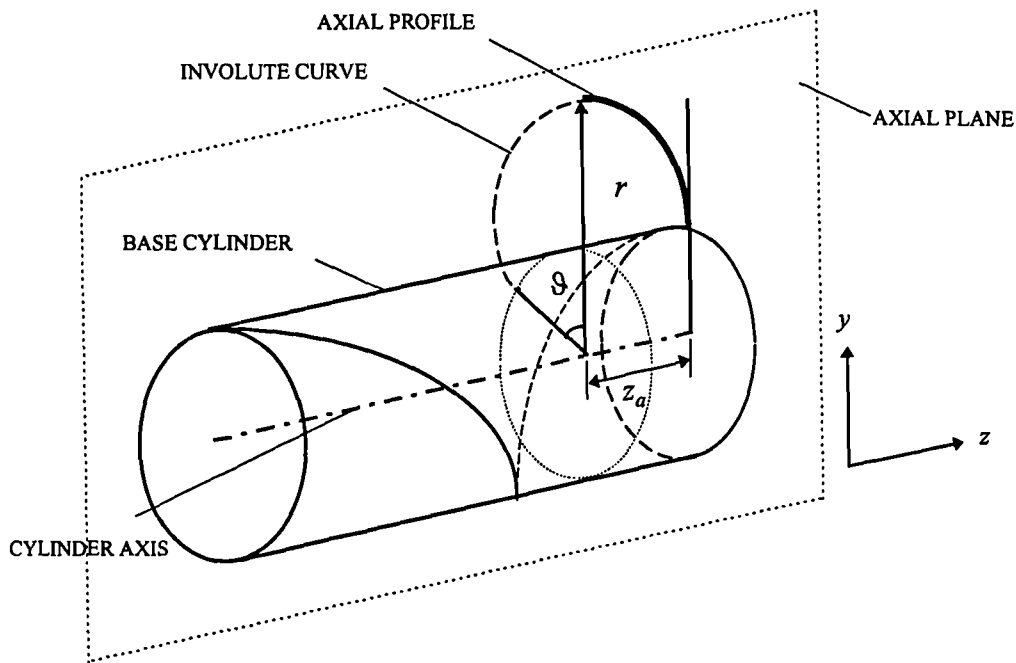
Figure 2.3 :   Defining a point in the development of the axial profile for the involute helicoid.

The radius value, r, becomes equivalent to a 'y_a' co-ordinate of the profile at this axial displacement in the system shown in Figure 2.3. By combining equations (1) and (2) the following equations are obtained for axial profile co-ordinates z_a and y_a :

Convolute helicoid :

$$z_a = \left(\sqrt{y_a^2 - r_b^2}\right)\tan\gamma - \left(\frac{l}{2.\pi}\right)\tan^{-1}\left(\frac{\sqrt{y_a^2 - r_b^2}}{r_b}\right)$$

Screw helicoid :

$$z_a = y_a \tan\gamma - \left(\frac{l}{2.\pi}\right)\tan^{-1}\infty \qquad\qquad [r_b = 0]$$

Involute helicoid :

$$z_a = \left(\frac{l}{2.\pi}\right)\left(\frac{\sqrt{y_a^2 - r_b^2}}{r_b} - \tan^{-1}\left(\frac{\sqrt{y_a^2 - r_b^2}}{r_b}\right)\right) \qquad \left[\tan\gamma = \frac{l}{2.\pi.r_b}\right]$$

2.2.3. Calculating rack section profiles of a worm thread

A rack section is the thread profile intersection with any plane parallel to the axial plane and offset by a value 'x'. The worm thread flank can be simulated using a series of helical paths. Each helix has the same lead value, but passes through a unique point on the axial profile. The relationship is described graphically in Figure 2.4. which shows the helix connecting point **A** in the axial plane and **B** in an offset plane.
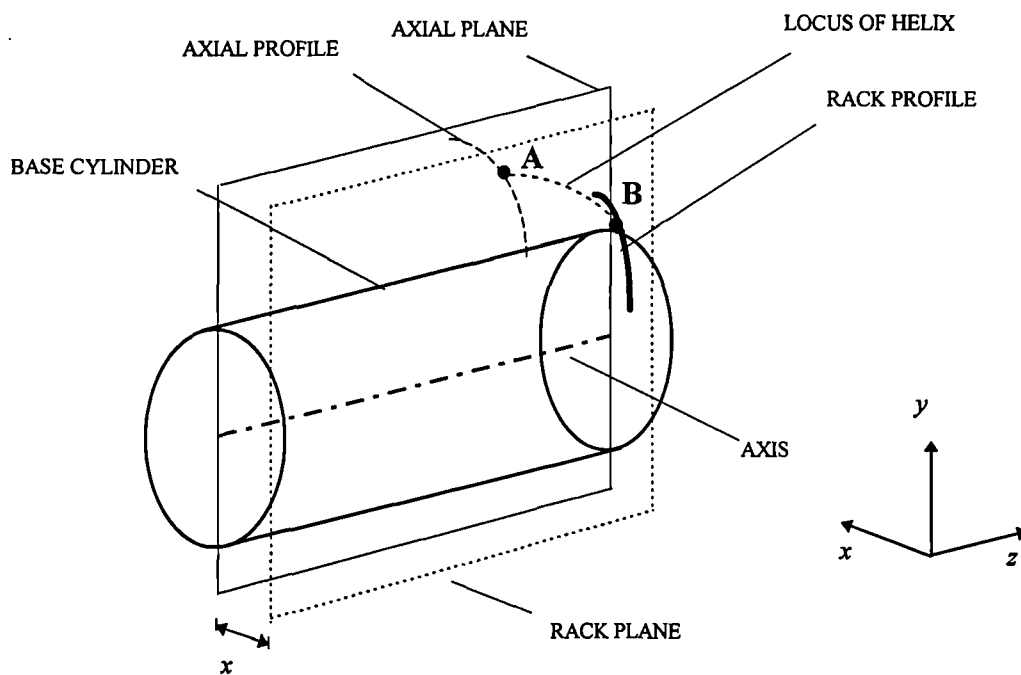
Figure 2.4 :   The development of the rack section profile in a plane parallel to the axial plane in which **A** and **B** are points on a common helical path.

The diagram in Figure 2.5 shows the helical path development into the offset plane when viewed along the base cylinder axis. This demonstrates clearly the triangular relationship between y_a, y, and x.
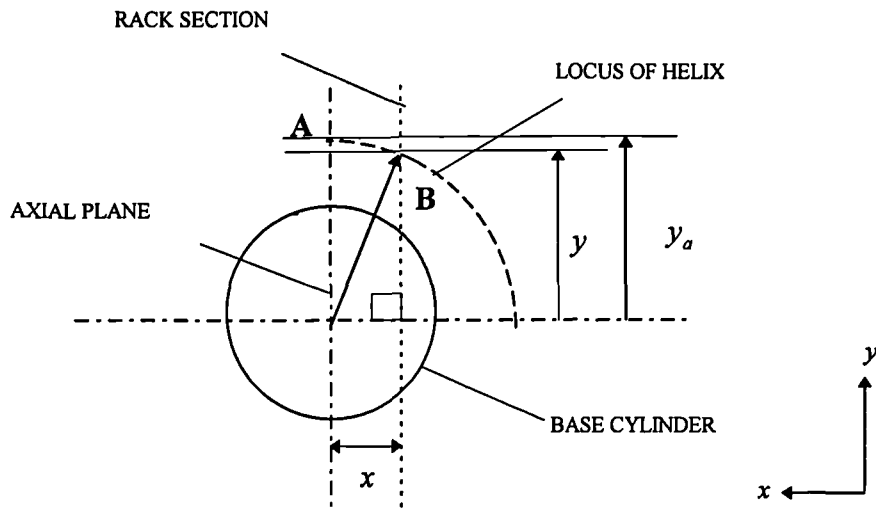
Figure 2.5 :   The intersection of a helix generated from an axial profile point with a
                rack plane at a distance x from the axial plane when viewed from the
                base cylinder axis.

Given that :

x_a, y_a, z_a are the co-ordinates of a point **A** on the axial profile ($x_a \Rightarrow x = 0$).

x, y, z are the co-ordinates of a point **B** on the worm thread on a helix

common to **A**.

For a point on the worm thread the following relationships hold for an axial profile
point and associated rack section profile point along a common helix :

$$z = z_a + \left(\frac{l}{2.\pi}\right) \sin^{-1}\left(\frac{x}{y_a}\right) \tag{3}$$

$$y = \sqrt{y_a^2 - x^2} \tag{4}$$

CHAPTER 2

2.2.4. The worm thread pressure angles

The pressure angles are crucial in determining the conjugate contact positions and consequently any relative error in the motion of the gear set. Differentiation of the profile equations (3) and (4) in section 2.2.3 for any given rack section provide the gradient and consequently the pressure angles for the worm thread form as shown in Figure 2.6.
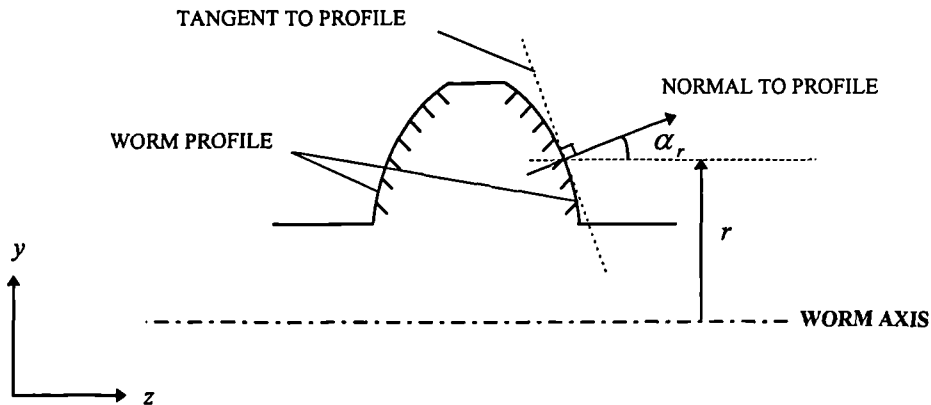
Figure 2.6 :   The pressure angle in an axial profile

The *rack pressure angle* α_r can be derived using the relationship between gradient and profile angle :

$$\alpha_r = \tan^{-1}\left(\frac{-1}{Gradient}\right)$$

$$\alpha_r = \tan^{-1}\left(\frac{-1}{\left(\frac{dy}{dz}\right)}\right)$$

$$\alpha_r = -\tan^{-1}\left(\frac{dz}{dy}\right) \qquad\qquad \left[\text{using the relation : } \tan(-\vartheta) = -\tan\vartheta\right]$$

Buckingham[10] demonstrated that this value can be calculated by substituting for z in this equation using defined profiles such as in (3) and (4).

Rack pressure angle for a screw helicoid :

$$\alpha_r = \tan^{-1}\left(\frac{y \cdot \sqrt{(y^2 + x^2)} \cdot \tan\gamma - l.x}{(y^2 + x^2)} \right) \tag{5}$$

Rack pressure angle for an involute helicoid :

$$\alpha_r = \tan^{-1}\left(\left(\frac{l}{2.\pi}\right)\left(\frac{y \cdot \sqrt{(y^2 + x^2) - r_b^2} - xr_b}{r_b \cdot (y^2 + x^2)} \right) \right) \tag{6}$$

The *axial pressure angle*, α_a, is the rack pressure angle in the axial section. This is obtained by using the value $x=0$ in equation (5) and (6) for the screw and involute helicoid form respectively. The *normal pressure angle*, α_n, is defined as an angle to the worm thread surface relative to the worm axis at a specific radius. It is formed by the helix angle of the worm thread, ψ, which for a helix of radius r and length l is:

$$\psi = \tan^{-1}\left(\frac{2.\pi.r}{l} \right) \tag{7}$$

The relationship between the axial pressure angle and normal pressure angle due to the helical form has been derived by Colbourne[20] as the following :

$$\tan\alpha_n = \tan\alpha_a \sin\psi \tag{8}$$

Substituting (7) into (8) gives the relation of the normal pressure angle to a point on the axial section profile :

$$\alpha_n = \tan^{-1}\left(\tan\alpha_a . \sin\left(\tan^{-1}\left(\frac{2.\pi.y_a}{l}\right) \right) \right) \qquad [r = y_a]$$

This value is important as it determines the line of action for the forces on the worm thread while transmitting a load and therefore affects both the efficiency and load capabilities. Usually a single value is stated for any design which is the pressure angle expected at a specific reference diameter. The choice of reference diameter and whether to use the axial or normal pressure angle is dependent on the design standard.

CHAPTER 2

2.2.5. Designation and dimensioning

For a given centre distance a it is possible to define a boundary between the gear centres in which a linear displacement parallel to the worm axis is equal to an equivalent rotational displacement about the wheel axis. Contact of worm and wheel is defined relative to this boundary as shown in Figure 2.7.
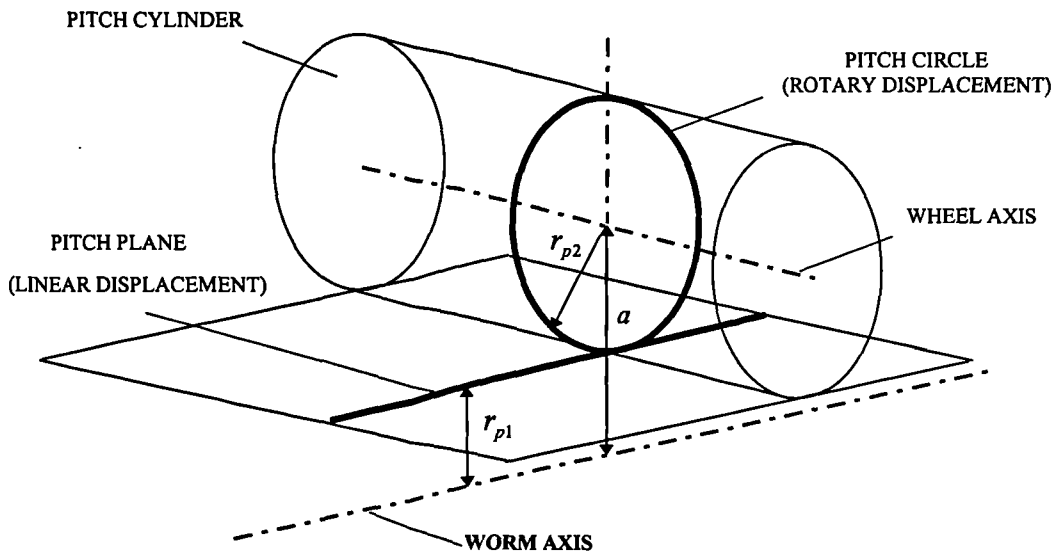
Figure 2.7 :   Conjugate contact dimensions relative to the pitch plane.

The distance of this boundary from the worm axis is the *worm pitch radius* value, r_{p1}. The *wheel pitch radius*, r_{p2}, is the distance from the wheel axis to the boundary and forms a *pitch circle* about the wheel axis. Analysis in all rack sections along the wheel axis produces a *pitch plane* parallel to both the worm and wheel axis, and a *pitch cylinder* about the wheel axis.

The number of worm threads, z_1, and wheel teeth, z_2, determine the ratio of the gear set. The circumference of the pitch circle is divided equally for each wheel tooth. This determines the thread and tooth spacing, known as the *pitch, p*. When p is known then the lead value needed for the worm helix to maintain conjugate action is the pitch multiplied by the number of threads.

Due to the pitch plane relation this arc length is also the equivalent worm thread spacing in the axial section such that :

$$2.\pi.r_{p2} = p.z_2$$

This relation can also be arranged as :

$$\frac{p}{\pi} = \frac{2.r_{p2}}{z_2}$$

The pitch divided by π is represented by a factor known as the *module, m*. The *quotient, q*, is the number of modules in the worm pitch diameter and thus represents a scaling factor for the worm :

$$q = \frac{2r_{p1}}{m}$$

The choice of gear set design for a specified centre distance can be summarised by the *designation* of the gear set. The designation is defined in the following way :

DESIGNATION: z_1 / z_2 / q / m

This system was introduced as part of the process to rationalise and standardise worm gear production in industry by using fixed values of q and m. The worm and wheel are usually dimensioned in factors proportional to these values using some standard such as BS721[9], DIN[54][55][56], or AGMA[57]. The introduction of the designation system removed π from many of the calculations for these dimensions.

The compatibility of the dimensions and ratio of the gear set design are determined by the specific application for which it is intended to be used. This knowledge is generally at the discretion of industrial gear designers and based on empirical data.

2.3. CONJUGATE CONTACT

2.3.1. Conjugate point of contact

Conjugacy implies that ideal contact conditions exist between the driving and the driven component within a gear set. Conjugate contact must satisfy the *Law of Conjugate Gear Tooth Action* which states that in order to maintain a uniform rotary motion the normal to a rack section profile must pass through the same point on the centre line in each position of contact. The point is called the *pitch point* and is located at the intersection of the pitch plane with the common centre line. An example of the relation for a single position of contact in an axial section is shown in Figure 2.8, but this holds in each rack section through a worm thread.
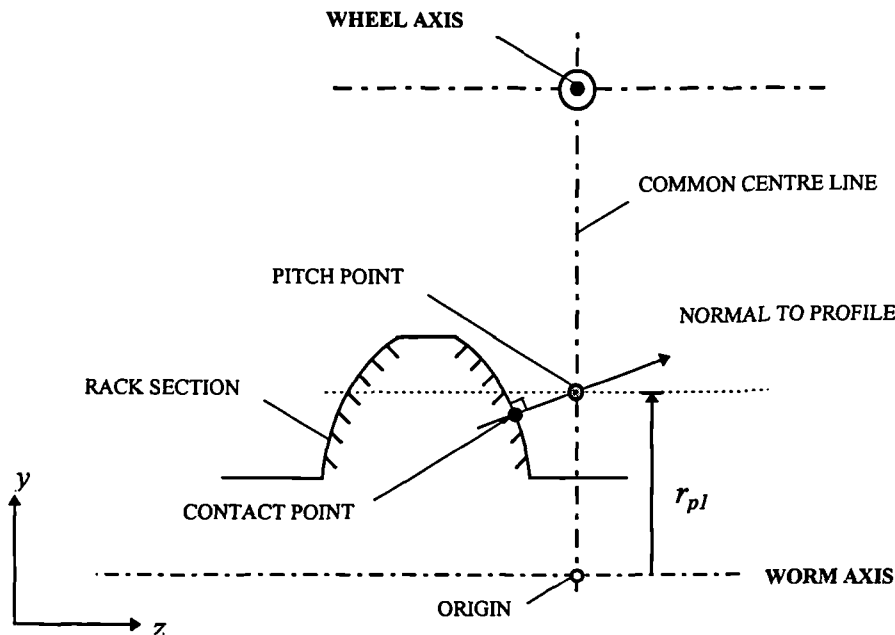
Figure 2.8 :   Conjugate contact in an axial section of an involute helicoid thread.

At a conjugate contact point, co-ordinates z and y have an associated rack pressure angle, α_r, such that the following relation holds :

$$\alpha_r = \tan^{-1}\left(\frac{y - r_{pl}}{z}\right)$$

2.3.2. Path of contact

By fixing one of the co-ordinates, an iterative calculation can be performed for any rack section to find a complementary co-ordinate and subsequent α_r which satisfies the conjugate contact relationship. An example of this is shown in Figure 2.9 for five sample rack sections of an involute helicoid which have offset values $x_1 = -b/2$, $x_2 = -r_b$, $x_3 = 0$, $x_4 = -r_b$, and $x_5 = b/2$ respectively, where b is the face width of the driven gear.

This can be repeated for the worm in a series of angular rotation positions, β_w. Each angular rotation is proportional to a rack profile displacement, u. For conjugate contact points at any displacement position the following equation holds in each rack section :

$$\alpha_r = \tan^{-1}\left(\frac{y - r_{p1}}{z + u}\right)$$

The locus of all the calculable conjugate contact positions on the worm profile is called the *path of contact*. This is shown in Figure 2.10 for each of the five sample rack sections described above.

There are two limits to the envelope of conjugate contact. The first is a negative pressure angle in the rack section profile. This can occur toward the root of the thread in rack sections with large offset values. In this case it is not possible to calculate a contact point since the normal can not pass through the pitch point at the associated displacement position. The second occurs when a *cusp* occurs along the path of contact. This point represents the minimum distance from the wheel axis for conjugate contact in the rack section. Any point further along the path of contact will cause destructive interference with the existing conjugate wheel profile generation.
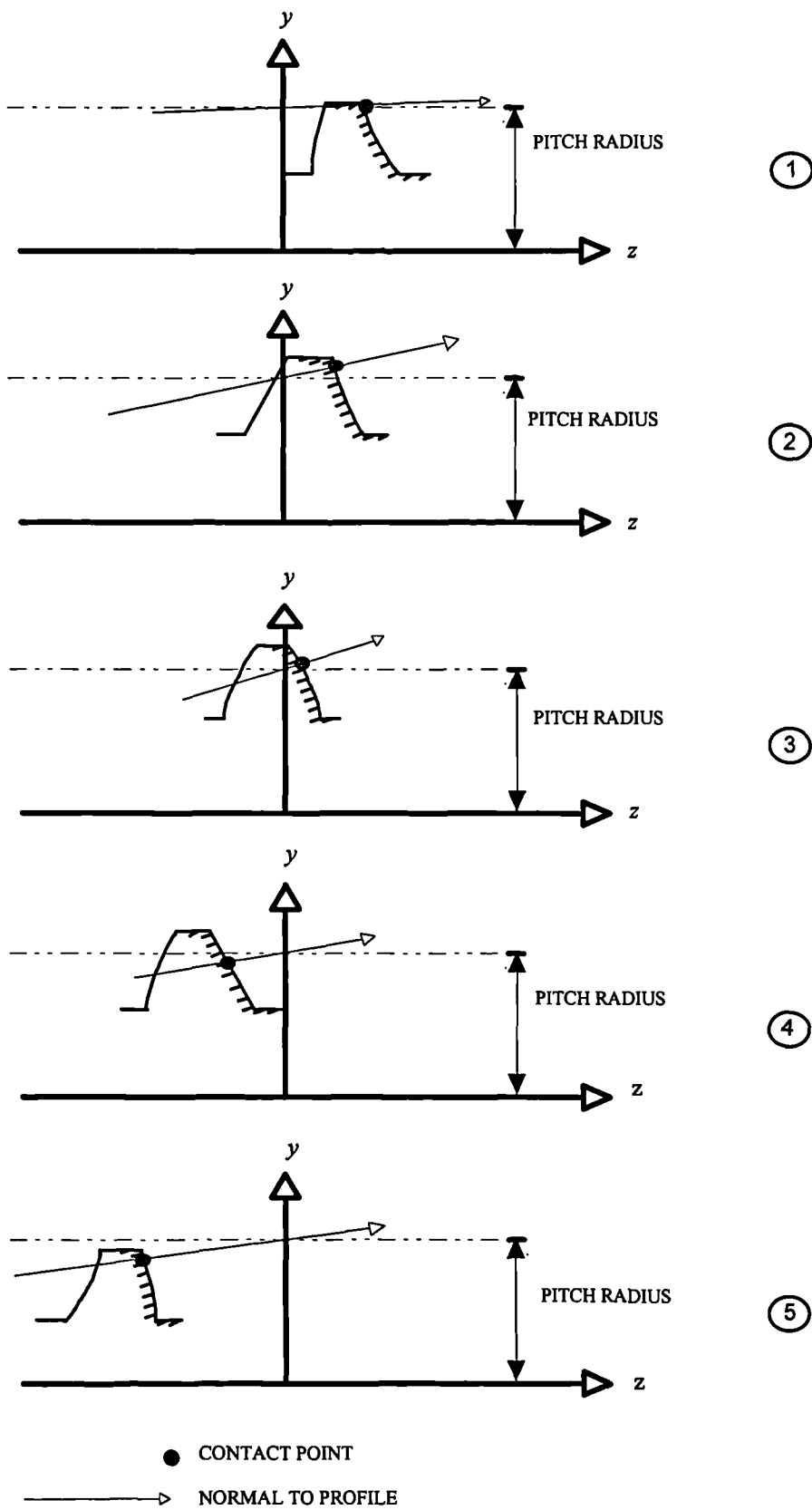
Figure 2.9 :   Contact points in five rack sections.
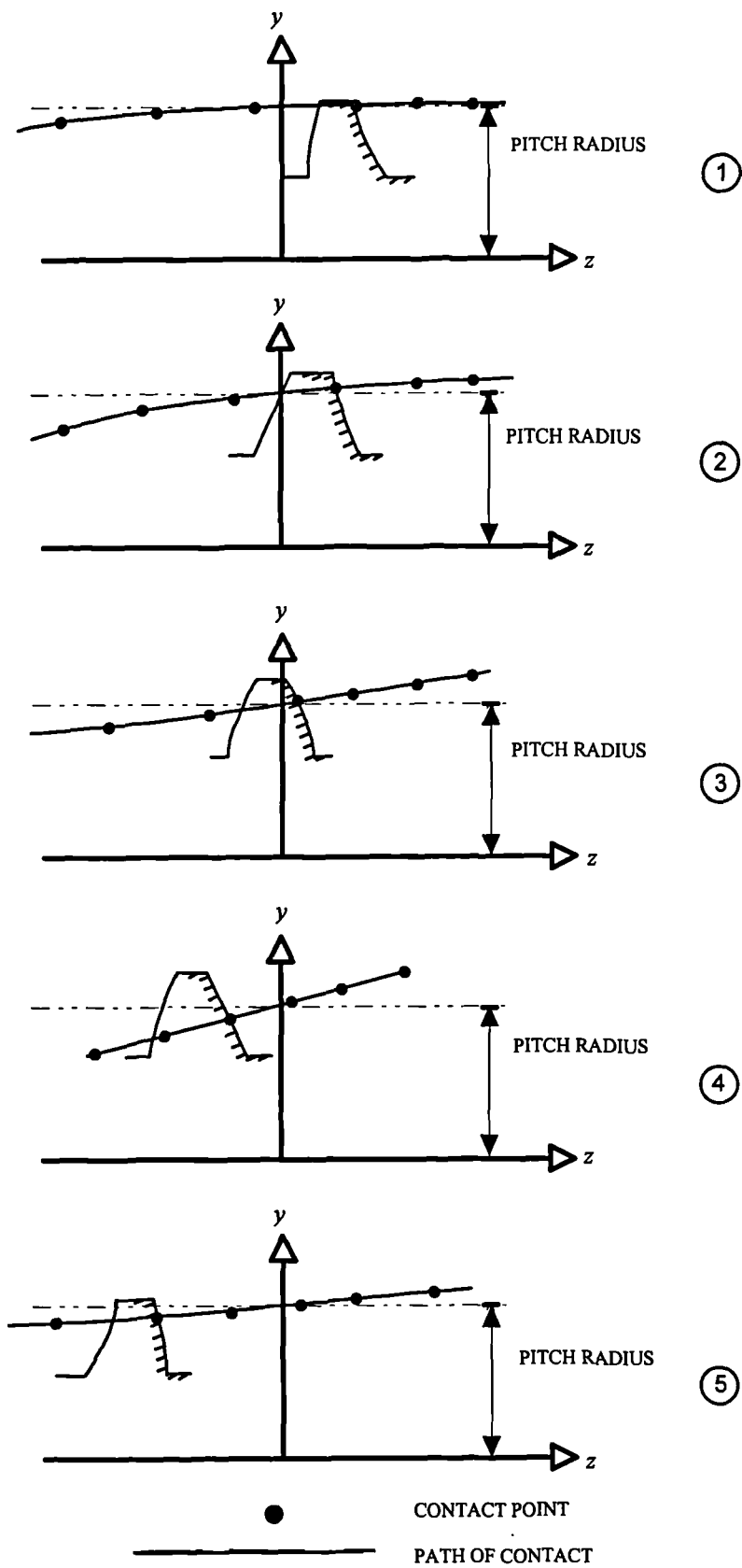
Figure 2.10 : Points of contact at six arbitrary displacements, and the path of contact in the five sample rack sections.

2.3.3.   Calculating the wheel tooth profile

In a conjugate wheel cutting process the tool thread form is identical to that of the worm. Sections of the worm thread are removed at regular intervals to form a series of cutting profiles, this process is known as *gashing*. The gearing ratio relative to the wheel is also maintained during the wheel generation. As a consequence the paths of contact in the cutting tool rack sections are identical to that of the worm. The conjugate contact points therefore become cutting points.

The gearing ratio is defined by the number of worm threads, z_1, and wheel teeth, z_2, and is maintained throughout the meshing cycle. The wheel completes z_1 revolutions for every z_2 revolutions of the worm. At each cutting point the rotary wheel displacement, β_2, is proportional to the cutter revolution in the same manner, and hence proportional to the axial displacement, u_0, of the cutter profile :

$$\beta_2 = \frac{2.\pi.u_0.z_1}{z_2.l_0}$$

The cutting point represents a point on the wheel tooth profile in the rack section as shown in Figure 2.11.
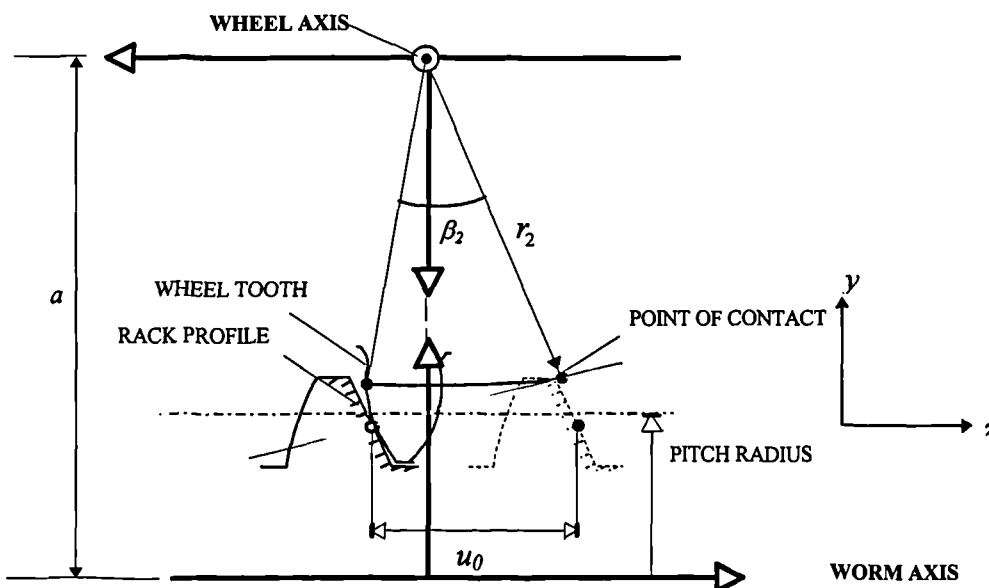
Figure 2.11 :   Generation of a point on the wheel tooth profile in a rack section.

Once the *centre distance*, *a*, representing the distance of the wheel axis from the worm axis along the common normal is known, the radius of the contact point on the wheel tooth profile, r_2, can be calculated :

$$r_2 = \sqrt{(z + u_0)^2 + (a - y)^2}$$

The wheel tooth profile in each rack section is generated by repeating this calculation for several contact points along the path of contact to find unique values of β and r_2 for each displacement. The wheel tooth form is given by combining the profile calculations from all of the rack sections. The resulting wheel tooth form is then described as being *conjugate to the worm*.

2.3.4.   Line of contact

The contact analysis in each rack sections can be indicated simultaneously by illustrating the complete gear tooth form when viewed in the direction of the worm axis. An example of this is shown in Figure 2.12 for the five sample rack sections established in section 2.3.2.

In Figure 2.12A the contact point is shown relative to the wheel tooth form for each rack section at a single arbitrary displacement. Joining the contact points in all these sections generates a conjugate *contact line* across the wheel tooth for this displacement as seen in Figure 2.12B. Increasing the number of rack sections creates a more continuous line of contact across the gear tooth face. This can then be repeated for a number of worm displacement positions creating a series of these contact lines during the meshing cycle as in Figure 2.12C.

WORM AXIS

PITCH PLANE

r_{p2}

CONTACT POINTS
(ONE ANGULAR POSITION)

(A)

WHEEL AXIS

① ② ③ ④ ⑤

WORM AXIS

LINE OF CONTACT
(ONE ANGULAR POSITION)

(B)

WHEEL AXIS

① ② ③ ④ ⑤

WORM AXIS

(C)

LINES OF CONTACT
(SEVERAL ANGULAR POSITIONS)

WHEEL AXIS
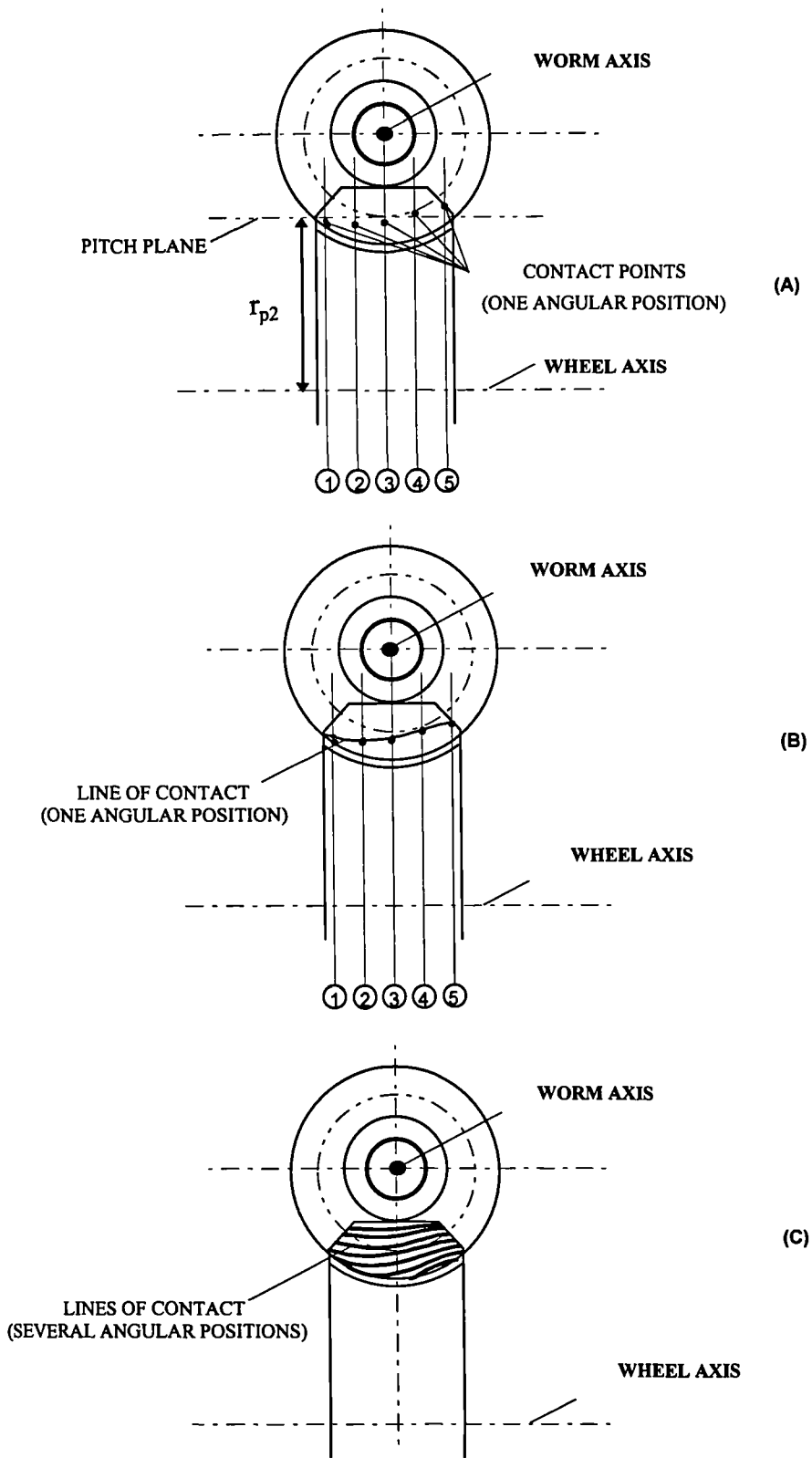
Figure 2.12 : Development of conjugate contact over a wheel tooth.

If enough sample displacements are considered, it can be seen that the continuous nature of conjugacy creates contact over the complete gear tooth face throughout the meshing cycle as in Figure 2.13. This is known as *full face* contact and is a characteristic of the conjugate gear set.
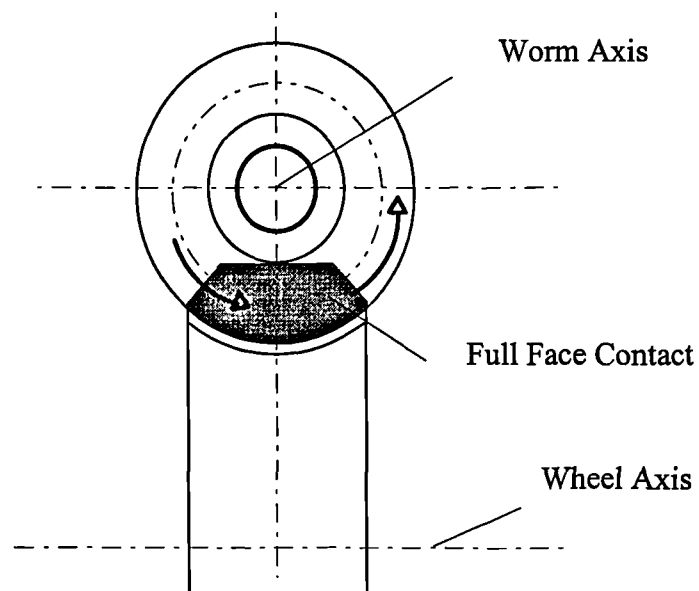
Figure 2.13 :   Diagram indicating full face contact through the gear meshing cycle in the case of a conjugate gear set.

2.4. CALCULATING MISMATCH CONTACT CHARACTERISTICS

2.4.1. The purpose of mismatch

Under operating conditions a worm gear set can experience severe heat fluctuations, abrasion, and elastic deformation of the contacting surfaces. The conjugate gear set is impractical as the full face contact condition does not allow clearance for the necessary oil lubrication of the surfaces. Wheel cutting tool parameters are therefore modified relative to the conjugate profile in industrial gear sets designs to avoid this situation. The cutting process consequently generates a wheel tooth form which is no longer conjugate to the worm. The modified parameters are collectively defined as the *mismatch*. A combination of mismatch parameters is chosen which produces a contact area which allows adequate clearance for lubrication of the contacting surfaces but maintains an area of contact large enough to avoid stress failure during operation. An arbitrary example is shown in Figure 2.14.
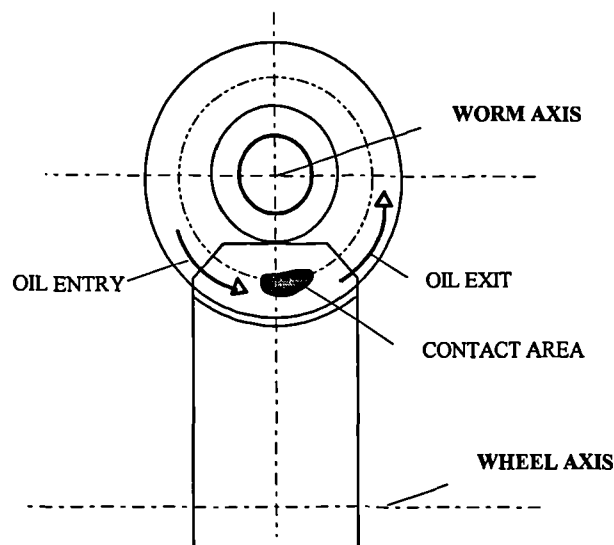
Figure 2.14 :   An example of a contact marking pattern for a mismatch worm gear set.

Studies by Janninck[18] and Colbourne[20] have shown how mismatch design parameters can influence the position and extent of the gear tooth relief, and consequently the marking pattern. Further discussion of the results and conclusions from these papers can be found in Chapter 5.

2.4.2. Wheel cutter modification due to mismatch parameters

2.4.2.1. Wheel cutter over-sizing

Wheel cutter over-sizing is a technique widely used to induce adequate entry and exit conditions for lubrication. The oversize value represents the dimension which is added to the worm at a reference diameter, d_p. This reference diameter is usually the pitch diameter or the mean diameter of the worm. The result of this is to shift each point on the worm profile away from the axis by half the over-size value as shown in Figure 2.15. The centre distance when cutting the wheel is changed to compensate for this increase in diameter.
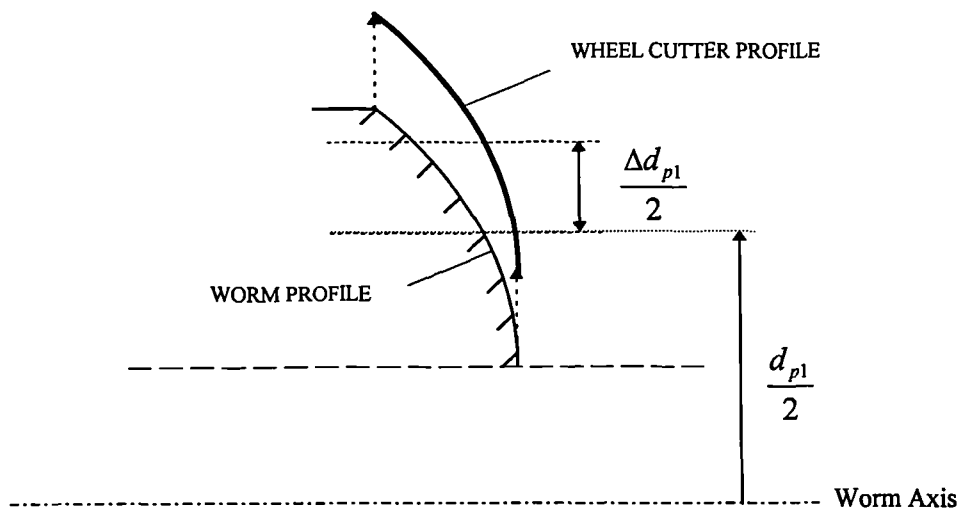
Figure 2.15 :   The direct increase in radius value shown in the axial section.

Though the axial profile is not affected, the contact path in each rack section changes due to a modification of the radius and normal pressure angle caused by the new helical paths of the thread flanks.

2.4.2.2. Changing the pressure angle

The axial pressure angle α_a at the reference diameter is derived by differentiating the equation of the axial profile as established in section 2.2.4. The axial profile of a screw helicoid is a straight line, therefore the axial pressure angle in a screw helicoid is a constant at all diameter values. The axial pressure angle in an involute helicoid is linked to the base cylinder diameter used for the involute helicoid generation. This is shown in equations (9) and (10) for the screw and involute helicoid respectively.

$$\alpha_a = \gamma \tag{9}$$

$$\alpha_a = \tan^{-1}\left(\frac{l}{\pi \cdot d_{p1} \cdot d_{b1}} \sqrt{d_{p1}^2 - d_{b1}^2} \right) \tag{10}$$

The profile and the pressure angle can be changed by choosing a different γ value. To achieve a change in axial pressure angle in an involute helicoid form the wheel cutter base diameter is modified as in Figure 2.16.
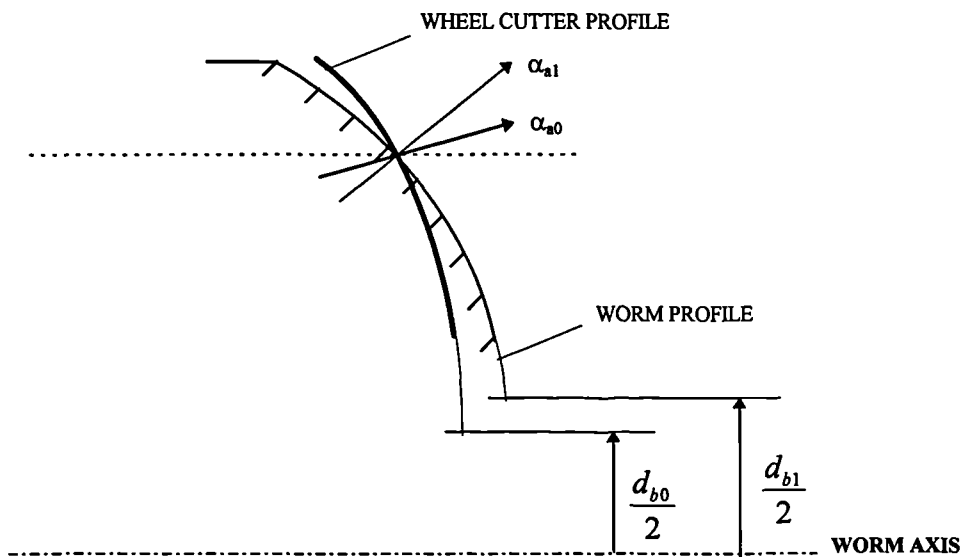
Figure 2.16 : The change in profile due to a change in base radius for an involute helicoid axial profile.

Rearranging equation (10) gives the following value for the base diameter needed to achieve a given axial pressure angle at a specific diameter, d :

$$d_b = \frac{d}{\sqrt{\left(\frac{\pi \cdot d \cdot \tan\alpha_a}{l}\right)^2 + 1}}$$

2.4.2.3. Profile modification

Relief can be created by adding metal to the basic involute profile of the wheel cutter. The modification value stated is the maximum profile change and occurs at the tip or root of the profile with all other values based upon some basic equation represented as a function of the diameter. The modification is usually applied symmetrically and normal to the profile about the mean diameter of the tooth. This process has mostly been performed by flat sided grinding wheels producing a linear relief over some length of the profile. CNC machines now allow any form to be transferred to the wheel cutter. An example of this which is often used in industry is parabolic relief as shown in Figure 2.17.
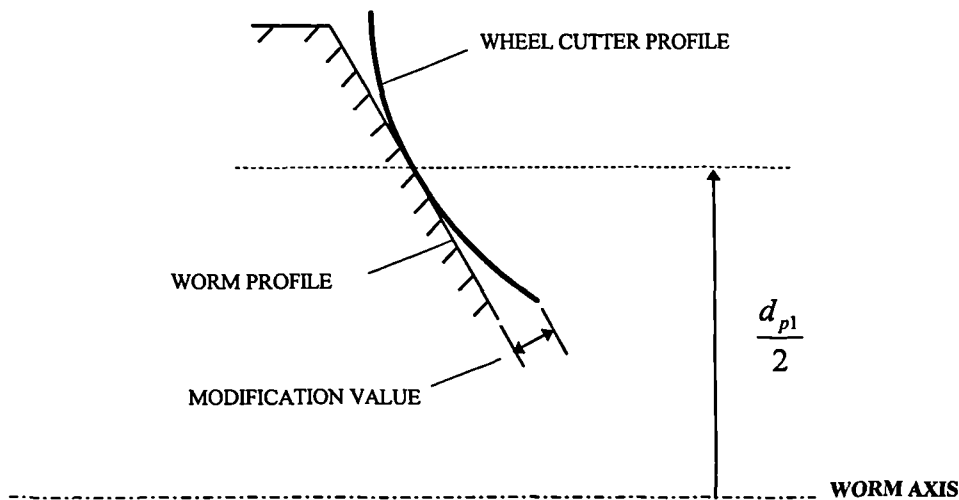
Figure 2.17 : The change in profile due to direct addition of surface material using a parabolic modification.

2.4.2.4. Changing the axis alignment

Normal worm and wheel alignment defines the angle between the axes, Σ_1, as 90° (or $\pi/2$). The cutting axis is often inclined at an angle Σ_0 during the wheel cutting process as part of the design method as shown in Figure 2.18. The angle of rotation is called the *tilt angle* (also known as the *swivel* or *tip angle*).
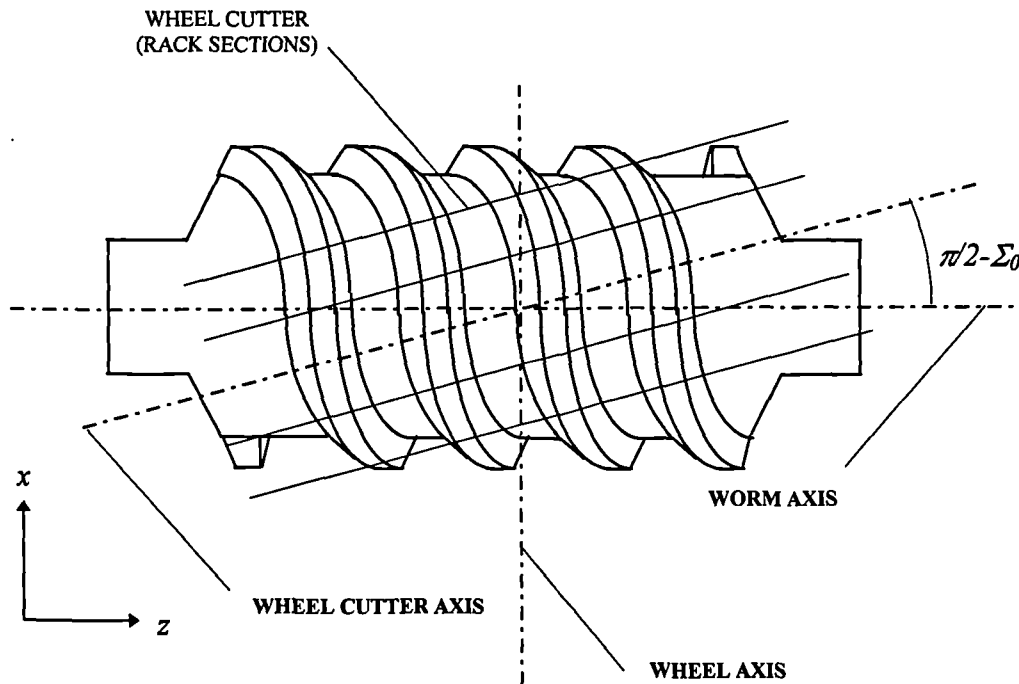
Figure 2.18 :   The modified alignment of the wheel cutter rack sections relative to the worm axis.

2.4.3. Wheel cutter design methods

The mismatch design method influences the relief applied to the gear tooth which in turn defines the area of contact for the worm thread. The parameters which define the wheel cutting tool can be varied independently, however, this does not lead to a scientific basis for the study of the effects of variations in design. A more acceptable form of analysis is to modify the parameters using a specific design method. In each design method the cutter is modified using one or more of the options described in the sections 3.1.1, 2, and 3 and fixing several relationships between the definition of the wheel cutter and worm dimensions. This has been analysed in some depth in a paper by Colbourne[20].

The diagrams in Figure 2.19 show the contours of 0.0005" and 0.0010" metal relief depth for an identical gear set based upon the designation given in Appendix D/1. The same design method is used in each case, the difference in contour pattern is caused by different wheel cutter design parameters.

$$\Delta d_{p1} = 0.15 \qquad \Sigma_0 = 89.18°$$

$$\Delta d_{p1} = 0.10 \qquad \Sigma_0 = 89.43°$$

$$\Delta d_{p1} = 0.00 \qquad \Sigma_0 = 90.00°$$
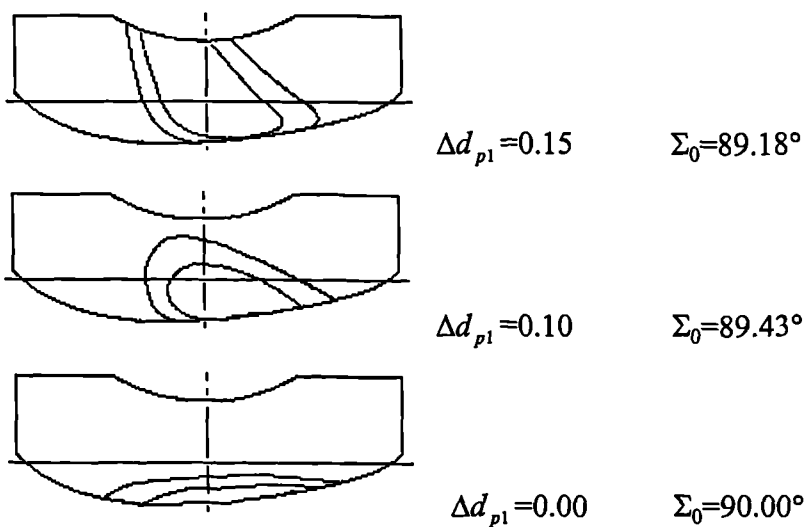
Figure 2.19 : The 0.0005" and 0.0010" contours of three alternative relief patterns produced by Colbourne using the normal pitch design method to define different wheel cutting parameters.

The final design must determine the contact conditions which best compensate for effects of the operating cycle. This is difficult due to the large number of variables needed to analyse any given application. This is multiplied by the extent of variation possible in each design and by the option to use a number of design methods. Examples of three of the more common methods are :

I.   NORMAL PITCH DESIGN METHOD

This method states that the normal pressure angle at the reference diameter of the worm and the wheel cutter are equal for a given over-size value.

$$d_{p0} = d_{p1} + \Delta d_{p1}$$

$$\alpha_{n1} = \alpha_{n0}$$

This method also states that the worm and wheel cutter have an equal lead normal to the flanks at a reference diameter. This generates the system shown in Figure 2.20.
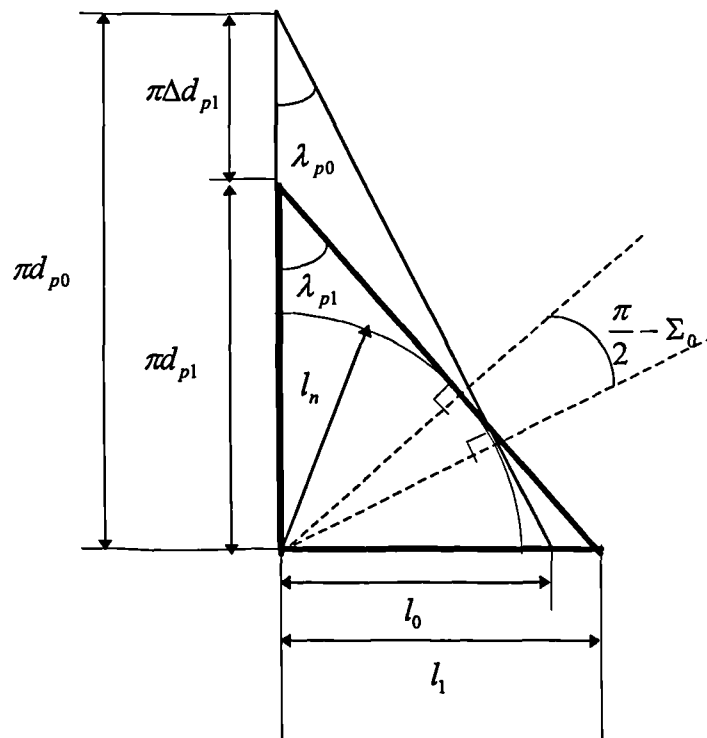
Figure 2.20 :   The diagrammatic representation of the relationship between the worm thread form and the respective wheel cutting tool helix at a reference diameter where Δd_{p1} is the oversize value.

The wheel cutter axis is inclined at an angle to the worm axis such that the lead (and therefore the pitch, p) is equal to that of the worm in a plane through the normal to the worm thread. A lead value for the wheel cutter must be found which satisfies this for the given over-size value. From the diagram it can be seen that :

$$l_n = \pi \cdot d_{p1} \cdot \sin \lambda_{p1} = \pi \cdot d_{p0} \cdot \sin \lambda_{p0}$$

The following relationships must then hold for the parameters :

$$\Sigma_0 = \lambda_{p0} - \lambda_{p1} + \frac{\pi}{2}$$

$$p_0 = \pi \cdot \left(d_{p1} + \Delta d_{p1} \right) \cdot \tan \left(\sin^{-1} \left(\frac{p_n}{\pi \cdot \left(d_{p1} + \Delta d_{p1} \right)} \right) \right)$$

II.   AXIAL PITCH DESIGN METHOD

The axial pitch method is similar to the normal pitch method. In this case the axial lead (and therefore pitch) is equal in both the worm and worm cutter for any over-size value.

$$d_{p0} = d_{p1} + \Delta d_{p1}$$

$$p_0 = p_1$$

III.   BASE PITCH DESIGN METHOD

The base pitch design method equates the lead/pitch of the worm and wheel cutter in the base diameter rack section.

$$p_1 \cos \alpha_{p1} = p_0 \cos \alpha_{p0}$$

The different methods generate distinct conditions of contact area and oil clearance. These also change over time as the parameters are modified when the cutting tool is re-sharpened. Design methods have often evolved based upon manufacturing strategy as well as contact conditions. Colbourne[20] states that the base pitch method can increase the life span of the wheel cutter. Ultimately it is for the gear set designer to choose both the most applicable design method and the values of the wheel cutter parameters which produce the optimum tooth form. Industrial sources state that any single method can not be expected to achieve this in every application.

2.4.4. Modified wheel tooth profile calculation.

Mismatch is achieved by varying several aspects of the wheel cutting process. The cutter profile can be changed either by designing the cutting tool from different parameters for the helicoid form (such as base cylinder diameter and lead), or by adding metal directly to the existing wheel cutter profile. Also, the generating process can be altered by inclining the wheel cutter axis relative to that of the worm.

The rack section model can still be used in the analysis of contact conditions in a mismatch gear set. The wheel cutter thread is generated in the same way as the worm about an axis. The cutter rack section co-ordinates are therefore not only subject to the axial displacement, u_0, but also a rotation of angle $\pi/2$-Σ_0. The linear displacement of the cutter profile, $(z_{r0} + u_0)$, equivalent to a cutter rotation is therefore not directed parallel to the axis. This implies that at the cutting point the associated cutter profile point is no longer at the initial rack section offset distance, x_{r0}, from the axial section. If values of x and z represent co-ordinates of a cutting point then :

$$x = x_{r0} \cos\left(\frac{\pi}{2} - \Sigma_0\right) + \left(z_{r0} + u_0\right) \sin\left(\frac{\pi}{2} - \Sigma_0\right)$$

$$z = x_{r0} \sin\left(\frac{\pi}{2} - \Sigma_0\right) + \left(z_{r0} + u_0\right) \cos\left(\frac{\pi}{2} - \Sigma_0\right)$$

41

Colbourne[20] derives equations which find the axial displacement of the tool for a given point on the cutter profile at an associated cutting point by relating the velocity components in the motion of the two contacting surfaces.

x_{r0}, y_{r0}, z_{r0} The wheel cutter thread co-ordinates.

n_{x0}, n_{y0}, n_{z0} The x, y, z axis components of the normal to the wheel cutter profile.

l_0 The lead of the wheel cutter thread.

z_0 The number of threads in the wheel cutting tool.

Δa The increment value for cutting centre distance.

$$u_0 = \left(\frac{1}{\cos\left(\frac{\pi}{2}-\Sigma_0\right)}\right)\left(\left(\frac{z_2 . l_{02} . n_{z0}}{2\pi z_0 . n_{y0}}\right) + x_{r0} \sin\left(\frac{\pi}{2}-\Sigma_0\right) + \left(\left((a+\Delta a)-y_{r0}\right)\left(\frac{n_{z0}\sin\left(\frac{\pi}{2}-\Sigma_0\right)-n_{z0}\cos\left(\frac{\pi}{2}-\Sigma_0\right)}{n_{y0}}\right)\right)\right) - z_{r0}$$

(11)

For rack section analysis, it is necessary to use these equations in an iterative process to find a profile point with a u_0 value which in turn gives wheel tooth co-ordinates with the same values of x as the x_{r1} values used for the worm rack sections. The wheel tooth profiles can then be compiled by relating the axial displacement at each point to the rotation of the wheel as described in section 2.3.3 :

$$\beta_2 = \frac{2.\pi.u_0.z_1}{z_2.l_0}$$

(12)

2.5.   CALCULATING MISMATCH CONTACT CHARACTERISTICS

2.5.1.   Gear tooth relief due to mismatch

The co-ordinates of the conjugate contact point in a rack section and the rack profile pressure angle at this point are found by using the equations defined by Buckingham[10] in section 2.3. The mismatch wheel profile co-ordinates are found using the theory described in the Colbourne[20] paper in section 2.4. By combining these two sets of theory a new calculation procedure has been developed through which it has been possible to determine and analyse contact conditions established by a given set of design parameters.

The first step in the calculation procedure is to establish the wheel tooth form generated by points on the cutting tool profile. The quantity of metal removed from the wheel tooth profile by a tool with mismatch design relative to the conjugate form is known as the *relief*. This is shown in Figure 2.21 for a single rack section.
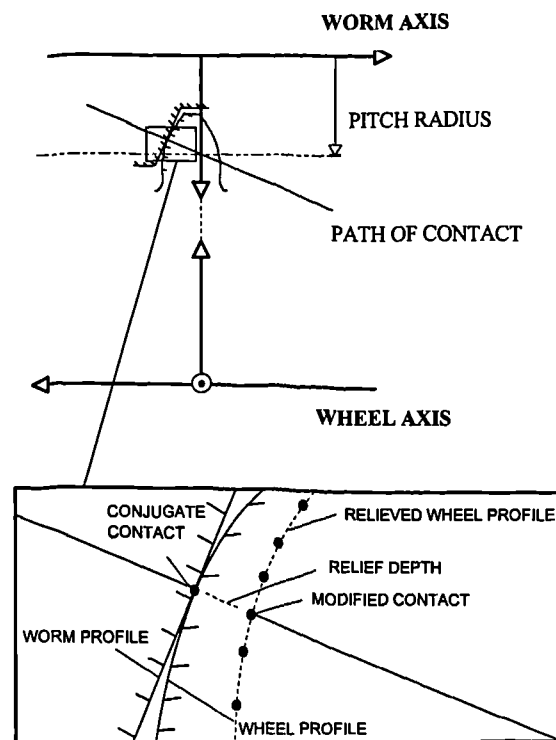
Figure 2.21 :   Wheel tooth relief in a rack section.

The calculations of gear tooth relief due to mismatch during the work presented in this thesis have used three assumptions :

- The change in path of contact due to mismatch is not significant in each rack section since the relief is small relative to the tooth surface curvature.

- Due to the relatively small scale of the modified profile, the length of the path of contact used to perform the analysis at any displacement position is short enough to be considered as a straight line projected at the rack pressure angle from the worm profile.

- The continuous tooth profiles can be represented by linear interpolation of the co-ordinates calculated for two adjacent wheel profile points without loss of accuracy given a density of at least four analysis points per millimetre of profile.

The first two assumptions have been used for gear analysis in previous research by Octrue[12] while working on load capacity. The close correlation of the theoretical and experimental results validated these assumptions. The third assumption was necessary to keep the calculations consistent whether using theoretically calculated or measured profiles. A more precise method is to find the exact modified contact point rather than interpolate between two adjacent points. This is possible for theoretical profiles which have a continuous profile, however this method could not be applied when using discrete profile co-ordinates produced by co-ordinate measuring machines. The effect can be minimised by calculating or measuring more profile points.

Discrete wheel tooth profile points can be calculated using the relation established by equations (11) and (12) in section 2.4.4. To determine a relief value in a rack section two consecutive wheel tooth analysis points, *P1* and *P2*, must be found which represent the part of the profile intersecting the path of contact. If such points exist on the wheel tooth profile, then by using the assumptions stated previously the relief calculation can be simplified as in Figure 2.22.
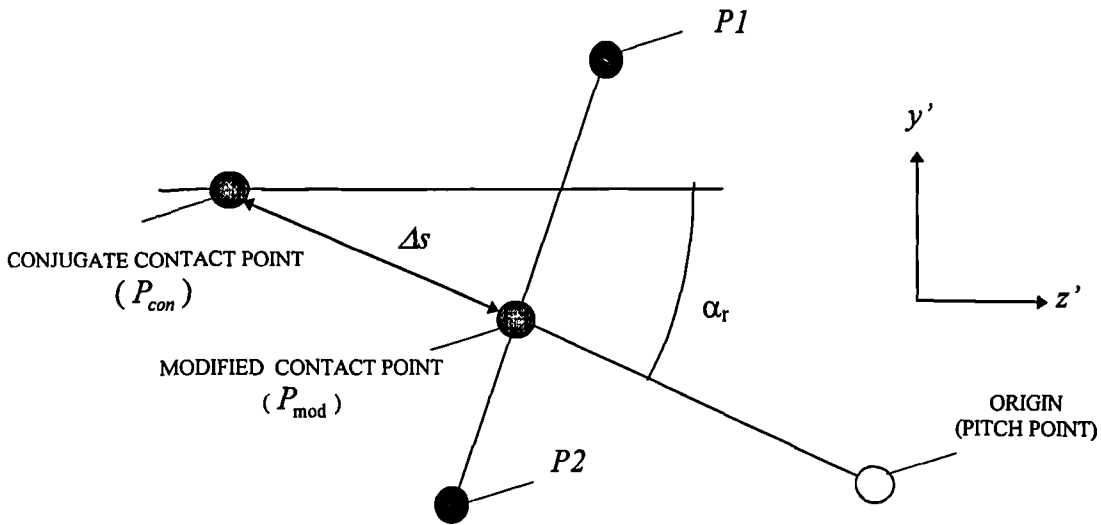
Figure 2.22:   Calculation of the relief value in a rack section.

Since the co-ordinates of the pitch point are also known, a temporary co-ordinate system is established using the pitch point as an origin. This has the relationship :

$$x' \Leftrightarrow x$$
$$z' \Leftrightarrow z \qquad (13)$$
$$y' \Leftrightarrow y - r_{p1}$$

From this simplified model the following relationships can be defined in the temporary co-ordinate system :

$$\tan \alpha_r = \frac{y'_{mod}}{z'_{mod}} \qquad (14)$$

$$y'_{mod} = y'1 + c(y'2 - y'1) \qquad (15)$$

$$z'_{mod} = z'1 + c(z'2 - z'1) \qquad (16)$$

$$\text{Where} \left[c = \frac{\overline{P1P_{mod}}}{\overline{P1P2}} \right]$$

CHAPTER 2

Substituting equations (15) and (16) into the relation in (14), c can be calculated :

$$c = \frac{y'1 - z'1\tan\alpha_r}{(y'1 - y'2) + (z'2 - z'1)\tan\alpha_r}$$

This value of 'c' can then be substituted back into equations (15) and (16) to obtain co-ordinates for the modified contact point. The modified tooth thickness due to the relief 'Δs' can now be calculated :

$$\Delta s = \sqrt{(y'_{mod} - y'_{con})^2 + (z'_{mod} - z'_{con})^2}$$

By compiling calculated relief values such as this at a series of displacements along the path of contact in each rack section, a map of relief due to mismatch can be generated for the gear tooth form. A *relief diagram* can be used to indicate a contour for any specified relief depth. This represents the boundary of points on the gear tooth with less than this specified depth of relief as shown in Figure 2.23. This technique can be used to examine the extent and position of the relief over the gear tooth and consequently where clearance is being created.
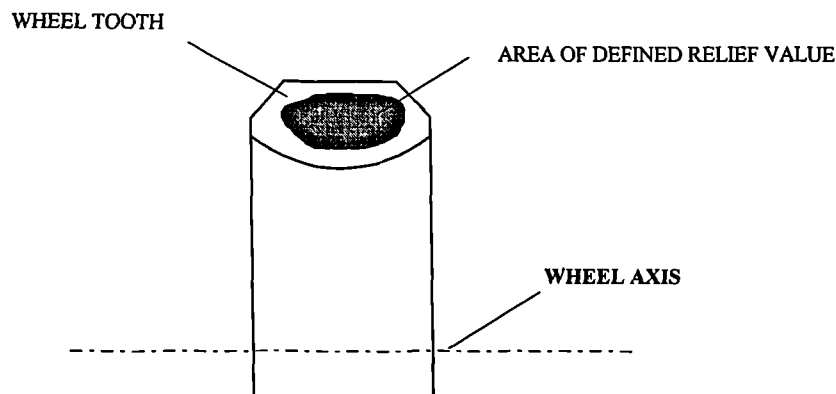
Figure 2.23 : An example of calculations for a single relief contour and bounded region at an arbitrary depth over a gear wheel tooth known as a relief diagram.

2.5.2. Transmission error

The relief generated by the mismatch modifies the wheel tooth profile and changes the point of contact in each rack section. This permits a linear shift of the worm profile along the worm axis, or an equivalent rotation in the wheel. The shift is calculated by first finding y_{mod} and z_{mod} from the y'_{mod} and z'_{mod} values defined in section 2.4.3 using the transformation in (13). Substituting the y_{mod} value into the worm rack profile equation gives an expected axial point of contact on the worm flank. The axial difference in position between this point and z_{mod} represents a linear *displacement error* as shown in Figure 2.24.
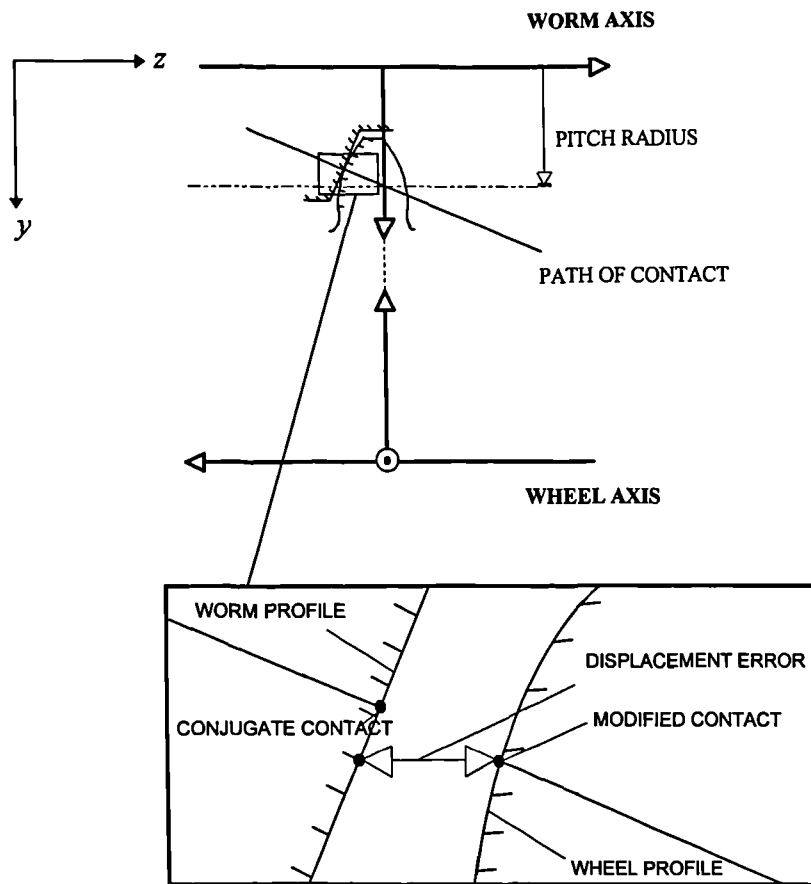
Figure 2.24 :   A diagram representing a displacement error in a single rack section.

The displacement error value can be determined in each rack section. The minimum value will cause contact between the flanks. This value is the *transmission error* and is defined as *the relative deviation in wheel position with respect to conjugate contact for a constant worm rotation*. This is usually expressed as a linear value at the pitch circle radius. Transmission error values are calculated at a series of positions through the meshing cycle. Plotting a series of error values against displacement position produces a transmission error graph for one tooth pair engagement as shown in Figure 2.25. Munro[25] states that by convention the transmission error is recorded relative to the driven direction, therefore wheel tooth rotation toward the worm thread caused by relief will create a negative transmission error.
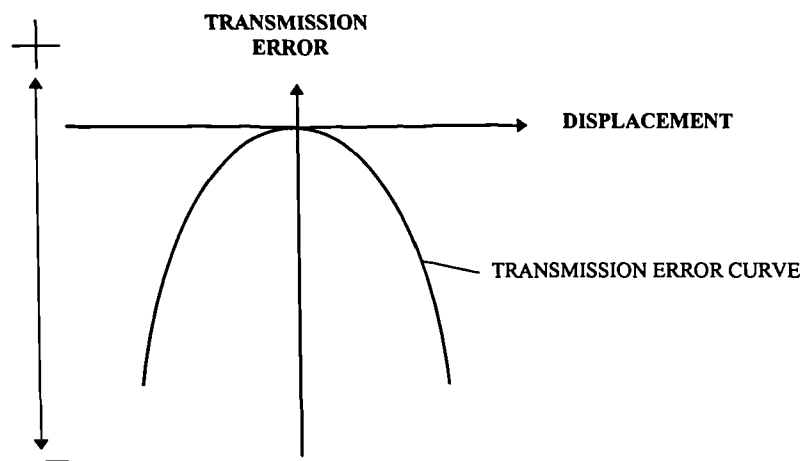
Figure 2.25 : Display convention for transmission error for a single engaging tooth pair.

In a theoretical contact condition each tooth pair will develop the same transmission error plot. These will by repeated at intervals equal to the worm thread or wheel tooth spacing. This interval spacing is the *pitch* value. The continuous transmission error curve, shown in Figure 2.26, is a result of the influence of adjacent tooth pair engagement as the worm is rotated. The transmission error at a point on this curve is determined by the minimum displacement error value calculable from all potential tooth pair engagements at each displacement position.
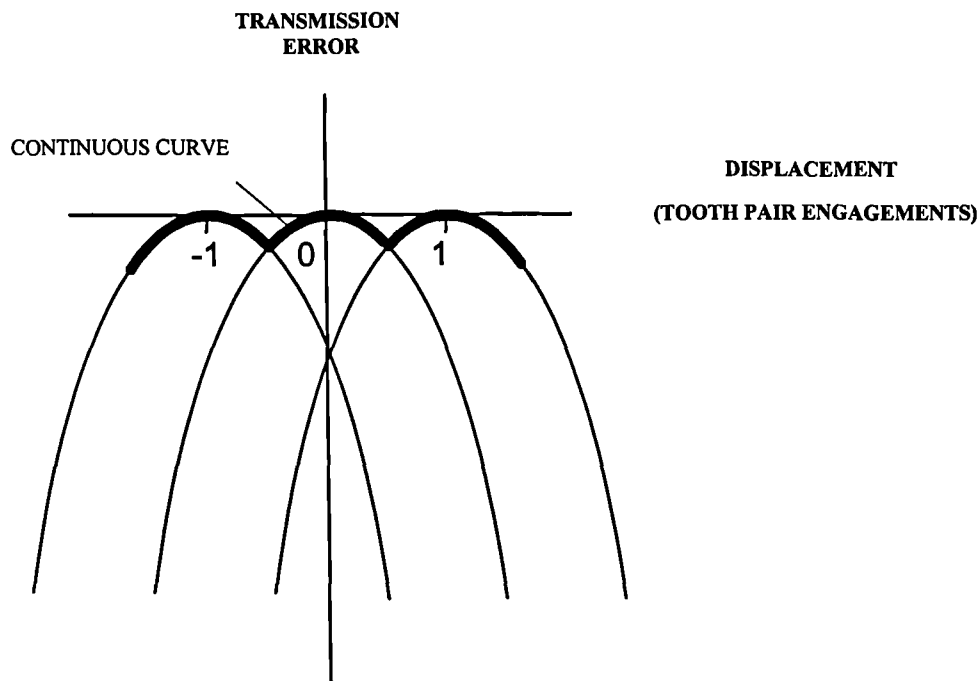
Figure 2.26 : Transmission error due to the transfer of contact between consecutive engaging tooth pairs.

2.5.3. Clearance between worm thread and wheel tooth flanks

Contact will occur in the rack section of the tooth pair engagement with the minimum displacement error value. To calculate flank clearance, the wheel position is first adjusted to that in which contact occurs. This point is determined by the transmission error calculations. For each contact point in a rack section, the gap between the worm thread and wheel tooth can be calculated at several positions. The gap value is the separation along the normal to the worm profile as shown in Figure 2.27, determined using the same method applied to the relief calculations in section 2.5.1.
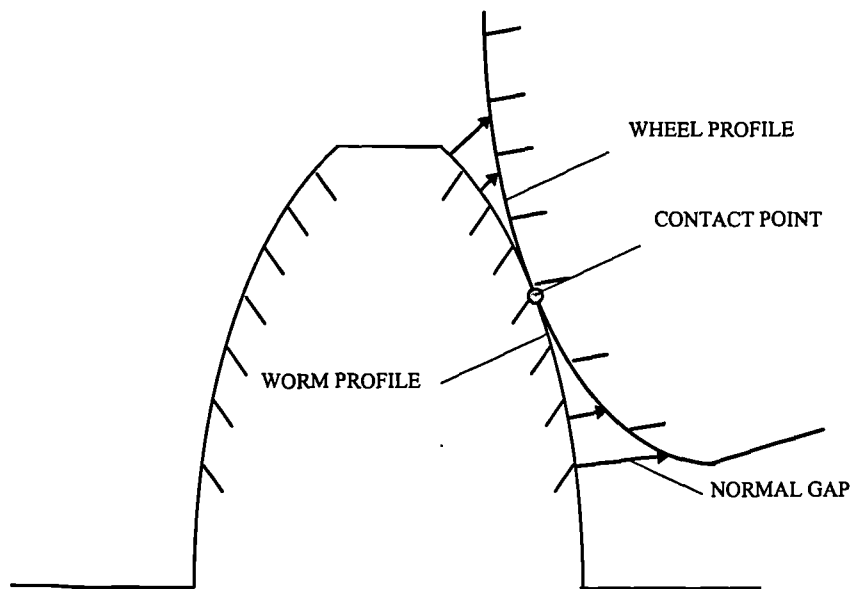
Figure 2.27 : An example of gap calculation over the full worm thread and wheel tooth profiles in a rack section at an arbitrary displacement.

All points on the wheel tooth profile which have less than a specified gap value can be determined. It is possible to repeat these calculations for the gap between the worm and wheel in all rack sections for a given displacement. Higher displacement error values in the other rack sections due to additional relief create an increased gap. This reduces the line of contact at any displacement position to a single *point contact* dependent upon the relief generated. The calculated gap region about the point of contact therefore no longer necessarily extends across the entire gear tooth face as in the conjugate case but exists over some area. An example of these features is shown in Figure 2.28.
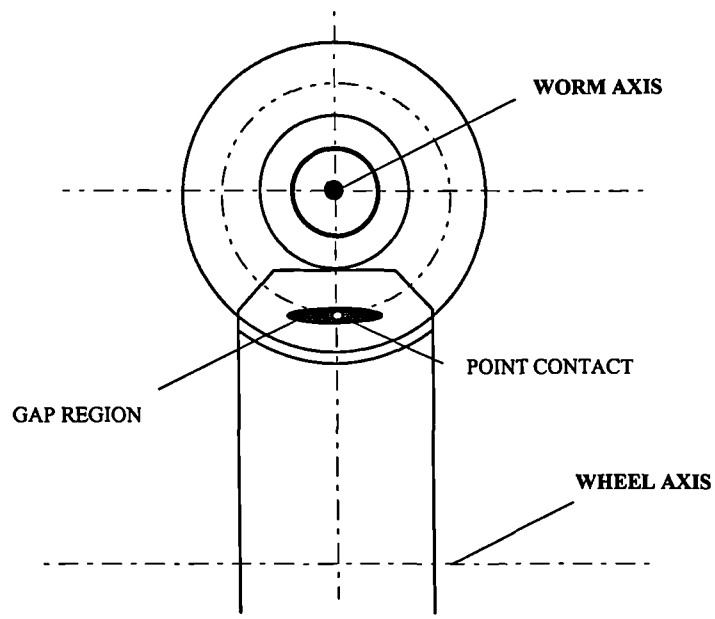
Figure 2.28 : An example of contact and maximum worm thread to wheel tooth gap of less than an arbitrary value at a single displacement due to mismatch parameters.

Repeating the calculations in all sections at a series of worm displacements during the meshing cycle builds a map of clearance over the gear tooth. The diagram in Figure 2.29 shows the contact point and a gap region calculation at 4 angular positions.
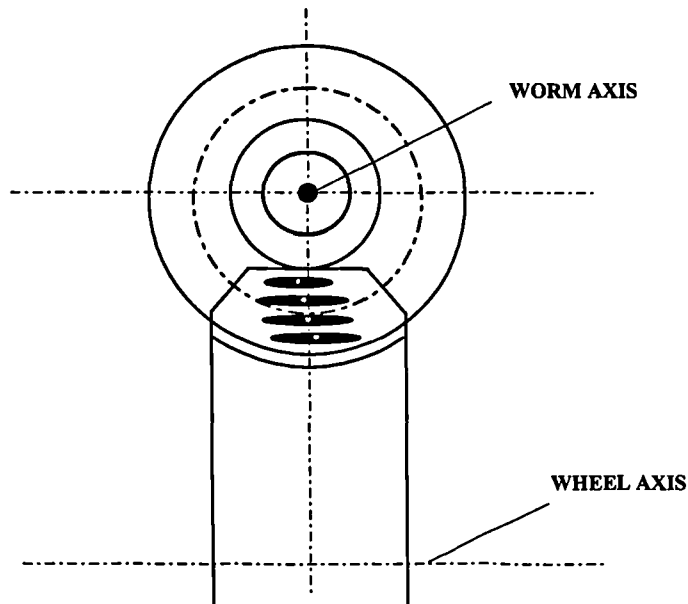
Figure 2.29 :   An example of contact points and gap calculations at a series of 4 displacements through the meshing cycle for a mismatch design.

If the displacement interval density is large enough, the compilation of gap calculations becomes an approximation of continuous contact. The information can then be used to produce a *clearance diagram* as in Figure 2.30.
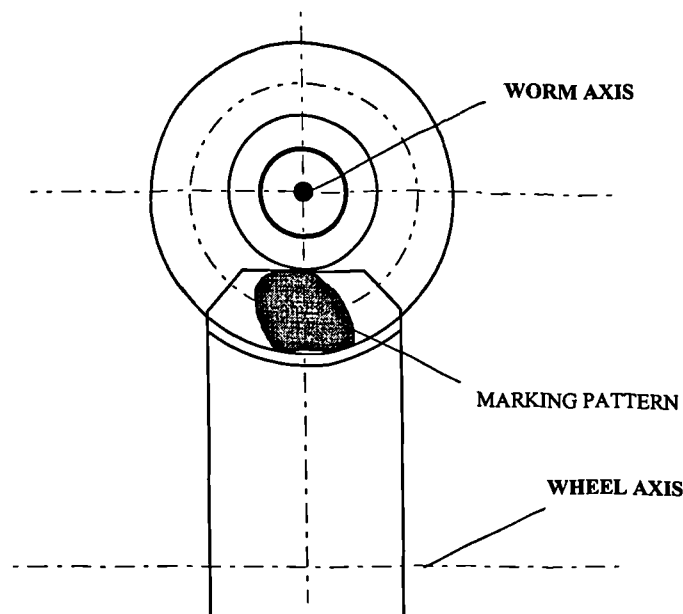
Figure 2.30 :   An example of a clearance diagram resulting from gap calculations at a series of displacements through the meshing cycle for a mismatch design simulating the contact marking pattern.

A maximum gap of approximately 10-15μm represents marking blue ink thickness. Any gap less than this value will theoretically permit one profile to be marked by ink transfer from the other. By identifying all of the positions on the profiles which satisfy this condition during the meshing cycle, the resulting clearance diagram simulates the *marking* or *bearing test*, often used in industry to examine contact conditions in manufactured gear sets.

The clearance diagrams resemble the relief diagrams to a large extent but they are different in one important respect. The gap calculations consider the transmission error in the gear tooth form and the contact of consecutive tooth pairs. The resulting marking pattern simulation will therefore be different as contact will not be maintained through the complete meshing cycle of a single tooth pair.

2.6. SUMMARY

A worm gear design is dependent upon selecting the designation based upon the application, load capacity, and efficiency. Though the geometrical principles are well known, these are largely skills learned through empirical research and development methods. It has therefore been impossible to record or report any distinct unique design routine during this chapter.

The conjugate gear set has characteristics of full face contact and no transmission error. A conjugate design does not allow for oil lubrication of the surfaces which affects the performance of the gear set while operating under a torque load. The wheel cutting tool has deliberately modified worm geometry to induce relief on areas of the wheel tooth relative to the conjugate form. The relief imposed on a wheel tooth form has a direct effect on the transmission error and contact marking pattern. The design must also define the correct mismatch parameters needed to induce a contact pattern appropriate for the intended application. It is critical to allow lubrication of the contacting surfaces while maintaining a substantial contact area.

Studies by Buckingham have identified the basis of development for several cases of worm gear geometry and shown the relationship of specific design parameters to the final thread profile. Further studies by Colbourne have derived equations which can be used to generate wheel tooth profiles using mismatched design parameters for the wheel cutter. By combining this work it is possible to model the effect of mismatch parameter variation on gear tooth form generation in the form of a relief diagram.

This has been taken further to develop calculations of continuous contact through the meshing cycle to derive the characteristics of transmission error and marking pattern. To better simulate the contact characteristics, these calculations must consider the influence of all the possible tooth pair engagements in the analysis model. This fact has been generally overlooked during previous analyses.

3. SOURCES OF CONTACT ERROR IN A WORM GEAR SYSTEM

3.1. INTRODUCTION

Developments in co-ordinate measuring machine technology since the 1980's have allowed component geometry to be inspected consistently to an accuracy of approximately 2-3µm[45]. This has enabled an investigation of the worm gear production process to be carried out. This chapter identifies sources of manufacturing error, and describes the methods used to record them.

A case study has recorded measurements for two sample gear sets in order to quantify and assess the influence of these error sources on contact conditions. Development of the theoretical equations established in Chapter 2 is described which has permitted such measurements to be used in the contact analysis in order to improve the accuracy of the model. This represents a new and unique aspect to worm gear contact analysis.

The theoretical contact conditions are subject to modification from the various error sources during production. Additional contact error sources from assembly and flank deformation due to a transmitted load have been identified. Further development of the theoretical analysis has allowed these aspects be included in the contact analysis in order to fully synthesise tooth pair engagement and improve the accuracy of the model. This also represents a new and unique aspect to worm gear contact analysis.

3.2. ERROR SOURCES FROM COMPONENT MANUFACTURE

3.2.1. Worm lead errors

These errors are a measure of the consistency of the rate of feed in the machine used to manufacture the worm and affect the required helical form of the component. The probe is set at a reference diameter and the associated lead angle as in Figure 3.1 The worm rotation and the linear feed of the probe parallel to the axis are then fixed relative to the lead value. During the translation of the probe, any deviations from the correct helix are recorded and indicate variations in lead. At each point of contact these lead errors are equivalent to an additional displacement Δu_l of the worm profile. They therefore contribute significantly to the transmission error measurement. While using these errors in calculations of contact conditions, it is important to know the interval of thread over which traces were obtained in order to relate the correct error value with the appropriate flank position.
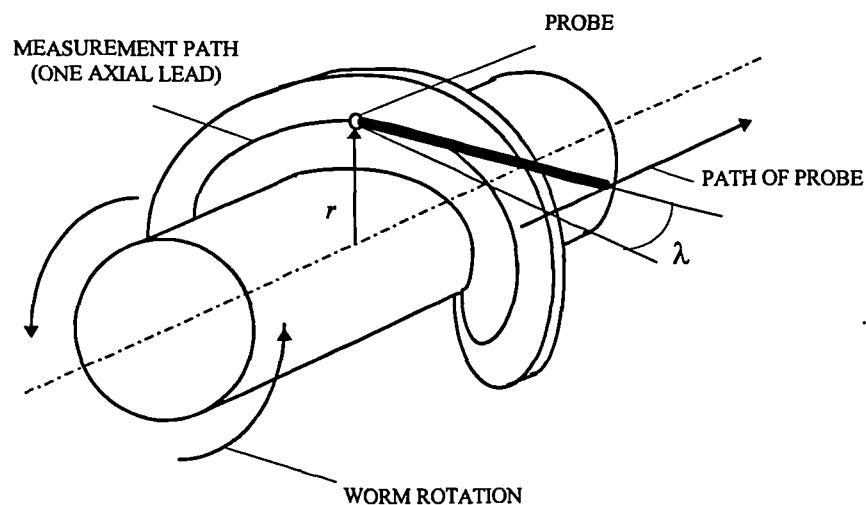
Figure 3.1 :   A diagram showing the probe setting during helical lead measurement.

Two worms of identical design were manufactured. The traces in Figure 3.2 show the results of lead error tests for these worms over exactly four axial tooth pitches. These are up to $12\mu m$ (0.0004") in magnitude and are similar in both flanks, and on both worms. This indicates that significant errors exist as a part of the manufacturing process due to the condition of the machine producing the components.

FLANK A   FLANK B   FLANK A   FLANK B
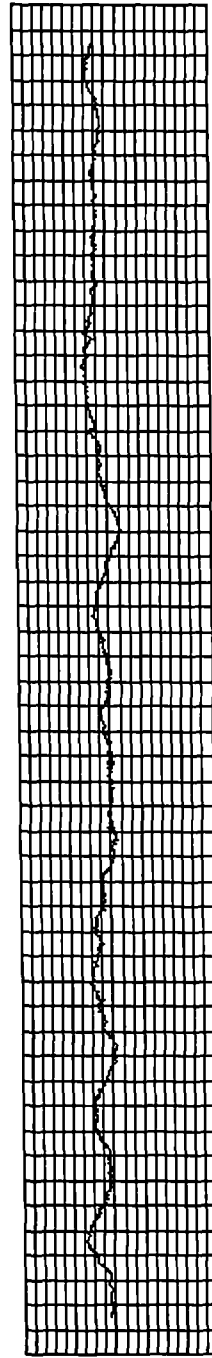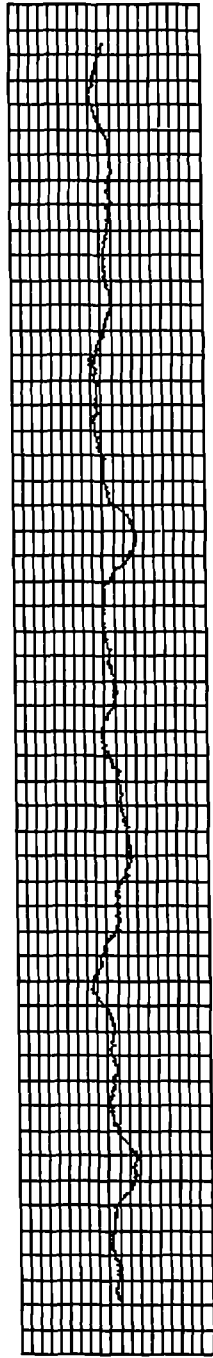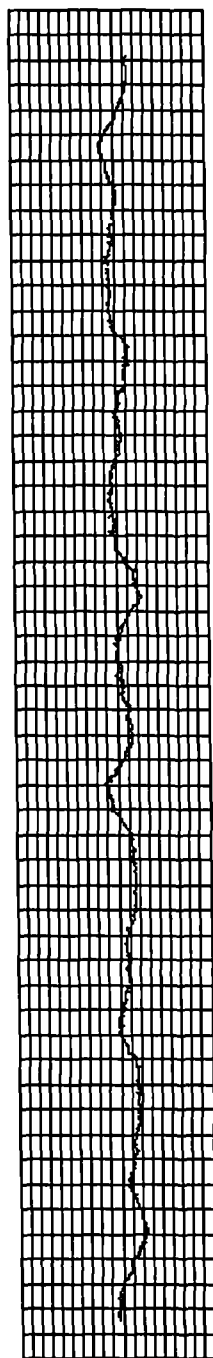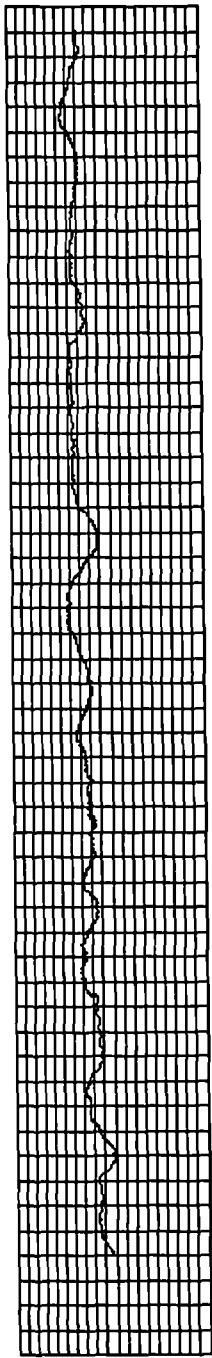
2.5μm   2.5μm   2.5μm   2.5μm

- METAL +   - METAL +   - METAL +   - METAL +

WORM 1   WORM 2

Figure 3.2 :   An example of measured worm lead errors for both flanks of two
                sample worms.

3.2.2. Worm profile errors

Helicoid geometry is based upon a straight line generator, represented by the generatrix described in Chapter 2. For the screw helicoid case this is in the axial plane, while for involute helicoid this is found in a rack section offset by the base cylinder radius. The worm thread form can therefore be easily generated by using a flat sided grinding wheel at the generator angle, γ, in the appropriate plane.

It is possible to record the variation of the helicoid worm thread profile by moving a probe over the thread between the tip and root using the generator line as a reference path. The involute helicoid measurement is shown in Figure 3.3 which also shows the required base lead angle setting of the probe in order to follow the straight line generator path.
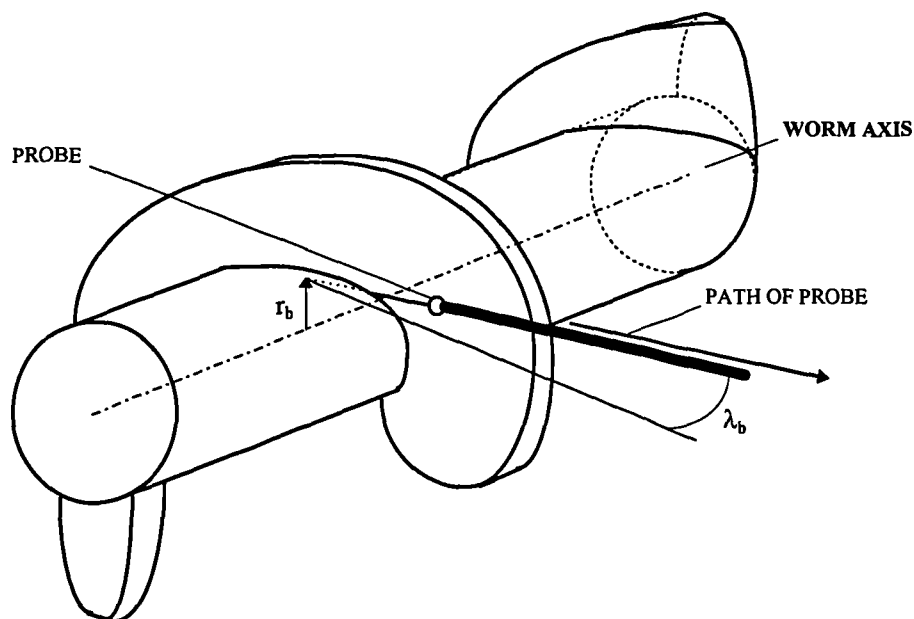
Figure 3.3 : A diagram showing the probe path during involute helicoid profile measurement.

Deviations from the straight line profile are recorded by the probe and represent the profile errors. Unlike the lead, these errors do not indicate problems with the machine but errors in the grinding wheel profile and setting relative to the flank. They can therefore be improved or even used to change the contact by modifying the grinding wheel settings.

The profiles of the flanks of the two worms described in section 3.2.1 were measured and the results are shown in Figure 3.4. These measurements show that the profiles of the worms are finished to within 1-2μm (0.00005") of the design profile, though this increased to 4μm (0.00015") toward the root of the Flank A in both cases. This degree of accuracy is possible due to the ease in controlling the straight line generator. These can be used in a contact calculation by direct substitution for theoretical worm profiles. The impact will be dependent upon the magnitude of the errors.
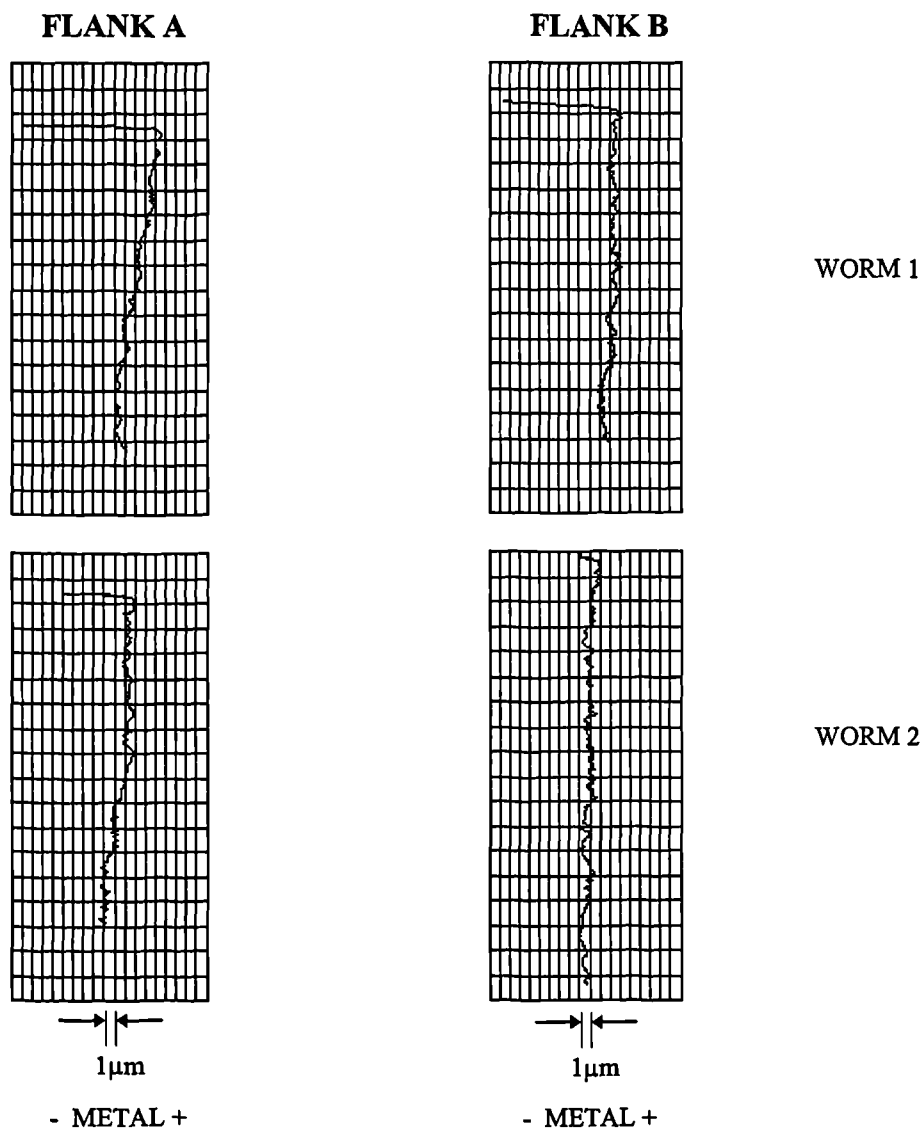
Figure 3.4 :   An example of measured worm profile errors for two sample worms.

3.2.3. Wheel cutter profile errors

The wheel cutting tool is itself a worm thread and can therefore be measured using the same techniques as in section 3.2.1 and 3.2.2. An alternative was to measure the profile co-ordinates digitally using a CNC machine tool. The digital measurements produced by the machine tool were stored on computer disk. These co-ordinates could be substituted directly for theoretical profiles to calculate a synthesised wheel tooth form.

Digital measurements of both cutting profiles of a conjugate wheel cutter manufactured using a standard cutter grinder machine are shown in Figure 3.5. These show significant errors of 5-10μm in some points on the profile.

Further tests were performed to investigate the sensitivity and repeatability of the machine tool measurements. Figure 3.6 shows the comparison of a wheel cutter profile errors measured using 50, 125, and 200 sample points along each profile. This shows that measurements using the CNC machine tool are repeatable to within 3μm, and that there is little detail excluded from the profile by using only 50 sample points along the cutter profile. The rogue measurement value indicating a 10μm error at the tip of one flank of the cutter is due to dirt on the profile which was removed for subsequent measurement cycles.

The majority of standard cutting tools are cut on cutter grinder equipment. Recent advances in CNC machine tool technology have allowed the cutting profile to be manufactured to an accuracy of around 2μm. The graph in Figure 3.7 shows the difference in profile error in two cutters of identical geometry cut using a standard cutter grinder and a CNC controlled grinding machine.
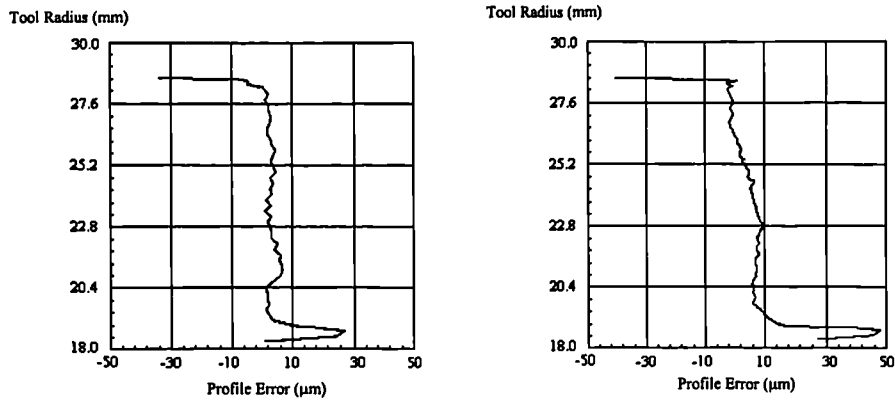
Figure 3.5 :   An example of measured wheel cutting tool profile error.
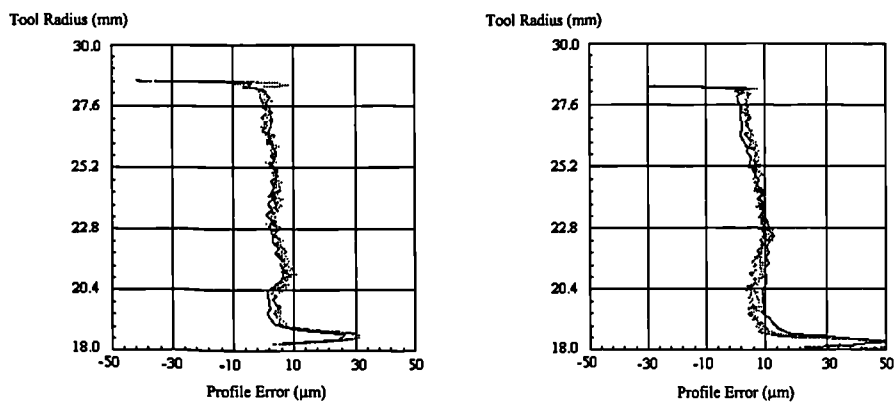
Figure 3.6 :   Examples of measured wheel cutting tool profile error for both flanks using 50, 125, and 200 sample points.
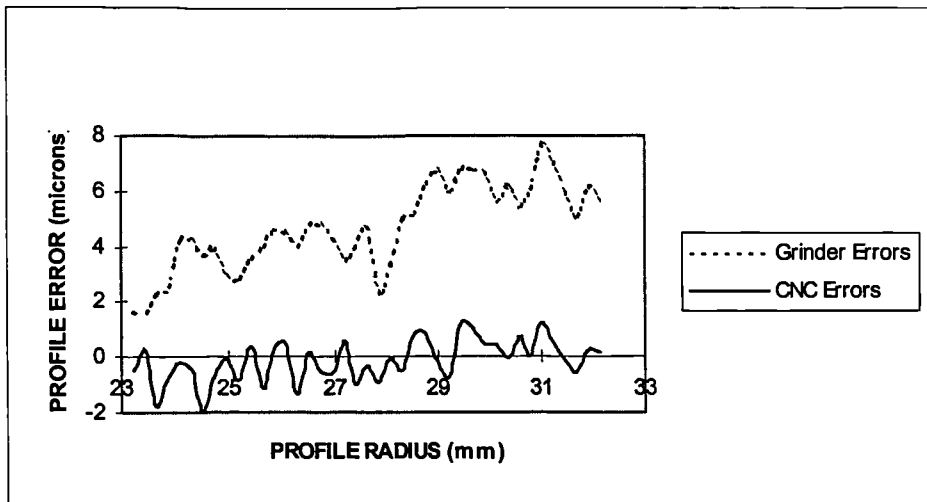
Figure 3.7 :   A plot of profile errors from gear cutting tools produced using a standard cutter grinder machine and a CNC machine tool.

3.2.4. Wheel tooth profile errors

Measurements of the wheel tooth profiles in axial and rack sections were recorded for two sample wheels. These profiles are in planes transverse to the wheel axis, as shown in Figure 3.8. Measurement of the profiles show the error in the generated wheel tooth form relative to a conjugate profile. Any deviations represent the relief for the section due to mismatch and manufacturing error.
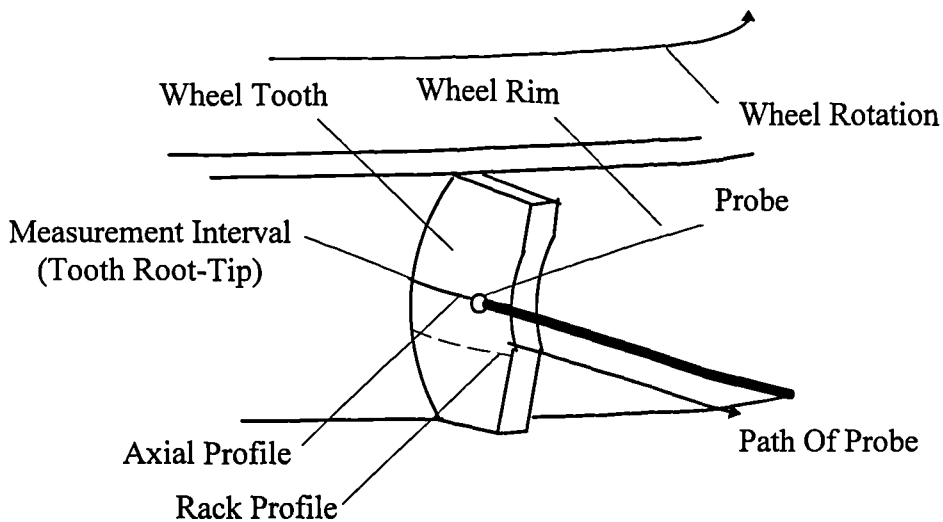
Figure 3.8 :   A diagram showing the probe path during the measurement of wheel tooth profiles.

Figure 3.9 shows a comparison of the conjugate wheel cutter profile errors as shown in section 3.2.3. and the profile errors measured in the axial section of the associated wheel tooth. This indicates that trends in cutter error position and magnitude are replicated in the wheel tooth form.

The measured profile errors are around 7-10µm which represents a significant influence on a conjugate wheel tooth contact. These errors act as relief which will automatically affect transmission error. They are also of a similar magnitude to the marking ink thickness and will therefore affect the contact marking of the tooth flank.
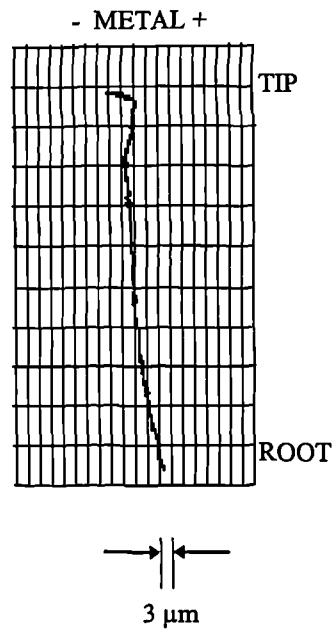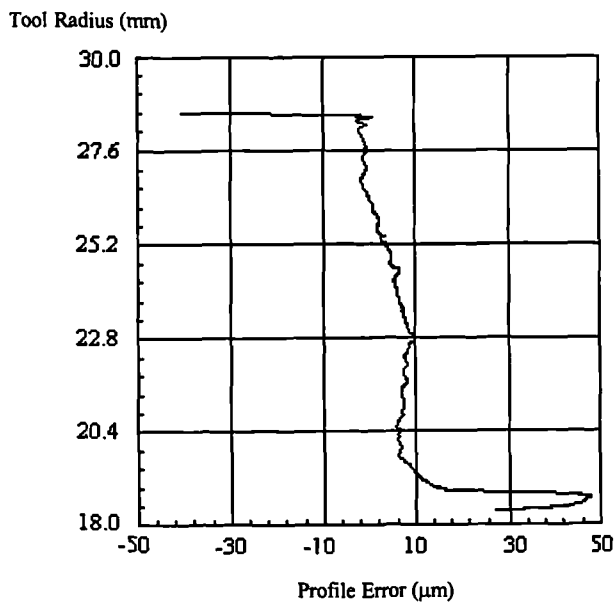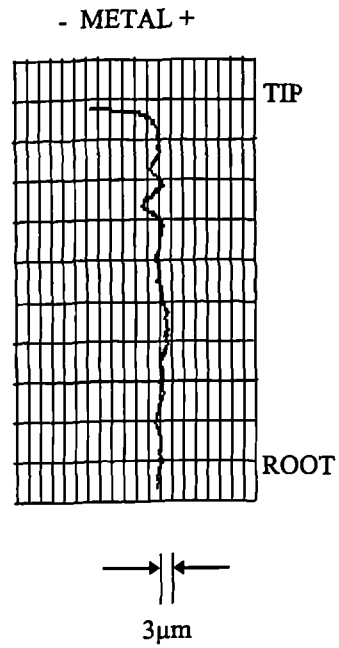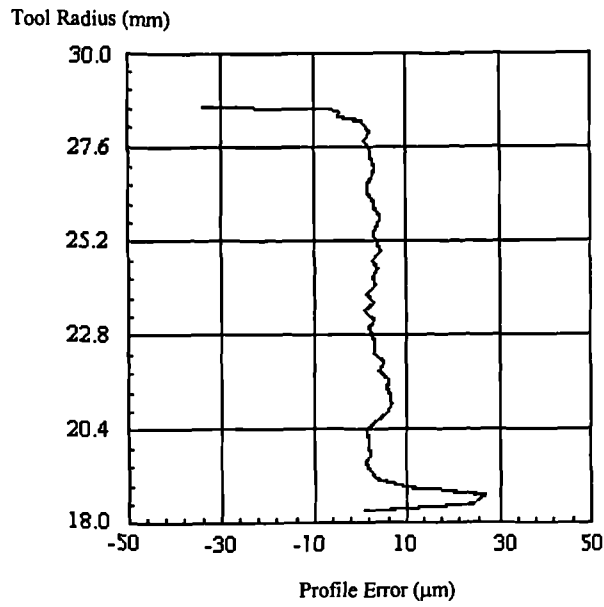
Figure 3.9 : A comparison of measured wheel cutting tool profile and wheel tooth profile errors.

Synthesised wheel tooth profiles were calculated using 50 points sampled along the 10.6mm depth of cutter profile equating to a point density of around 4-5 points/mm. The diagrams in Figure 3.10 show a comparison of synthesised and measured profile errors in the axial section for a sample wheel cut by the tool measured in section 3.2.3.
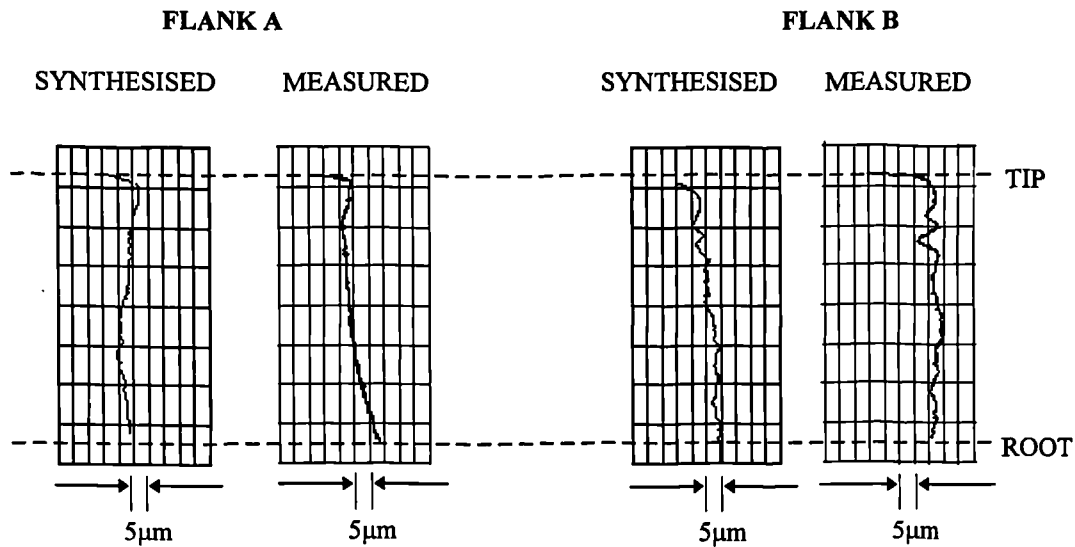
Figure 3.10 : Examples of synthesised and measured wheel tooth profile errors in an axial section.

Comparisons of synthesised and measured profile errors were also made in other transverse wheel planes using the same point density. The graphs in Figure 3.11 show comparisons of calculated and measured profile error in four other rack sections for this sample wheel at offset values of -14mm, -8mm, 8mm, and 14mm. The same profiles were measured for a second sample wheel tooth form which included mismatch parameters. The profiles of the associated cutting tool was manufactured were also measured. The graphs in Figure 3.12 show the resulting theoretical, synthesised and measured profiles in the axial plane for this sample. The theoretical calculations indicate that there is relief in this wheel tooth form design caused by the mismatch parameters. Considering that the measuring machines used had an accuracy of 3-5μm which could induce additional slope in the profile measurements, the relief in the measured profiles is generally well replicated in the synthesised profiles. These results show that it is possible to calculate the wheel tooth form using measured wheel cutter profiles to within 2-3μm.
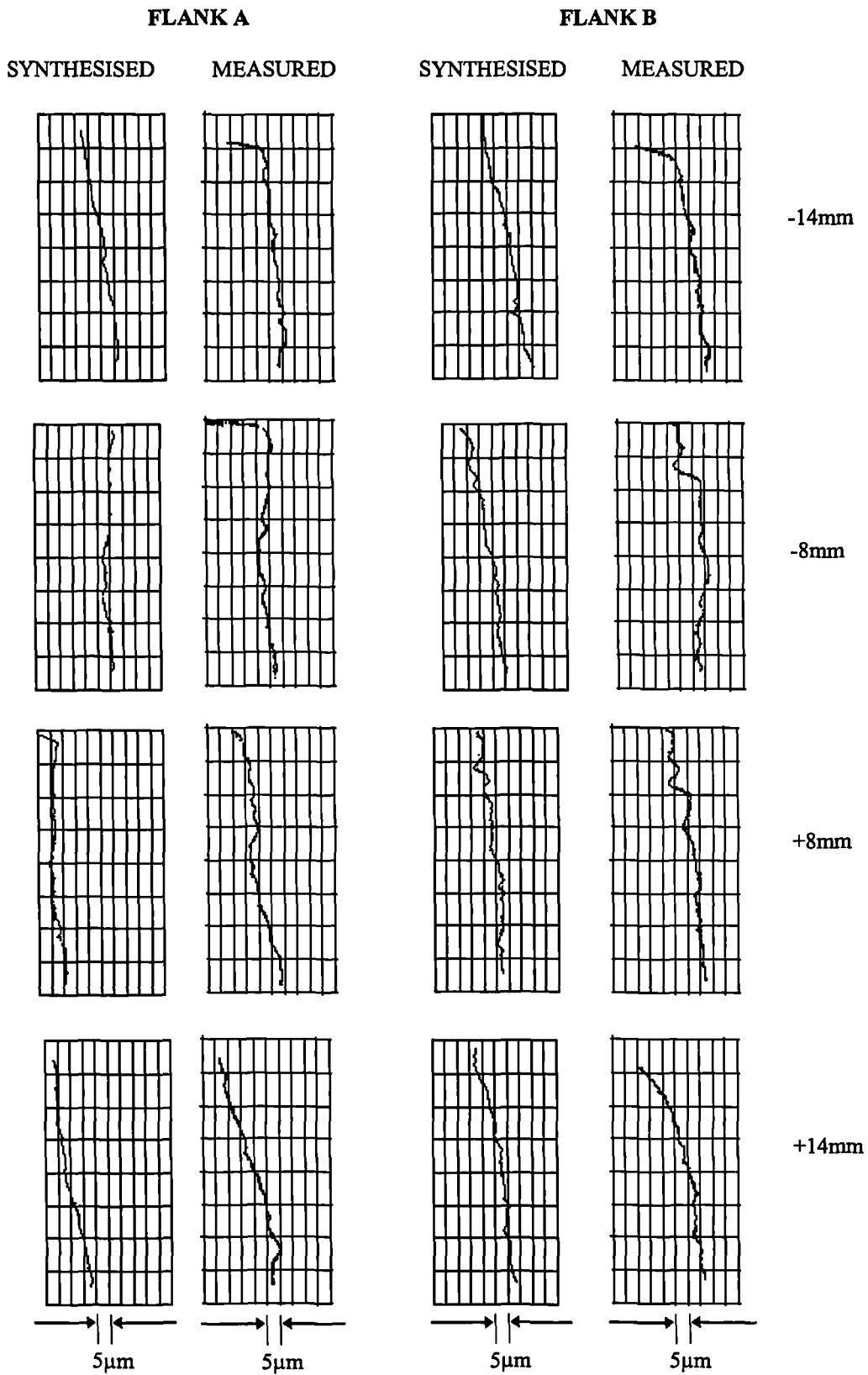
Figure 3.11 : A comparison of synthesised and measured wheel tooth profiles at several centre height displacements.

FLANK A   **FLANK B**
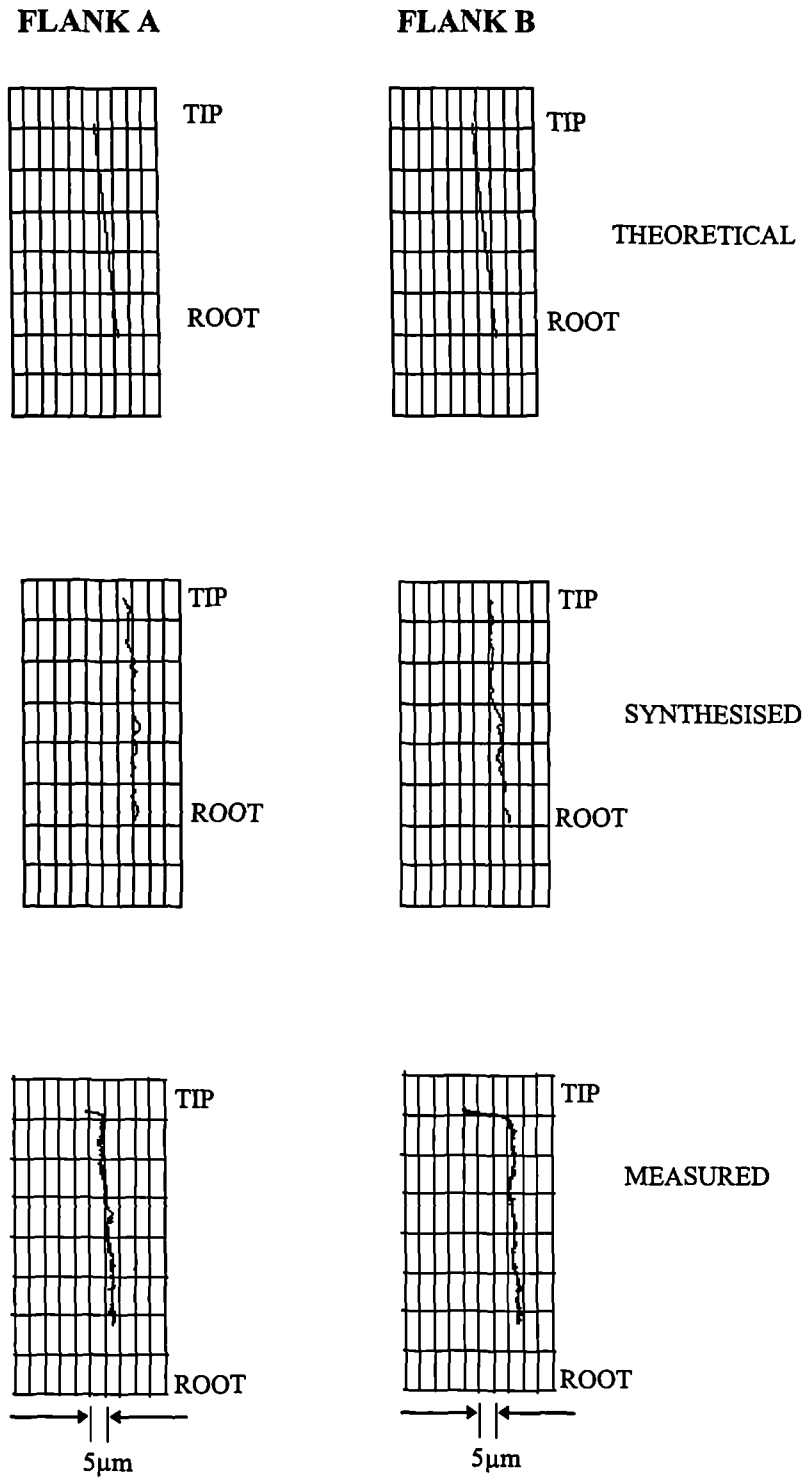
Figure 3.12 :   A comparison of theoretical, synthesised and measured profile errors in the axial profile of a sample mismatch design wheel.

3.2.5. Wheel tooth pitch errors

These errors are a measure of the kinematic accuracy of the hobbing machine in the consistency of the rate of feed of the cutting tool and the relative rotation of the hob and wheel blank. This implies that they are similar to the lead errors in that they depend upon the condition of the machine producing the component.

The diagram in Figure 3.13 shows the measurement procedure for recording the consistency of spacing between wheel teeth. The probe is fed and retracted radially to a reference diameter of the gear wheel once every tooth pitch over a full gear revolution. The deflection caused by the metal surface is recorded.

The data is checked for errors in two ways, the tooth to tooth spacing which represents the difference between consecutive teeth, and the cumulative error which refers to the error relative to a datum tooth flank. Examples of measured error of this kind are shown in Figure 3.14 for tooth to tooth and cumulative error in a 50 tooth gear wheel.

The wheel errors can contribute substantially to the transmission error value. These errors represents a direct addition to the displacement error calculation as $\Delta\beta_2$, and therefore cause premature or late engagement of a worm thread and wheel tooth inducing tip contact and excessive transmission error readings. In severe cases this may lead to vibration and shock loading problems during operation. An even distribution of the teeth, shown by the cumulative pitch, is important to reduce this effect but it is crucial to minimise the tooth to tooth error since severe differentials between consecutive engagements will accentuate the problem.
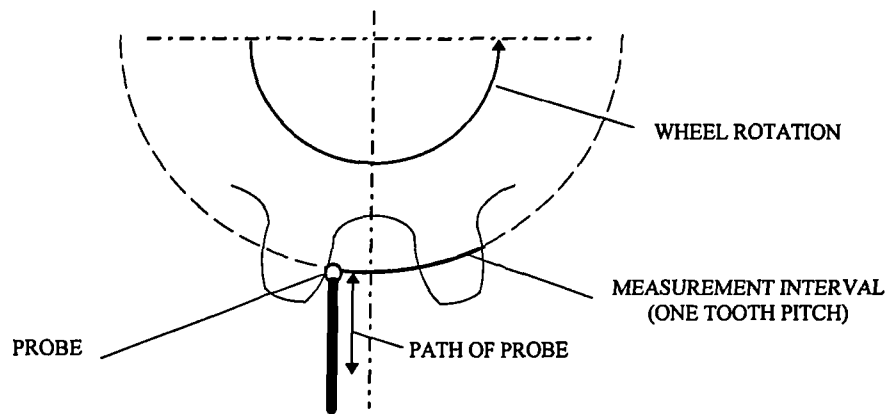
Figure 3.13 : The probe path of during involute helicoid wheel tooth pitch measurement.
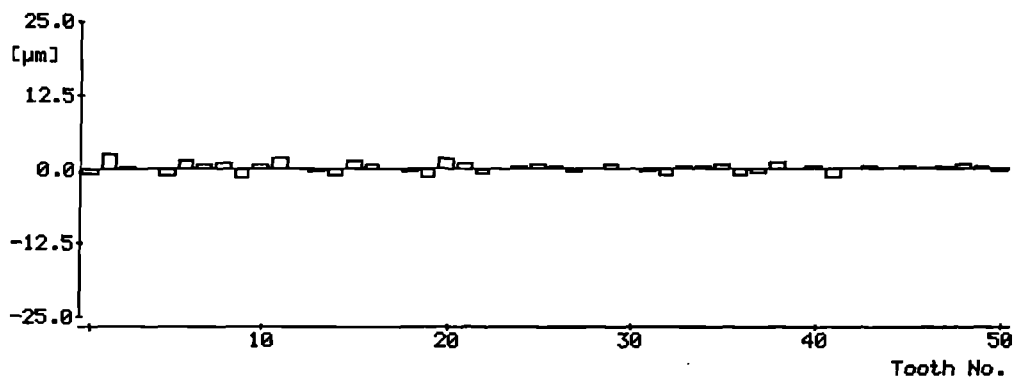
TOOTH TO TOOTH PITCH ERROR
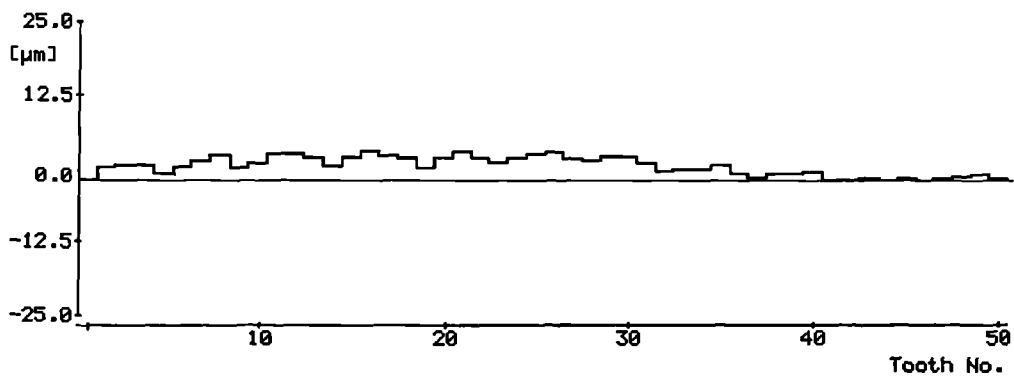
CUMULATIVE PITCH ERROR

Figure 3.14 : An example of measured wheel pitch errors for a single flank using a sample wheel with 50 teeth.

3.3.   ERROR DUE TO DISPLACEMENT OF THE GEAR SET AXES

The position of the gear set can change the relative relief due to profile modification in the equations of each rack section during contact analysis. The calculations of contact characteristics are therefore directly affected.

Changes in centre distance and height are due to manufacturing tolerances between surfaces of the worm gear box and affect the values of centre distance by Δa, and rack section offset by Δx when used in the contact analysis model. Eccentricity occurs in the components and is due to the misalignment of the shaft during machining. Eccentricity of the wheel causes a sinusoidal error in centre distance over a period of one wheel revolution, while that of the worm creates a cyclic variation in both centre distance and centre height increment value but are 90° out of phase. These alignment effects are additive and are defined in Figure 3.15.
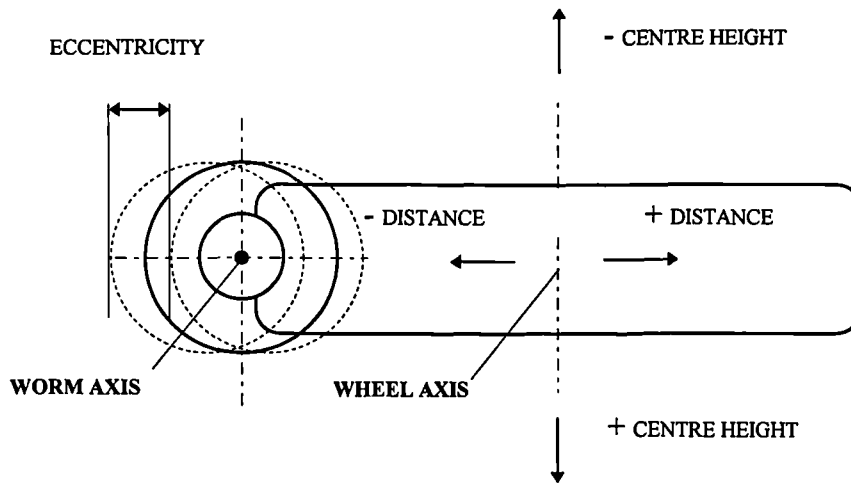
Figure 3.15 :   The definition of axial displacements for a worm gear system.

Values of 25μm for centre distance and height error, and 2-3μm for eccentricity are used by industrial collaborators for high precision applications. The effects for a specific assembly can be monitored by mounting probes against reference surfaces.

The effect of misalignment can be included in the model of contact conditions. This model can also be used to assess the effect on contact of further alignment changes which occur under load due to deflections of the shaft axis in the bearings.

3.4. ERROR SOURCES DUE TO AN OPERATING LOAD

3.4.1. Worm thread and wheel tooth bending

The torque load transmitted by a gear system imparts a force at the contact point. The rack section analysis system acts as a series of cantilever beams to resist this force. This leads to a bending of the worm thread and wheel tooth as shown in figure 3.16.
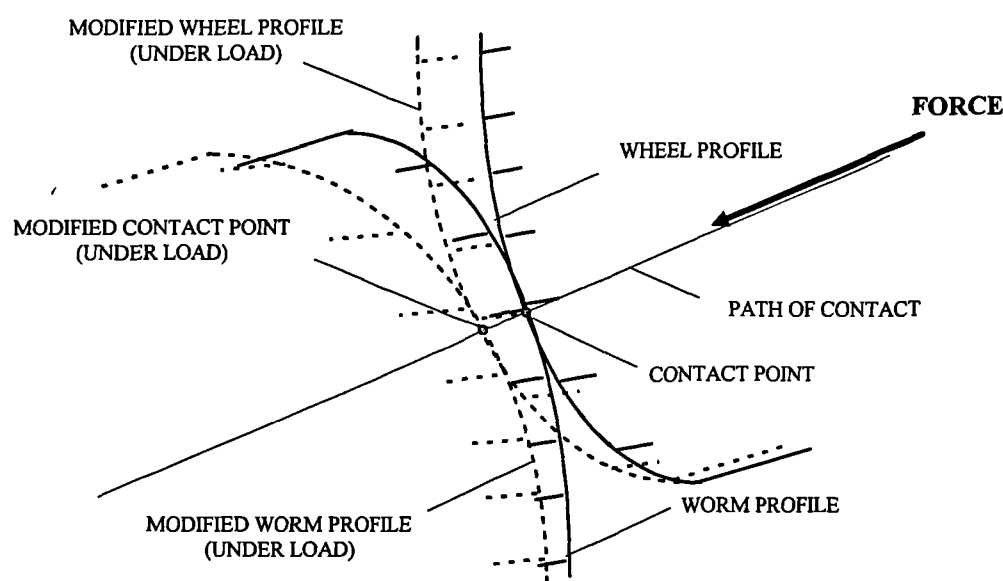
Figure 3.16 : A diagram showing the change in contact in a rack section due to bending under torque load considered when calculating transmission error.

This diagram also shows that the new contact point along the path of contact represents a shift in wheel position equivalent to a rotation. This contributes directly to the transmission error calculation. Further, the bending will reduce the displacement error value in adjacent tooth pair engagements. If the load is sufficient then the bending effect may reduce the displacement error to zero and allow contact. As a result of the contact occurring there will be a contribution to the load resistance.

If the under lying changes in transmission error through the tooth engagement cycle can be said to be analogous to an AC electrical signal then the change in mean value due to deformation represents a DC shift, as described by Munro[59].

3.4.2. Worm thread and wheel tooth compression

The diagram in Figure 3.17 shows the effect of a Hertzian compression on the contacting surfaces in a rack section due to a torque load. The extent of the compression is greatly exaggerated in this diagram, however this does demonstrate how the effect modifies the contact point and influences the transmission error value.
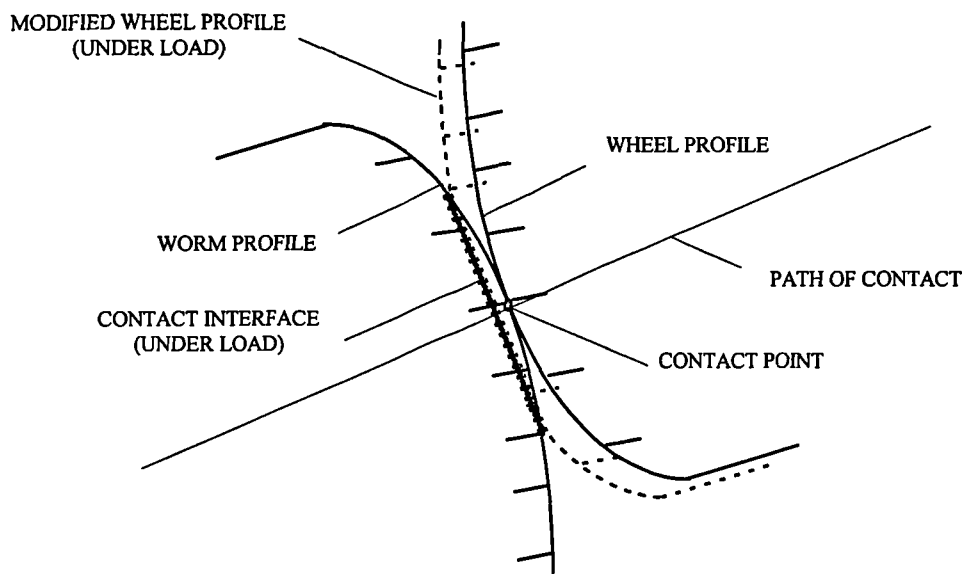
Figure 3.17 : A diagram showing the change in contact in a rack section due to tooth compression under torque load considered when calculating transmission error.

As in section 3.4.1., if the load is high enough then this effect may become greater than the relief value in rack sections other than that which is used to establish the contact point. As a result of the contact occurring in this case there will be a contribution to the load resistance from such sections.

Again, the resulting change in mean transmission error value due to deformation represents a DC shift as described by Munro[59]. Surface compression is also important when considering lubrication as it influences the entrainment of oil. Work by Dyson, Evans & Snidle[60] has produced formulae which can be used in association with clearance calculations to investigate the effect of mismatch parameters on oil film formation during gear set operation.

3.4.3. Modelling deformation under load

3.4.3.1. The linear stiffness model

The linear stiffness model uses a single constant value per unit facewidth, k, as a combined stiffness value for both the worm and wheel material when calculating total deformation under load. The model divides the worm thread and wheel tooth into thin slices across the facewidth using rack sections of equal width δb. These slices act as a series of independent springs of stiffness k which are cropped by the relief value, Δs, calculated for the slice using the theory in section 2.5.1. At any specified position during the engagement cycle, the springs are considered to be compressed by the applied load. It can be seen in Figure 3.18 that the rack section will make no contribution to the resistance of the load unless the compression value is at least equal to the relief value. A compression value, e_{dc}, is sought iteratively to equate the applied force, F, generated by the torque load, to the resistive force in the spring system.
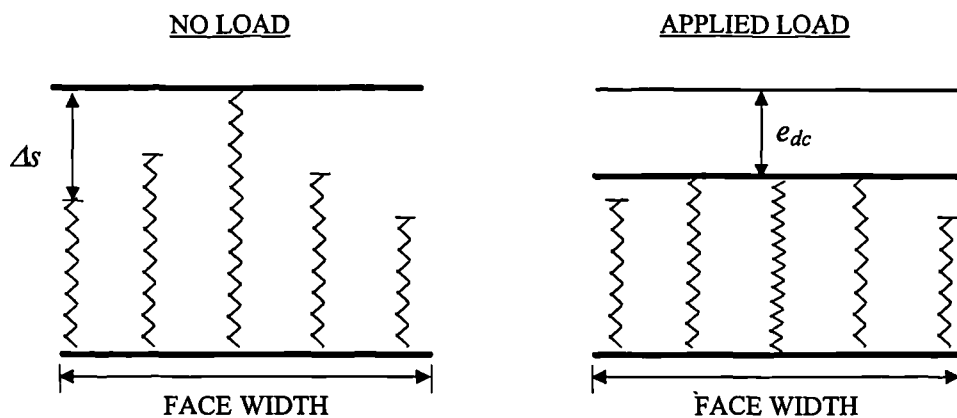
Figure 3.18 : A diagram showing the thin slice model before and during an applied torque load for calculating transmission error due to tooth deformation using five slices.

In making these calculations two important points must be considered. The first is that the force in each slice acts at the rack pressure angle and therefore the tangential component must be determined. The second is that the deformation permits engagement from more than one thread and wheel pair.

If there are N rack sections which can contribute to the load after considering all possible tooth pair engagements then the linear stiffness model involves finding a solution to the following equation :

$$F = k\delta b \sum_{i=1}^{N} (e_{dc} - \Delta s_i) \cos \alpha_{r_i} \qquad \forall \Delta s \le e_{dc}$$

A value of e_{dc} which satisfies this condition represents the DC shift or mean transmission error level due to tooth deformation.

3.4.3.2. The variable stiffness model

The variable stiffness model expands upon the linear stiffness model, however the thin slice analysis principle can still be applied. This model considers local variation in stiffness due to position on the contacting surface. The stiffness values are influenced by two main aspects of geometry and the contact position in the engagement cycle.

The value at any point contact in one slice increments the stiffness in adjacent slices across the tooth width in the form of a normal distribution. Contact in any other slice due to deformation has a similar normal distribution which is directly additive to the existing stiffness values. In this way the thin slices are no longer considered independent of each other. Further, the amplitude of the distribution curves diminish as the contact point moves away from the root dependent upon the engagement.

The basic equations of a normal distribution curve are readily available in statistical literature such as Weimer[61], however research by Oda et al[35][36] on spur and helical gear tooth forms has shown that the shape of the distribution curve can be greatly influenced by geometry. A function dependent upon contact position on the thread or tooth surface is used to determine the total stiffness value for each point, and replaces the constant k as in the following equation :

$$F = \delta b \sum_{i=1}^{N} f(x_i, y_i, z_i)(e_{dc} - \Delta s_i) \cos \alpha_{r_i} \qquad \forall \Delta s \le e_{dc}$$

3.4.3.3. The finite element model

Though a finite element model often takes considerable development, recent attempts have been made to apply this technique to gearing. Litvin et al[62] and Narayan et al[63] have produced results which simulate theoretical load effects for gear systems. Lack of measured validation makes it difficult to conclude whether this method is any more accurate than direct calculation using a simpler model.

3.4.3.4. Determining the tooth deformation model

The variable stiffness model was rejected since there was not enough experimental data to formulate a complete function to use in developing a model of all gear tooth forms. The finite element method was rejected mainly on the basis of time taken to complete the calculations since one of the objectives of the research work during this project was to produce calculations to be used in software as a practical design tool.

The method used for the transmission error analysis under load during this research program was the linear stiffness model. Smith[12][13] states that the linear stiffness model for spur and helical gear tooth contact uses a stiffness value of 14.0 N/mm/μm. The worm system model incorporated a proportional reduction in elasticity from 213 GPa to 111 GPa[64] to compensate for the phosphor bronze tooth contact of the wheel. The initial choice of stiffness constant therefore was set at 10.5 N/mm/μm.

3.5. SUMMARY

The position and extent of the contact marking pattern, and the magnitude of the transmission error curve are defined by the mismatch design. This can be based upon one of several different design methods. The parameters defining the final specification using any design method can be varied to produce specific, or even optimum, contact conditions.

Manufacturing errors of the gear components and gear box can greatly modify the theoretical calculations of contact. Some error sources, such as lead errors, are highly dependent upon the accuracy of the machine used to produce the component. Other error sources, such as wheel cutter profile, are more controllable and can be improved by 50% using accurate CNC machine tools.

By measuring the manufacturing errors it is possible to include them as part of the calculation in a model of contact. These can be used to assess the quality of a newly completed gear set, or to investigate any problems that exist in an existing system. A point density measurement of 4-5 points/mm on a wheel cutter profile is a high enough sensitivity to calculate the actual wheel tooth form to an accuracy of 2-3μm. A higher density produces no significant increase in accuracy.

The deformation of the thread and tooth under load during operation directly contribute to contact calculations and transmission error. These deformations can be modelled using several different techniques. The linear stiffness model has been chosen not only because of its simplicity but because of the lack of published deformation data for worm gear teeth, and time restrictions.

4. NEW SOFTWARE DEVELOPMENT

4.1. INTRODUCTION

The ability to model the effects of design and contact conditions on the performance characteristics of any gear system is becoming increasingly important in research and development. This has proven difficult for a worm gear system due to the complex geometry which dramatically increases the number of calculations necessary for a comprehensive analysis. Within the last ten years the improvement in computing speed has overcome this problem to such an extent that a full contact analysis can be completed within a time period of a few seconds.

A review of the software currently available for worm gear analysis was completed. This identified the essential elements for gear analysis. Based on this review, new software was developed to enhance and extend analysis techniques in order to form a more complete package. During this development, the collaborating companies associated with this research were consulted to keep the software facilities directly relevant to industry.

4.2. A REVIEW OF AVAILABLE SOFTWARE

4.2.1. Trials of software for the calculation of worm gear contact characteristics

Work by Centre Technique Des Industries Mecaniques (CETIM) based in France has produced a very graphical analysis package which provide a visual illustration of worm gear geometry. The options for analysis includes multiple design methods, and scaled displays of the thread forms in several different planes. Despite the range of options, this analysis is restricted to the ideal geometry and contact conditions case which assumes perfect profiles in each component and a conjugate wheel tooth form. Since no mismatch parameters are possible, the value of this software is limited when considering operational worm gear design.

Software has been written by Colbourne[20] using contact calculations based upon a vector calculus method of designs including mismatch parameters. The parameter variation offers the potential to investigate the influence of worm gear design on contact conditions. There are two separate programs, one to study the effect of design on gear tooth relief, and the other to analyse the subsequent contact conditions.

The first program calculates the gear tooth form for given worm and hob parameters. The relief at any specified depth is then indicated by a contour line over the gear tooth. In the second program, the instantaneous transmission error value and the subsequent clearance between a defined worm thread and wheel flank at an any point during the meshing cycle are calculated. In this respect the software is a far more powerful tool than that produced by Octrue (CETIM), however it is still restricted to analysing design only, and does not have the capacity to model misalignment or machining errors.

When defining a new design or experimenting with design parameter combinations, it is necessary to cycle through all of the parameters. It is also necessary to repeat the contact analysis at several positions through the meshing cycle to compile a transmission error graph or contact diagram. These factors increase the time taken to complete an analysis. This program is limited to the analysis of a single tooth pair engagement cycle. To fully analyse contact conditions within the worm gear system it is necessary to consider the simultaneous contact for several tooth pair engagements.

A software package to analyse worm gear contact has also been developed by the Design Unit at the University of Newcastle-upon-Tyne. Each design parameter can be entered individually, or auto-designed by computer calculations based on the designation and using one of the BS, DIN, or ISO standard methods of dimensioning. The options for defining contact conditions allow linear misalignment of the axes, or 'offset', values during the gear cutting and meshing cycles. It also allows several forms of linear and parabolic profile modification to be applied to the wheel tooth form.

Results from this program indicate the gear tooth relief, transmission error, and the clearance (with an option to view the instantaneous clearance between the worm and wheel in three displacement positions simultaneously). The disadvantages of this system are that it takes several minutes to complete a nominal analysis for contact over approximately three axial pitches of worm displacement, and that it requires support software to operate in the Windows environment.

4.2.2. Literature review of software predictions of worm gear characteristics

The authors Litvin and Kin[23] have also produced software analysis of worm gear geometry. This incorporates the ability to calculate transmission error including axis offset misalignment conditions in the worm gear system. The graph of transmission error shows a series of overlapping curves suggesting that only one tooth pair was considered in this model.

Literature produced by Narayan et al[63] illustrates a software package which has been produced to calculate loading stress for a worm gear design. From these, the transmission error under a torque load is derived. When performing these calculations the contact conditions for multiple simultaneous tooth pair engagements are considered to derive the true contact conditions. The method uses a finite element technique which generally takes far longer to process than direct calculation. No detail is given for how long the calculations take to perform and so this program may prove impractical for progressive design research purposes. Despite the title of the paper, there is also no analysis of the error effects induced during the production of the gear sets, the machining error refers to changes in the design parameters.

4.2.3. Summary of existing software

Elements of these programs are the calculation of gear tooth relief, transmission error (under various contact conditions), and flank clearance. Ease of data entry, integral displays and analysis functions have also been considered in some cases, although these are not essential to the program operation.

The time taken to produce the results has often been overlooked, and no assessment has been made regarding the difference in sensitivity of the final results for each of the calculation methods. No program offers a complete calculation analysis as an integral part of its operation. Though there are various options available to change the theoretical contact conditions of the gear sets by design, these programs do not permit the analysis of machining or operating error effects encountered during production. In all of these cases of worm gear software development no experimental validation of the calculated results is offered.

4.3. THE NEW SOFTWARE PACKAGE

A new software program was developed to corroborate and expand upon the work completed in this area. The program was written for use in an MS-DOS environment which reduced computer requirements and removed the need for additional support software. Following the review and appraisal of the existing software available for gear system analysis, the important functions necessary to perform a complete study of operating characteristics were identified. The new software was developed to contain the significant features common to most of the existing software :

- Analysis of multiple geometry worm gear sets.
- Profile modification of the basic geometry.
- Misalignment of the system.
- Calculation of gear tooth relief.
- Transmission error calculation.
- Data storage and recall.

Though some of these features can be found in other software they were not found collectively in a single package. To expand upon this range of analysis, the options offered by the new software introduce the following additional features :

- Operating error protection.
- A model of error sources induced during production and operation.
- Prediction of contact meshing conditions considering multiple tooth pairs.
- Continuous transmission error graph for the specified design.
- Simulated contact marking pattern.
- Full wheel engagement analysis option.
- Transmission error for a gear system operating under a torque load.
- Fourier analysis of transmission error wave forms.

4.4. PROGRAM OPERATION

4.4.1. The new software operating system

4.4.1.1. The menu system

The display in Figure 4.1 shows the three menus used for these tasks are marked MAIN MENU, DATA MANAGER, and RESULTS MENU and the program function options available under each menu. The main menu is used to control the priorities of the user. This allows access to the data manager, a new analysis for the current gear set specification, or the recall of results calculated during a past analysis cycle. The design specification can be entered using the data manager menu. This allows the entry, saving, recall, or modification of a design specification. The results menu is used to select the analysis of contact characteristics calculated for the current gear set design specification during the simulation cycle.

4.4.1.2. Gear set data entry and modification.

It is frequently necessary to change the gear specification during the research and development of a gear design. The program operates a one key entry system allowing the user to default an entry to the current value allowing fast and efficient design input. A further increase in operating speed has been made by sectioning the input of parameter definitions to worm, hob, and gear design so that a full specification does not have to be entered after each modification. The complete specification is displayed after each amendment and can be reviewed at any time during the program operation by using the option from the main menu. An example of the full gear set specification display is shown in Figure 4.2 for a complete sample set of worm gear parameters. When recalling or saving data from a file, a protection facility has been provided which checks whether a file exists or is being over-written. Further protective features and warnings have been placed throughout the program which prevent performing calculations on an incorrectly defined design. The appropriate error message is displayed to inform and guide the user in each case.

MAIN MENU	DATA MANAGER	RESULTS MENU
1. DATA MANAGER	1. ENTER NEW GEAR SET DATA	1. PROFILES
2. RUN SIMULATION CYCLE	2. CHANGE WORM DESIGN DATA	2. TRANSMISSION ERRORS
3. CURRENT GEAR SET DATA	3. CHANGE GEAR CUTTER DESIGN DATA	3. RELIEF
4. RECALL STORED RESULTS	4. CHANGE GEARING DATA	4. CLEARANCE
5. EXIT PROGRAM	5. IMPORT DESIGN DATA	5. LOADED SYSTEM ANALYSIS
	6. SAVE DESIGN DATA TO FILE	6. FOURIER ANALYSIS
	7. CONVERT TO MILLIMETRES	7. MAIN MENU
	8. UNITS ARE IN INCHES	
	9. MAIN MENU	

Figure 4.1 :   The three control menus and associated options.

	WORM	HOB
Type	:Screw	:Screw
Axial Pressure Angle	:20.0000°	:19.9346°
Root Diameter	:47.346	:47.346
Pitch Diameter	:63.500	:63.500
Outside Diameter	:79.654	:79.654
Calliper Depth	:8.077	:8.509
Calliper Thickness	:12.446	:12.700
Lead	:50.800	:50.698
No. of Threads	:2	:2
Profile Modification	:0.000	:0.038
Profile Shift	:0.000	:3.810
Tilt Angle	:0.000°	:0.820°
Gear Centres/Extension	:132.814	:1.905

	WHEEL
Gear Teeth	:25
Gear Wheel Outside Diameter	:225.044
Throat Radius	:23.673
Gear Face Width	:50.800

Figure 4.2 :   The full specification display for a sample gear design.

4.4.2. Control of contact conditions

4.4.2.1. The gear wheel cutting cycle

The screen display in Figure 4.3 shows the default settings for the wheel cutting cycle options page. The calculation of gear tooth form for the specified design is performed by the gear cutting cycle. These are based upon the theory derived in Chapter 2 for worm gear mismatch analysis.

The program uses fixed geometry options of involute or screw helicoid forms as specified by the input in the gear specification. An option exists to import a file of pre-determined cutting tool co-ordinates. These can be created by direct calculation of any arbitrary profile or CNC measurement of an existing cutter profile.

The sensitivity of the analysis is controlled by the parameters specified at this stage. The number of rack sections and profile points can be changed. A larger number increases the co-ordinate point density over the gear tooth and consequently the accuracy of the analysis improves.

The axis alignments during the cutting process can be defined using options in this page. The centre height, centre distance, and cutter eccentricity can be changed relative to the design cutting axis. This is kept independent of the running alignment settings to resemble the production process. An option also exists to include a chamfer in the wheel tooth form.

The command keys are identified at the bottom of the display. If the gear tooth form has been calculated previously and the parameters have not been modified, an option exists to bypass this process moving directly to the meshing cycle control page. If this option is selected and the gear set parameters have not been modified since the previous cutting cycle then the existing gear tooth form co-ordinate file is used by the gear set mesh analysis. If the parameters have been changed any attempt to use this function will result in an error message and the user will be returned to the main menu.

4.4.2.2. The gear set meshing cycle

The display screen represented in Figure 4.4 shows the default options for the worm and wheel meshing cycle. The extent of the analysis is controlled in the options on this page. The long analysis calculates characteristics over one revolution of the gear wheel. This can be changed to a short analysis which calculates the number of teeth needed to perform an analysis of contact for the system over a wheel rotation interval equivalent to two worm lead displacements. This can be controlled further by altering the number of sample points taken over the specified interval.

The axis alignments during the meshing cycle can be changed using options at this stage. As in the wheel cutting cycle analysis the centre height, centre distance, and worm eccentricity about the axis can be specified.

It is possible to analyse the effect of synthesised or measured wheel pitch, and worm lead errors on the contact conditions. The displays in Figure 4.5 and Figure 4.6 show an example of this using the display screens for the entry of arbitrary error values of wheel pitch and worm lead error respectively for a short analysis of the sample worm gear specification.

The final section shows the default names for the data files which are labelled individually for easier analysis. These file names can be changed by the operator. They can be recalled in future use of the program using the option given in the main menu.

The command keys are identified at the bottom of the display. If the parameters defining the gear set specification and analysis conditions have not been changed, an option exists to bypass this process moving directly to the results menu. If this option is selected when there has been no change to the parameters since the previous mesh cycle, the results menu is shown representing options for the current gear set analysis. If this is selected and no analysis has been performed for the current design specification, then an error message is displayed and the user is returned to the main menu.

GEAR CUTTING CYCLE

Cutter File Name   :hobtools.dat
Co-ordinate File Name   :gearform.dat

Number of Rack Sections :40
No of profile points   :50

AXIS SETTINGS.

Cutting Height Offset   :0.000000
Cutting Centre Offset   :0.000000
Cutting Eccentricity   :0.000000

WHEEL CHAMFER.

    Chamfer Inset   :0.000000
    Chamfer Angle   :0.000000

    ENTER - Mesh Settings Y - Change Current Settings N - Run Cycle

Figure 4.3 :   The default options page for the gear wheel cutting cycle.

GEAR MESHING CYCLE

   Long Or Short Analysis   :2
   Number Of Sample Points :65

AXIS SETTINGS.

    Running Height Offset   :0.000000
    Running Centre Offset   :0.000000
    Worm Eccentricity   :0.000000
    Set Wheel Pitch Errors :No
    Set Worm Lead Errors   :No

DATA FILE NAMES.

    Transmission Error File   :teerrors.dat
    Relief File   :greliefs.dat
    Clearance File   :markings.dat

    ENTER - Results Menu Y - Change Current Settings N - Run Cycle

Figure 4.4 :   The default options page for the worm gear meshing cycle.

WHEEL TOOTH PITCH ERRORS

AMPLITUDE
(MICRONS)

5.00   —

2.50   —

0.00   ￢

-2.50   —

-5.00   ￢ | | | | | | |
            1   2   3   4   5   6   7

TOOTH NUMBER :4
ERROR VALUE   :4.50 microns

SPACE - Next   TAB - Change Direction   ENTER - Run Cycle
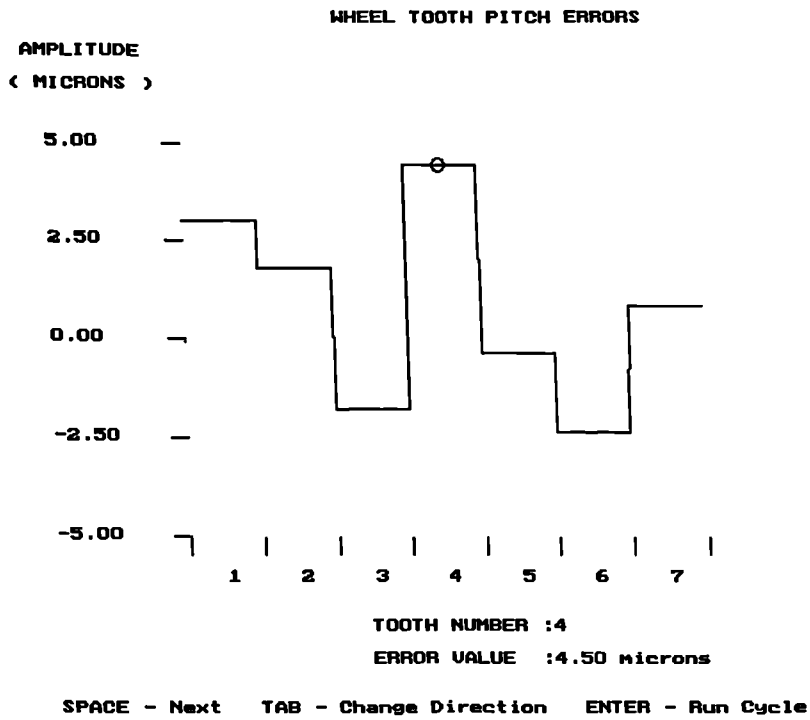
Figure 4.5 :   The wheel tooth pitch errors input screen used during the program.

WORM THREAD LEAD ERRORS

AMPLITUDE
(MICRONS)

5.00   —

2.50   —

0.00   ￢

-2.50   —

-5.00   ￢

AXIAL POSITION :-2.0000 inches
MEASUREMENT STEP :1
ERROR VALUE :0.20 microns

SPACE - Next   TAB - Change Direction . ENTER - Run Cycle
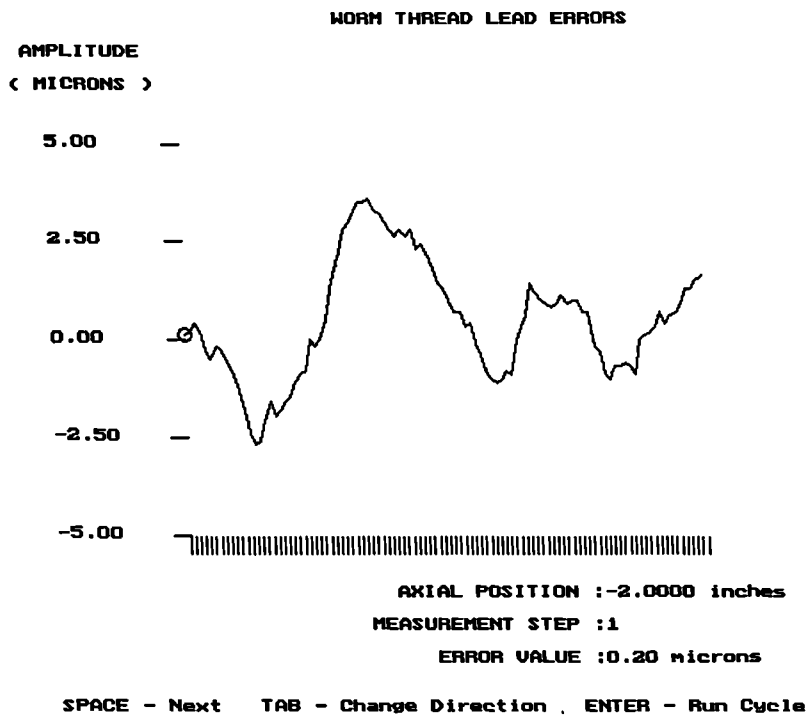
Figure 4.6 :   The worm lead error input screen used during the program.

4.4.3. The result display and analysis options

4.4.3.1. Worm and wheel cutter profile generation

Using this option the profile of the worm thread or wheel cutting tool are represented on a graph. The profile can be displayed in the axial or normal section. The plot in Figure 4.7 represents the axial section through the worm thread for the sample specification.

```
Y CO-ORDINATE          WORM PROFILE
   (INCHES)            AXIAL SECTION

  1.57

  1.38

  1.20

  1.01

  0.83
        -0.369   -0.185   0.000   0.185   0.369

              X CO-ORDINATE
                 (INCHES)
```
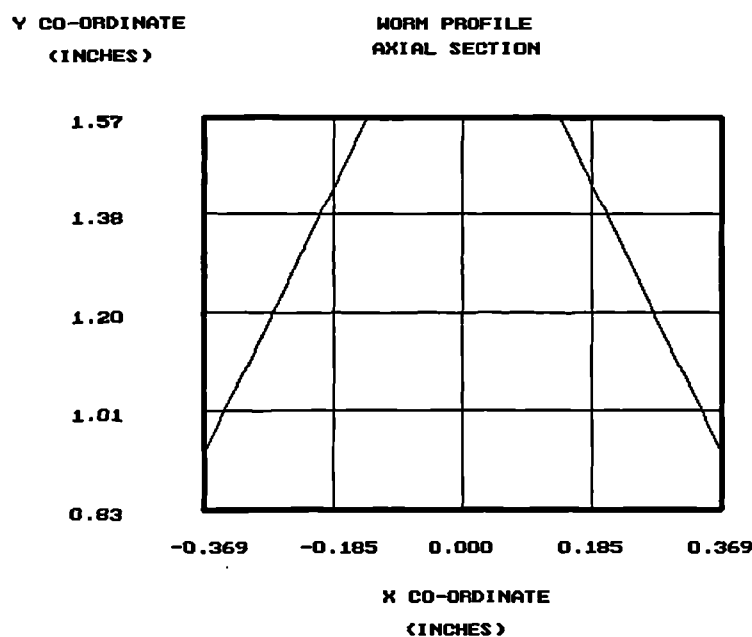
Figure 4.7 :   An example of the profile graph option using the worm thread of the sample gear design viewed in the axial section.

On a 640x480 screen, a 12mm X-axis dimension implies that individual pixels represent in excess of 25μm intervals and are therefore too large to accurately represent the actual thread form. This problem is exaggerated as the thread form thickness increases. Though these graphs were not sensitive enough to be used directly in the manufacturing process, it was possible to write the co-ordinates of the profiles to a computer file. These files can be used in conjunction with CNC machine tools as part of a digital control cutting or measuring program.

4.4.3.2. Transmission error graph for a worm gear design

A 2 lead interval is defined as the short analysis of the contact conditions for the sample specification. The graph in Figure 4.8 represents the transmission error over 2 lead displacements of a 2-start worm equivalent to 4 tooth pitches. It shows the dominant trace over the interval when considering all potential tooth pair engagements at each position through the meshing cycle. The absolute value of this wave form is displayed in microns representing the magnitude of the transmission error.
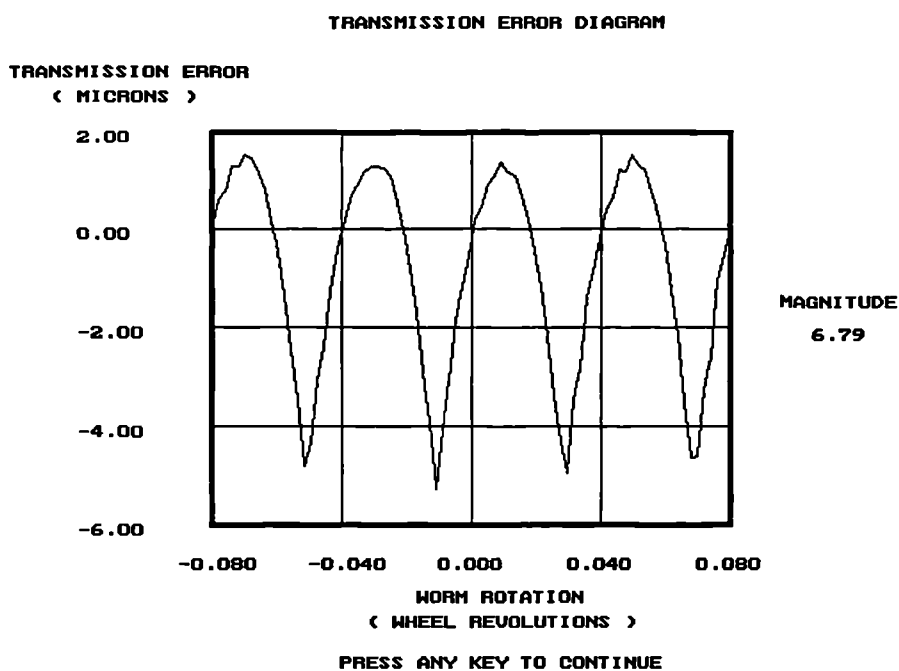
Figure 4.8 :   The 'short' analysis transmission error for the sample gear design.

This wave form considers contact due to changes in design parameters, manufacturing error sources, and shaft alignment but it does not consider deformation of the components under load.   Analysis of operation under a torque load is described in section 4.4.3.5.

4.4.3.3. Gear tooth relief diagrams

When designing worm gear sets, the relief between the worm thread and wheel flank is important for establishing areas of contact as discussed in Chapter 2. The relief is calculated by the new software during the meshing cycle. The results can be viewed by the program using this option. The display in Figure 4.9 shows the default screen for the relief over the gear tooth form derived from the sample specification. The region indicated in this diagram is at the $10\mu m$ default level used by the program. It is possible to instantly view the relief region at alternative depths without repeating the mesh analysis by using the command keys. The diagram shows the gear tooth in the correct aspect ratio with the scale automatically derived from the specification. In some designs, more than one area of the tooth may have relief within the bound set by the specified depth. The display uses a shaded area rather than a contour to indicate contact thereby eliminating any confusion in identifying the required region.

Using CNC measuring machines it is possible to measure wheel tooth profiles in sections transverse to the wheel axis. Measurements in this plane represent analysis in an axial rack section of the worm. A direct comparison of calculated and measured relief profiles can be made using the new software. The values used to generate the relief diagram can be selected by the program to isolate the calculated relief in each profile section through the gear tooth. The graph in Figure 4.10 shows the default relief profile which represents results calculated in the axial section of the worm using the sample gear design. The scales of the graph are defined by the maximum and minimum relief, and the maximum and minimum radius of the complete gear tooth form regardless of the currently displayed section.

The profile relief can be displayed in any of the rack sections specified at the gear cutting cycle stage. The number of the current section displayed can be changed using the command key options given at the bottom of the screen. An example of this is shown in Figure 4.11 which shows relief diagrams for a selection of five rack sections across the gear tooth form generated by the default settings to analyse the sample gear design.

GEAR RADIUS
(MILLIMETRES)

112.52

103.00

93.48

83.96

74.44

-25.400   -12.700   0.000   12.700   25.400

FACEWIDTH
(MILLIMETRES)

SPACE - Next   TAB - Change Direction   ENTER - Relief Profiles
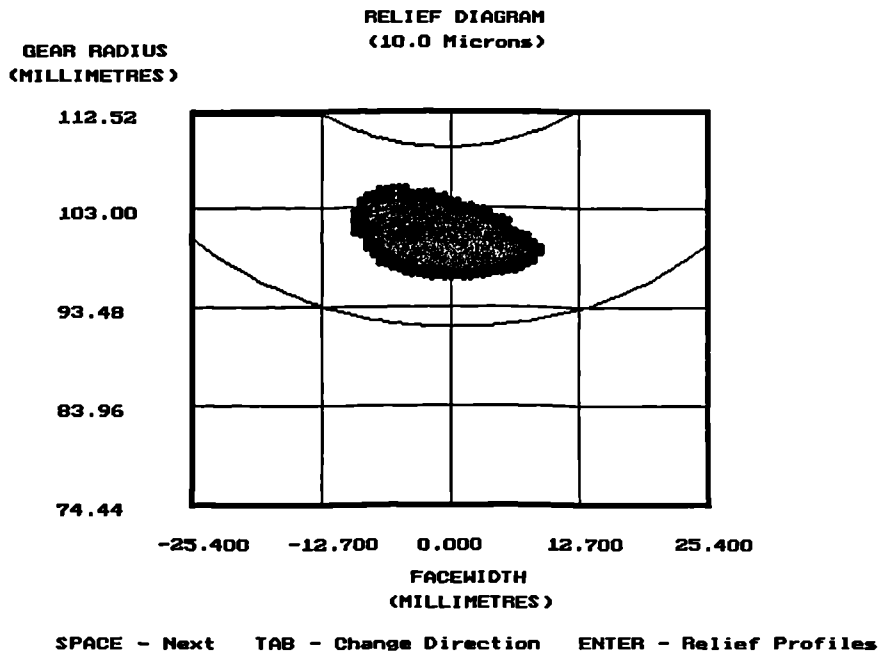
Figure 4.9 :   The default relief diagram for the sample gear design.

PROFILE RELIEF

RELIEF VALUE   SECTION :0
(MICRONS)

0.00

-36.25

-72.50

-108.75

-145.00

95.445   99.673   103.901   108.129   112.357

TOOTH RADIUS
(MILLIMETRES)

SPACE - Next   TAB - Change Direction   ENTER - Results Menu
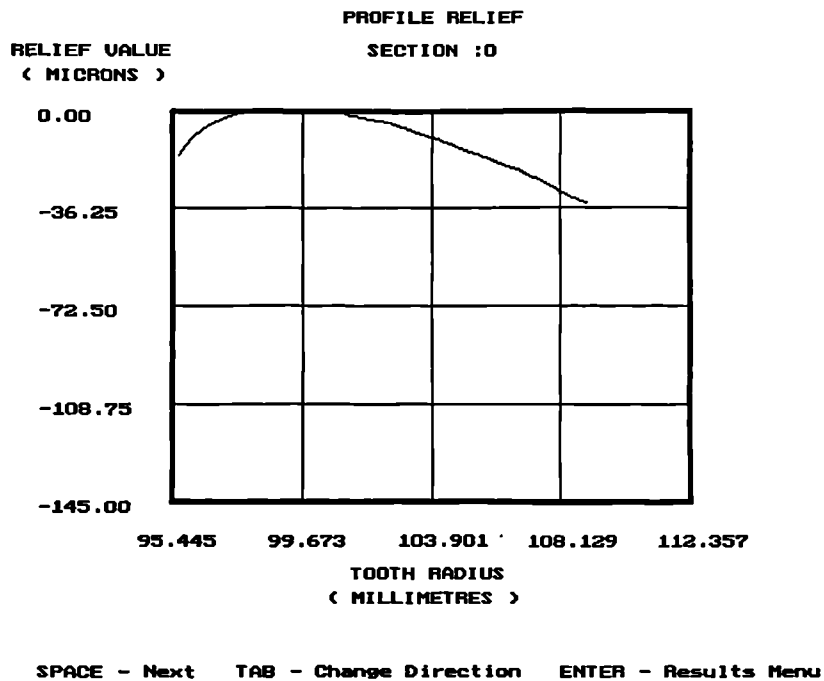
Figure 4.10 :   The profile relief in the axial section (section 0) for the sample gear
tooth design.

(PROFILE SECTION NUMBER)
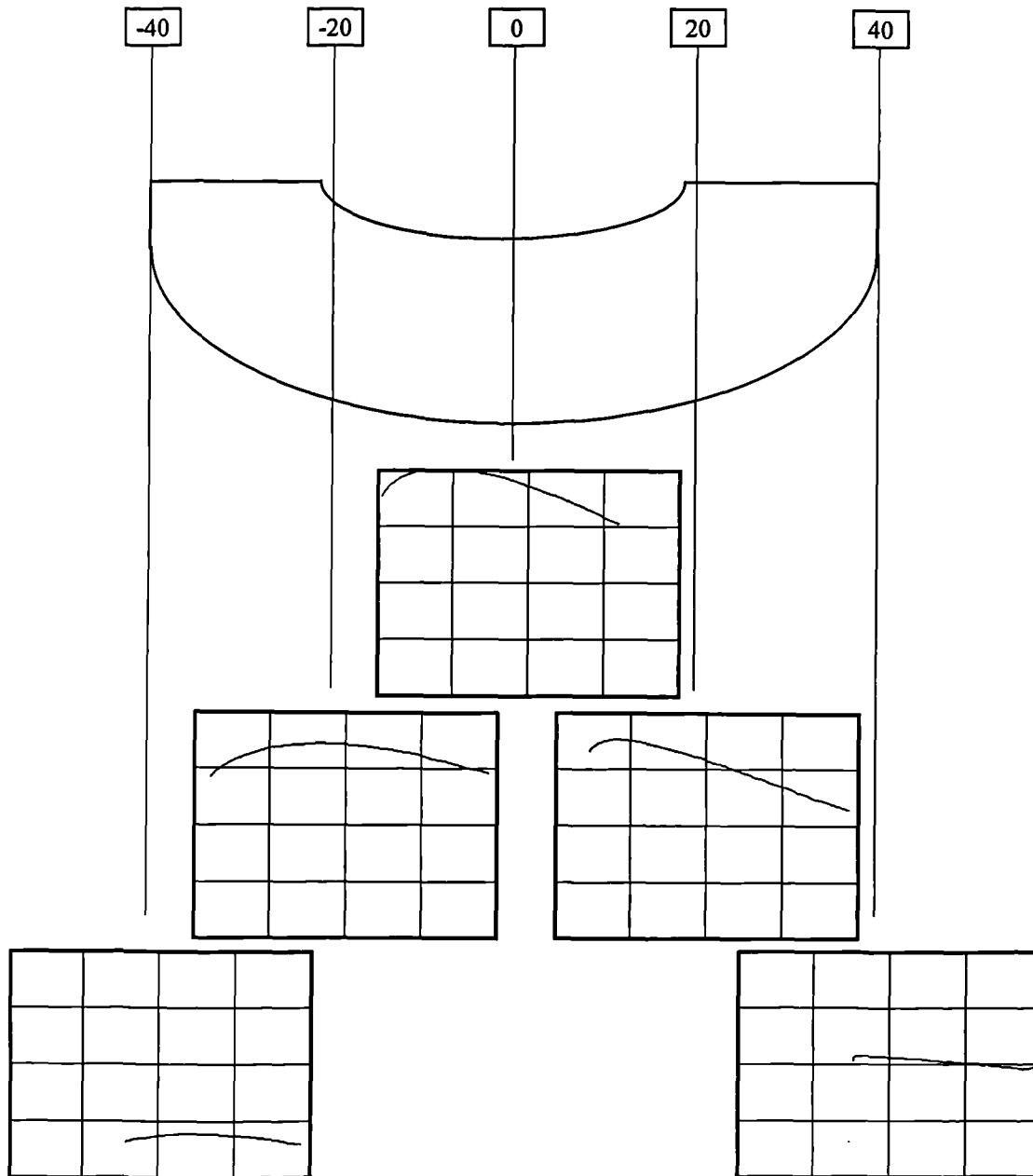
Figure 4.11 : The changes in profile relief across the wheel tooth generated by the sample gear design.

4.4.3.4. Clearance diagram

The clearance between each tooth and the worm thread is calculated during the meshing cycle at all meshing positions over the selected analysis interval. The display in Figure 4.12 shows the composite of all these calculated clearances for the sample specification during the meshing cycle. The calculations displayed take into account any additional clearance due to transmission error from adjacent tooth pair contacts. This is a theoretical simulation of the marking, or bearing, test performed by industry to validate the contact conditions between the worm thread and wheel flank as described in section 2.4.5. The display shown represents the 10μm default level used by the program. It is possible to view the clearance region at alternative depths by using the indicated command keys without repeating the mesh analysis.

Again the diagram shows the clearance over the gear tooth in the correct aspect ratio with the scale automatically derived from the specification. This display also uses a shaded area rather than a contour to indicate clearance over the specified region. The current clearance value for the indicated region is shown by the display.

4.4.3.5. Transmission error for a loaded worm gear system

The meshing cycle establishes the relief values over each tooth used in the contact analysis. These values are used to perform the load analysis model calculations as described in Chapter 2. The relief values are stored in a data file and can be instantly retrieved. This enables the computer to perform calculations at any load level for the current design without repeating the meshing cycle.

The load analysis option shows the calculated transmission error for a specified load relative to the no load transmission error curve calculated during the meshing cycle. The graph in Figure 4.13 shows an example of the display screen for this facility using the sample design specification under a 500 Nm torque load. The transmission error at this load is displayed relative to the graph of the no load transmission error in order for the user to gauge mean transmission error effects. The calculations can be repeated for any load level using the command keys as indicated in the display.

CLEARANCE DIAGRAM
(10.0 Microns)

GEAR RADIUS
(MILLIMETRES)

112.52

103.00

93.48

83.96

74.44

-25.400   -12.700   0.000   12.700   25.400

FACEWIDTH
(MILLIMETRES)

SPACE - Next   TAB - Change Direction   ENTER - Results Menu
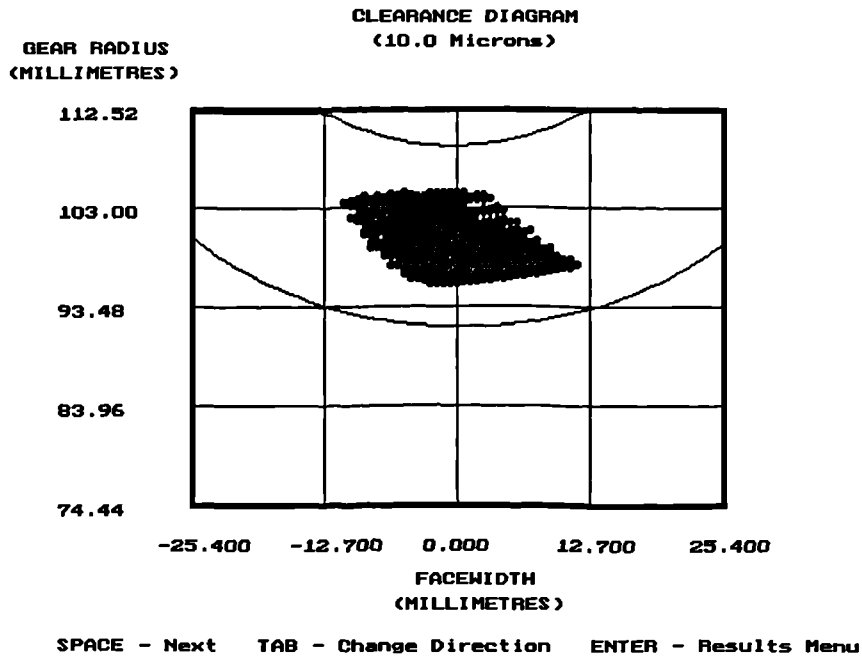
Figure 4.12 :   The clearance diagram for the sample gear design simulating the
contact marking pattern using a 10μm ink thickness.

TRANSMISSION ERROR DIAGRAM

TRANSMISSION ERROR   TORQUE :500 Nm
(MICRONS)

2.00
                                                    —— 0 Nm
-7.75

-17.50

-27.25
                                                    —— 500 Nm
-37.00

-0.080   -0.040   0.000   0.040   0.080

WORM ROTATION
(WHEEL REVOLUTIONS)

SPACE - Next   TAB - Change Step Size   ENTER - Results Menu
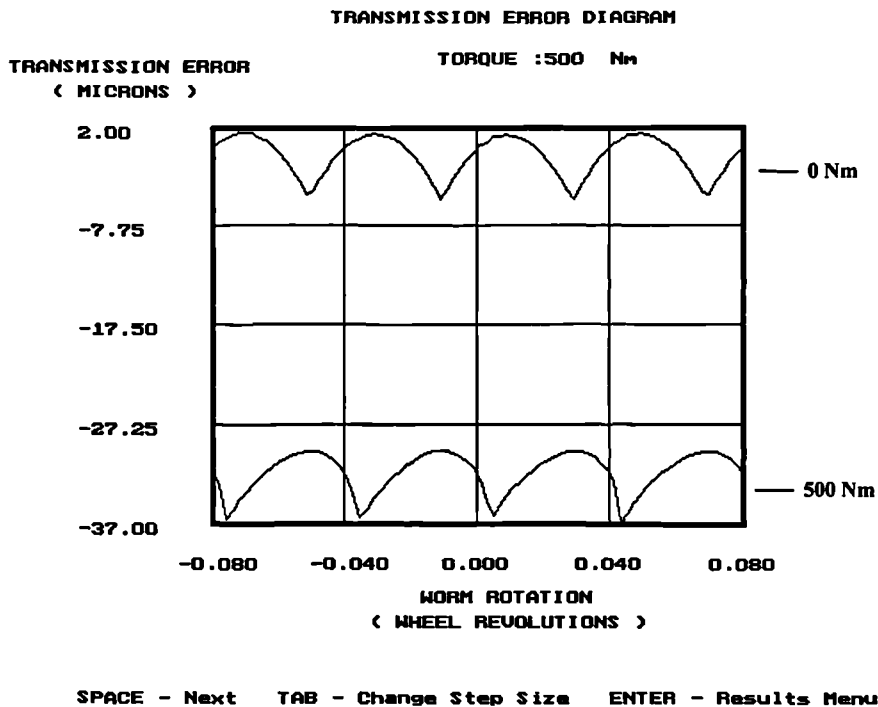
Figure 4.13 :   The graph of the effect on transmission error for the sample gear
design under a 500 Nm load.

4.4.3.6. Fourier frequency analysis

The principle and development of the Fast Fourier Transform (FFT) routine has been well documented by sources such as Ramirez[65] and Bringham[66]. It is a valuable investigative tool which can identify the individual frequency components of a wave form.

Fourier analysis has become an important part of understanding the source and consequences of gear set transmission errors. This can be used to investigate contributions to the composite transmission error from distinct error sources which affect the theoretical contact conditions and therefore influence the wave form. It can also be used to relate the transmission error to noise and vibration problems which occur during operation.

A Fourier analysis option within the program removes the time needed to process and format the data, and the expense of purchasing a separate analysis package. The function is based upon the code written by Press et al[67] specifically for computer programmers. This function provides a frequency spectrum in cycles per revolution (cyc/rev) of the wheel for the transmission error wave calculated for the contact conditions calculated during the meshing cycle. It is also possible to analyse the transmission error curve produced by the load analysis option using this same function.

The display shown in Figure 4.14 shows the transmission error calculated for the sample gear specification and the resulting frequency spectrum for the wave form. This displays the spectrum for the first 250 cyc/rev frequencies. The peaks indicated at 25 cyc/rev and further harmonics in this spectrum reflect the 25:2 ratio of the sample gear specification used. The display also indicates the mean (or DC) transmission error level for the wave, as well as the frequency and the amplitude of the currently indicated frequency. The amplitudes for each of the frequencies over the spectrum range can be viewed by using the command keys displayed at the bottom of the page.

TRANSMISSION ERROR DIAGRAM

TRANSMISSION ERROR
(MICRONS)

MAGNITUDE
6.79

WORM ROTATION
(WHEEL REVOLUTIONS)

PRESS ANY KEY TO CONTINUE

FOURIER ANALYSIS

AMPLITUDE
(MICRONS)

DC SHIFT : -0.83

FREQUENCY : 1

AMPLITUDE : 0.01

FREQUENCY
(PER WHEEL REV)

SPACE - Next   TAB - Change Direction   ENTER - Results Menu
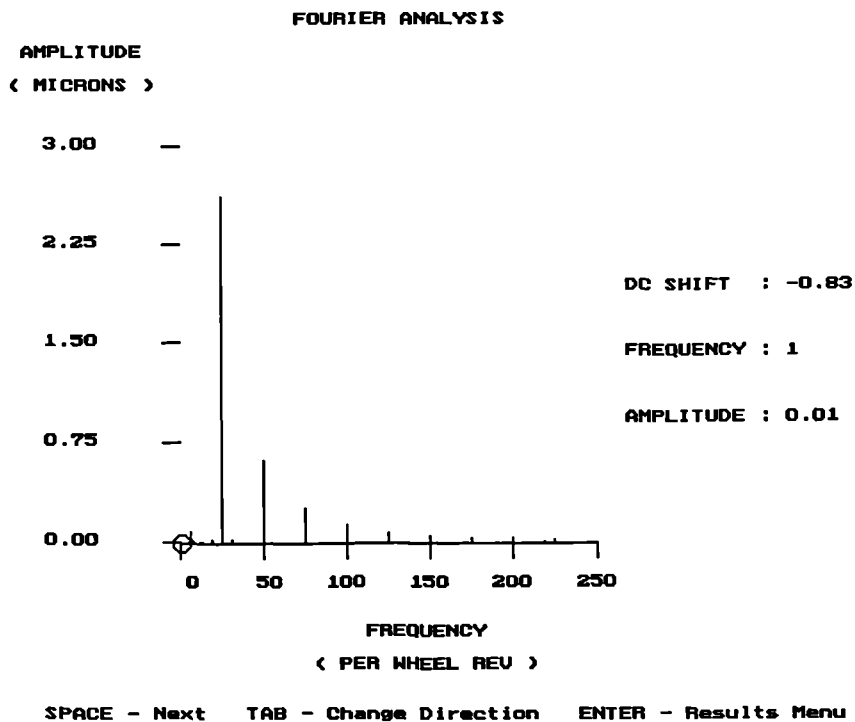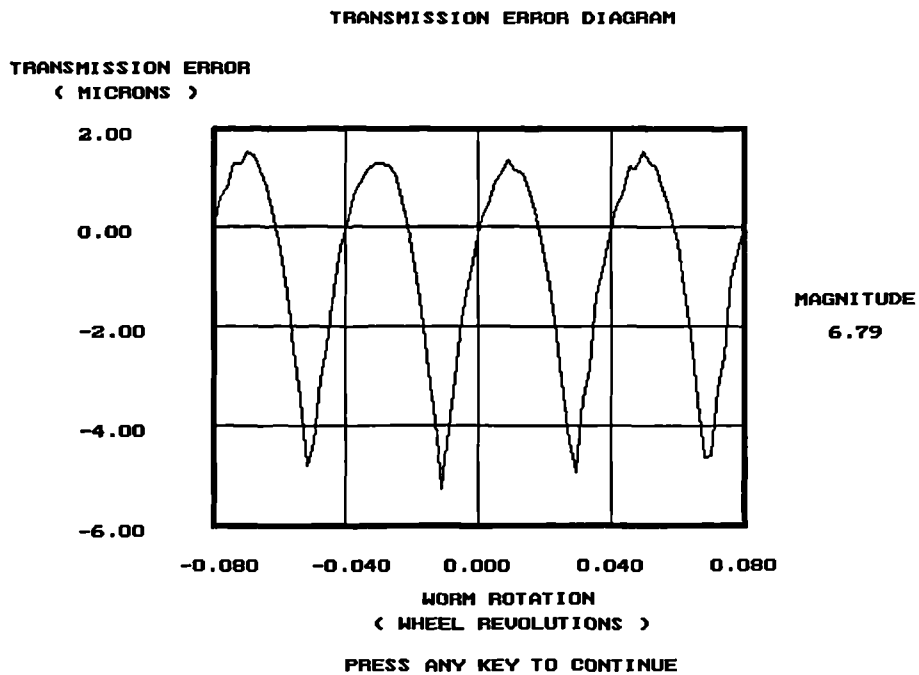
Figure 4.14 :   The Fourier analysis frequency spectrum for the transmission error
wave form calculated for the sample gear design.

CHAPTER 4

4.4. SUMMARY

The completed program offers the following advantages over other existing software programs for worm gear analysis :

- Ease of operation.
- Protective features.
- Analysis speed.
- Analysis of manufacturing and operating error sources on contact conditions.
- Composite contact marking simulation for multiple tooth pair engagements.
- Continuous transmission error calculation.
- Transmission error in systems under a torque load.
- Fourier analysis of transmission error wave form.

Once a full set of data has been entered, the analysis performed by the gear cutting and meshing cycle is completed in approximately 15 seconds using the default settings for the program on a 100 MHz machine with a 16 Mb memory. This allows a fast analysis of worm gear design with the potential to perform several design iterations within a few minutes to optimise the contact characteristics as required. As a result it is possible to use the new software as a practical and efficient analysis tool to complete the following tasks :

- Develop contact geometry for new worm gear forms.
- Analyse and improve contact conditions in various existing helicoid designs.
- Investigate and assess manufacturing quality.
- Optimise design parameters for specific operating conditions.
- Trouble shoot problems in existing gear systems.

5. SOFTWARE VALIDATION

5.1. INTRODUCTION

The literature review in Chapter 1 has shown that there are many methods for calculating gear design and several computer programs have been produced to perform them. It also showed that there were some areas of analysis which have not been covered or validated. The new computer software uses the calculation technique described in Chapter 2 to analyse worm gear design and the effects of potential error sources identified in Chapter 3. These new features give certain advantages over other software packages as shown in Chapter 4, however in order for this software to become justified as a practical investigative tool it must be fully validated.

Computer software predictions of gear set characteristics were validated in three stages. The first was to compare the calculations of gear tooth relief generated by the software with equivalent calculations described in published literature performed by several independent sources using alternative methods. The second was to select an existing industrial design and compare the correlation of gear tooth relief, marking pattern and transmission error characteristics with as many existing software sources as possible. The third stage was to produce several test gear sets under controlled manufacturing conditions and compare measured characteristics with the new software program predictions.

5.2. VALIDATION OF THEORETICAL CALCULATIONS USING EXISTING DESIGN SPECIFICATIONS

5.2.1. Comparison of screw helicoid gear tooth relief using existing literature

Previous work produced by Janninck[18] and Colbourne[20] has compared relief calculations on an existing worm gear design specification. The gear set specification listed in Appendix D/1 was used to assess the initial theoretical calculations of gear relief made by the new computer software with results produced by these two authors. Prediction of 0.0005" and 0.0010" relief contours calculated by Janninck for this

specification are shown in Figure 5.1, while Figure 5.2 shows the equivalent Colbourne calculations. The new software calculations of relief are shown in Figure 5.3 for depths of 13µm and 25µm which represent the closest metric values for direct comparison with the Janninck and Colbourne diagrams.

Though the regions of relief are approximately in the same positions on the gear tooth face, there are some visible differences between the Janninck and Colbourne calculations of exact contours at 0.0005" and 0.0010" relief for this specification. Colbourne suggests that the reasons are the way in which profile modification is applied to the original gear cutter profile and the direction in which the relief is calculated which can be axial or normal to the tooth surface. A further reason could be that Janninck used only the calculated points as shown in his paper to derive the contours, which is approximately 6 profile points in each of 10 rack sections, while the Colbourne analysis used 21 profile points in each of 81 rack sections for the calculations. This represents a significant increase in point density over the gear tooth which implies that this interpolation will be a more accurate representation of relief.

Comparison of the Janninck calculations with the new software results shows the same conclusions as those drawn by Colbourne for the sample design given in Appendix D/1. Despite the difference in display technique, there is a correlation to within 1µm between the Colbourne calculations and those made by the new software. The only significant difference is the appearance of a small region of 25µm relief indicated by the new software in the exit corner of the gear tooth which does not exist in the other diagrams. This may be caused by the difference in sensitivity between the interpolation contour and discrete area display techniques.

The new software used 40 profile points in each of 81 rack sections to make the relief calculations. This shows that when analysis is performed there is little advantage obtained by using a higher point density than that chosen for the default by Colbourne. Because of this 40 profile points in each of 81 rack sections were used as the point density distribution default for all further analysis by the new software.

Figure 5.1 :   Calculation of relief contours by Janninck at contours of 0.0005" and 0.0010" for the screw helicoid gear specification in Appendix D/1.

Figure 5.2 :   Calculation of relief contours by Colbourne at contours of 0.0005" and 0.0010" for the screw helicoid gear specification in Appendix D/1.

Figure 5.3 :   Calculation of relief from the new software for regions of 13 and 25 microns for the screw helicoid gear specification in Appendix D/1.

5.2.2. Further comparison of screw and involute helicoid gear tooth relief

The initial comparison for a screw helicoid gear set specification produced good agreement with the Colbourne software. A further screw helicoid gear specification, as listed in Appendix D/2, was used to confirm the theoretical calculations of gear tooth relief. In Figure 5.4 the contours of 0.0005" and 0.0010" relief for this specification are shown as calculated by the Colbourne software. Figure 5.5 shows the predictions of the 13μm and 25μm relief regions from the new software for this specification. Once again there is a very close 1-2μm correlation in the calculations.

The involute helicoid is the worm gear form preferred by British industry. It was therefore necessary to compare the relief calculations using this form. An involute helicoid specification as listed in Appendix D/3 was then analysed using the method described for the screw helicoid specifications. The results obtained from the Colbourne program are shown in Figure 5.6, while Figure 5.7 represents the equivalent results produced by the new software. Though there is in general a good agreement between the calculation methods, small differences in the indicated region are evident in this case. The minimum relief point in the new software calculations has moved toward the centre of the tooth form. This may be due to the differential in point density used for the two sets of calculations, or inherent differences in the calculation method. Not enough information about the Colbourne method of calculation is known at this point to investigate further.

Figure 5.4 : Calculation of relief contours by Colbourne at contours of 0.0005" and 0.0010" for the screw helicoid gear specification in Appendix D/2.
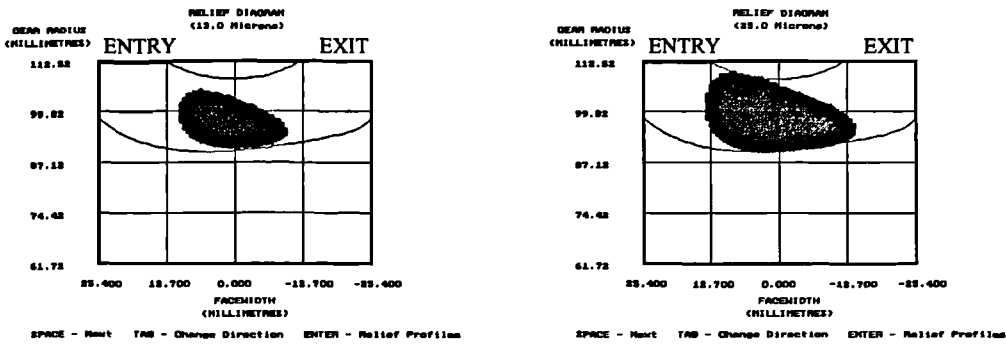
Figure 5.5 : Calculation of relief from the new software for regions of 13 and 25 microns for the screw helicoid gear specification in Appendix D/2.
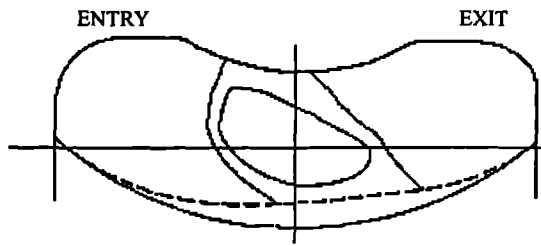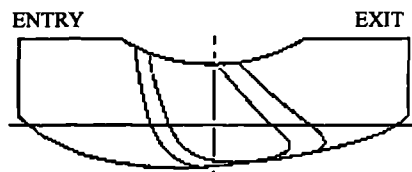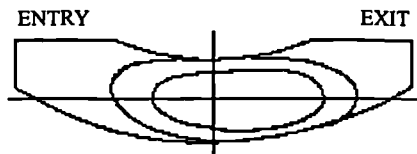

Figure 5.6 : Calculation of relief contours by Colbourne at contours of 0.0005" and 0.0010" for the involute helicoid gear specification in Appendix D/3.
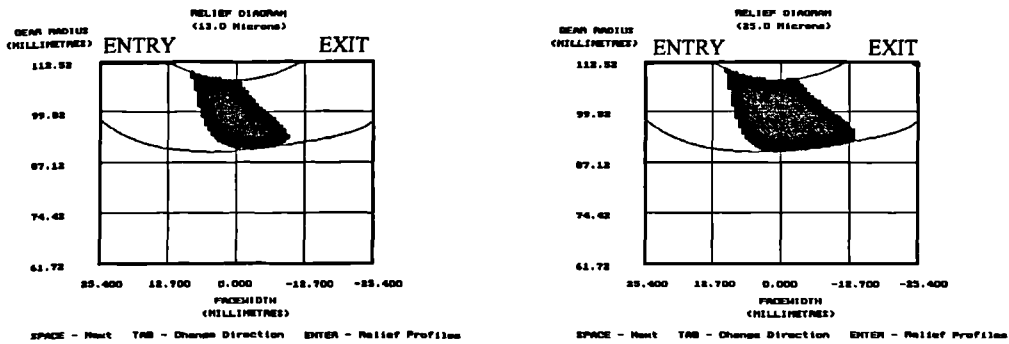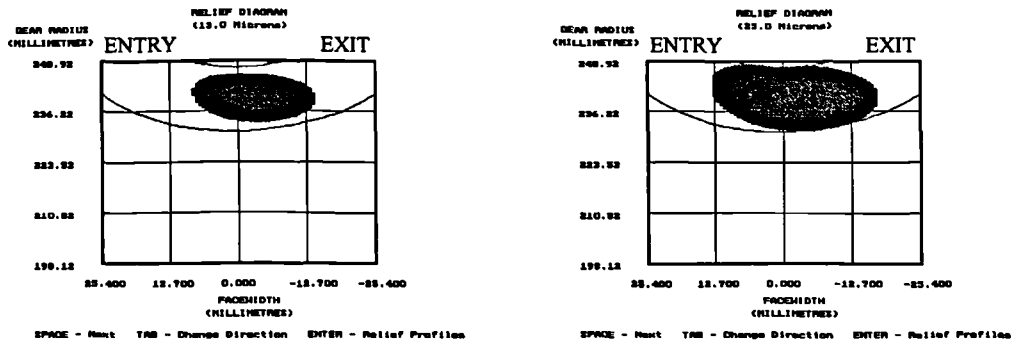

Figure 5.7 : Calculation of relief from the new software for regions of 13μm and 25μm for the involute helicoid gear specification in Appendix D/3.

5.2.3. Comparison of software calculations for theoretical transmission error

The predictions of transmission error calculated by the new software and the Colbourne software were compared. The graphs shown in Figure 5.8 and Figure 5.9 compare the predicted transmission error plot for a single tooth pair engagement for the Appendix D/2 and Appendix D/3 specifications respectively. These graphs correlate to within 2μm, any difference could be due to either a subtle change in the design specification through rounding error or an inherent variation in the method for calculating the point of contact between the two programs. The difference in transmission error magnitude should be expected since a difference in the calculated gear tooth relief form reported in section 5.2.2. will induce this.

5.3. COMPARISON OF RELIEF CALCULATION USING AN INDUSTRIAL DESIGN SPECIFICATION

The Janninck and Colbourne analysis of gear sets used to validate the new computer program in previous sections of this chapter were published in the late 1980's and based upon an American Gear Manufacturers Association (A.G.M.A.) design standard. An existing industrial involute helicoid specification was chosen from a British manufacturer as a new arbitrary and independent design for further validation. This specification can be found in Appendix D/4. Calculations of the gear tooth form made using the new software are shown in Figure 5.10 indicating theoretical gear tooth relief of 13μm and 25μm. These were compared to calculations of 0.0005" and 0.0010" relief contours using the Colbourne program, shown in Figure 5.11. A further source of validation was the software produced by the Design Unit based at the University of Newcastle Upon Tyne. The diagram in Figure 5.12 shows the results from this program for the Appendix D/4 design. This indicates 0.0010" and 0.0005" relief using a thick and a thin line respectively at a series of constant distances from the wheel axis across the wheel tooth. There was an excellent correlation in the results from both sources for this specification. This shows that theoretical gear tooth relief can be calculated by independent methods to within approximately 2μm.

A COMPARISON OF THE NEW SOFTWARE TRANSMISSION ERROR CALCULATIONS WITH RESULTS FROM COLBOURNE SOFTWARE USING THE SCREW HELICOID SPECIFICATION IN D/2
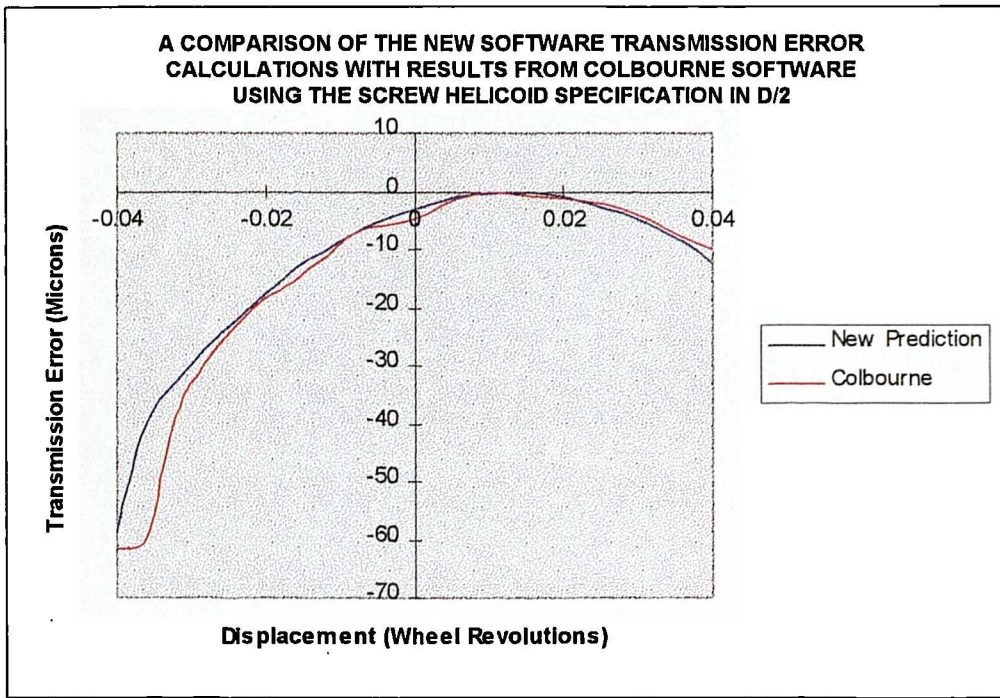
Figure 5.8 :   Compared software predictions of transmission error for the screw helicoid specification D/2.

A COMPARISON OF THE NEW SOFTWARE TRANSMISSION ERROR CALCULATIONS WITH RESULTS FROM COLBOURNE SOFTWARE USING THE INVOLUTE HELICOID SPECIFICATION IN D/3
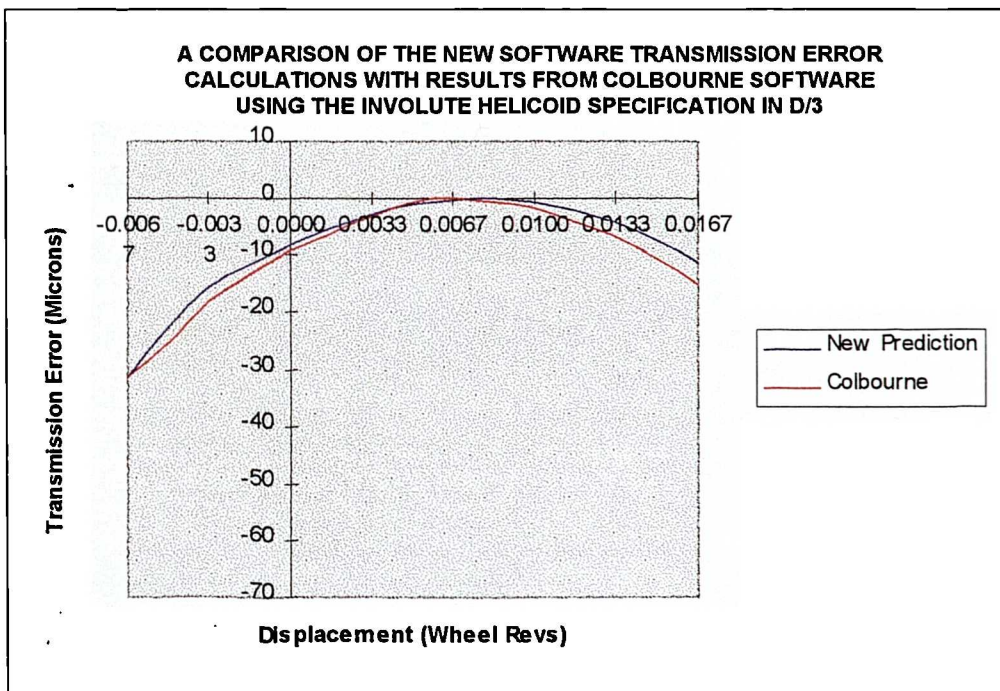
Figure 5.9 :   Compared software predictions of transmission error for the involute helicoid specification D/3.
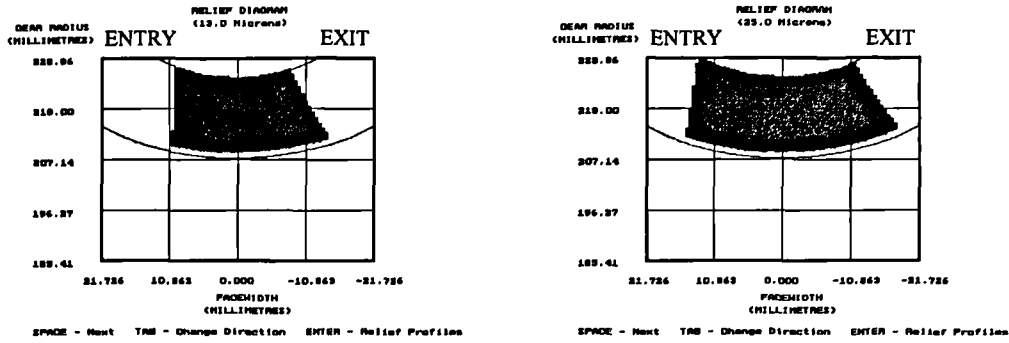
Figure 5.10 : Calculation of relief from the new software for regions of 13 and 25 microns for the involute helicoid gear specification in Appendix D/4.
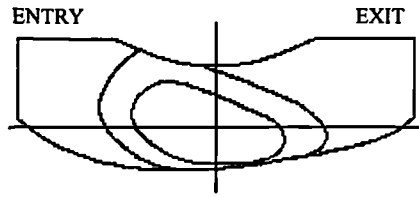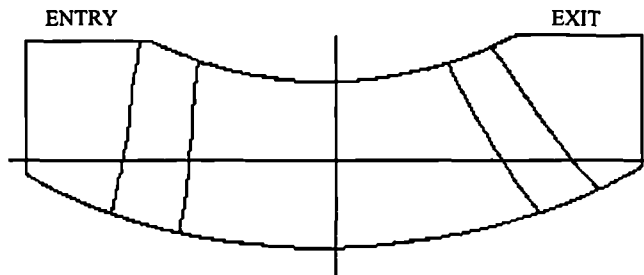

Figure 5.11 : Calculation of relief contours by Colbourne software at contours of 0.0005" and 0.0010" for the involute helicoid gear specification in Appendix D/4.


Figure 5.12 : Calculation of relief along lines of equal radius across a gear tooth by Hu software at depths of 0.0005" and 0.0010" for the involute helicoid gear specification in Appendix D/4.

5.4. VALIDATION OF CALCULATED CHARACTERISTICS USING MANUFACTURED GEAR SETS

5.4.1. Recording manufactured gear set characteristics

The next step was to compare the software predictions with measurements recorded using production gear sets. The two gear sets used in Chapter 3 to investigate production errors were used for this.

Two gear sets were made based upon an existing standard production gear design with a 50:1 ratio and 152.4 mm (or 6") centre distance. Though both sets used the same worm design, the wheel tooth designs were different. The first was a conjugate set in which, by definition, the wheel cutter tool was a copy of the worm thread profile and followed the path of the worm thread during the cutting process. A conjugate gear set would fail under operating conditions due to lack of lubrication, however the design is of great use for research purposes as a control sample. The theoretical characteristics of no transmission error and full face contact expected from this gear set imply that any errors detected would stem from the production process itself. This wheel is referred to as 'Wheel A' for the purpose of this analysis, and the design can be found in Appendix D/5. The second was produced using a wheel cutter design which would allow satisfactory oil entry and exit clearance. This wheel will be referred to as 'Wheel B' for this analysis and the design can be found in Appendix D/6.

Calculations were completed by the software for contact marking and transmission error using the gear set design information only. This represented the theoretical gear set characteristics. A record was kept of any manufacturing error sources detected through the production process. Including these in the software calculations of marking pattern and transmission error produced a synthesised prediction of gear set characteristics. A marking test was performed using micrometer blue as an indicator of contact and clearance between the flanks of both wheels and the threads of the respective worms. The transmission error was also recorded using a single flank testing machine. These tests represented the measured characteristics used in comparison with the theoretical and synthesised calculations.

5.4.2. Computer model predictions for a manufactured conjugate gear set

Calculations were made by the new software for the theoretical contact marking pattern based upon the gear set data alone for a conjugate gear design. The results can be seen in Figure 5.13 for the both wheel flanks, referred to as Flank A and Flank B of the gear tooth. The contact marking was then calculated using the wheel cutter profile, eccentricity, and linear axis misalignment error sources detected during the production process. The subsequent synthesised contact marking patterns are shown in Figure 5.14 for both wheel flanks. These were compared with the record of actual marking recorded for the completed gear set as shown in Figure 5.15 for both wheel flanks. The theoretical and synthesised transmission errors were also calculated by the new software and compared to the measured results obtained by the single flank tester. The results are shown in Figures 5.16, 5.17, and 5.18 respectively for Flank A, and Figures 5.19, 5.20, and 5.21 for Flank B.

The comparison of these results indicates several points of interest. The synthesised errors for Flank A highlighted the grooved area of tooth which is distinct in the recorded case while this is not true in the comparison of results for Flank B. Here the synthesised errors appear to produce no effect despite several grooved areas indicated by the recorded case. This may be due to an inconsistency in the thickness of marking blue ink on application and during contact. Alternatively, this may be due to the mode of display within the software itself. Each of the points on the gear tooth which is calculated to be within the clearance value required is indicated by a circle of two pixels. This may extend the indicated region into an area which is not in the specified range and hence give a false representation of the extent of the marking.

The agreement of the transmission error is good in both flanks. The amplitude in Flank A correlates to within a 1μm tolerance. The same can be said for the Flank B results in general, the only distinct difference being the amplitude of the severe peak recorded in the signal. Though the synthesised transmission error for Flank B identifies a peak caused by the series of grooves indicated in the recorded marking pattern, it is 5μm smaller in magnitude.
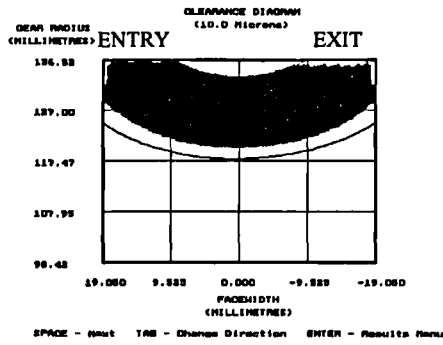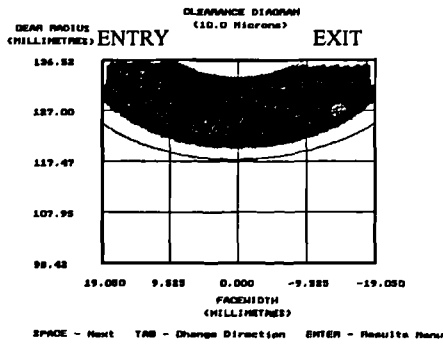
FLANK A   FLANK B

Figure 5.13 :   Theoretical marking pattern for Wheel A.
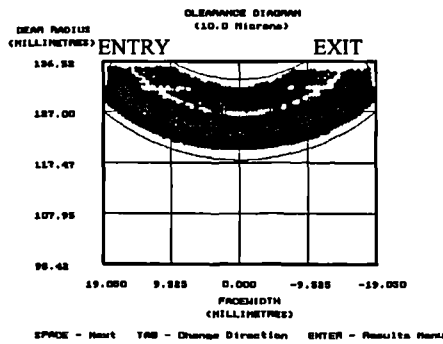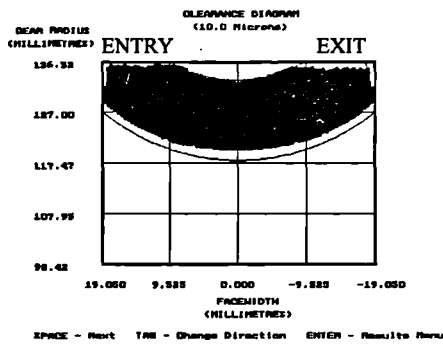
FLANK A   FLANK B

Figure 5.14 :   Synthesised marking pattern for Wheel A.
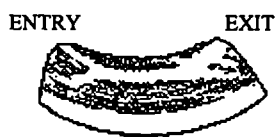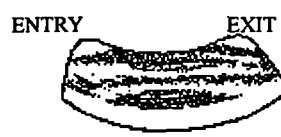
FLANK A   FLANK B

Figure 5.15 :   Recorded marking pattern for Wheel A.
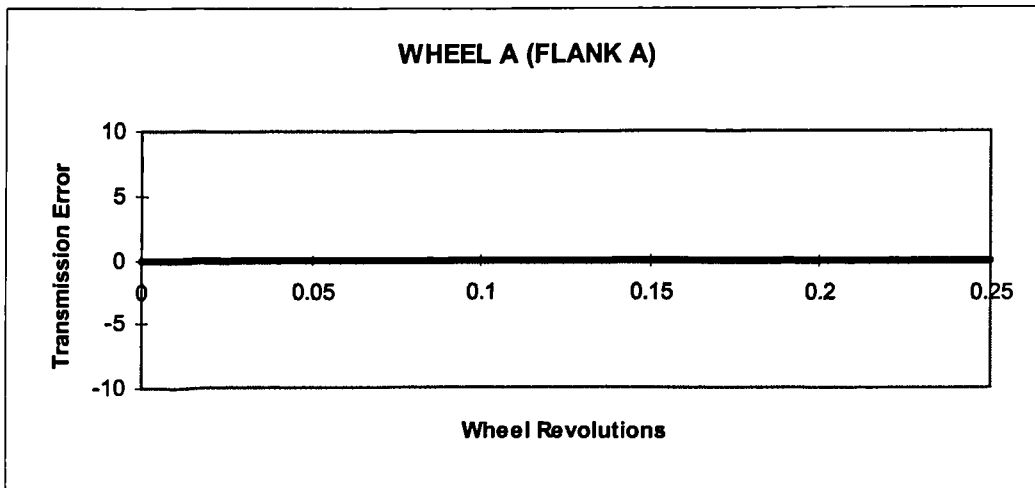
Figure 5.16 : Theoretical transmission error for Wheel A (Flank A).
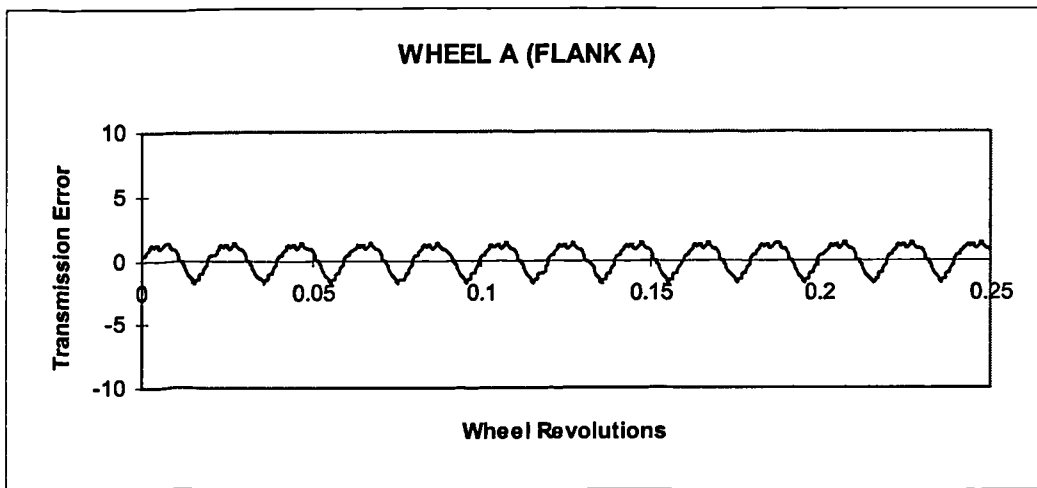
Figure 5.17 : Synthesised transmission error for Wheel A (Flank A).
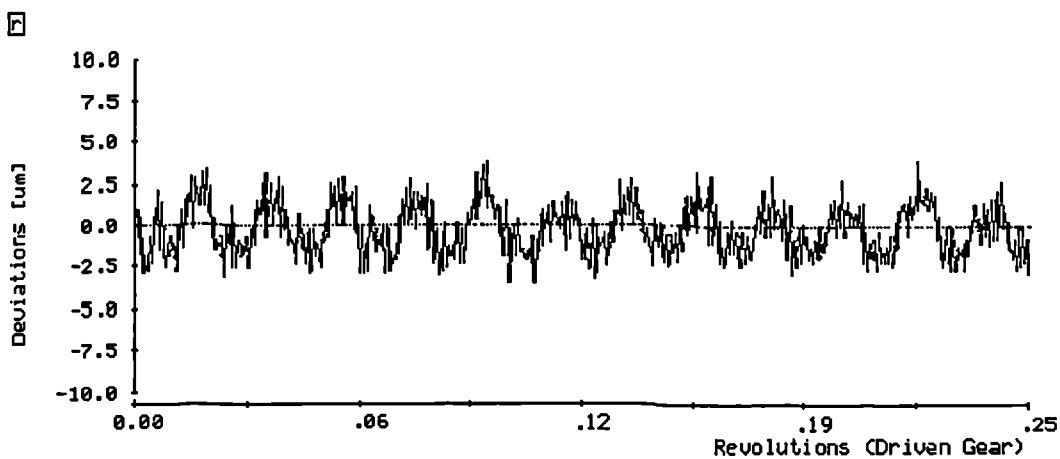
Figure 5.18 : Measured transmission error for Wheel A (Flank A).
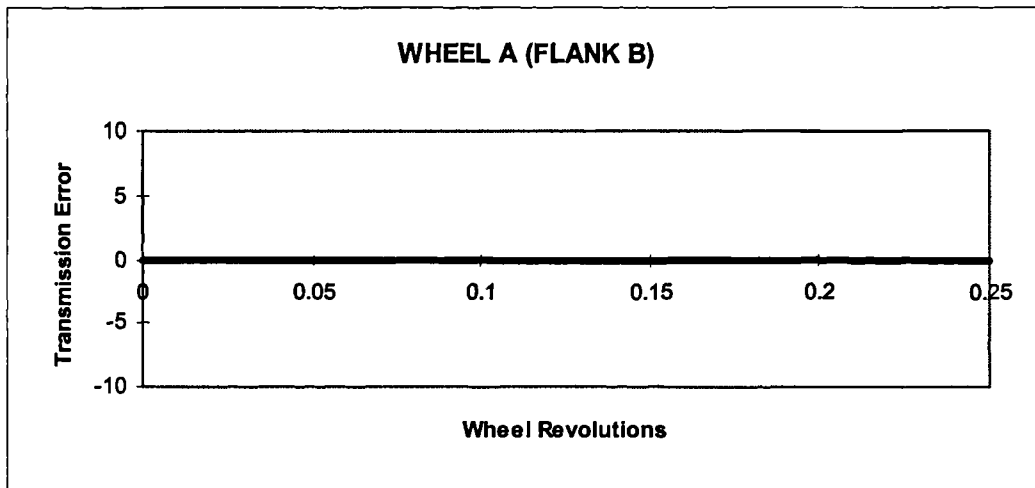
WHEEL A (FLANK B)

Figure 5.19 :   Theoretical transmission error for Wheel A (Flank B).
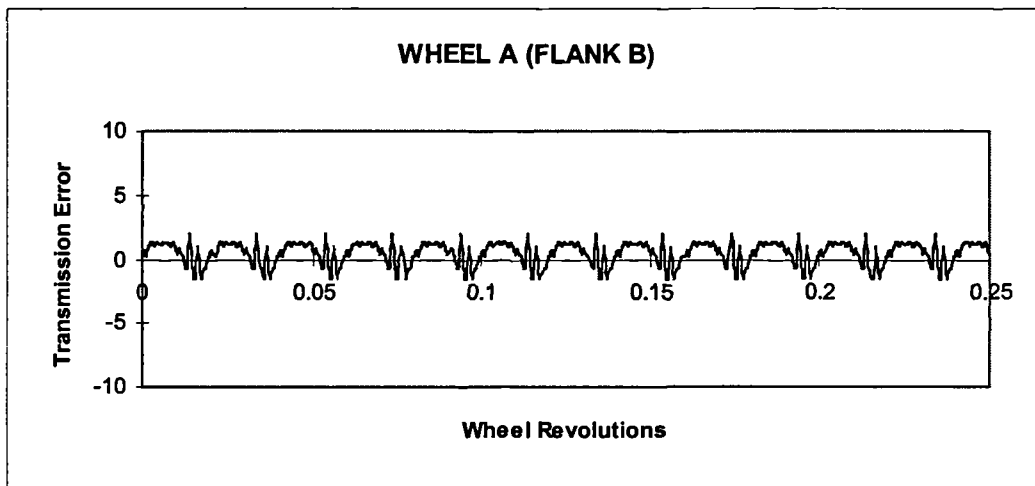
WHEEL A (FLANK B)

Figure 5.20 :   Synthesised transmission error for Wheel A (Flank B).
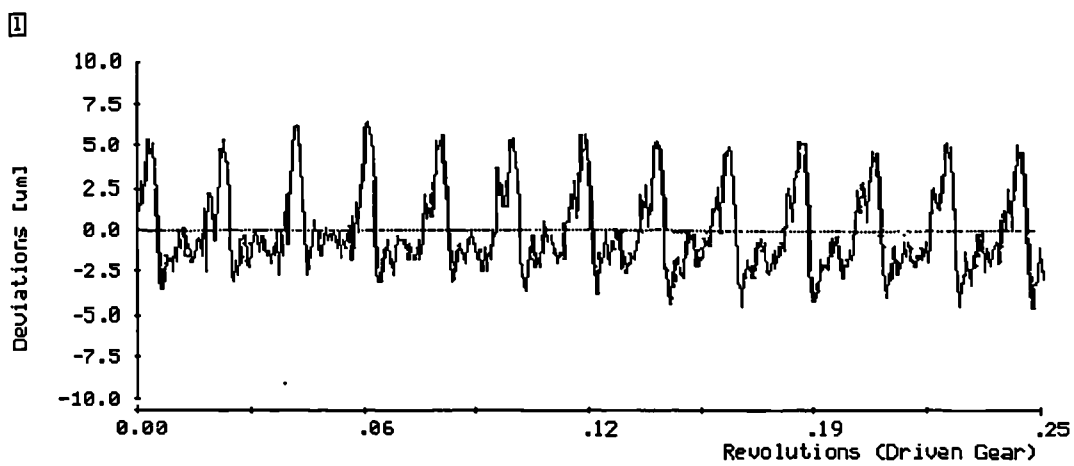
Figure 5.21 :   Measured transmission error for Wheel A (Flank B).

5.4.3. Computer model predictions for a manufactured standard design gear set

The second set was a standard full design including all the mismatch parameters which would be included in a design process to make an operational gear set. The analysis of gear set characteristics performed for Wheel A was repeated for the set using Wheel B. Predictions of theoretical and synthesised gear set characteristics were made by the new software and compared to the measured data. The theoretical, synthesised and recorded contact marking patterns for this wheel are shown in Figures 5.22, 5.23, and 5.24 respectively. Also, the transmission error results are shown in Figures 5.25, 5.26, and 5.27 respectively for Flank A, and Figures 5.28, 5.29, and 5.30 for Flank B.

An immediate observation taken from these results is that the synthesised contact markings are significantly different from those intended by the theoretical design. The most likely source of this is cutter profile error. For Flank B up to 50% of the tooth contact is lost. This may have a significant effect on initial stress on the tooth if it were to be driven under a torque load. Despite being different from the theoretical calculations, the synthesised predictions are a good representation of the recorded markings.

There is a significant increase in transmission error from 2μm magnitude in the theoretical design to 8μm magnitude in synthesised calculations for Flank B and 6μm magnitude for Flank A. Again the synthesised transmission error represents the measured error well with a magnitude correlation to within 1.5μm. The wave signal forms show good correlation in Flank A, but only a fair similarity in Flank B as the minor of the two measured peaks is just evident in the synthesised results, but has not been completely defined.
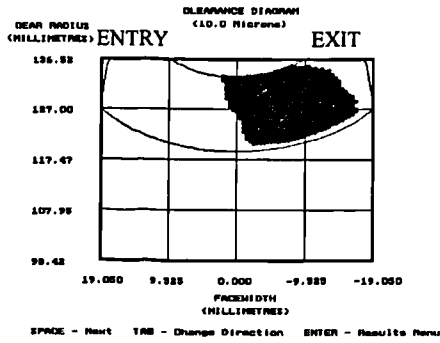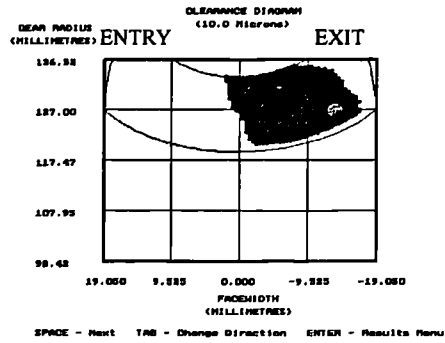
Figure 5.22 :   Theoretical marking patterns for Wheel B.
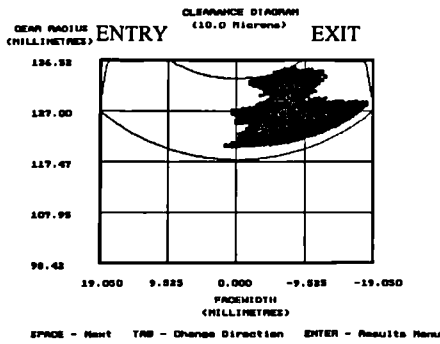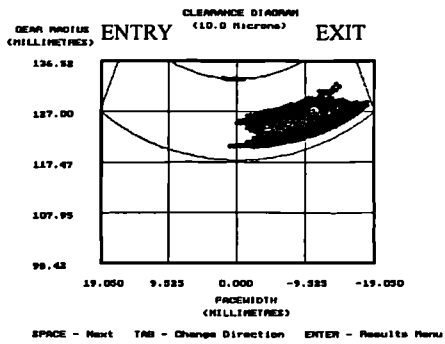
Figure 5.23 :   Synthesised marking patterns for Wheel B

Figure 5.24 :   Measured marking patterns for Wheel B.
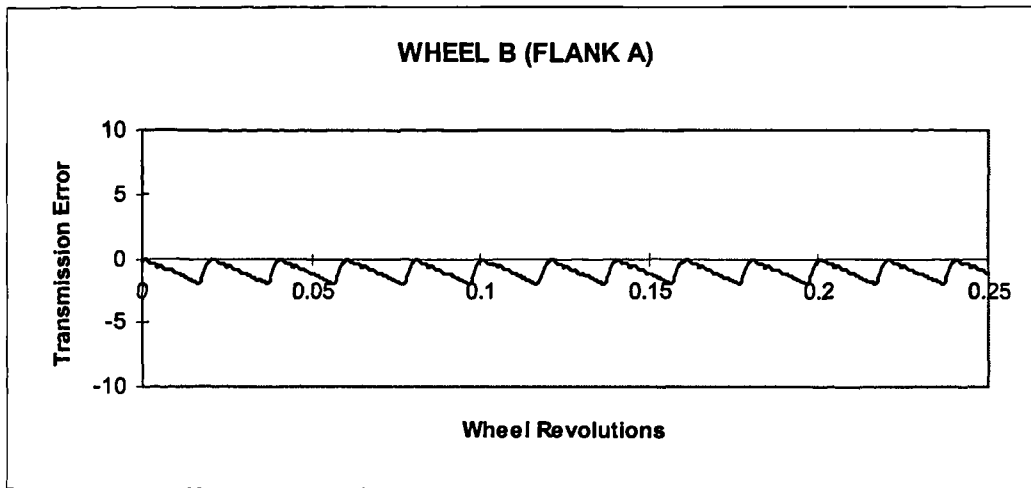
Figure 5.25 : Theoretical transmission error for Wheel B (Flank A).
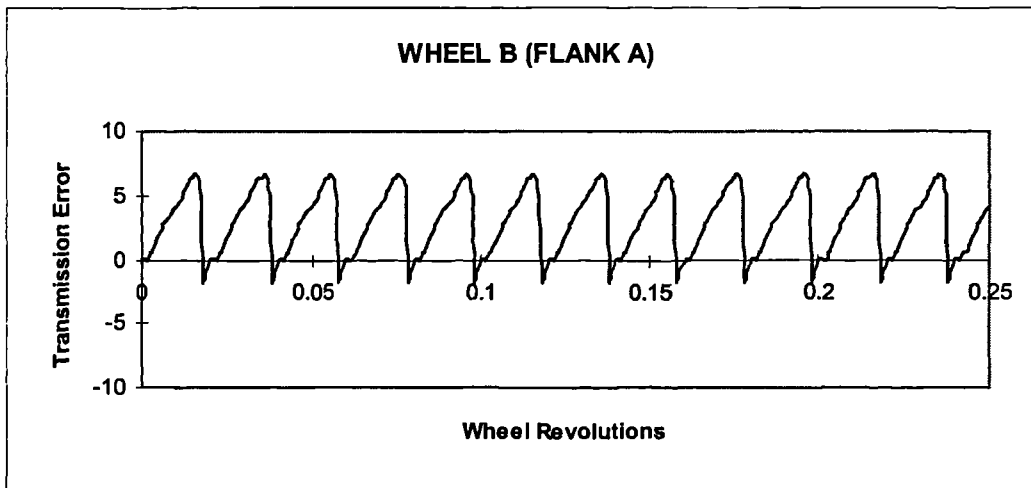
Figure 5.26 : Synthesised transmission error for Wheel B (Flank A).
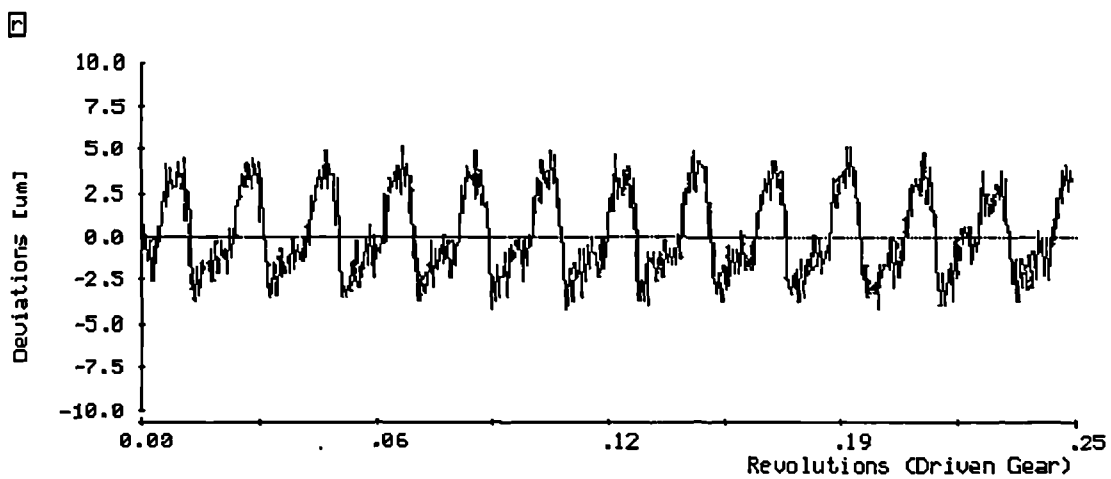
Figure 5.27 : Measured transmission error for Wheel B (Flank A).
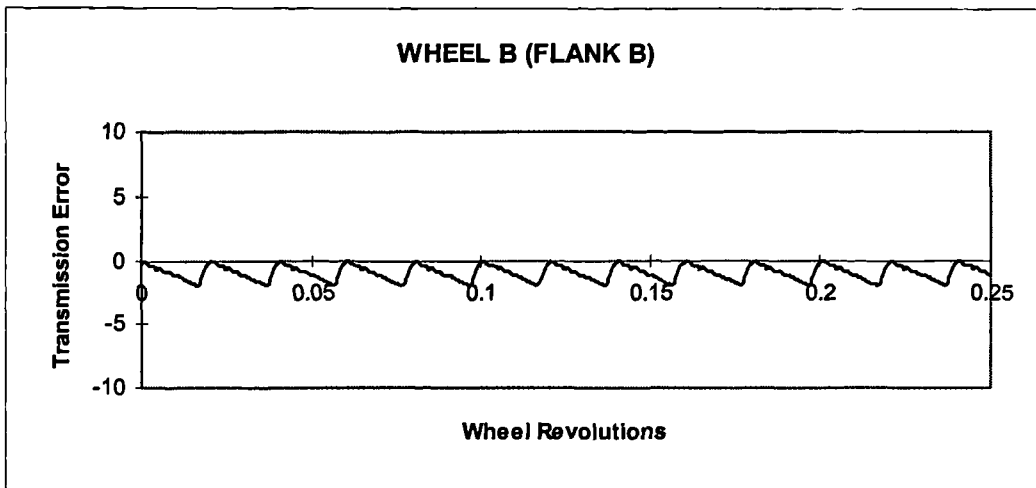
Figure 5.28 :   Theoretical transmission error for Wheel B (Flank B).
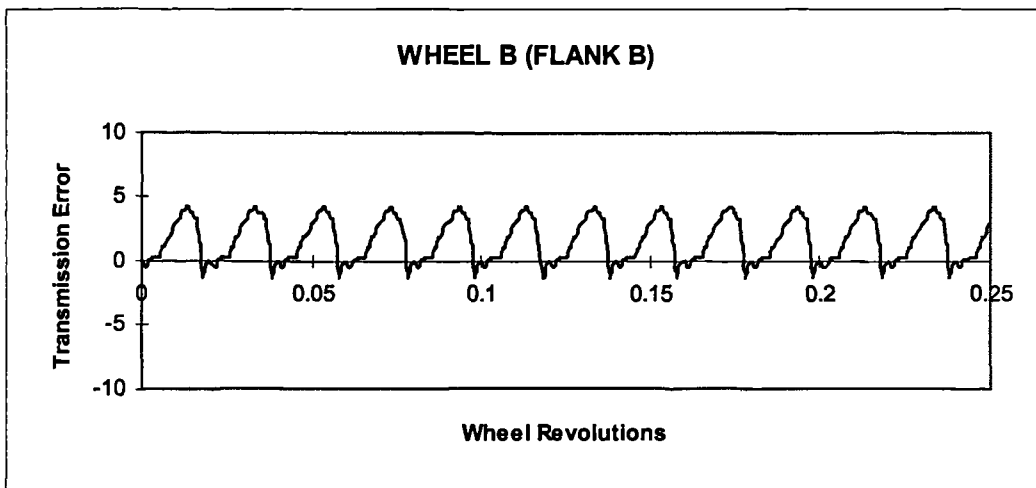
Figure 5.29 :   Synthesised transmission error for Wheel B (Flank B).
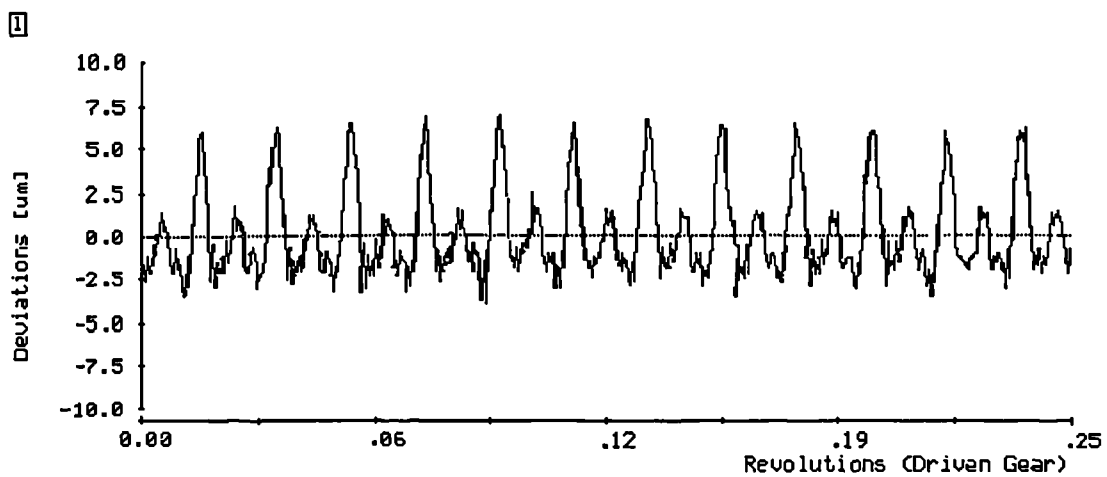
Figure 5.30 :   Measured transmission error for Wheel B (Flank B).

5.5.   CORRELATION OF CONTACT MARKING WITH MULTI-START DESIGN SPECIFICATIONS

In industrial worm gear production it is often necessary to produce a worm with more than one thread because of the fixed range of module values used, or to achieve a specific ratio.   These are referred to as multi-start gear sets and are generally characterised by a high lead angle value of 7° or more. It is possible to manufacture gear sets with worm forms containing around 20 threads.   The analysis of worm gear contact defined in section 2.4.3 relied on the three stated assumptions in the relationship of the worm rack and wheel profile when defining the geometry to calculate contact conditions.   The inherent exaggerated curvature of a multi-start design may affect these fundamental assumptions by causing a relatively large difference between the paths of contact of the worm and wheel cutter in each rack section.

To investigate this effect some sample marking patterns from industrial sources were gathered for operating gear sets with multi-start specifications, although it was not possible to obtain transmission error plots or measure error sources for these gear sets to make synthesised predictions of characteristics.   These were compared with theoretical predictions of contact marking made by the new computer program based upon the gear design information. The comparison of predicted and recorded contact marking pattern for a 56:3 ratio design is shown in Figure 5.31, while Figure 5.32 shows the comparison for a 59:5 ratio design. From the comparisons it can be seen that a close contact marking simulation is achievable for worm designs with up to 5 threads. This suggests that the assumptions in the theory necessary for calculating clearance can still be applied under these conditions. The specifications for these designs are listed in Appendices D/5 and D/6 respectively.
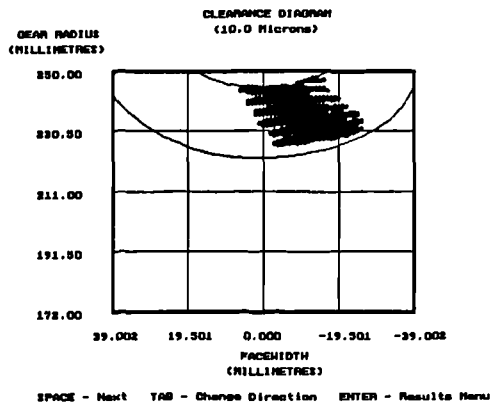
Figure 5.31 :   Comparison of a theoretical and recorded marking pattern for a 56:3 ratio worm gear set.
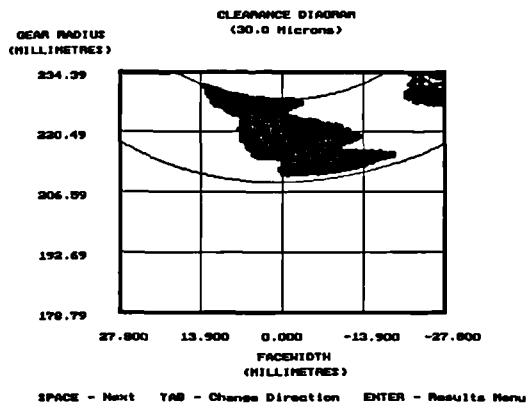
Figure 5.32 :   Comparison of a theoretical and recorded marking pattern for a 59:5 ratio worm gear set.

5.6. SUMMARY

The theoretical calculations of gear tooth relief, transmission error, and clearance have been validated against several independent sources. This has been confirmed using existing designs obtained from published literature and arbitrary new designs chosen from industrial design libraries.

The results in this chapter have shown that including measured error sources has a calculable and visible influence on the resulting characteristics. The synthesised analysis has been a far more accurate representation of contact characteristics. There is a strong correlation between the synthesised and measured marking pattern. There is not such a precise correlation for every case for transmission error magnitude, but the majority of the results agree to within 2μm.

Differences in marking pattern can be attributed to a combination of inconsistency in ink thickness and the exaggerated marking area produced by the computer display method within the software. The reason for any difference in transmission error wave form may be due to wheel cutter profile wear in the range of 1-2μm during the wheel cutting process and in general the manufacturing error sources used with the synthesised model were in the order of only a few microns. Also, the use of discrete measurement points does not fully describe the continuous wheel tooth surface. Undetected errors may have created variations in the actual contact conditions resulting in unexpected peaks relative to the calculated wave form. When making comparisons of this kind it should be taken into consideration that the Co-ordinate Measuring Machine (CMM) profile and other error measurements have typical tolerances of ±2μm and that there are some inherent misalignment tolerances of ±25μm in the worm gear system upon assembly. A further significant source of discrepancy may come from the simulation of worm lead error effects within the contact model. Research into these factors is necessary for the development of a more complete model of worm gear contact.

The results show that the software is a good contact mesh model once given the correct contact conditions. This suggests that the software is a good tool for both gear set analysis and development as it allows experimentation in existing or new worm gear design techniques, investigations into individual error effects on contact conditions, and assessment of tolerance to error sources for a particular application before production.

6.   TEST RIG DEVELOPMENT

6.1.   INTRODUCTION

A test rig was designed and constructed by Holroyd, one of the collaborating companies, to investigate the transmission error behaviour of a worm gear set during operation under load. Several items of data acquisition equipment were fitted to this test rig to record operating characteristics.

The test rig enabled an investigation of worm gear transmission error under load to be carried out for several gear designs and operating conditions. Using the measurements recorded by the data acquisition equipment, it was possible to isolate the component of the transmission error due to deformation of the worm thread and wheel tooth while under a torque load. The accuracy of the equipment allowed a model of contact characteristics under load to be developed for use with the new software.

6.2.   THE TEST GEAR BOX ASSEMBLY

6.2.1.   The test gear box elements

A cross section through the design is shown in Figure 6.1 with the worm and wheel mounted in position. The test gear box structure is very rigid in order to limit the effect of case distortion due to load. The rigid construction imposes a limit on the possible dimensions of test gear sets to designations which are based upon a single centre distance. The final design was manufactured to hold a gear set with 152.4 mm (or 6") centre distance. It is possible to introduce small variations in centre distance by placing or removing shim plates between the mating surfaces of the worm and wheel housings. It is also possible to adjust the centre height of the gear set by using slip gauges to change the alignment of the worm housing relative to a reference surface as shown in Figure 6.2 representing the view of the test box along the worm axis.
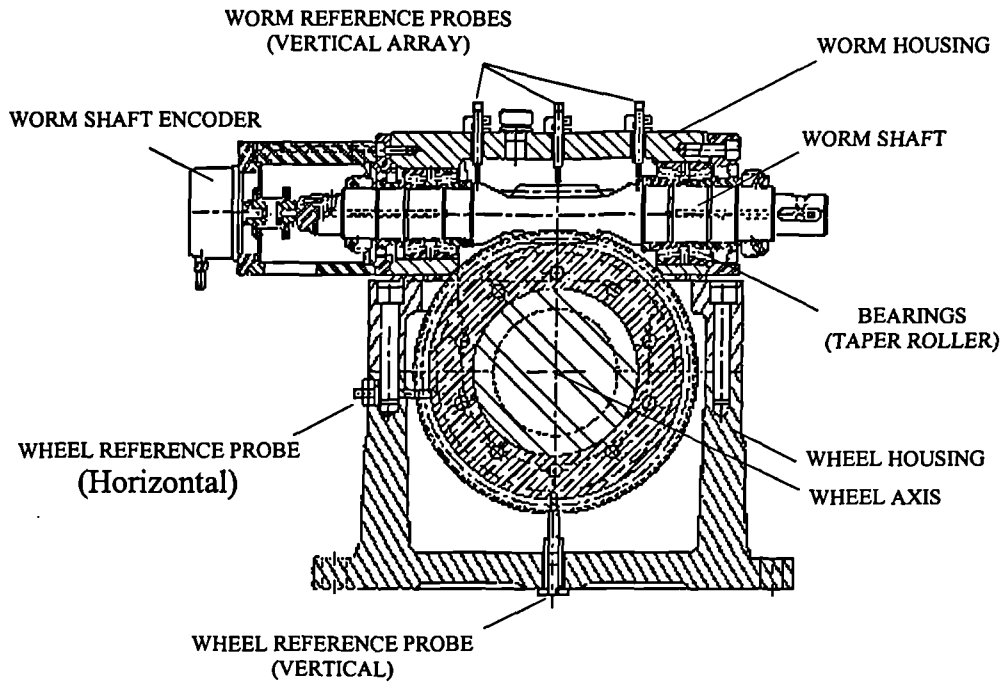
Figure 6.1 : A section through the worm gear test box of the test rig with the gear set viewed along the wheel axis.
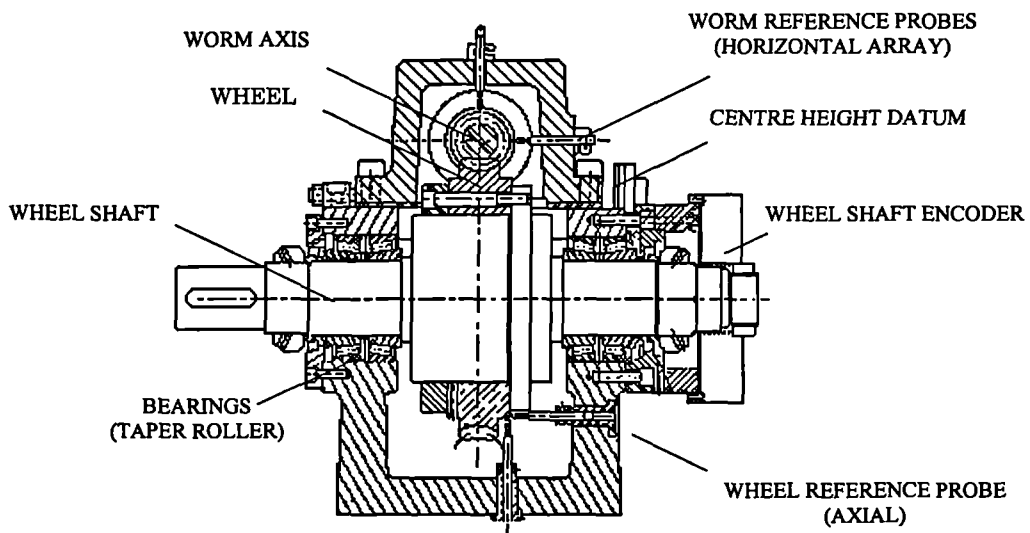
Figure 6.2 : A section through the worm gear test box of the test rig with the gear set viewed along the worm axis.

The worm and wheel shafts are mounted in the housings using double row taper roller bearings as used for machine tool spindles. The table in Figure 6.3 shows the stiffness values for these bearings.

COMPONENT	BEARING TYPE	RADIAL STIFFNESS (N/μm)	AXIAL STIFFNESS (N/μm)
Worm	Free	1120	90
Worm	Fixed	1360	130
Wheel	Free	1640	120
Wheel	Fixed	1640	120

Figure 6.3 :   A table of the stiffness values for the taper roller bearings used in the test rig to hold the worm and wheel shafts.

The test box assembly has comprehensive data acquisition equipment. Probes are mounted in several key positions on the test box to monitor the movement of the components of the gear system and their housings during operation. The diagrams of the test box show the probes which were set to run against the reference bands of the gear set to monitor the radial displacement in each component and the deflection under load leading to misalignment and eccentricity. Digital rotary encoders monitor relative angular position of the worm and wheel shafts as shown in the section viewed along the wheel shaft and the worm shaft of Figure 6.2 and Figure 6.3 respectively. The data from these encoders is collected and processed for analysis by a computer system which records the differential between a transmitted and expected number of square wave pulse signals to determine the transmission error.

The recorded measurements from the data acquisition equipment were used to identify the changes in contact conditions of the gear set and investigate the consequences on transmission error for a given torque load applied by the test rig assembly.

6.2.2. The probe unit

Movements of the gear set components and distortion of the test gear box housing are recorded using probes. Initially two types of probe system were assessed to measure these displacements while operating under a torque load. The first probe system monitors changes in eddy currents set up in the target surface, while the second measures by direct contact using linearly varying displacement transducers (or L.V.D.T.) probes. The eddy current probe system was rejected because of problems in measuring displacements repeatable to less than $10\mu m$ and the fact that the response became erratic or collapsed when the probe was not directed at exactly 90° to the target surface. Using the LVDT probes it was possible to make measurements repeatable to within $1\mu m$ accuracy. The measurements were recorded on a visual display gauge and on thermal strip paper. These were used to investigate the extent of movement in the gear set and assess the impact of the change in contact conditions.

6.2.3. Digital encoders for the input and output shafts

The input and output shafts of the test gear box are fitted with digital rotary encoders produced by Heidenhain. The worm shaft encoder was a ROD 250 model producing 18000 signal pulses per revolution. The encoder mounted on the wheel shaft is a RON 806 model with 36000 signal pulses per revolution. This wheel encoder signal is passed through a 702B EXE unit, also produced by Heidenhain, which produced a 25 fold interpolation quadrature signal. The resulting rotary accuracy of this system is around 0.3 arc seconds. Each encoder contains one marker pulse signal which can be used as a reference angular position while recording shaft movement. The reference marker on the wheel shaft encoder was used during the test rig operation to ensure that the measurements of transmission error were referenced to the same wheel angular position for each test. To facilitate the positioning of the encoders during a change of gear set they are fixed by doweling to ensure correct mounting within tolerances upon reassembly of the box.

6.2.4. The computer and data processor

A GFM computer, model GP-30, was used to collect, store and analyse the data provided by the encoder units mounted on the worm and wheel shaft of the test gear box. The transmission error over several gear revolutions in either direction can be monitored. The backlash for a gear set can also be recorded by continuously measuring the difference in signal pulses for a single gear rotation in both directions at a series of target angular positions. For any test the measured data values and the Fourier series analysis of the recorded transmission error wave can be written to a MS-DOS file on diskette for further analysis.

6.2.5. Rotary shaft speed indicator.

The digital encoders connected to the input and output shaft of the test box are capable of indicating rotary speed. This can be displayed by the computer screen. To initially validate this system, an independent shaft rotary speed indicator was fitted to the rig. The rig was run at input speeds of 100-300 rpm in 50 rpm intervals. The values displayed by these two systems for the worm shaft rotary speed agreed to within 0.1 rpm over the testing period. The speed indicator was necessary to check the hydraulic brake gear pump characteristics and was used extensively in controlling the operating conditions while recording transmission error under load.

6.3. THE TEST RIG ASSEMBLY

6.3.1. The test rig components

The test gear box is fitted to the other elements of the test rig as shown in Figure 6.4. The drive input is supplied by a 4kW geared motor which develops 2.2kW @ 1440 rpm. The geared system connected to this motor reduces the rotary speed by a 3.9:1 ratio which limits the input to the worm shaft to between 50 and 370 rpm. The output from the test box is transmitted to a speed step-up helical gear box with a 1:49.07 ratio. This in turn is connected to a braking system which generates a torque load. The torque is measured using a strain gauge arrangement mounted on the coupling shaft between the output shaft of the test box and the step up box, as shown in Figure 6.5.

6.3.2. The hydraulic brake system

The brake system comprises a gear pump attached to the output shaft of the step-up box circulating 320 cSt. oil from a 420 lt. reservoir. The oil flow returning to the tank passes through a pressure relief valve. This valve is used to impose a restriction on the flow which causes a pressure build up in the oil pipe generated by the gear pump action. The pressure build up induces a torque in the gear pump which is transmitted back through the gear system. Changes in the pressure level through the valve are indicated by a pressure gauge mounted on the return to the tank.

The pressure relief valve is fitted to a housing, shown in Figure 6.6., and initially had an operating pressure range of 7 - 25 bar. Oil pressure in the valve is controlled by turning a screw on the valve unit, as shown in Figure 6.7, which compresses an internal spring. The resulting force in the spring restricts the movement of an oil seal covering several venting holes. Oil entering the valve has to achieve the equilibrium pressure required to compress the spring enough to expose the venting holes to the cavity before flow can continue. A gauge inserted into the housing unit registers the pressure.

PRESSURE GAUGE

PRESSURE RELIEF VALVE

HYDRAULIC BRAKE OIL
(RESERVOIR)

4 KW MOTOR

INPUT SHAFT COUPLING

TEST GEAR BOX

OIL FLOW   GEAR PUMP   STEP-UP BOX
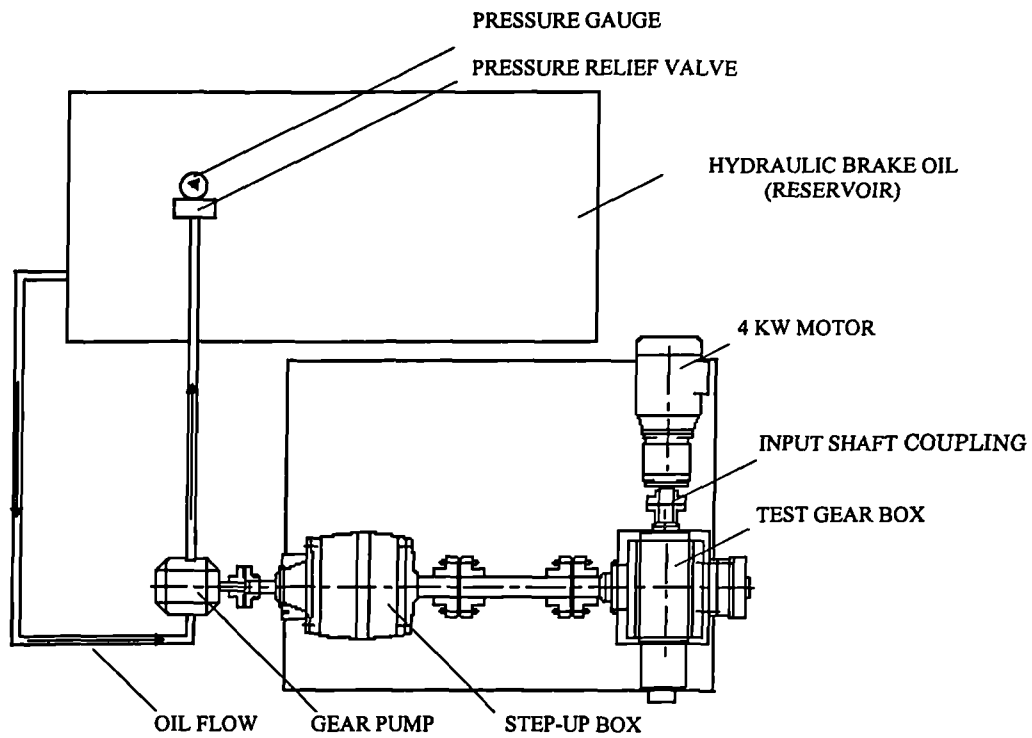
Figure 6.4 :   The test rig assembly top elevation.

STEP-UP BOX

OUTPUT SHAFT
COUPLING

GEAR PUMP

TEST GEAR BOX

FRAME
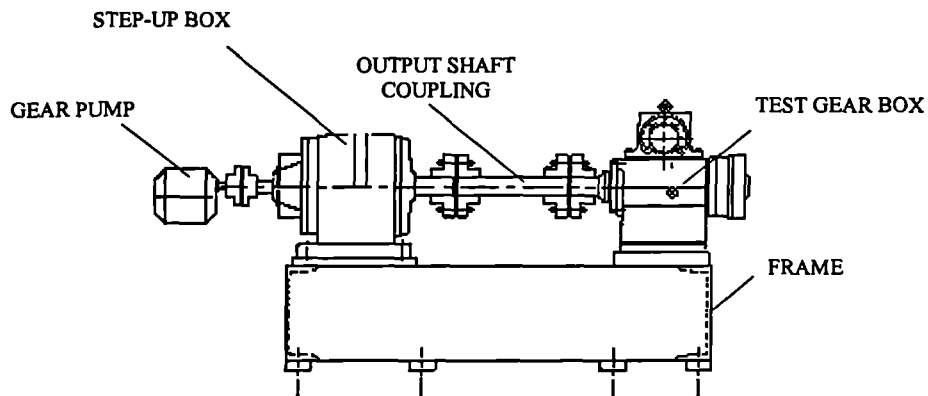
Figure 6.5 :   The test rig assembly side elevation.

PRESSURE RELIEF VALVE

VALVE HOUSING UNIT

OIL FLOW OUT

TAPPED HOLE
(CONNECTION TO TANK)

TAPPED HOLE
(PRESSURE GAUGE)

TAPPED HOLE
(CONNECTION TO RETURN FLOW)

OIL IN
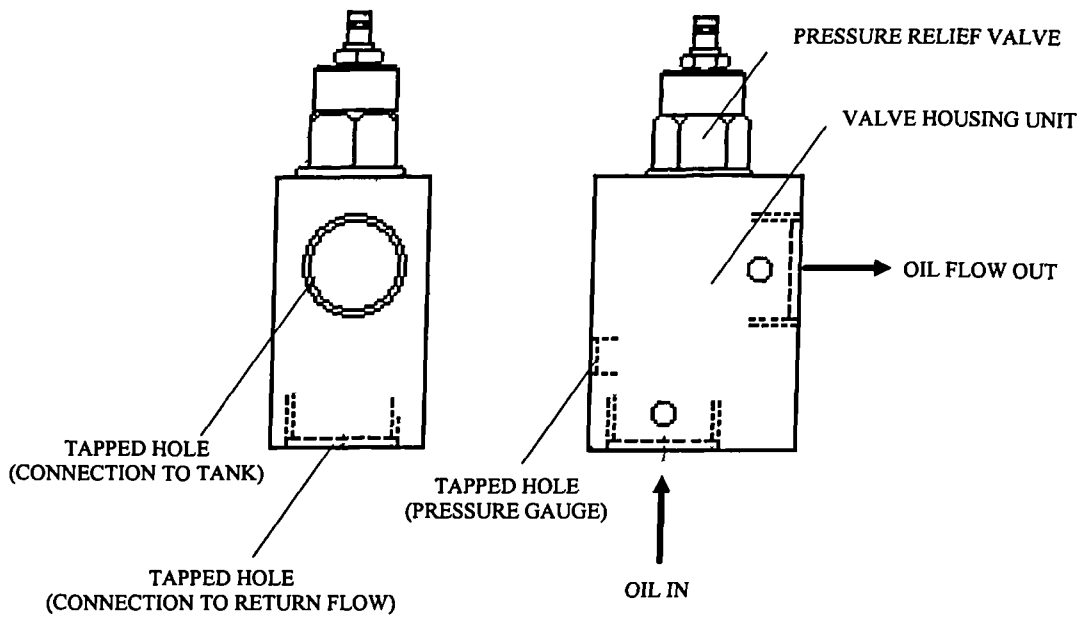
Figure 6.6 :   The Housing For The Pressure Relief Valve.

ADJUSTING SCREW THREAD

INTERNAL CAVITY

SPRING

OIL SEAL

FLOW INTO HOUSING UNIT

VENTING HOLE

FLOW FROM RETURN HOSE
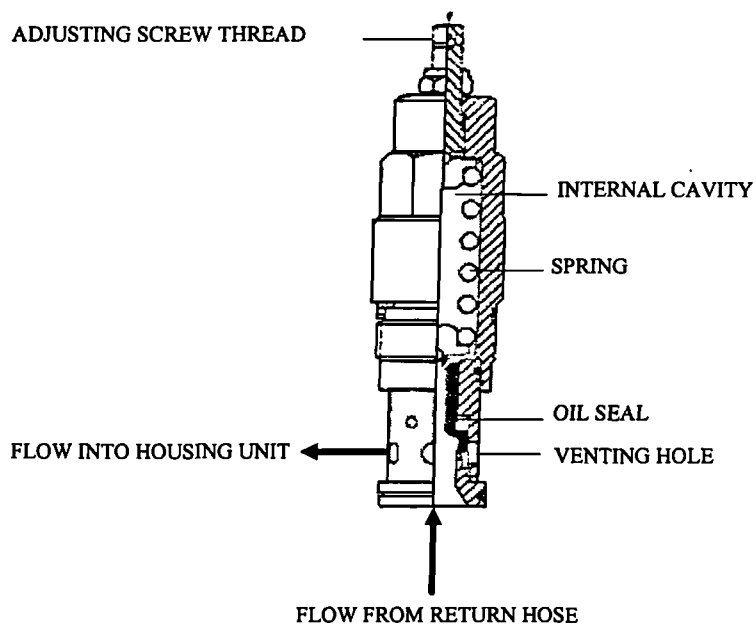
Figure 6.7 :   The Pressure Relief Valve Of The Hydraulic Brake System.

6.3.3. The test rig torque meter

6.3.3.1. Electrical calibration of the torque meter

Four strain gauges are arranged as a Wheatstone Bridge circuit on the output shaft connecting the test box to the step up box. Two 45° chevron strain gauges of equal resistance, R_{g1-4}, are mounted on either side of the output shaft from the test box. Resistors pairs R_{g1} R_{g2} and R_{g3} R_{g4} are mounted diametrically opposite on this shaft. This active 4 gauge formation then eliminates any bending effects within the readings so that only pure torque is registered.
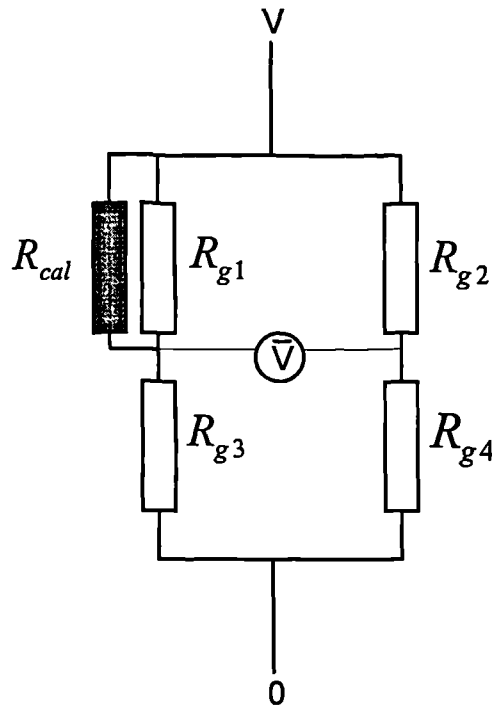
Figure 6.8 :   The 4 strain gauge Wheatstone bridge arrangement used by the torque meter and the calibration resistor.

The calibration was performed using a simulation resistor. A resistor of specific value, R_{cal}, was placed in the circuit as shown in the Figure 6.8 arrangement. An induced voltage differential, $\bar{V}$, was registered across the gauges. This represented the calibration voltage drop across the resistor bridge needed to simulate the defined 2500 Nm torque value. The calibration resistor was then removed. Any torque applied to the output shaft was represented by a linearly proportional change in this voltage drop reading.

The process for calculating a resistance value to simulate the operating conditions in the circuit is as follows. The first step is to calculate the principal stress, σ, of the shaft under these conditions. This was then used to calculate the principal strain, ξ_p, resulting from a 2500 Nm calibration torque. The equations and values necessary for this were obtained from Parker[71], and define the following relations :

$$\sigma = \frac{16M}{\pi d^3} \qquad (1)$$

$$\xi_p = \frac{\sigma(1+\upsilon)}{E} \qquad (2)$$

Where :

M	= CALIBRATION TORQUE	= 2500 Nm
d	= SHAFT DIAMETER	= 60 mm
E	= YOUNG'S MODULUS	= 2.13×10^{11} Pa
ν	= POISSON'S RATIO	= 0.333

When substituting these values and the relationship in (1) into (2) this gives :

$$\xi_p = \frac{4 \times 16 \times M}{3 \times \pi \times (d \times 10^{-3})^3 \times E} = 369 \times 10^{-6} \qquad (3)$$

Using the equations found in Perry & Lissner[72] the value of the calibration resistor needed to represent this calibration torque condition for the output shaft is then calculated :

$$R_{cal} = \frac{R_g}{\xi_{Tot} \times G_f} - \frac{R_g}{2} = \frac{R_g}{\xi_p \times 4 \times G_f} - \frac{R_g}{2} \qquad (4)$$

R_g	= STRAIN GAUGE RESISTOR VALUE	= 1000 Ω
G_f	= STRAIN GAUGE FACTOR	= 2.105
ξ_{Tot}	= COMBINED STRAIN	= $\xi_p \times 4$

When substituting these values and the relationship in (3) into (4) this gives :

$$R_{cal} = \frac{1000}{0.001476 \times 2.105} - \frac{1000}{2} = 321 k\Omega$$

6.3.3.2. Torque meter validation through mechanical calibration

The electrical calibration method used in the test rig facilitated a quick and easy method of ensuring a consistent record of torque reading. However, the multiple calculations involved in the process of defining a calibration value and the potential error tolerances in the stated values for each parameter made it necessary to validate the electrical system of calibration. This was done by comparing a series of meter readings with a known mechanical torque.

The mechanical torque was applied by mounting a lever arm in the horizontal position to the coupling bar of the output shaft. A series of known masses were suspended from this bar at a recorded distance from the shaft axis. The resulting torque was calculated and compared to the readings registered by the torque meter system.

The results are shown in table in Figure 6.9 with the graph shown in Figure 6.10 showing this relationship over the full range of the electrical and mechanical calibrations. It can be seen from the results that the electrical calibration gives a reading correct to within 2-3% of the actual torque value. The method was thus deemed to be an acceptable for future test rig calibration.

Mass (kg)	Applied Torque (Nm)	Registered Torque (Nm)	Error (%)
0	0.00	0.00	0.00
10	82.50	85.00	2.33
20	165.00	170.00	2.63
30	247.00	252.50	2.02
40	329.50	335.00	1.55
50	412.00	420.00	1.83
60	494.50	502.50	1.54
70	577.00	590.00	2.16
80	659.00	670.00	1.61
90	741.50	757.50	2.09
100	819.00	830.00	1.30

Figure 6.9 :   A table of results recording the mechanically applied torque, the torque value registered by the torque meter, and the resulting percentage error value.
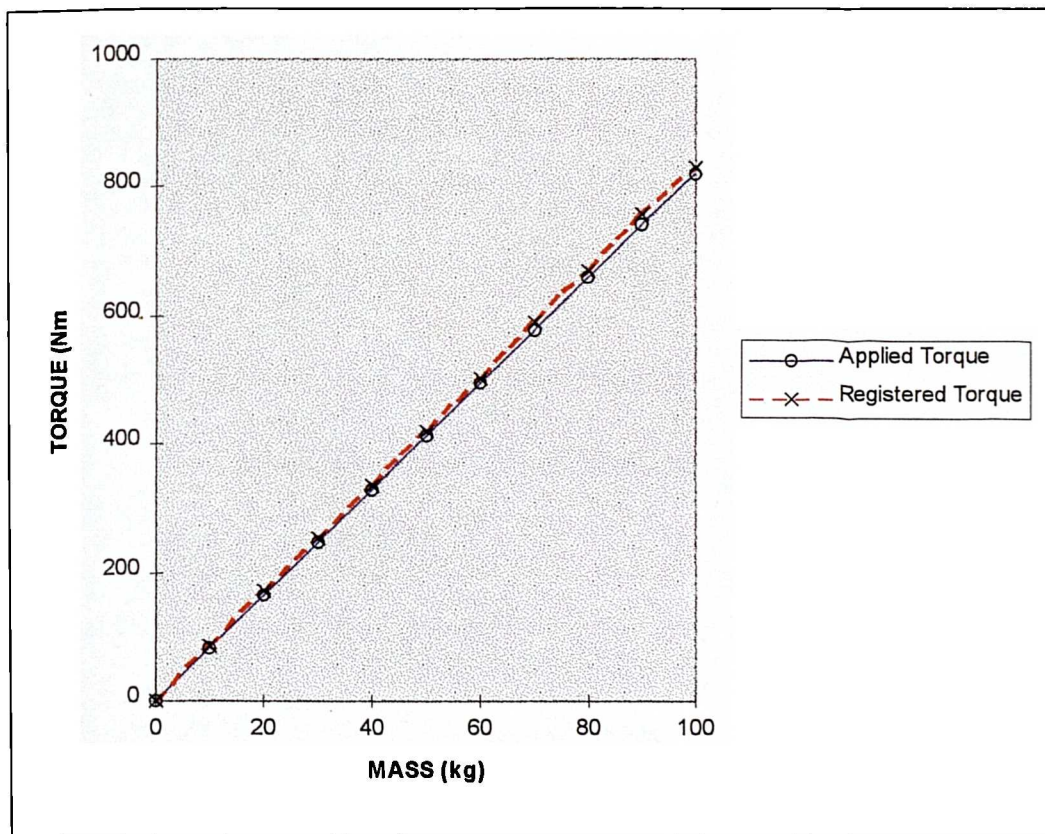
Figure 6.10 :   A graph of results recording the mechanically applied torque and the value registered by the torque meter.

CHAPTER 6

6.4. Testing initial test rig operating conditions

6.4.1. Gear pump performance characteristics

Tests were performed on the completed test rig to assess the performance of the equipment under operating conditions. A series of input shaft speed and output torque readings were recorded for a range of constant hydraulic brake oil pressures. The graphs of torque/speed and power/speed characteristics of the gear pump are shown in Figure 6.11 and Figure 6.12 respectively for values of 0, 3, 5, 6.9, and 8 bar.

The results show that the constant 8 bar hydraulic brake oil pressure represents the upper bound for recording results over a full range of operating speeds within the 2500 Nm design limit of the test rig. The results of the power/torque characteristic curve at constant 6.9 bar were found to be consistent with the manufacturer's data for gear pump characteristics.

The most significant results were represented by the 0 and 5 bar constant pressure test readings. The pressure valve used in the brake system had a main operating range of 7-25 bar pressure. Below the 6.9 bar value it was not possible to obtain a set of readings over the full range of operating speeds as shown by the constant 5 bar curve. It was not possible to operate the rig under any brake pressure below 3.5 bar without totally removing the valve. In this case a 0 bar oil pressure existed in the brake system. The curves representing the 0 bar results indicate that there was still a torque generated in the gear system which increases linearly with operating speed. This torque can be attributed to mechanical losses transmitted through the step-up box, friction generated in the bearings, and oil flow resistance through the brake pipe circuit. This is present in the development of the curves in each of the constant brake oil pressure tests.

These results indicated that the rig was operating correctly and the gear pump power/speed characteristics were performing as expected. Modifications were needed to the equipment to improve the operating range as there were some operating conditions which were not possible below the constant 6.9 bar line.
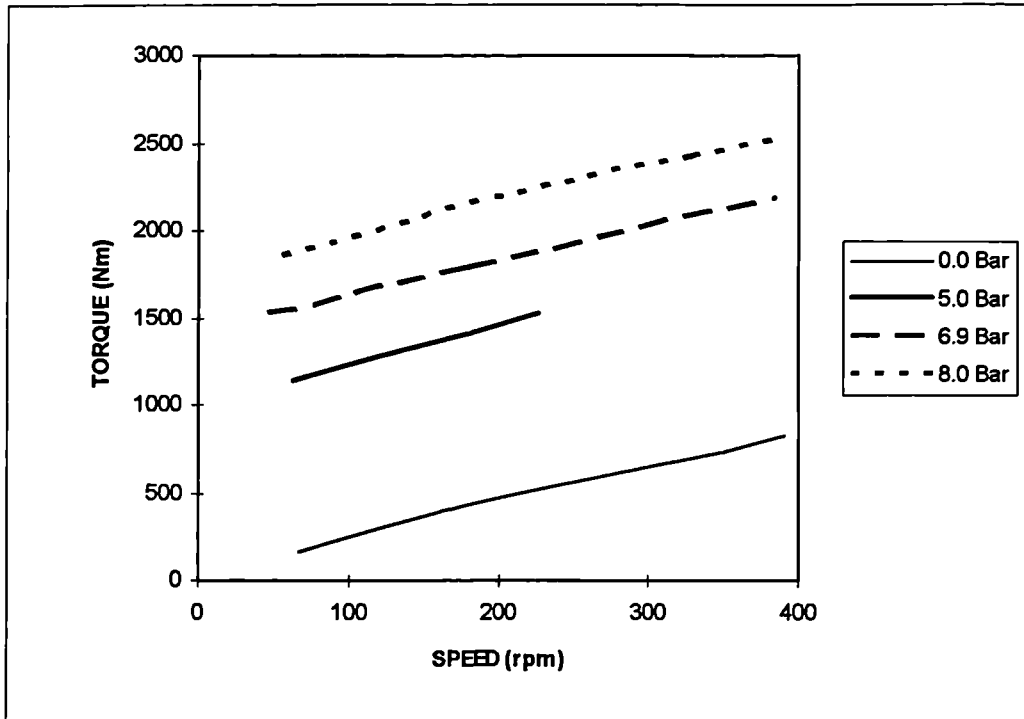
Figure 6.11 :   A graph of the torque/speed operating characteristics for the gear pump
at a range of constant brake oil pressure values.
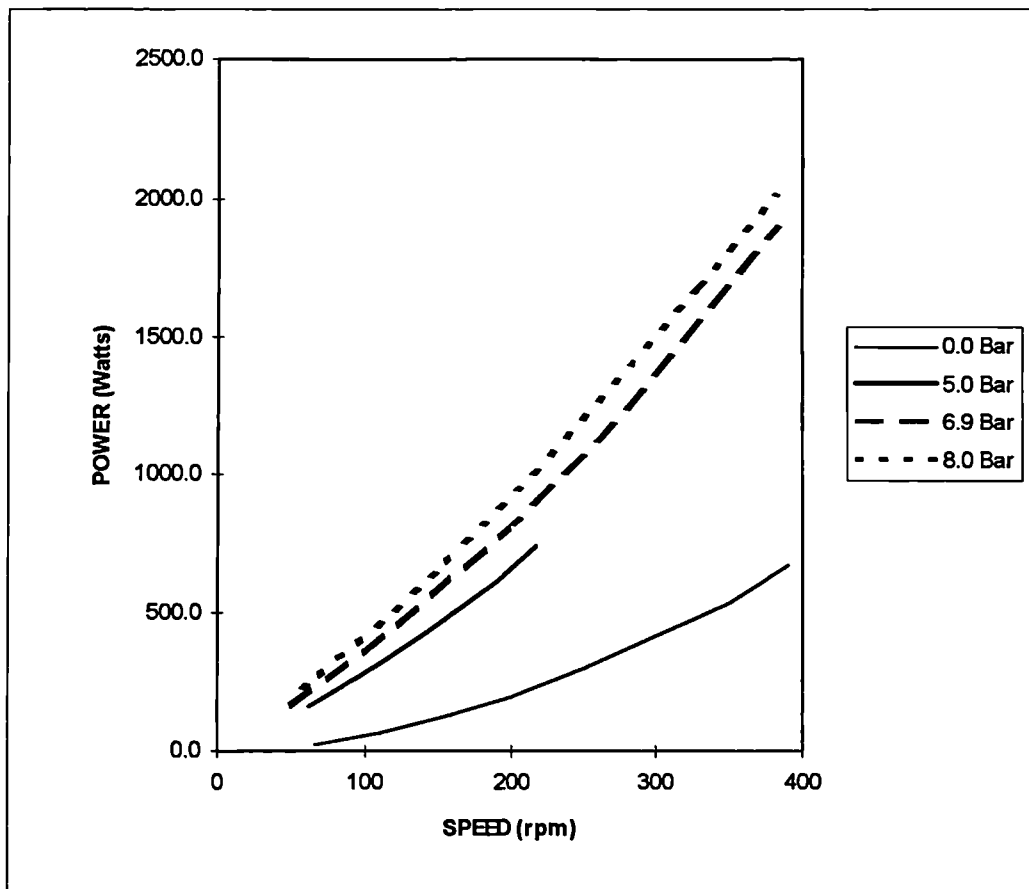
Figure 6.12 :   A graph of power/speed operating characteristics for the gear pump at a
range of constant brake oil pressure values.

6.4.2. The influence of operating time on gear pump characteristics

Tests were performed to establish the stability of the gear pump characteristics after the test rig had been operated for a period of time while driving a torque load. A range of input motor speeds and subsequent torque values were recorded for a constant 6.9 bar hydraulic brake oil pressure. The test gear box was then driven at a constant 150 rpm input shaft speed under a constant 1000 Nm torque load. The process of recording speed and torque values at a constant 6.9 bar was repeated after a 45 and 90 minute duration of operation. The data recorded at these three intervals is tabulated in Figure 6.13, while Figure 6.14 shows the graph of the calculated power/speed characteristics for the gear pump.

This series of results shows that even though the test rig was not intended to operate for periods of longer than a few minutes, initial testing indicated that the gear pump characteristics remained stable for at least 90 minutes of operation.

Speed	Angular Velocity	Pressure	Torque	Speed	Power	
(r.p.m.)	(rad/s)	(bar)	(Nm)	(output)	(Watts)	
49.1	5.142	6.9	1628	0.1028	167.4	
99.0	10.367	6.9	1713	0.2073	355.2	
200.6	21.007	6.9	1940	0.4201	815.1	0 MINS
294.3	30.819	6.9	2143	0.6164	1320.9	
384.0	40.212	6.9	2355	0.8042	1894.0	

Speed	Angular Velocity	Pressure	Torque	Speed	Power	
(r.p.m.)	(rad/s)	(bar)	(Nm)	(output)	(Watts)	
45.7	4.786	6.9	1538	0.0957	147.2	
88.4	9.257	6.9	1638	0.1851	303.3	45 MINS
178.0	18.640	6.9	1763	0.3728	657.3	
290.0	30.369	6.9	2138	0.6074	1298.6	
370.0	38.746	6.9	2285	0.7749	1770.7	

Speed	Angular Velocity	Pressure	Torque	Speed	Power	
(r.p.m.)	(rad/s)	(bar)	(Nm)	(output)	(Watts)	
38.0	3.979	6.9	1550	0.0796	123.4	
127.0	13.299	6.9	1658	0.2660	441.0	90 MINS
178.7	18.713	6.9	1738	0.3743	650.5	
280.0	29.322	6.9	2042	0.5864	1197.5	
375.0	39.270	6.9	2249	0.7854	1766.4	

Figure 6.13 :   The table of results for tests for power/speed characteristics of the hydraulic brake gear pump during operation.
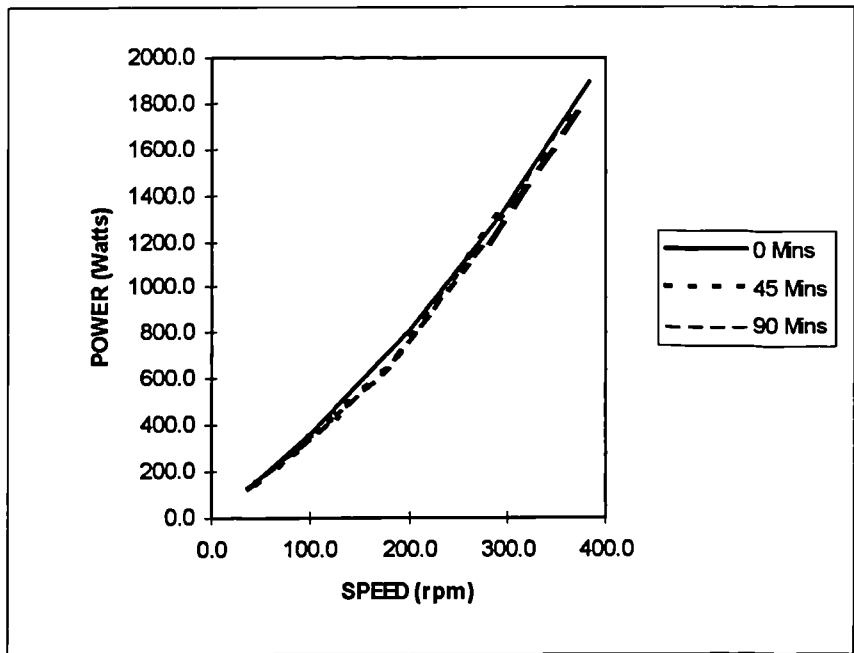
Figure 6.14 :   The change in power/speed characteristics of the hydraulic brake gear pump during operation.

6.4.3. Improving the test rig operating range through modifications to the test rig equipment

6.4.3.1. Replacing the pressure relief valve to the oil reservoir inlet

The torque supplied to the system was provided by a pressure relief valve on the flow by an adjustable valve on the inlet to the oil reservoir. The original design specification for the rig called for pressure adjustment on the brake mechanism from 0 - 10 bar. The 7 - 25 bar pressure relief valve was replaced by a new valve with a 3.5 - 16 bar range. It was then possible to obtain characteristics at constant pressure conditions as low as 2 bar over the full operating speed range of the test rig. It was not possible to reduce the torque to zero in order to operate the test gear system under no load conditions using this method alone.

6.4.3.2. Modifications to the hydraulic brake system.

The replaced pressure relief valve still induced torque in the brake system when fully opened. To compensate for this, a pipe system was designed to allow flow through the gear pump and had a facility to reduce pressure in the system. This was achieved using a valve connected to the input and output of the oil supply for the gear pump. The diagram in Figure 6.15 shows the pipe network needed to achieve this and the installation position of this oil circulation unit relative to the test rig assembly. When opened this valve creates a short circuit in the hydraulic system which bypasses the reservoir. The local circulation allowed the oil pressure in the brake system to be reduced to zero. By using this system it is possible to operate the rig at all constant hydraulic pressures from 0-8 bar through the entire operating speed of the rig and consequently lower torque. The diagram also shows the position of the two flow control valves. These allow oil to flow in both directions through the gear pump. This enables the test gear set to be driven in either direction without disconnecting the pipe system.
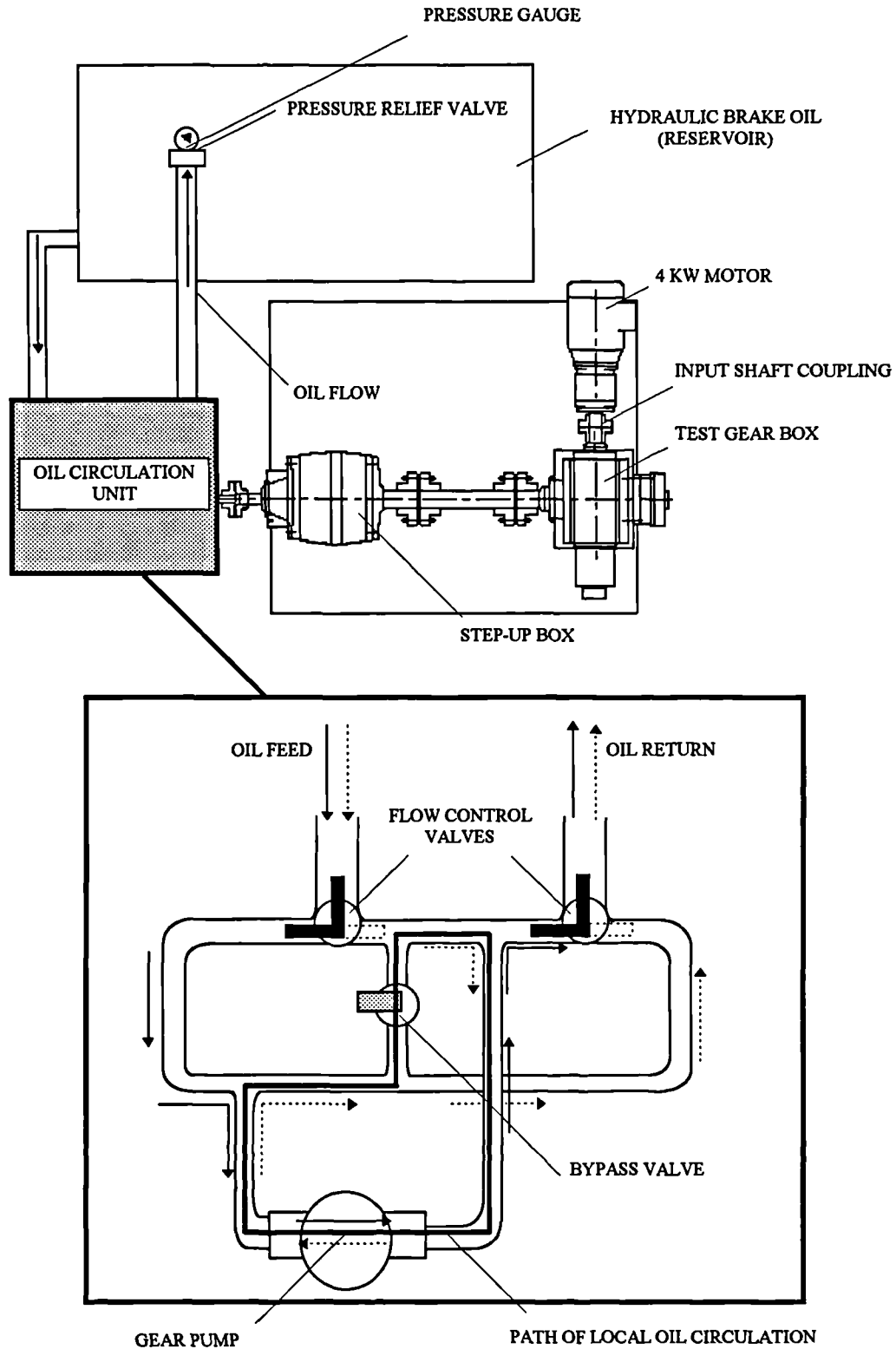
Figure 6.15 : The bypass valve pipe and flow control system as part of an oil circulation unit in the test rig assembly as viewed in the top elevation.

6.4.4. Modified gear pump performance characteristics

The assessment of the equipment using gear pump characteristics used in Section 6.4.1 was repeated to investigate the influence of equipment modifications made as a consequence of the initial testing. A range of input operating speeds and subsequent torque values were recorded for a series of constant hydraulic brake oil pressures.

The graphs in Figure 6.16 and Figure 6.17 show the torque/speed and power/speed characteristic curves at constant brake oil pressure levels of 0, 1, 3, 5, 6.9, and 8 bar. The graphs in Figure 6.18 and Figure 6.19 show the torque/speed and power/speed characteristic curves for the results recorded in the reverse direction.

Oil flow through the gear pump was reversed to expose any bias in the system creating additional torque. Torque values were recorded at a range of input operating speeds for a constant brake oil pressure of 6.9 bar. To further validate the stability of the characteristics during operation, a test was performed after the rig had driven each flank of a gear set for 4 hours at 150 rpm input shaft speed under 1000 Nm torque load. The graph of the torque/speed and power/speed characteristics under these conditions are shown in Figure 6.21 and Figure 6.22 respectively. These results were compared to the data obtained from the test rig for the initial 6.9 bar series.

The results show that using the bypass valve system dramatically improved the range of operating conditions for the test rig as demonstrated by the 1 bar curve. The reduction in the loop length of oil circulation made possible by the bypass valve short circuit reduced the torque induced by pipe friction effects. The 0 bar curve of the torque/speed graph indicates that a torque still exists. This implied that some inherent torque remains in the test rig assembly. It is only possible to operate the test gear box under zero load by removing the coupling from the output shaft to the step up box, and therefore disengaging all mechanical braking effects. The results also show that the characteristics have not changed as a result of the equipment modifications, and that there is a stability over an 8 hour operating period.
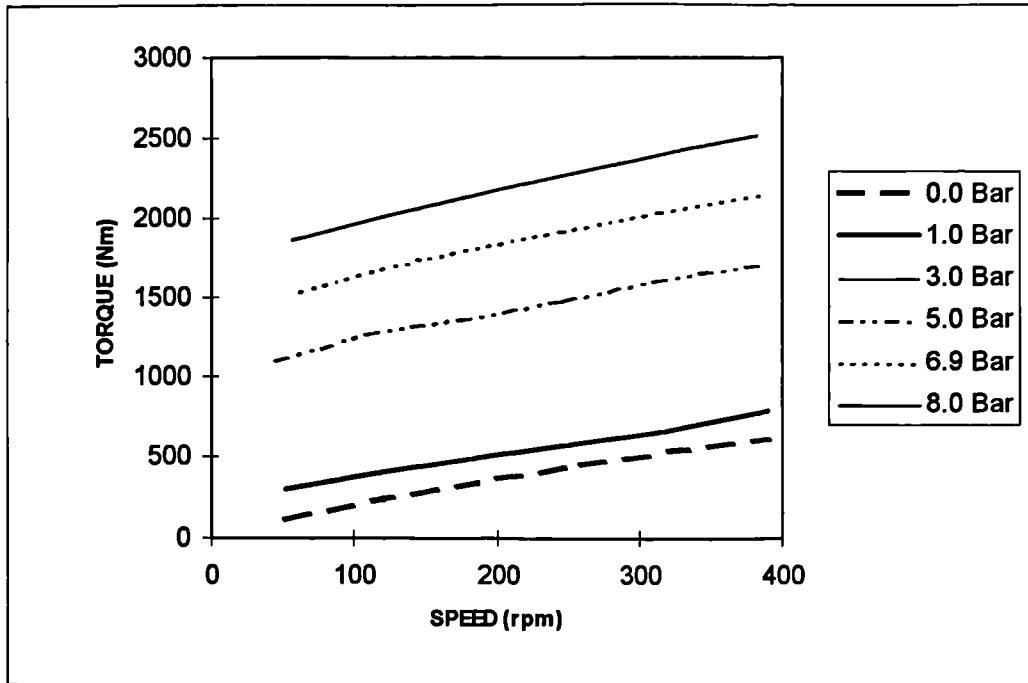
Figure 6.16 : A graph of torque/speed characteristics of the test rig brake gear pump through a series of constant oil pressure values driving in the forward direction.
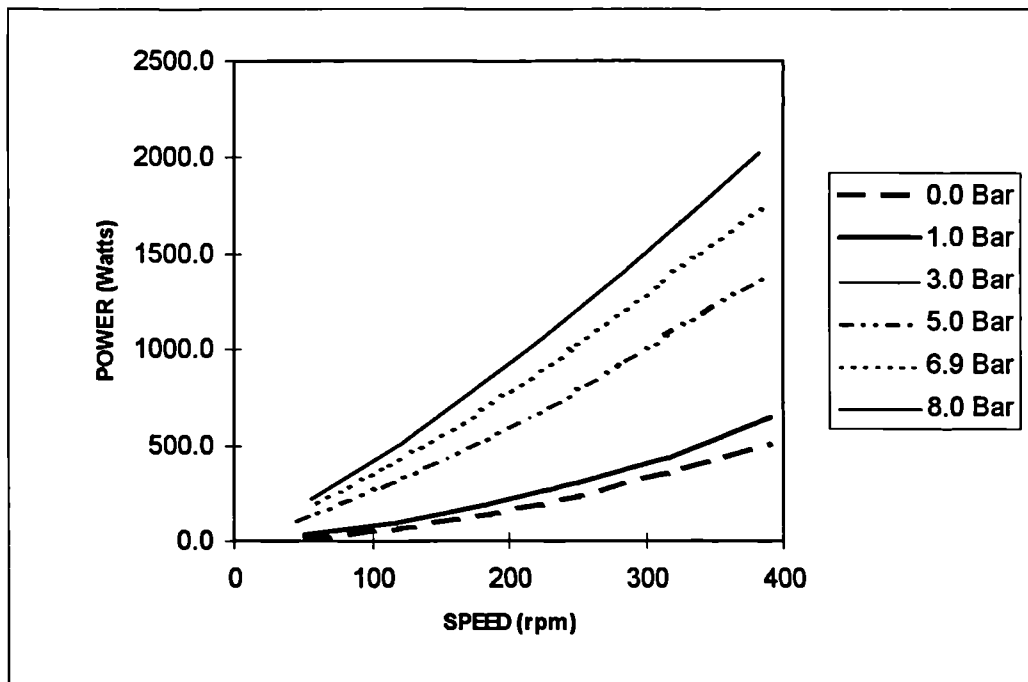
Figure 6.17 : A graph of power/speed characteristics of the test rig brake gear pump through a series of constant oil pressure values driving in the forward direction.
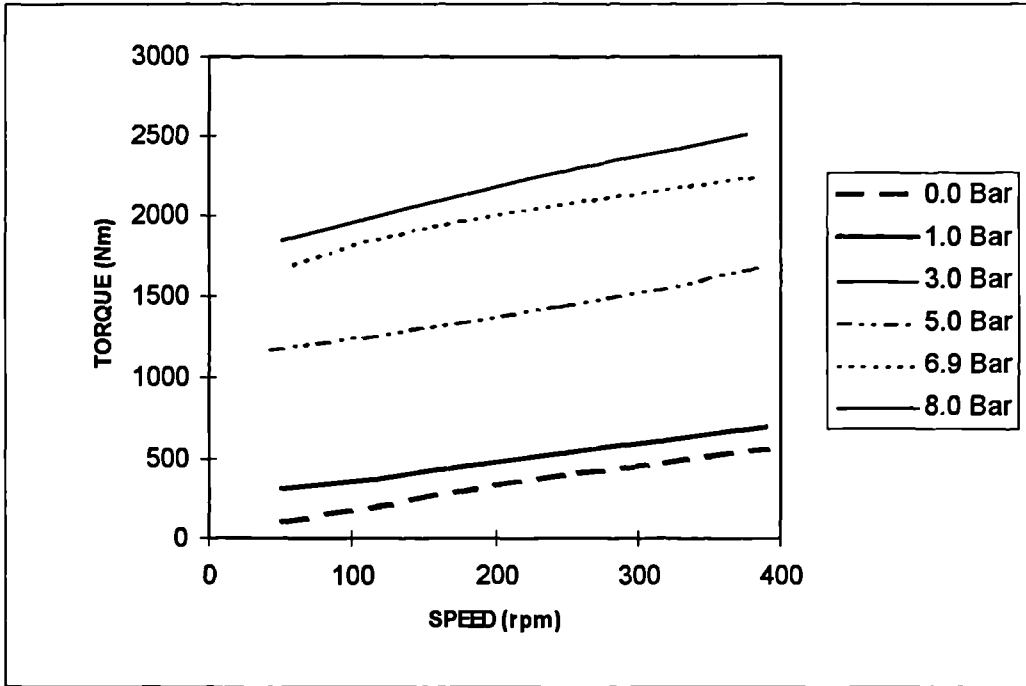
Figure 6.18 : A graph of torque/speed characteristics of the test rig brake gear pump through a series of constant oil pressure values driving in the reverse direction.
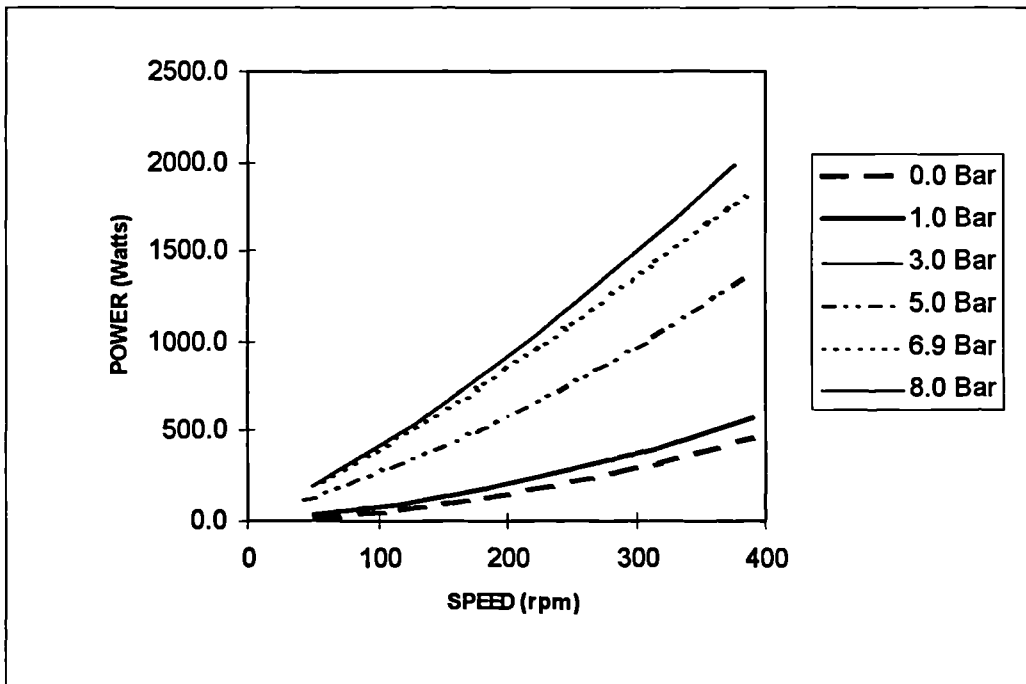
Figure 6.19 : A graph of power/speed characteristics of the test rig brake gear pump through a series of constant oil pressure values driving in the reverse direction.
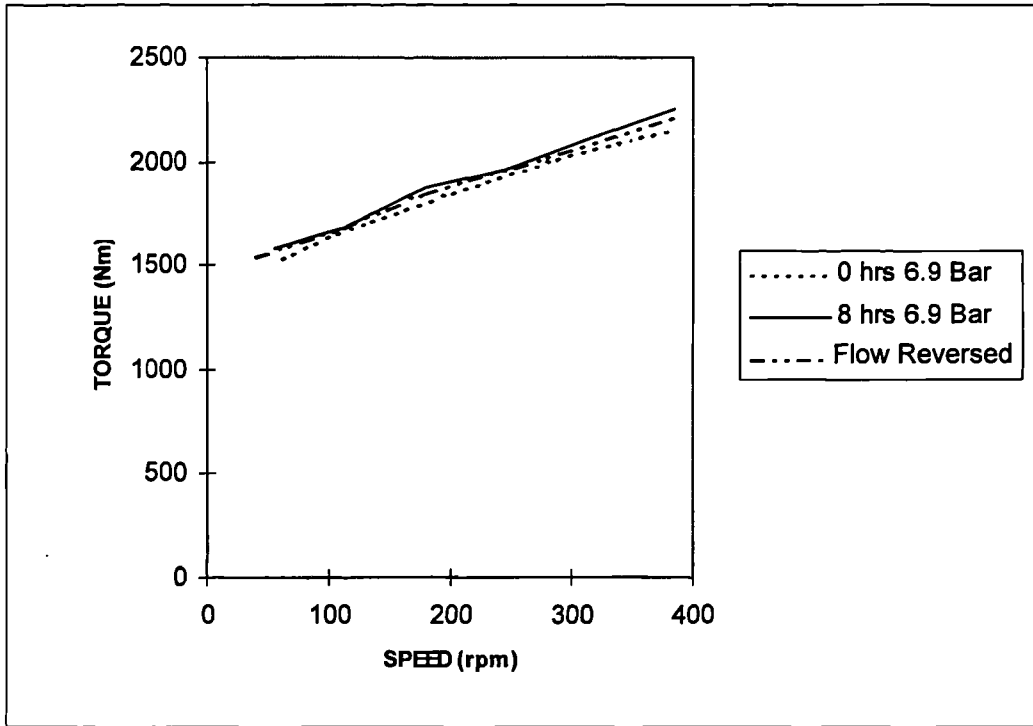
Figure 6.20 : A graph of torque/speed characteristics of the test rig brake pump starting from rest, after 8 hours operation, and with the flow of hydraulic brake oil reversed.
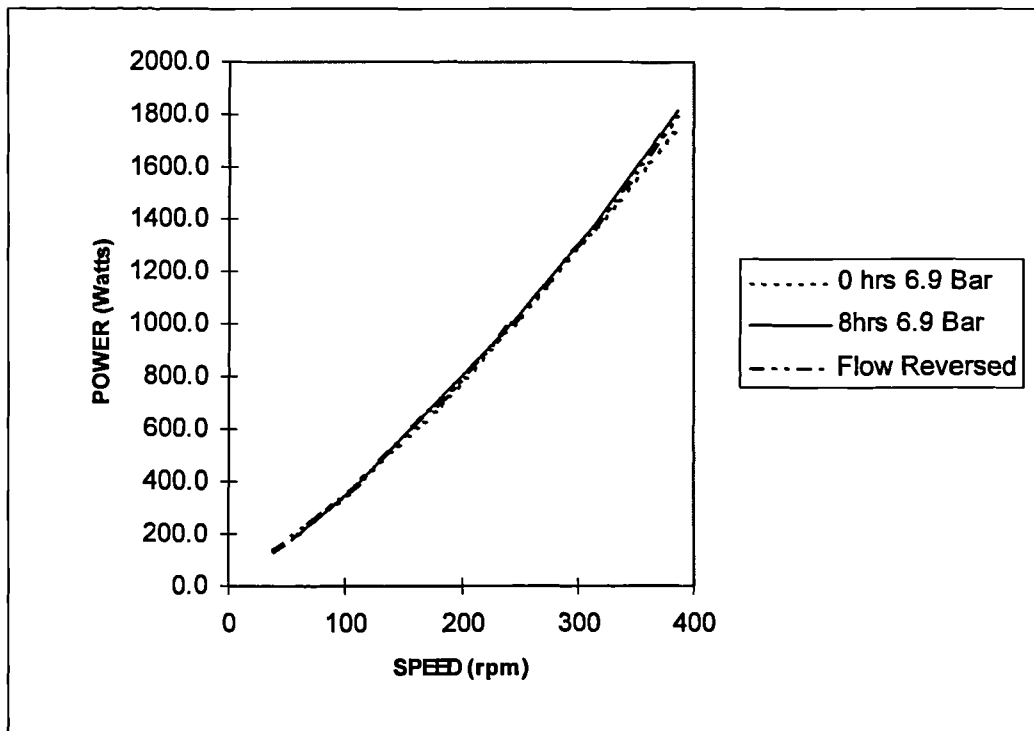
Figure 6.21 : A graph of power/speed characteristics of the test rig brake pump starting from rest, after 8 hours operation, and with the flow of hydraulic brake oil reversed.

6.5. TEST GEAR BOX MOVEMENT

6.5.1. The arrangement of probes monitoring gear box movement

To ensure an accurate computer model representing actual contact conditions, several probes were placed around the test box. This was to assess to what extent distortions in the box and component deflection in the bearings create misalignment of the worm gear system. The diagram in Figure 6.22 shows the probe placements at crucial reference locations on the components and the housing surfaces of the test gear box.

The probes marked 1 and 2 detected radial movement and deflection on the worm shaft reference bands relative to the bearing housings, probe 3 detected similar movement for the wheel reference band. The probes marked 4 and 5 record axial movement of the worm and wheel shafts respectively. Recorded movement of the worm and wheel housing are made relative to the frame upon which the test gear box is mounted. The probes marked 6 and 7 detect movement in the worm housing parallel to the worm axis and the wheel axis respectively. The probes numbered 8 and 9 monitor the same effects for the wheel housing. From these probe measurements it is possible to determine the modified alignments for the worm gear system due to component deflection and housing distortion at a given load.

6.5.2. Radial component movement under no load

To investigate the assembled alignment of the worm and wheel components, two probes were set against the worm machining reference bands and a third against that of the wheel. These probes are marked 1, 2, and 3 in the Figure 6.22 diagram of probe points. The traces in Figure 6.23, Figure 6.24, and Figure 6.25 were taken by these three probes respectively for a test gear set operating under no load in the forward and reverse directions during one rotation of the gear wheel. These show that the eccentricity of the worm is not more than 3µm total indicated run-out (t.i.r.), and within 10µm t.i.r. for the wheel over one revolution.
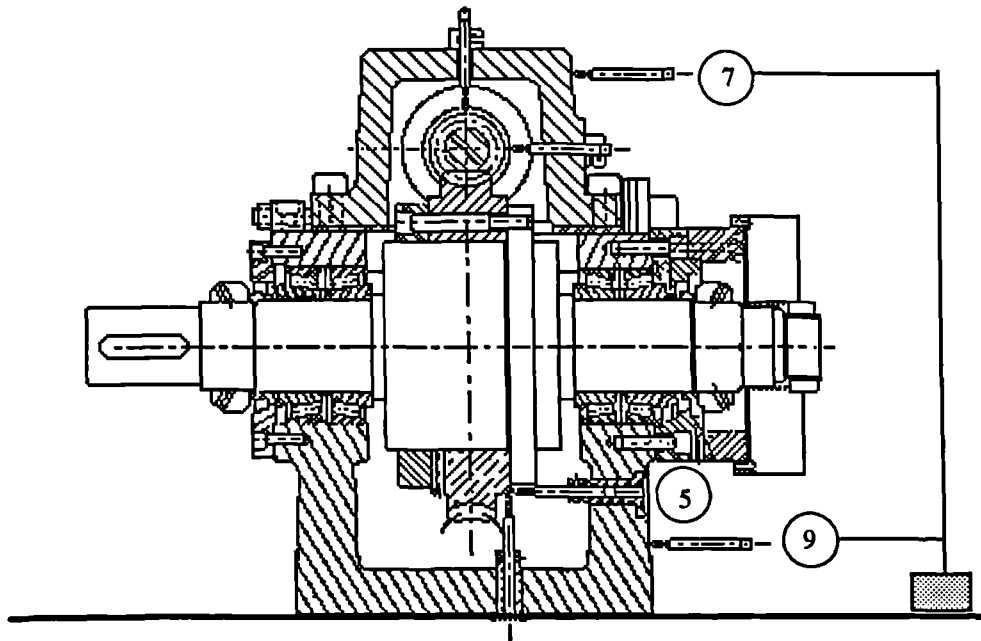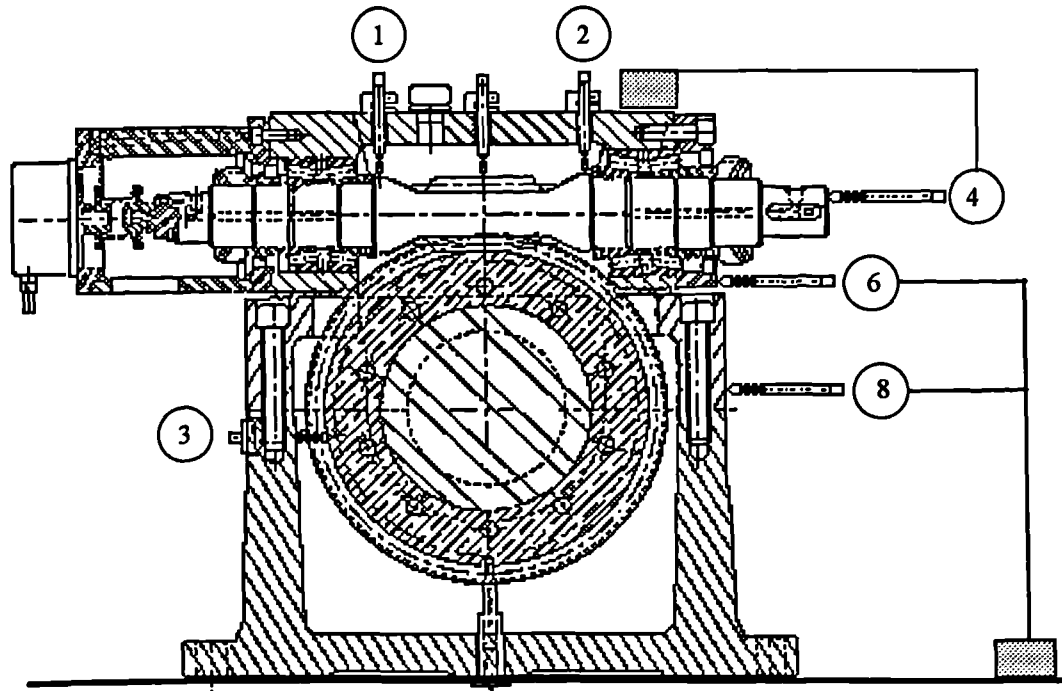
Figure 6.22 : A diagram of probe points monitoring component and housing movement in the test box assembly under load.

FORWARD   REVERSE
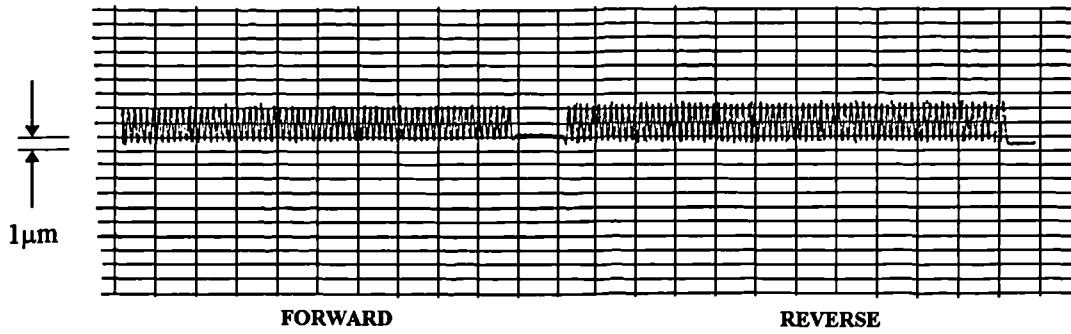
Figure 6.23 :   Eccentricity recorded in the worm reference band by probe 1 over one revolution of the wheel under no load driving both flanks.

FORWARD   REVERSE

Figure 6.24 :   Eccentricity recorded in the worm reference band by probe 2 over one revolution of the wheel under no load driving both flanks.

FORWARD   REVERSE
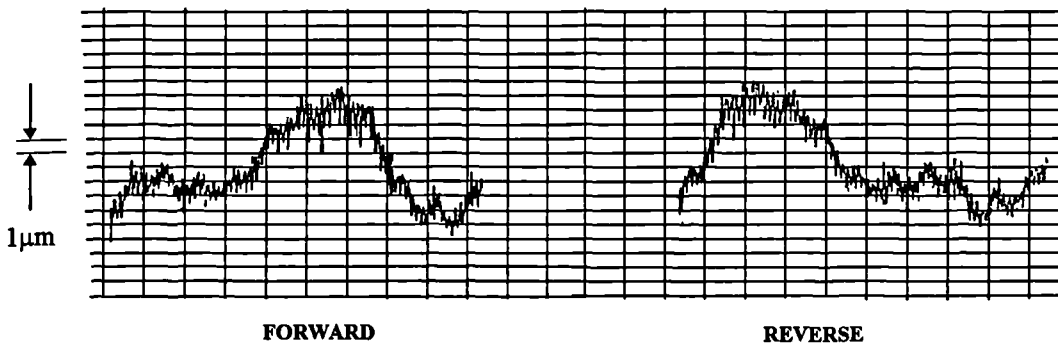
Figure 6.25 :   Eccentricity recorded in the wheel reference band by probe 3 over one revolution of the wheel under no load driving both flanks.

6.5.3. Radial component movement under an operating load

The three probes described in Section 6.5.2 are also used to record component movement while driving both the forward and reverse flanks under an operating load. The recording period was extended over several gear wheel rotations to investigate any change which may affect contact conditions during a test. Traces from the worm reference band probes were taken at 1000 Nm and 2000 Nm torque levels. The results in Figure 6.26 show that the eccentricity in the worm was at a maximum of around 5μm for probe 1, while Figure 6.27 shows that this value is never more than 2μm for probe 2 using the same load levels. In both cases the most significant effect is a deflection in the centre of oscillation of the trace under load from the no load datum. This represents an increase in centre distance of 10μm at 2000 Nm load. Similar measurements were taken for the wheel using probe 3 with the operating load gradually reduced from 2000-0 Nm over several gear wheel rotations in the forward and reverse directions. The deflections of the probe as shown in Figure 6.28 indicate that the wheel moves 8-10μm from the datum position which exists while operating under no load.

From these results it can be seen that there is distinct eccentricity in the components and that they deflect under load. Though these effects can be included in the computer model their magnitudes are small enough to be irrelevant to the final result since they are a fraction of the assembly tolerance values.
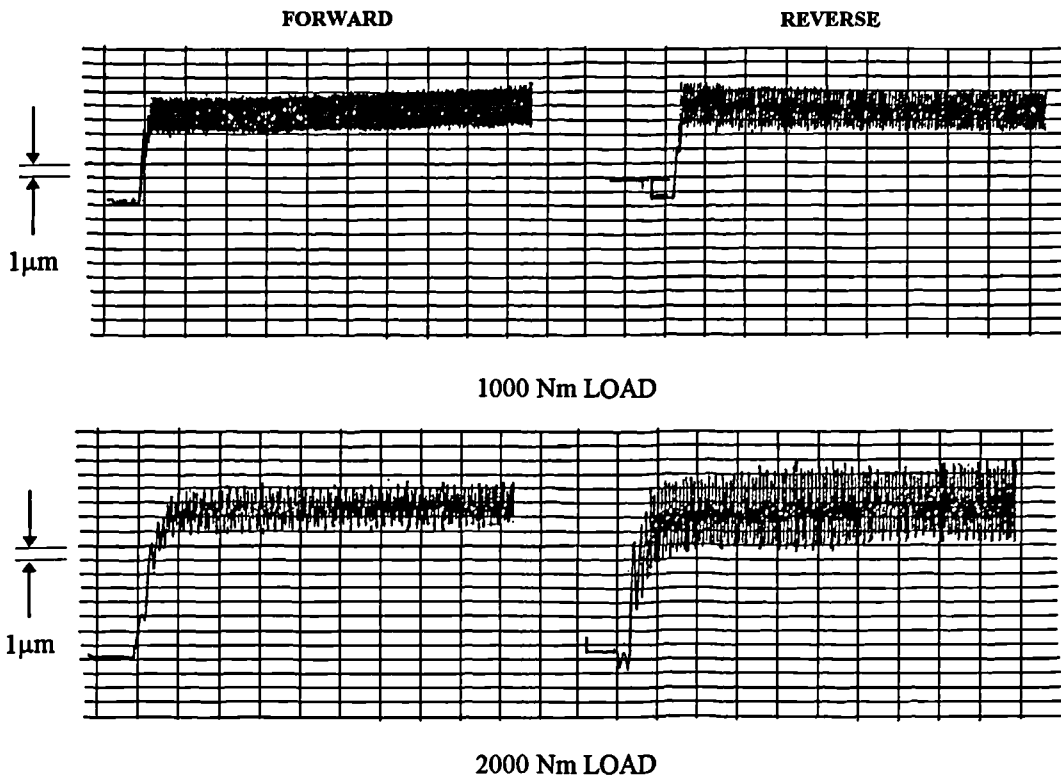
Figure 6.26 : The worm reference band trace from probe 1 for both flanks while driving a wheel under loads of 1000 Nm and 2000 Nm.
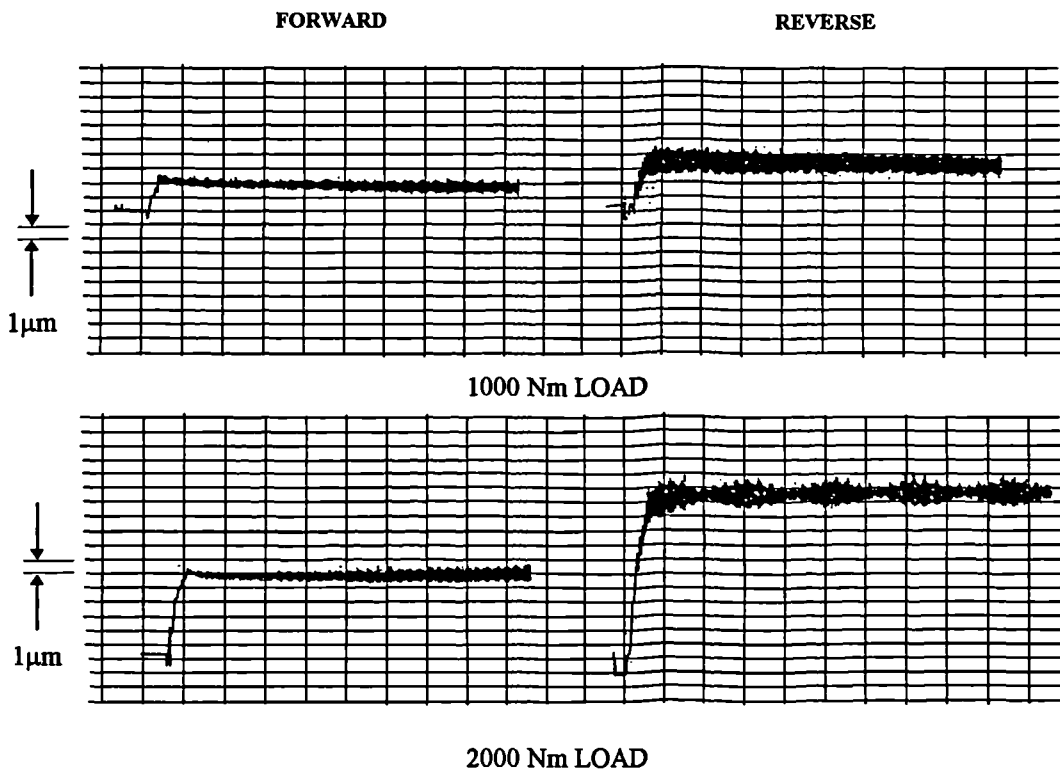
Figure 6.27 : The worm reference band trace from probe 2 for both flanks while driving a wheel under loads of 1000 Nm and 2000 Nm.
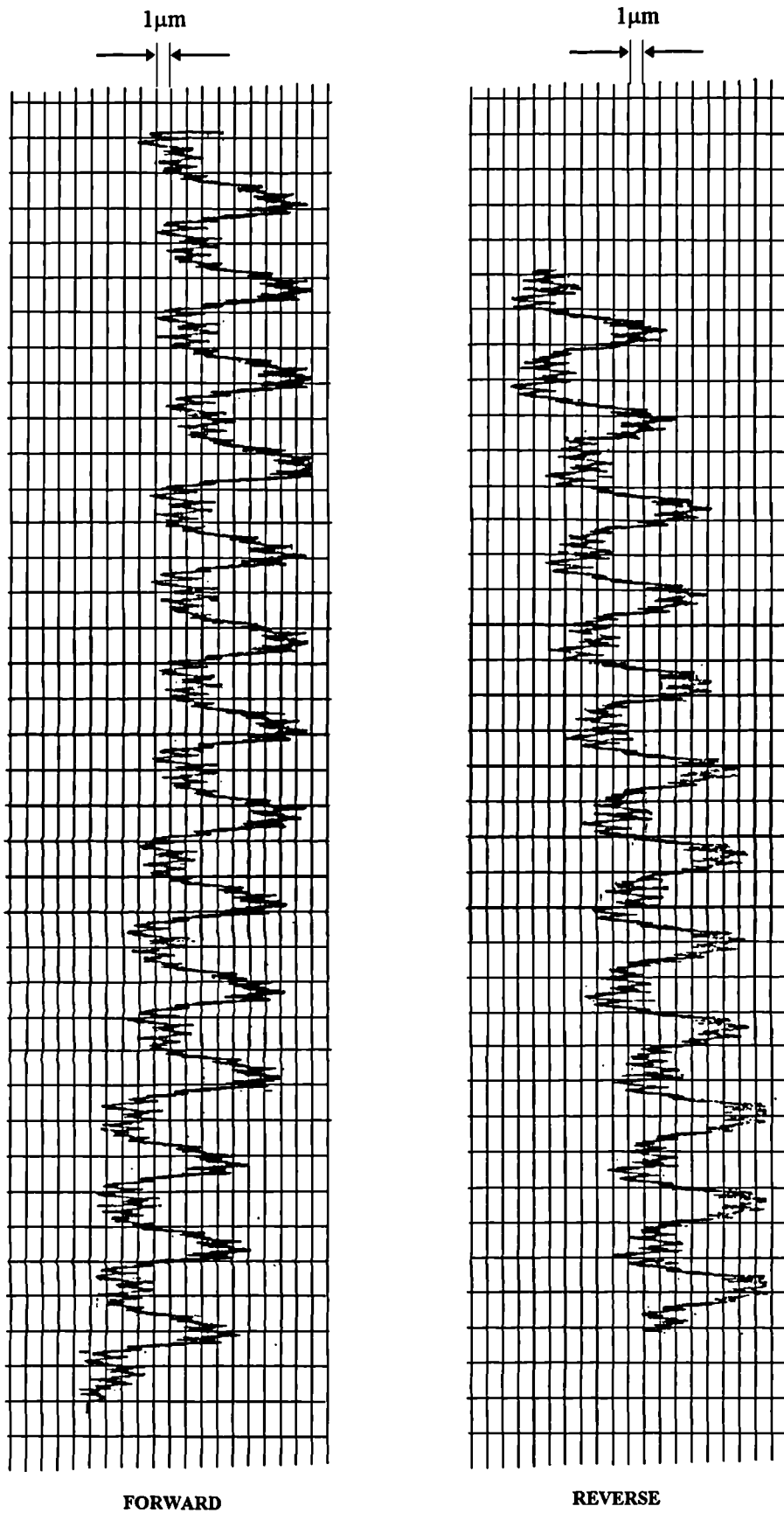
Figure 6.28 : The wheel reference band probe trace for both flanks under loads of 2000-0 Nm.

6.5.4. Axial movement of the gear set components under an operating load

The probes 4-9 described in section 6.5.1 recorded the axial displacements of the components under a series of loads from 0-2000 Nm in 500 Nm intervals in both the forward and reverse directions. The results define the modified position of the gear set axial datum caused by movement in the worm and wheel shaft bearings. The results of the probe readings are shown in Tables 6.1.

Torque	Forward Movement	Reverse Movement	Torque	Forward Movement	Reverse Movement
(Nm)	(Microns)	(Microns)	(Nm)	(Microns)	(Microns)
0	0	0	0	0	0
500	20	-23	500	2	-1
1000	35	-37	1000	5	-2
1500	60	-63	1500	7	-3
2000	94	-92	2000	8	-7

PROBE 4   PROBE 5

Table 6.1 :   The tables of results recording worm and wheel axial movement under load.

Probe 4 indicated that there was a substantial axial movement of the worm in the bearings of 94μm when operating under 2000 Nm load. This is of the same order of magnitude as the tooth deformation effects in the test gear set. Movement in this direction is registered by the encoders as additional wheel movement or tooth deformation, and is therefore carefully monitored. Probe 5 shows that the wheel axial displacement is much smaller at around 8μm for the same load. The difference in magnitude can be explained by the fact that the gear set used during the test was a 50:1 ratio with a 20° normal pressure angle. This created a line of action at the contact point on the gear set of approximately 22° to the worm axis and 85° to the wheel axis. The component of force along the wheel axis is therefore greatly reduced.

6.5.5. Movement of the worm and wheel housing under an operating load

During the tests described in Section 6.5.4, probes 6-9 recorded the movement of the worm and wheel housing. The results in Table 6.2 show the associated probe deflections.

Torque	Forward Movement	Reverse Movement
(Nm)	(Microns)	(Microns)
0	0	0
500	7	-10
1000	17	-16
1500	26	-26
2000	31	-36

PROBE 6

Torque	Forward Movement	Reverse Movement
(Nm)	(Microns)	(Microns)
0	0	0
500	5	-6
1000	9	-11
1500	16	-15
2000	20	-18

PROBE 7

Torque	Forward Movement	Reverse Movement
(Nm)	(Microns)	(Microns)
0	0	0
500	5	-5
1000	11	-11
1500	16	-16
2000	22	-20

PROBE 8

Torque	Forward Movement	Reverse Movement
(Nm)	(Microns)	(Microns)
0	0	0
500	1	-2
1000	4	-5
1500	9	-7
2000	11	-10

PROBE 9

Table 6.2 :   The tables of results recording worm and wheel housing movement under load.

The results show that the worm housing has moved further in the worm axial and wheel axial direction compared to the wheel housing in each operating condition. As a consequence, there was a change in centre height and axial movement in the worm relative to the datum position defined for no load. The differential of the movement with the wheel housing created $14\mu m$ and $10\mu m$ offset values for alignment and axial profile shift in the worm respectively. These values were considered when defining the model of the worm gear system. The test box comprises separable worm and wheel housing units which are bolted together. Movement or distortion of the bolts at the interface could account for the differential in the probe readings. A box which is cast as a whole unit may produce a different result.

6.5.6. Using probe measurements to model worm gear system offset modifications due to load

The changes in alignment of the gear set in the wheel axis direction can be neglected for the computer model as the composite effect falls within the 25μm tolerance value for centre height during assembly. The significant result derived from these measurements is the large axial movement of the worm which directly translates the thread profile. The axial movements of the components in the bearings are greater than those in the radial direction since the axial stiffness of the bearings are approximately a factor of 10 smaller than those in the radial direction. The fact that the major component of force under load is directed along the worm axis explains the excessive displacement recorded in this direction. This motion is compounded by an additional movement of the worm housing relative to the wheel housing. The combined effect moves the worm thread profile axially relative to the wheel without an associated rotation in the shaft which is directly additive to the backlash recorded by the computer calculations of the encoder signals. However, the probe readings are used to remove the effects and isolate the effects of tooth deformation as described in Section 6.6.2.

6.6. LOADED TRANSMISSION ERROR ACQUISITION AND ANALYSIS

6.6.1. Recording the tooth to tooth transmission error

6.6.1.1. Transmission error signal acquisition

To assess the data acquisition capabilities of the equipment, transmission error tests were performed at a series of loads from 0-2000 Nm in 500 Nm intervals. The results shown in Figure 6.29 show data recorded over a full wheel revolution against both flanks of a sample gear set. The results for tests performed at 1500 Nm load and over indicated a beating effect which distorts the signal. This effect made it difficult draw direct conclusions for the gear set transmission error characteristics. It was therefore necessary to process the wave form data and remove this effect before analysis could begin.

A Fourier analysis of the wave forms is given in Figure 6.30 for the transmission error signal samples taken at the 2000 Nm load level. This shows a significant amplitude at 49 cycles per wheel revolution. The test gear set has a ratio of 50:1 while the step-up gears have a 1:49.07 (to 2 d.p.) ratio. The period of this beating effect was found to be approximately 1.1 wheel revolutions. This combination identified the step-up box which connects the brake to the output shaft of the test box as the source of this effect.

The amplitude variation was caused by small torque variations imposed by the differential of the two gear ratios which subsequently created small oscillations in axial position of the worm shaft due to movement in the bearings. An example of this relationship is recorded in Figure 6.31 which shows a transmission error signal including the beating effect and the corresponding cyclic variation in worm axial shaft movement recorded during the test. It was necessary to remove this effect before correct analysis of gear set characteristics could be performed.
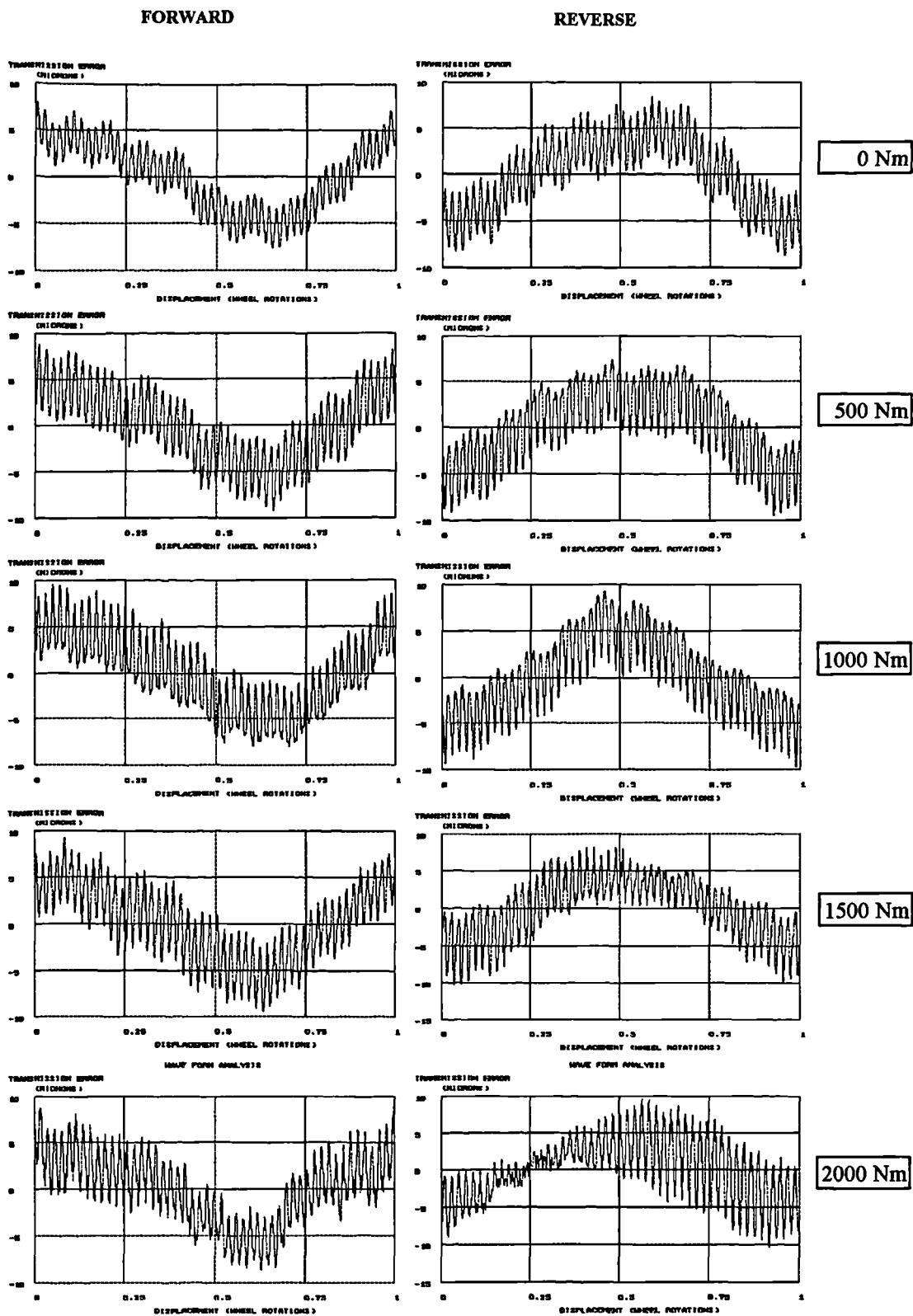
Figure 6.29 : The initial transmission error wave signals recorded for a standard set of test rig results.
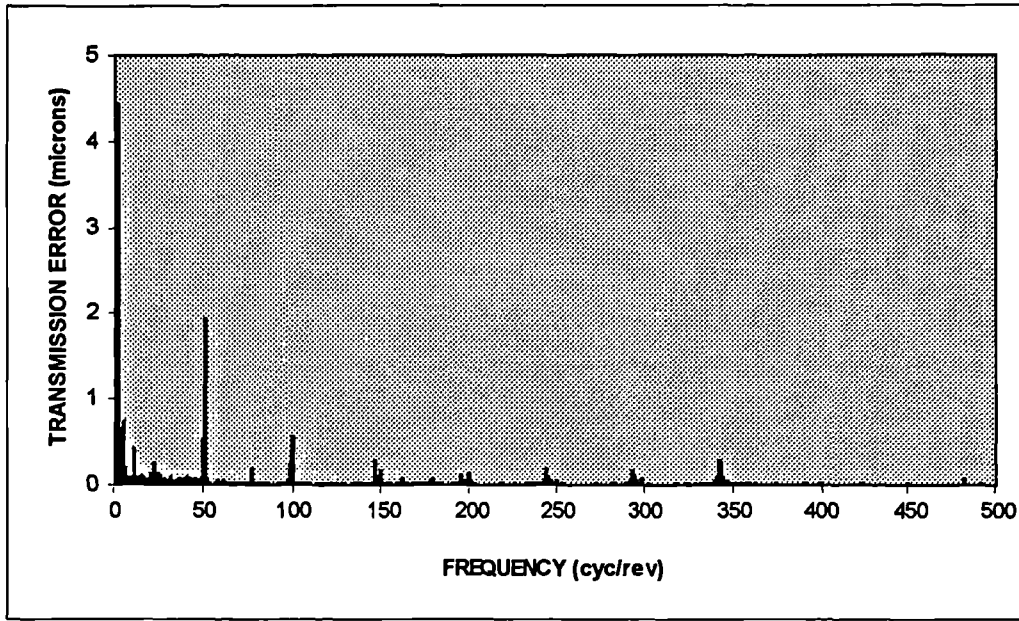
FORWARD
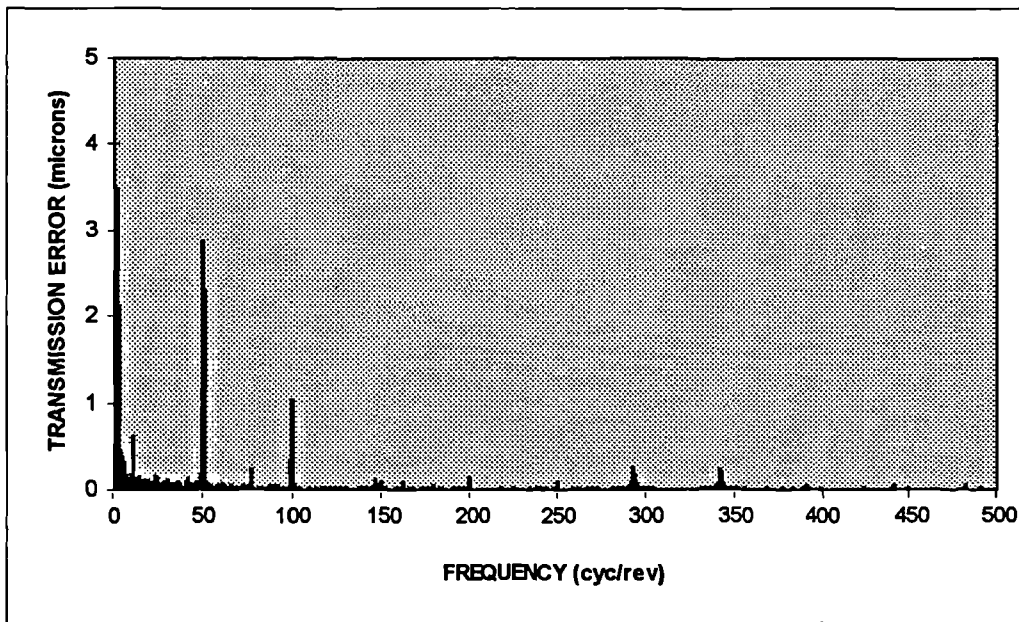
REVERSE

Figure 6.30 : The Fourier analysis frequency spectrum for the 2000 Nm load test sample.
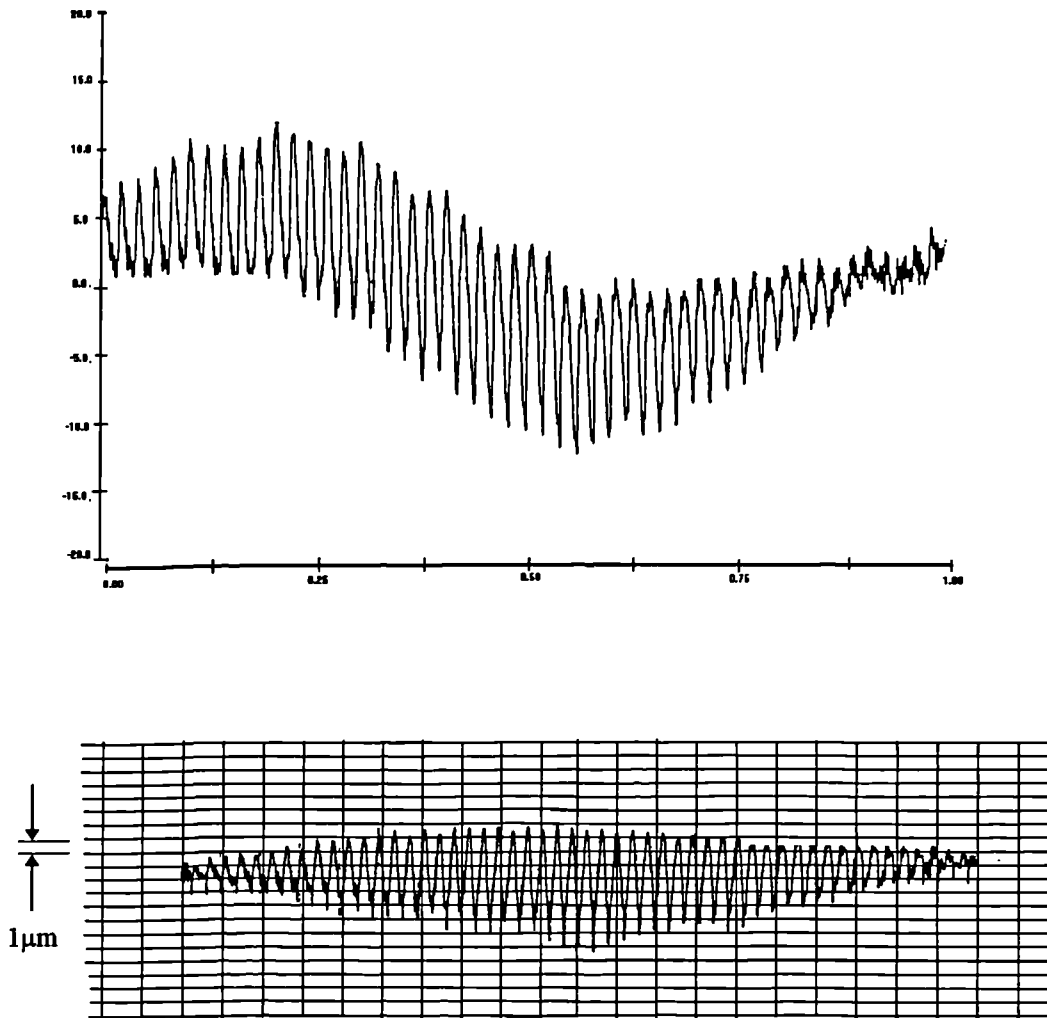
Figure 6.31 : The interference signal in the transmission error recorded by the GP-30 computer for a single wheel revolution and the associated worm shaft movement during this period.

6.6.1.2. Filtering the transmission error signal

The graph in Figure 6.32 shows a data sample taken directly taken from test measurements in which the beating effect is distinct. A Fourier analysis of this signal was carried out using data recorded over a full beating period. The exact 49.07 cycle/rev harmonic components of the wave form were removed. The graph in Figure 6.33 shows the wave form for the data sample after this filter had been performed. A second Fourier analysis of this measured data was carried out using the data sample recorded over one wheel revolution. This produced a spectrum with integer frequencies from which the significant 49 cycle/rev harmonics were removed. The significant frequencies were those with amplitude greater than $0.15\mu m$, which represented the accuracy of the data acquisition equipment. The graph in Figure 6.34 shows the wave form after this filter had been carried out.

Analysis of the sample data filtered over a full beating period indicated that it was still possible to detect a beating effect. The reason for this was that the method used contained an error function based upon rounding of the step-up box ratio and the subsequent definition of the beating period. This error function had a frequency of 49.07 cycles/rev and therefore created a beating effect with a $1-2\mu m$ amplitude. The graphs show that the simplified method using integer frequencies of tooth cycles per wheel produced a far more consistent wave.

The problem in using this method was the loss of information on the required wave form by ignoring some relevant frequencies. Tests were performed to ensure that a significant influence was not lost by ignoring lower amplitude harmonic frequency values or side band frequencies (excluding the dominant 50 cycle/rev frequency harmonics) created in the frequency spectrum by the non integer ratio in the step-up box.
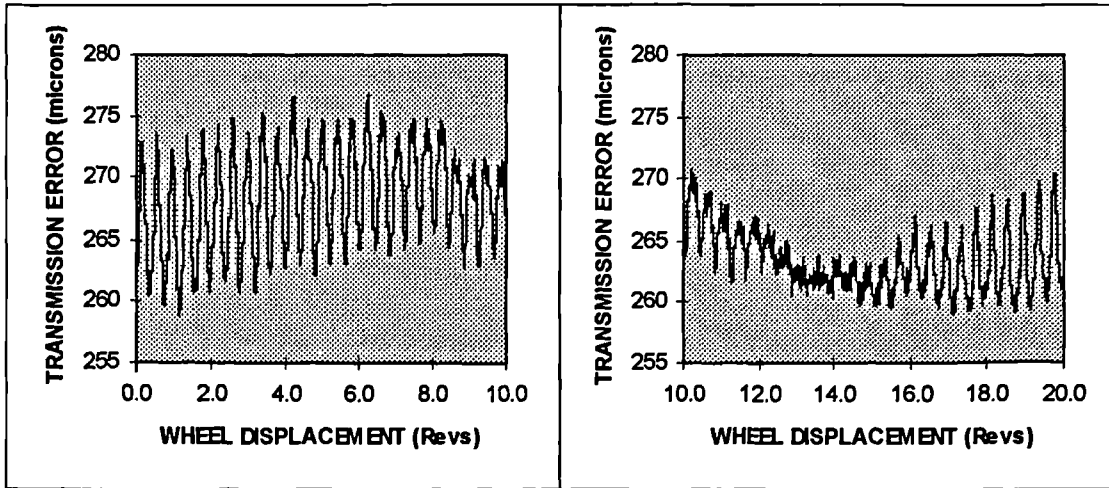
Figure 6.32 : The measured data signal containing an interference effect.
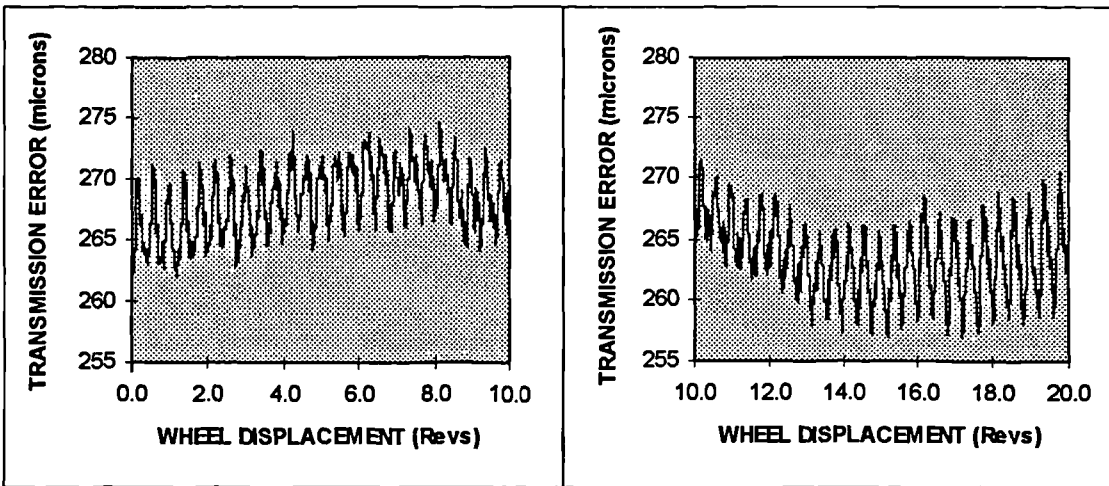
Figure 6.33 : The interference signal filtered for the significant 49.07 cycle/rev frequencies from data recorded over a beat period.
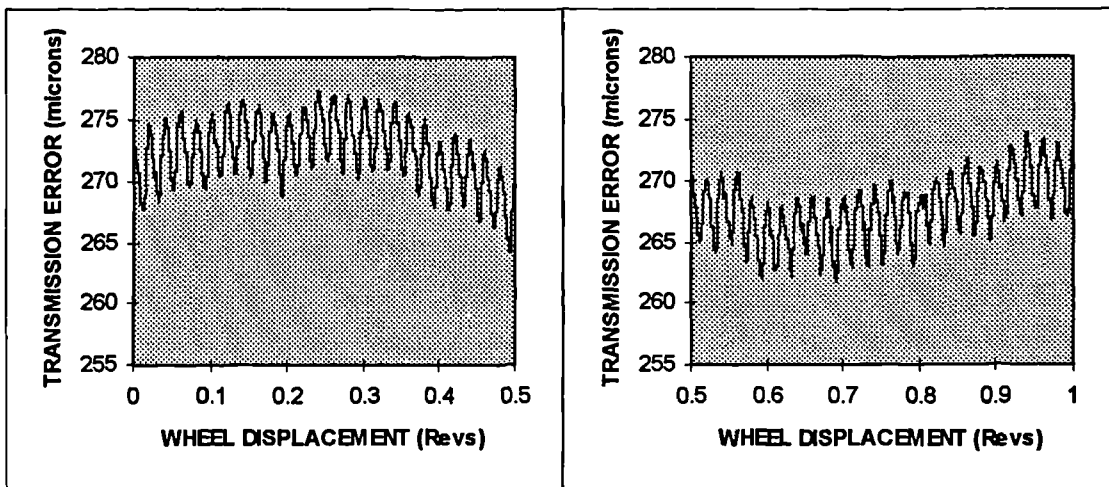
Figure 6.34 : The interference signal filtered for the significant 49 cycle/rev frequencies from data recorded over one wheel revolution.

CHAPTER 6

The transmission error plot in Figure 6.35 shows the result over five teeth engagements with only the significant 49 cycle/rev harmonics removed from the sample wave. Figure 6.36 shows a plot for the same interval with all of the 49 cycle/rev harmonics removed from the sample wave form. Figure 6.37 shows the result of filtering all significant 49 cycles/rev harmonics and adjacent side band frequencies. From the results in these graphs it can be seen that there is no significant change in wave form by filtering frequencies other than the 49 cycles/rev harmonics. Changes in local and total amplitude are well within a 1μm level.

6.6.1.3. The filtered transmission error signal

The graphs in Figure 6.38 represent the initial transmission error data results after filtering of the significant 49 cycle/rev harmonic interference frequencies as described in section 6.6.2.2. This shows that the filtering process has removed the interference effect throughout the series of test results.

This in itself is not proof that this represents the transmission error signal from the test gear box alone. To ensure this it would be necessary to replace the step-up box system with a different ratio, perform a similar filter on a new set of measurement data, and check the correlation in the filtered transmission error signal. A more efficient alternative would be to stiffen the worm bearings axially and reduce the problem. Installing a different braking mechanism may remove the problem, however it should be considered that alternative braking mechanisms may also generate some form of interference signal.
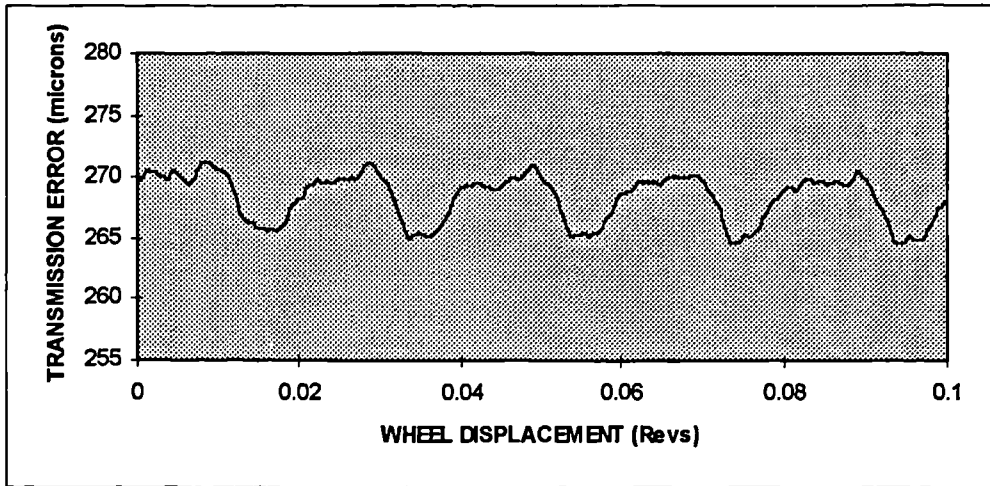
Figure 6.35 :   Signal filtered for significant 49 cycle/rev frequencies.
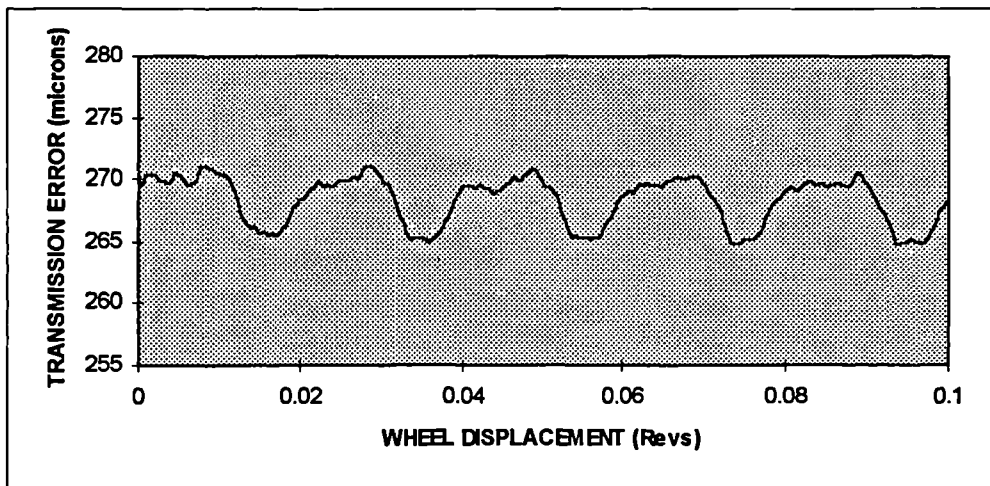
Figure 6.36 :   Signal filtered for all 49 cycle/rev frequencies.
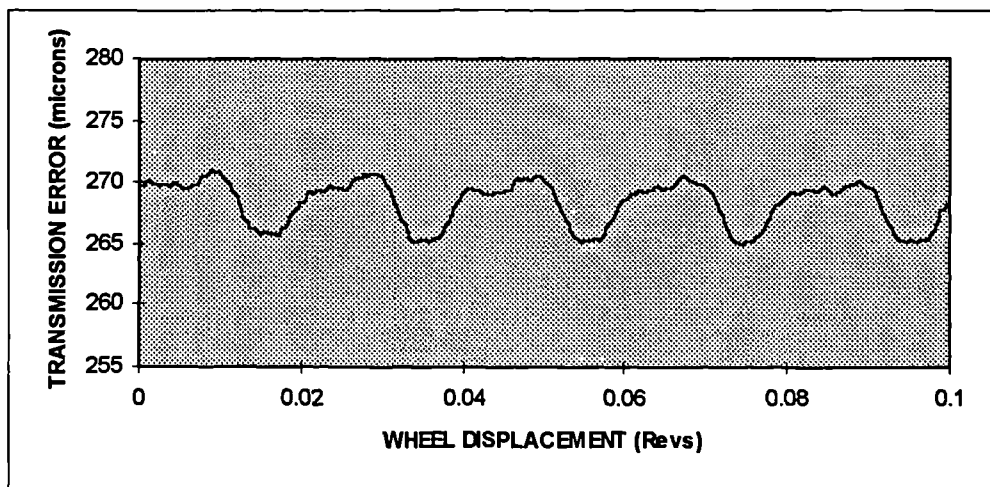
Figure 6.37 :   Signal filtered for all 49 cycle/rev and significant side band frequencies.
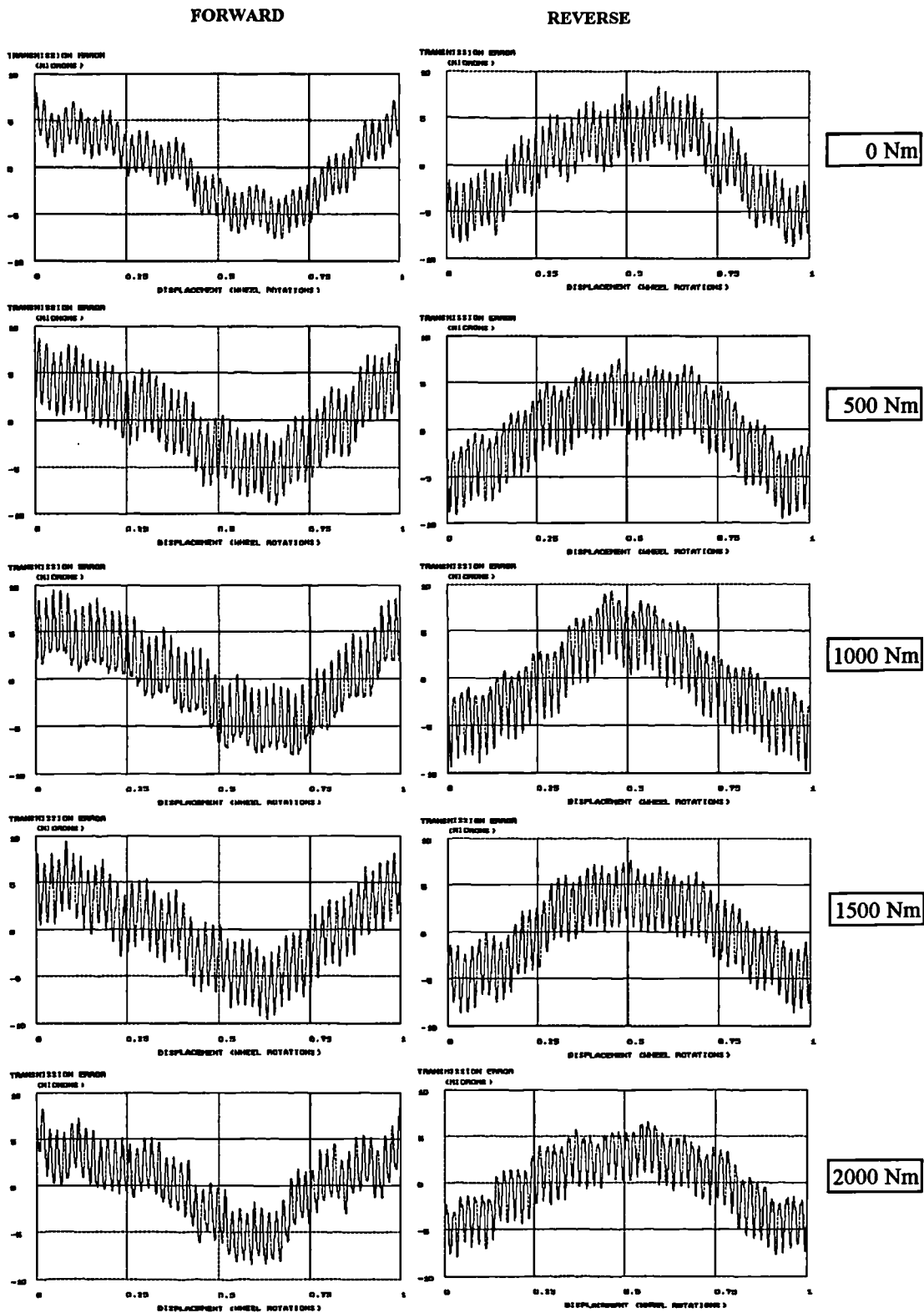
Figure 6.38 :   The filtered transmission error wave signals recorded for a standard set
of test rig results.

6.6.1.4. The repeatability of the tooth to tooth transmission error signal

To investigate the repeatability of a single test for transmission error under load, two tests were performed on a worm gear set under identical operating conditions. This was repeated for a different load to investigate the variability of this result. An initial test was performed on the gear set operating at 150 rpm input shaft speed driving a 1000 Nm load. The test rig was allowed to settle for 1 hour and the test was repeated. The graph in Figure 6.39 shows the resulting transmission error signal generated during the test over a period of five tooth engagements, or 0.1 wheel revolutions. This procedure was then carried out with the gear set operating at 150 rpm input shaft speed driving a 1500 Nm load. The graph in Figure 6.40 shows the results from this repeat test.

The signals from the first load interval test show a correlation in form but a variance in magnitude for the transmission error signal. The second load interval comparison test shows a far greater correlation in all aspects of the control and repeat signals. These results implied that tests under identical conditions on the test rig could have a variance of 1-2μm amplitude in the transmission error signal.
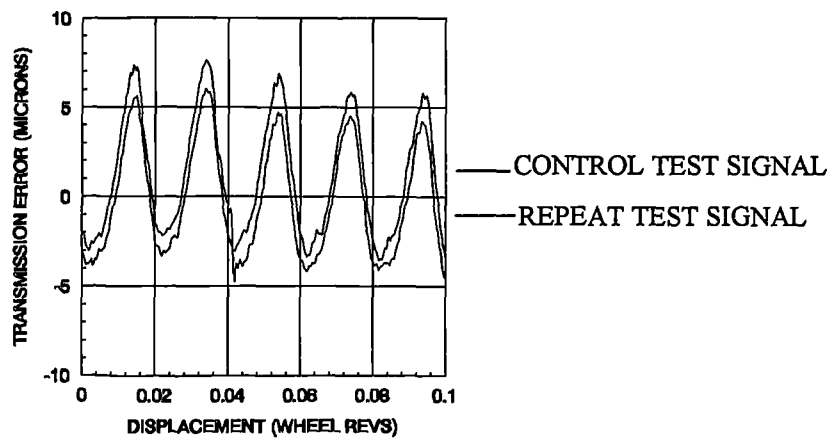
Figure 6.39 : The repeatability of the transmission error signal under a 1000 Nm load operating at 150 rpm input shaft speed.
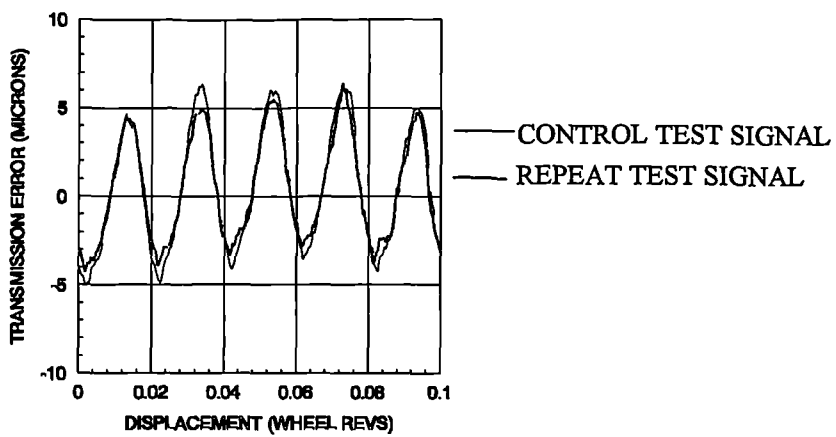
Figure 6.40 : The repeatability of the transmission error signal under a 1500 Nm load operating at 150 rpm input shaft speed.

6.6.2. The mean transmission error value

6.6.2.1. Isolating the tooth deformation component using backlash

The graph in Figure 6.41 shows an example of a transmission error recorded during a bi-directional test on a sample gear set under no load. In this test, the wheel is driven in the forward direction for one revolution and then in the reverse direction for one revolution. The test rig computer calculates the average backlash, value B_0, of the gear set using the differential of the position error data at a specified number of target positions of the wheel shaft. The graph in Figure 6.42 shows the backlash, B_{dc}, recorded when this test is repeated for the same gear set while operating under load. This increase in backlash was due to tooth deformation, movement of the components within the bearings, and modified housing alignment of the test gear box while operating under load as indicated by the probe measurements taken in Section 6.5. The axial worm movement relative to the wheel axis contributes directly to the registered backlash value. This effect is removed by adding the worm axial movement in the bearings relative to the housing, detected by probe 4, to the differential in displacement between the movement of the worm and wheel housings given by probes 6 and 8 respectively. This is achieved using a single probe with a datum on the wheel housing detecting movement directly from the end of the worm shaft. The diagram in Figure 6.43 shows this probe arrangement and a record of the axial movement, Δu, of the worm recorded during the bi-directional test. This clearly shows the three distinct phases for the test period of forward driving, stopping and changing the brake pipe valve settings, and then reverse driving. The backlash component due to deformation is established by subtracting the worm movement and the backlash value under no load from the total backlash value. Dividing this by two establishes the value for a single flank driving direction assuming an equal effect between the two flanks. Therefore, if e_{dc} represents the mean transmission error level measurement caused by tooth deformation, then this value is determined by :

$$e_{dc} = (B_{dc} - B_0 - \Delta u)\,/\,2$$
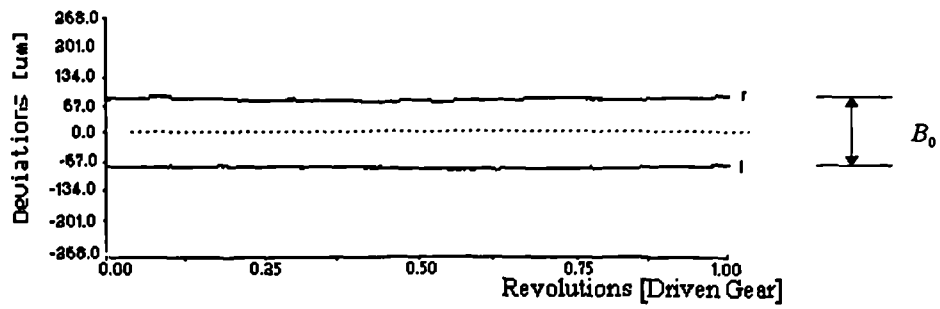
Figure 6.41 : The backlash recorded through a bi-directional test for a test gear set operating under no load.
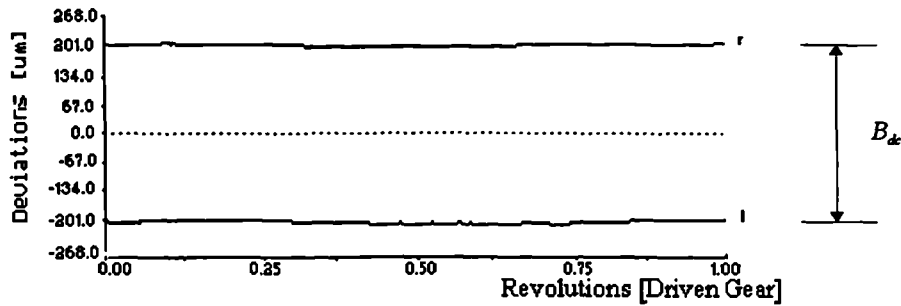
Figure 6.42 : The backlash recorded through a bi-directional test for a test gear set operating under 1500 Nm load.
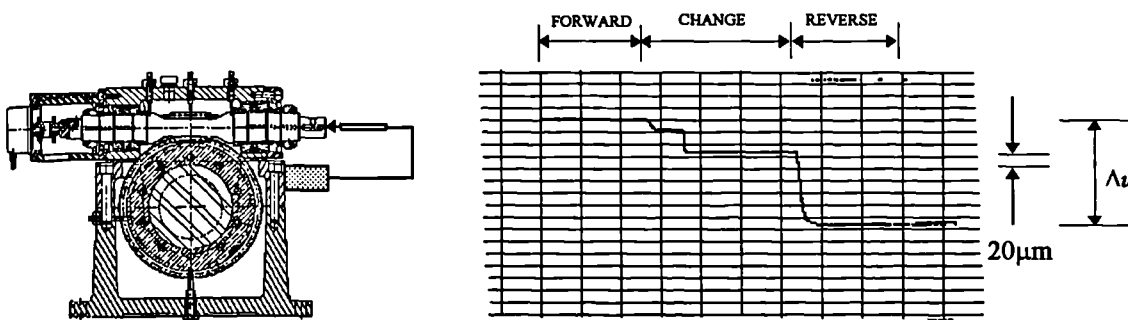
Figure 6.43 : The axial worm shaft movement recorded through a bi-directional test for a test gear set operating under 1500 Nm load.

6.6.2.2. Isolating tooth deformation using continuous measurement

An alternative method to that proposed in Section 6.6.3.1 was considered for establishing mean transmission error which avoids the assumption of an equal distribution of tooth deformation value between the flanks. This method continuously records transmission level over several revolutions of the worm gear while driving in the same direction through the standard test series operating conditions. The record must be continuous since the datum is reset for each test and the relative changes in transmission error are otherwise lost.

The graph in Figure 6.44 shows an example of the transmission error recorded over five revolutions. The load is decreased after each revolution from 2000-0 Nm in 500 Nm intervals over this period while running at a constant 150 rpm input shaft speed. The sine wave fluctuation in the graph at each interval is due to eccentricity of the wheel, however, there is a distinct change in mean transmission error level which represents the tooth deformation and worm shaft movement. The trace in Figure 6.45 indicates the actual axial movement in the worm shaft during this test. As described in the backlash method, this contributes directly to the indicated transmission error level and must be removed.

Repeatability of mean transmission error value using this method could not be achieved consistently to better than 20μm tolerance. This was due to the fact that the test rig required a settling period after each load variation to allow for movement in the bearings and changes in hydraulic brake oil pressure. The movement occurring during this period interfered with the continuous signal and made establishing mean transmission error levels difficult, incurring high tolerance values. Further disadvantages of this method are that a Fourier spectrum could not be established for the curve since the measurements are not cyclic. Also, it is not possible to obtain results for constant operating conditions over exactly one revolution. Though an attempt could be made to process the data by separating the data using results obtained from the files written to MS-DOS disk, this is very impractical and time consuming with no guarantee of an improvement in the validity of the measurements.
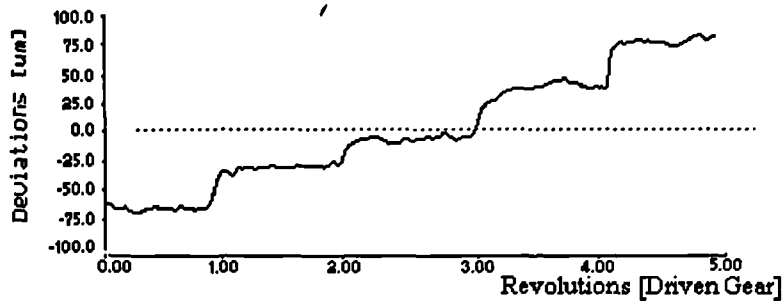
Figure 6.44 : The transmission error levels recorded for a single direction test over five wheel revolutions for a test gear set operating under 500 Nm load intervals from 0-2000 Nm .
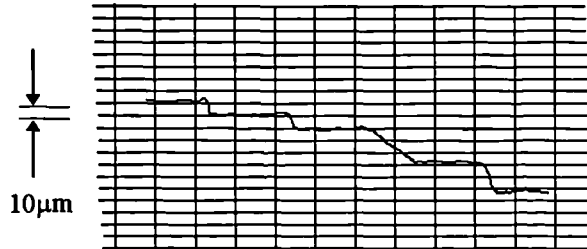
Figure 6.45 : The axial worm shaft movement recorded for a single direction test over five wheel revolutions for a test gear set operating under 500 Nm load intervals from 0-2000 Nm .

6.6.2.3. The repeatability of the mean (or DC) transmission error signal

A series of tests was performed to investigate the repeatability of the procedure described in Section 6.6.2.1 for establishing mean transmission error. A bi-directional test was performed on an unloaded gear set to obtain a nominal backlash value. Five bi-directional tests were then performed at 1 hour intervals on the gear set while operating at 150 rpm input shaft speed under a 1500 Nm torque load. The backlash value and worm shaft movement were recorded for these tests. The mean transmission error level was determined using these values.

The transmission error signal measured under these conditions was filtered to remove the interference effect on both flanks. The graphs in Figure 6.46 show the results of the series of five tests for transmission error signals from the forward and reverse driving flanks of the test gear. These graphs suggest that it is possible to establish a mean transmission error level to within 5μm using this method.

FORWARD   REVERSE
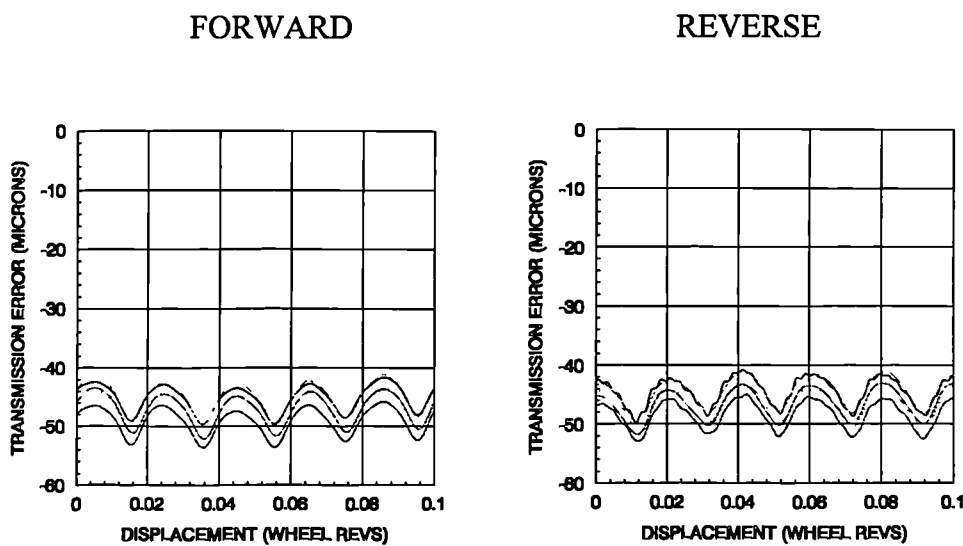
Figure 6.46 :   A series of mean transmission error repeatability tests for a worm gear set operating under 1500 Nm load at 150 rpm input shaft speed.

6.6.3. The influence of lubrication on transmission error

The contacting surfaces were lubricated using a 220 cSt mineral oil. A test was performed on a test gear set to assess the influence of this oil on the contact conditions between the worm thread and gear wheel teeth during the meshing cycle.

The gear set was initially cleaned of oil and the lubrication system was disconnected from the test gear box. The transmission error signal from the gear set for a full wheel revolution was recorded while operating under no load. The oil lubrication supply was then re-connected to the gear box and a further recording of transmission error was taken under the same operating conditions.

The graph in Figure 6.47 shows a sample of the transmission error signals taken over a five tooth engagement interval of wheel rotation from both the dry and lubricated contact condition tests. These show that the transmission error wave form and magnitude is well within the limits of repeatability described in Section 6.6.2.4 previously. It can therefore be concluded that the lubricating oil does not significantly influence the contact conditions of a gear set when sampling the transmission error signal.
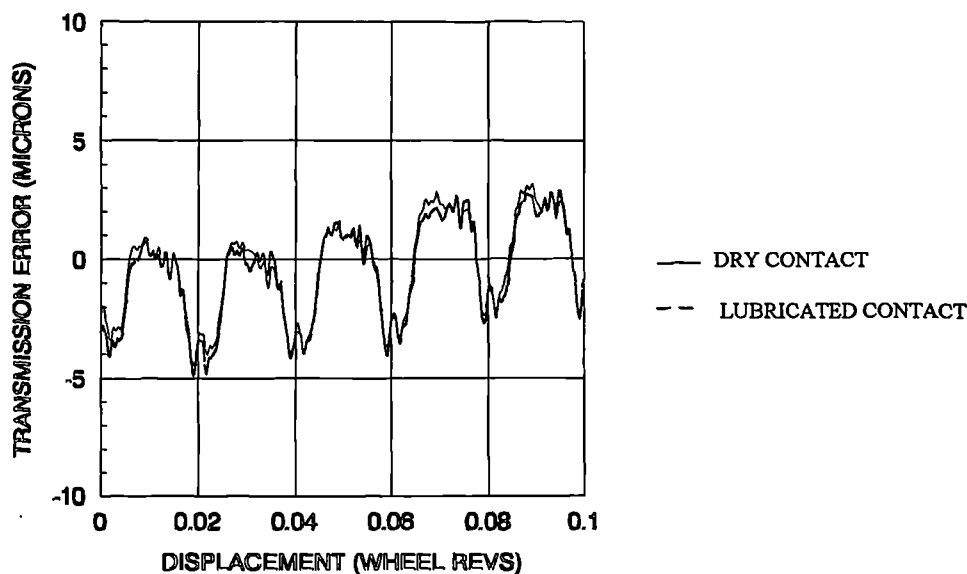
Figure 6.47 : A comparison of transmission error during dry and lubricated contact of an unloaded gear set.

6.7.   SUMMARY

The elements used in the test rig assembly were checked and calibrated. This equipment enabled measurement of transmission error to be recorded for a 152.4mm (6 ") centre distance gear system mounted in the test gear box.

Errors in the nominal assembly contributed directly to the transmission error data recorded. By placing probes at reference points over this test gear box it was possible to record misalignment in the gear set components and distortion of the housing assembly due to operation under a torque load. These deviations were assessed for their importance in attempting to model the worm gear contact conditions.

An interference effect in the transmission error caused by the differential between the step up and test gear boxes was filtered from the data. A method was devised which isolated the mean level due to tooth deflection in the test gear set while transmitting a torque load. The resulting wave magnitude was consistent and repeatable to approximately 1-2μm, with the mean level repeatable to within 5μm. Further tests showed that the lubrication oil used for the test gear set had no effect on contact conditions.

From the commissioning tests it was determined that the test rig could provide suitable data to carry out an investigation of worm gear accuracy under a torque load. The results obtained are described in Chapter 7 and 8.

7. INVESTIGATIONS OF WORM GEAR TRANSMISSION ERROR CHARACTERISTICS UNDER LOAD

7.1. INTRODUCTION

To ensure consistency in the transmission error data, the operating range of the test rig was restricted to 100-300 rpm worm speed and 0-2000 Nm braking torque. This was in order to keep well within the limits of performance defined by the initial test of the rig assembly reported in section 6.4. A standard series of loaded transmission error measurements was defined as intervals of 500 Nm from 0-2000 Nm with an operating speed of 150 rpm on the input shaft. From this it was possible to compile transmission error characteristics for a worm gear system through load by plotting the data at each load interval on the same graph. The graph for each series of tests represented a Harris Map for the gear system, named after Prof. Stephen Harris[26] who developed the technique during the 1950's and 60's while analysing spur gear performance characteristics.

The data was collected as a series of bi-directional tests for backlash using the GP-30 computer. The diagram in Figure 7.1 illustrates the forward and reverse driving direction convention of the shafts used during testing.
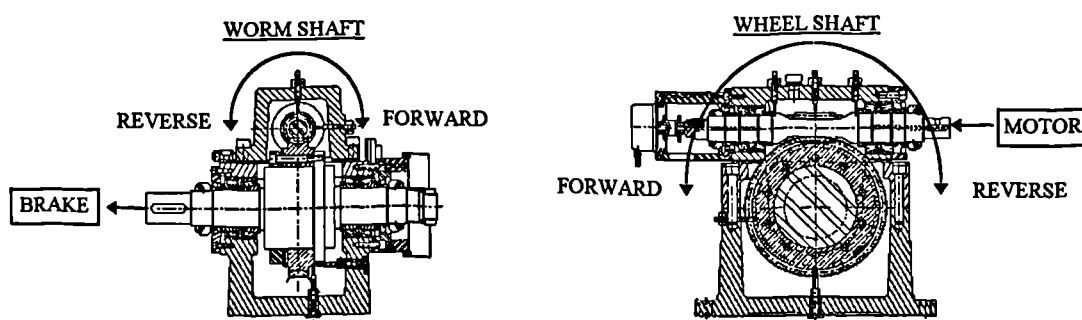
Figure 7.1 :   A diagram showing the definition of shaft rotation operating direction.

The transmission error and contact marking of the gear sets while under no load were recorded to use as further software validation. The test rig was then used to obtain transmission error results through a range of loads for these sets while under various operating conditions such as running speed and misalignment. Data from the experimental tests was used to develop a model of transmission error under load for use in the new software program.

Three gear sets were designed by the software based on an existing industrial designation using a 50:1 ratio and 152.4 mm (6") centre distance. The worm was made from steel to the standard BS 1970 (pt 1) Grade 665M17 and finished to a high standard resulting in profile errors of only 3µm and lead errors of less than 6µm thus reducing the potential error effects from these sources. The wheels were made from phosphor bronze to the standard BS 1400 Grade PB2C. Due to the difference in elasticity between the two components it was expected that most of the significant load effects during operation would be influenced by the wheel and therefore the same worm was used in each set.

The sets were designed using different techniques to induce individual characteristics for investigation. In each case the main criterion for the design was an initial contact marking which allowed entry and exit clearance for lubrication. The comparison of synthesised and measured characteristics made in sections 5.4 and 5.5 were considered a close enough correlation to allow the software to be used as a design tool for this task. The contact marking pattern and transmission error comparisons made in section 5.4 were repeated for the worm mating with each wheel under no load for further software validation. The gear sets were then installed in the test rig to investigate the effect of design techniques on transmission error while operating under load.

7.2. THE CORRELATION OF CALCULATED AND MEASURED CONTACT CHARACTERISTICS FOR THE TEST GEAR SETS UNDER NO LOAD

7.2.1. Comparisons of calculated and measured characteristics for a standard industrial gear set design (Wheel 1)

The first gear set included a wheel produced using an industrial design method based purely upon the designation, the design is listed in Appendix D/9. For this sample the program was used to confirm the satisfactory contact conditions of the design. This set was used as a control to study the effects of load on transmission error for a standard industrial design.

Predictions of theoretical and synthesised gear set characteristics were made and compared to the measured data collected. The theoretical, synthesised and recorded contact marking patterns for this wheel are shown in Figures 7.2, 7.3, and 7.4 respectively. Also, the transmission error results are shown in Figures 7.5, 7.6, and 7.7 respectively for the forward driven flank, and Figures 7.8, 7.9, and 7.10 for the reverse flank.

As in section 5.4, the marking patterns for this analysis show that including manufacturing errors influences the calculated clearance as can be seen from the discrepancies in theoretical and synthesised results on both flanks. Further, it shows that the synthesised calculation give a better representation of the actual contact conditions when compared to recorded data.

The transmission error analysis for this gear set driven in the forward direction shows some distinct correlation of the theoretical and measured signal in both magnitude and form. The synthesised error plot does not correlate well in form or magnitude. The depression effect is evident in the synthesised results obtained while driving in the reverse direction. In this case the measured signal resembles both the theoretical and synthesised calculations to within 1-2μm. Complete correlation at this scale is difficult to achieve due to the magnitude of the errors involved relative to the accuracy of the measuring equipment used.
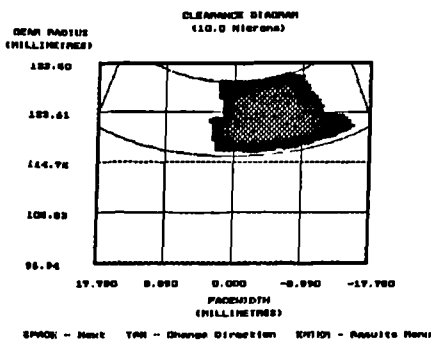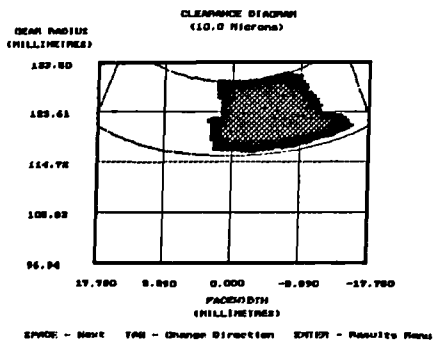
FORWARD   REVERSE

Figure 7.2 :   Theoretical marking pattern for Wheel 1.

FORWARD   REVERSE

Figure 7.3 :   Synthesised marking pattern for Wheel 1.

FORWARD   REVERSE

Figure 7.4 :   Measured marking pattern for Wheel 1.

WHEEL 1 (FORWARD)
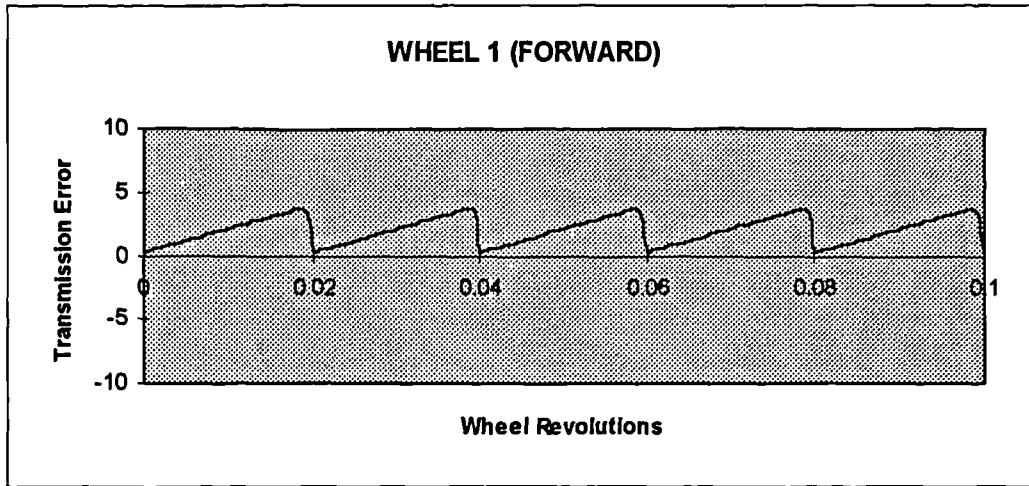
Figure 7.5 : Theoretical transmission error for Wheel 1.

WHEEL 1 (FORWARD)

Figure 7.6 : Synthesised transmission error for Wheel 1.

WHEEL 1 (FORWARD)

Figure 7.7 : Measured transmission error for Wheel 1.

Figure 7.8 :   Theoretical transmission error for Wheel 1.

Figure 7.9 :   Synthesised transmission error for Wheel 1.

Figure 7.10 :   Measured transmission error for Wheel 1.

CHAPTER 7

7.2.2. Comparison of calculated and measured characteristics for a standard industrial design with wheel cutter profile modification (Wheel 2)

A second wheel was produced using the specification of the standard wheel in section 7.2.1. The wheel cutter was designed with metal added to the profile inducing additional relief on the tip and root of the wheel teeth. This wheel was used to investigate the influence of relief on transmission error wave form analogous to work completed by Munro and Yildirim[33] on spur gear sets under torque loads. The aim was to apply a relief which would minimise the transmission error wave amplitude at an operating load of 2500 Nm. This value was chosen as it was the upper design limit for the test rig, however it was later found to be outside the operating range of the assembly.

The new software program was used to simulate the bending effect of the gear teeth using a linear stiffness model as defined in Chapter 3 with a value for the stiffness constant, k, of 11.5N/mm/μm. The calculated effects on transmission error magnitude for a series of linear and parabolic relief values at this 2500 Nm load is shown in Figures 7.11 and 7.12 respectively.

For optimisation during operation at the 2500 Nm design load, the minimum magnitude of calculated transmission error was chosen. For the forward driven wheel flank design this was 0.064 mm (0.0025") of linear profile modification, and 0.128 mm (0.0050") of parabolic profile modification on the reverse flank. Using CNC grinding machines it was possible to produce a wheel cutting tool with both a linear and parabolic profile modification in order to study the effects on a single wheel.

The no load analysis was repeated using this gear wheel and the test worm. The theoretical, synthesised and recorded contact marking patterns for this wheel are shown in Figures 7.13, 7.14, and 7.15 respectively. The transmission error results are shown in Figures 7.16, 7.17, and 7.18 respectively for the forward driven flank, and similarly Figures 7.19, 7.20, and 7.21 for the reverse flank. There is an excellent agreement with both flanks for both marking pattern and transmission error analysis.
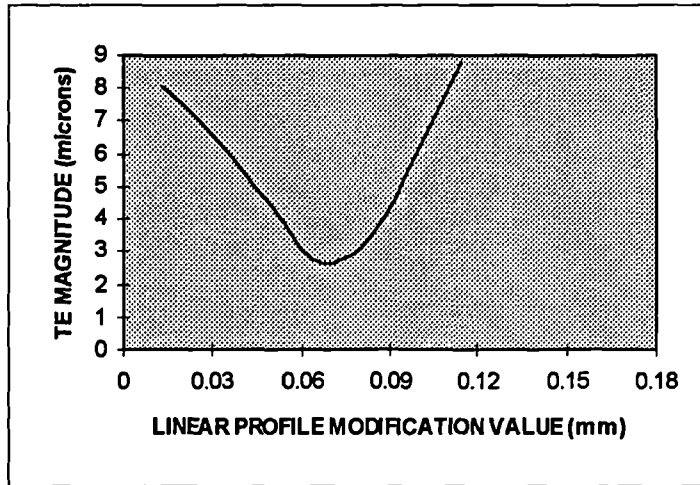
Figure 7.11 :   A graph of the change in theoretical transmission error magnitude under
2500 Nm load with respect to fly tool linear profile modification.
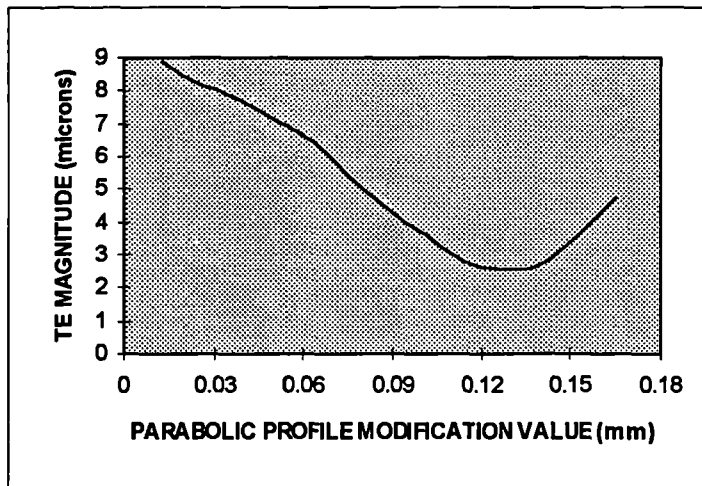
Figure 7.12 :   A graph of the change in theoretical transmission error magnitude under
2500 Nm load with respect to fly tool parabolic profile modification.
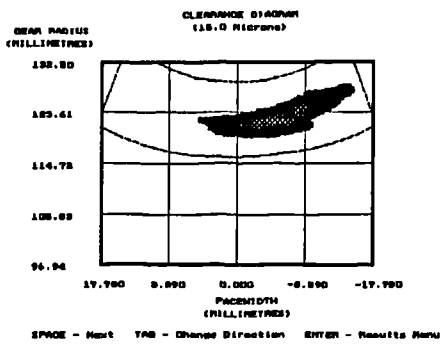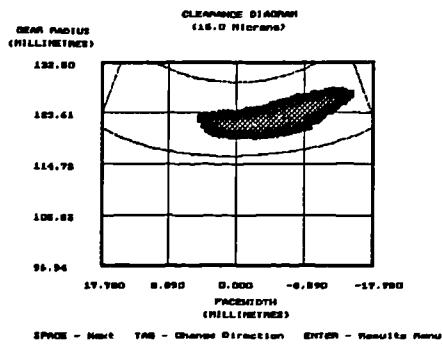
FORWARD (LIN)   REVERSE (PAR)

Figure 7.13 : Theoretical marking pattern for Wheel 2.
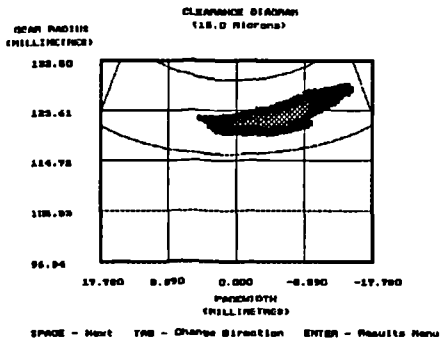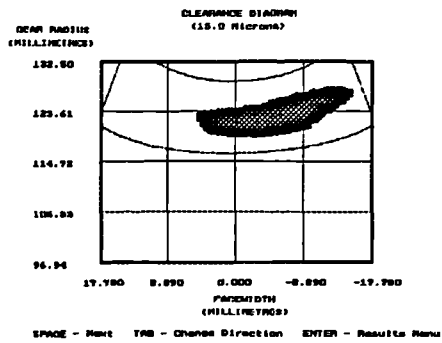
FORWARD (LIN)   REVERSE (PAR)

Figure 7.14 : Synthesised marking pattern for Wheel 2.
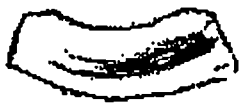
FORWARD (LIN)   REVERSE (PAR)

Figure 7.15 : Measured marking pattern for Wheel 2.
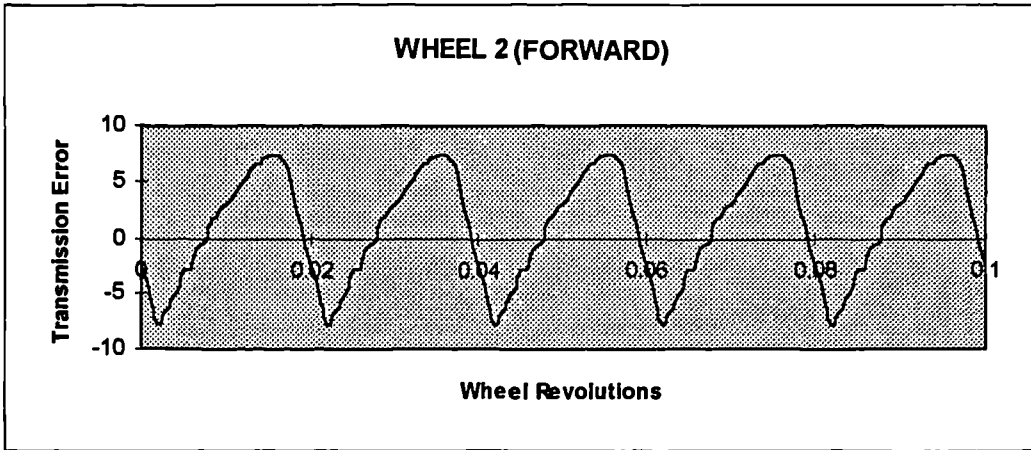
Figure 7.16 :   Theoretical transmission error for Wheel 2.
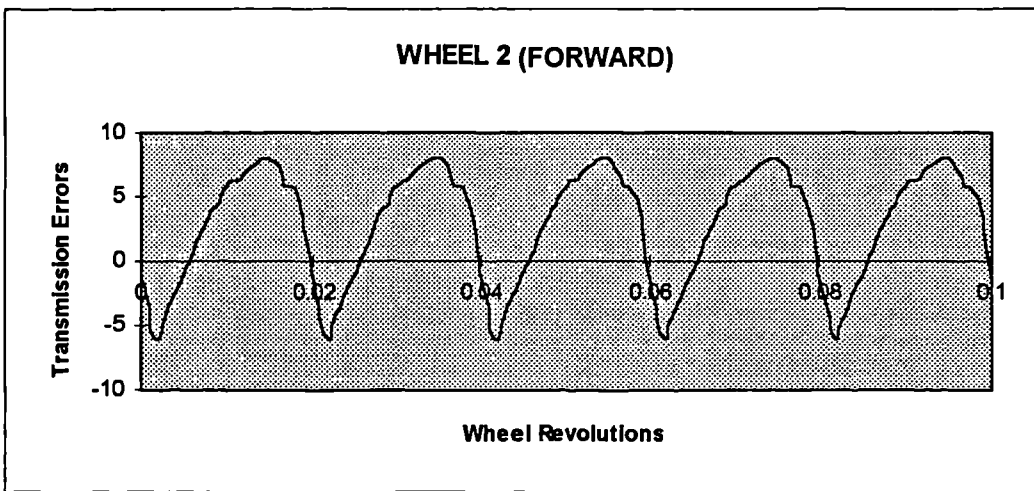
Figure 7.17 :   Synthesised transmission error for Wheel 2.
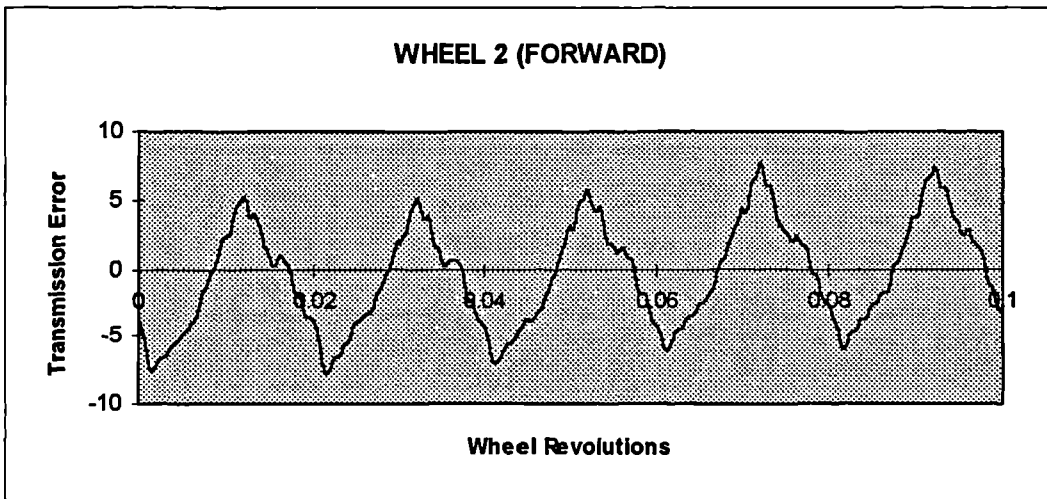
Figure 7.18:   Measured transmission error for Wheel 2.
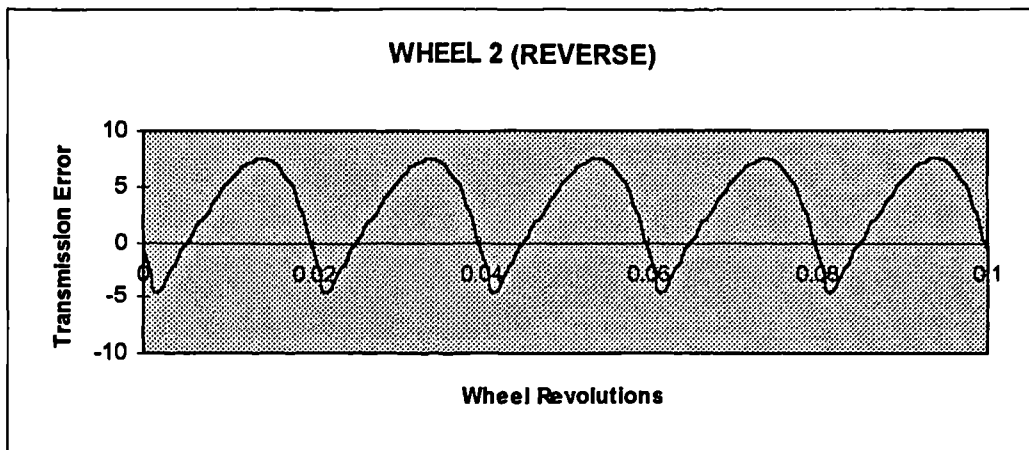
Figure 7.19 :   Theoretical transmission error for Wheel 2.
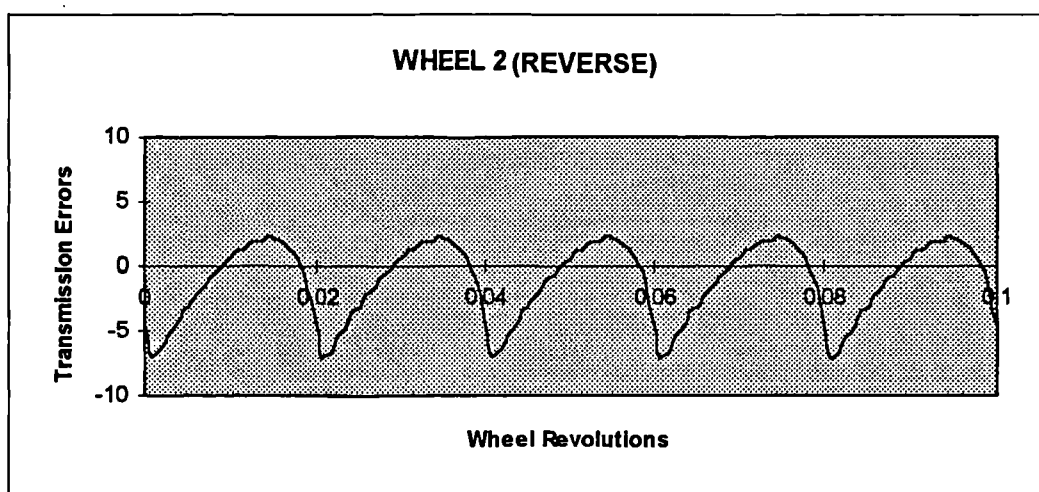
Figure 7.20 :   Synthesised transmission error for Wheel 2.
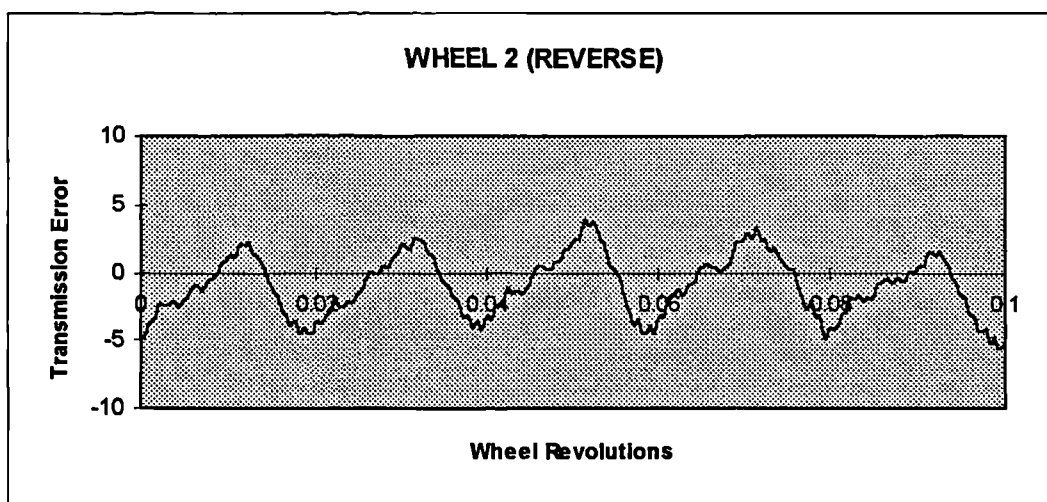
Figure 7.21 :   Measured transmission error for Wheel 2.

7.2.3. Comparisons of calculated and measured characteristics for a wheel design using an oversize wheel cutter (Wheel 3)

The third design combines the worm parameters as used in the first and second designs with an oversized wheel cutting technique. This is often used by industry to give a combination of contact marking pattern in the centre of the gear wheel tooth from tip to root and maintain satisfactory lubrication conditions. This wheel was used to examine the influence of different fundamental design methods on similar gear systems under load by direct comparison with Wheel 1.

The new software was used to analyse wheel designs with a range of oversize values in order to minimise the transmission error under load while maintaining a sufficient entry and exit clearance in the tooth form. A graph of transmission error magnitude for a series of oversize values is shown in Figure 7.22. The oversize value of 2.286 mm (0.090") was used for the wheel cutter design as this represented the minimum theoretical transmission error while still satisfying the lubrication conditions. The full gear set design specification is listed in Appendix D/10.
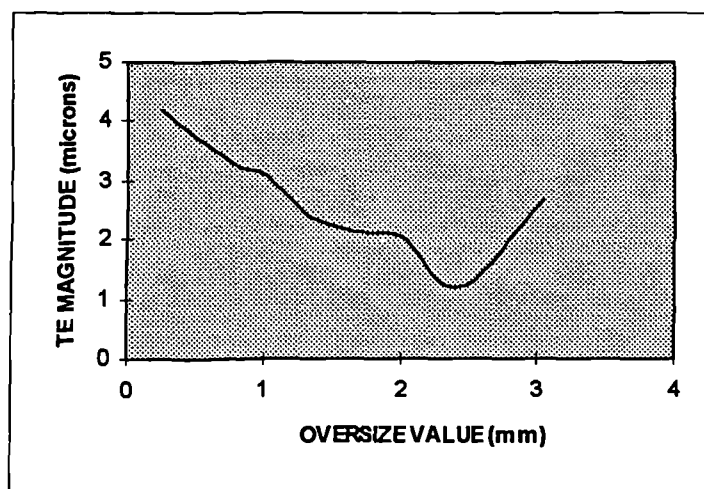
Figure 7.22: A graph of the change in theoretical transmission error magnitude under 0 Nm load with respect to fly tool oversize value.

The theoretical, synthesised and recorded contact marking patterns for this wheel are shown in Figures 7.23, 7.24, and 7.25 respectively. The transmission error results for this design are shown in Figures 7.26, 7.27, and 7.28 respectively for the forward driven flank, and Figures 7.29, 7.30, and 7.31 for the reverse flank.
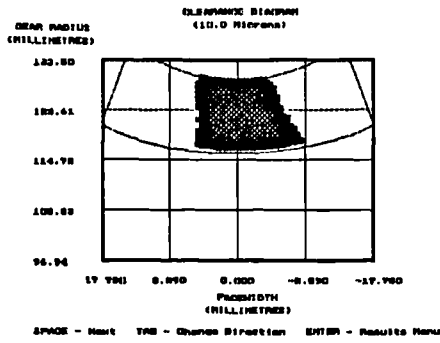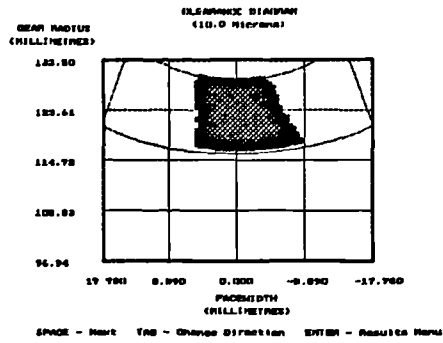
FORWARD   REVERSE

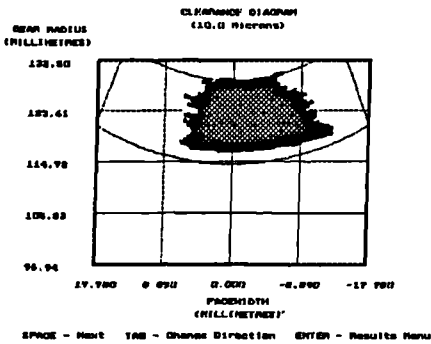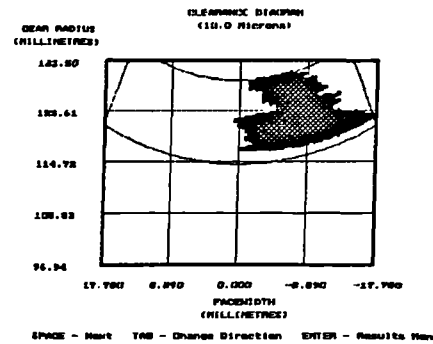Figure 7.23 :   Theoretical marking pattern for Wheel 3.
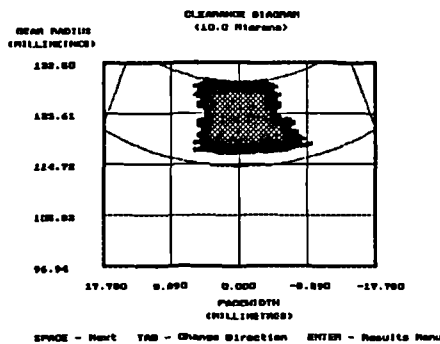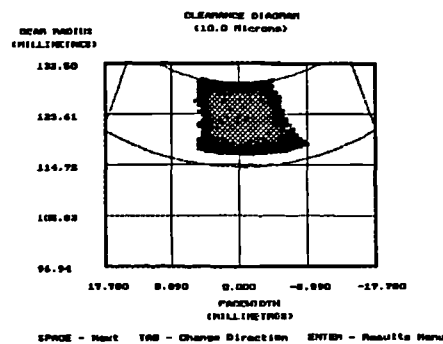
FORWARD   REVERSE

Figure 7.24 :   Synthesised marking pattern for Wheel 3.

FORWARD   REVERSE

Figure 7.25 :   Measured marking pattern for Wheel 3.
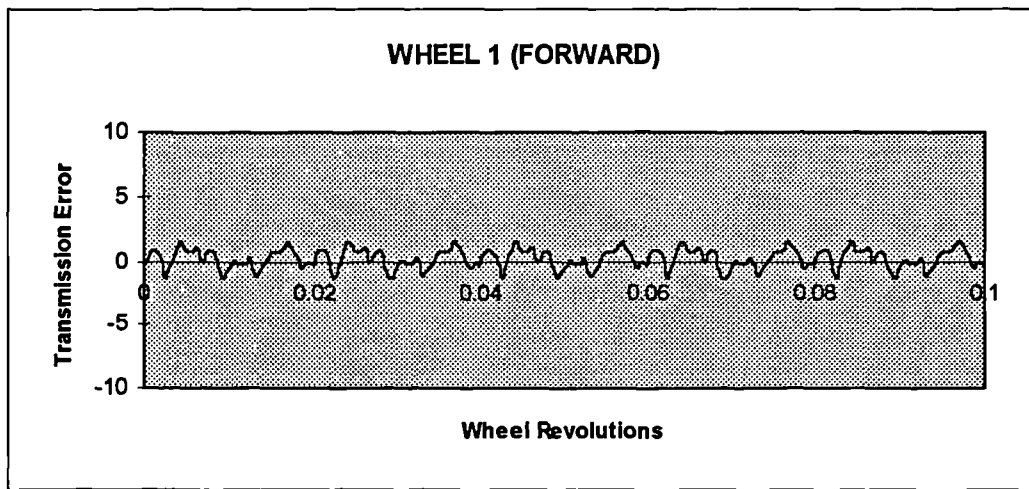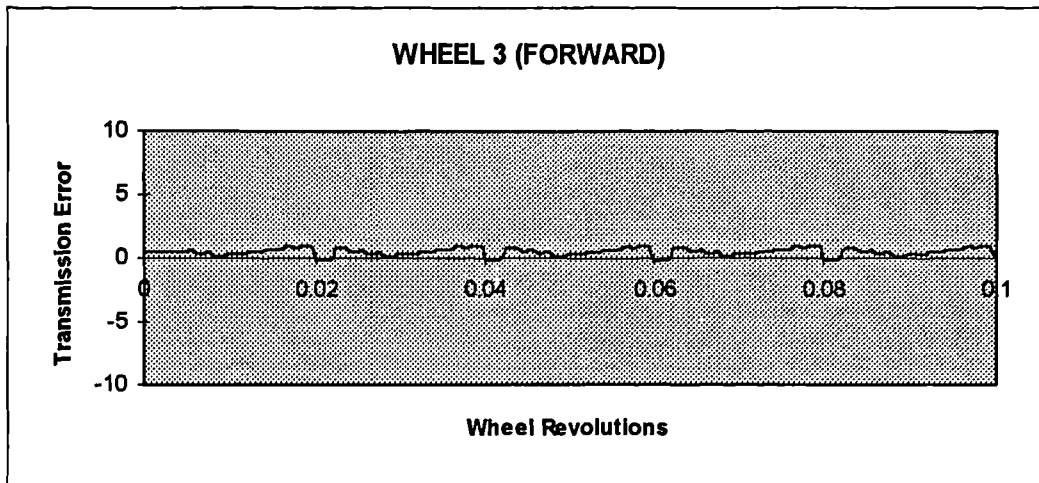
Figure 7.26 :   Theoretical transmission error for Wheel 3.
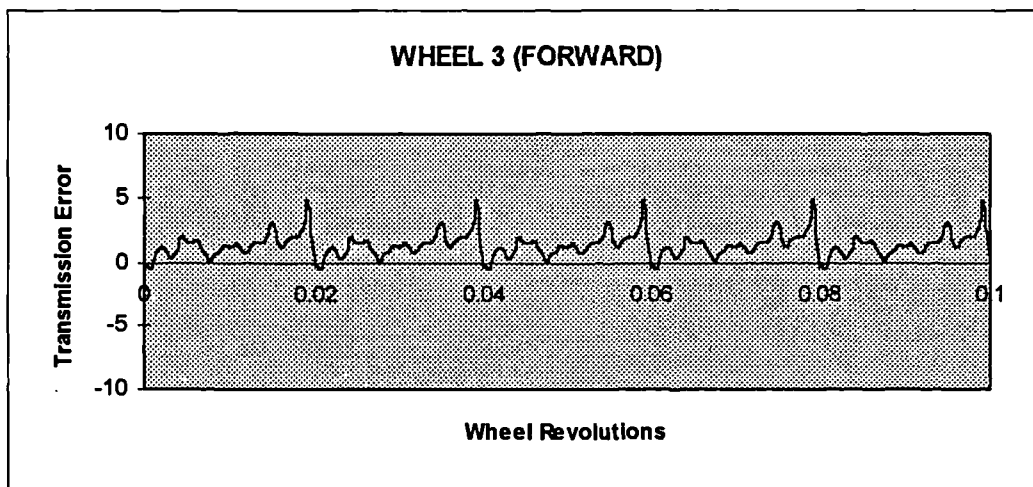
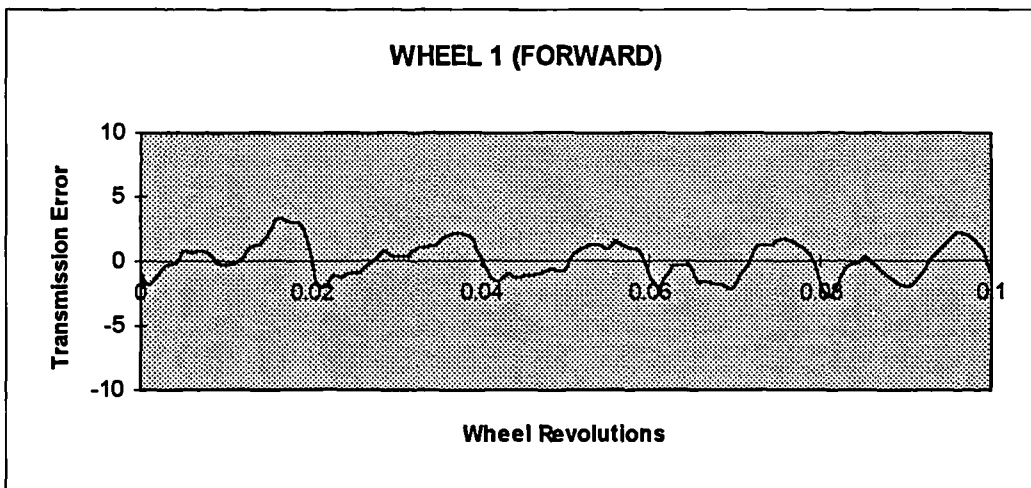Figure 7.27 :   Synthesised transmission error for Wheel 3.
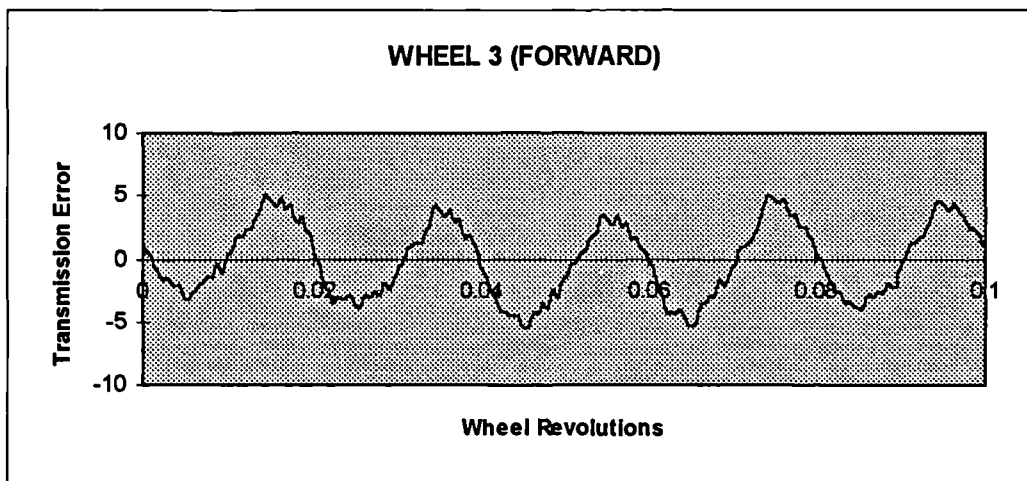
Figure 7.28 :   Measured transmission error for Wheel 3.

CHAPTER 7
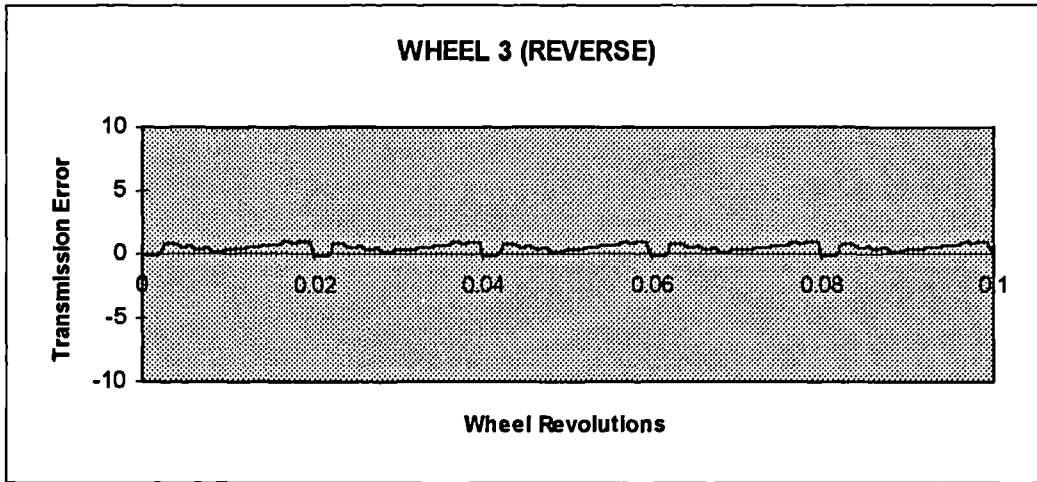
Figure 7.29 :   Theoretical transmission error for Wheel 3.
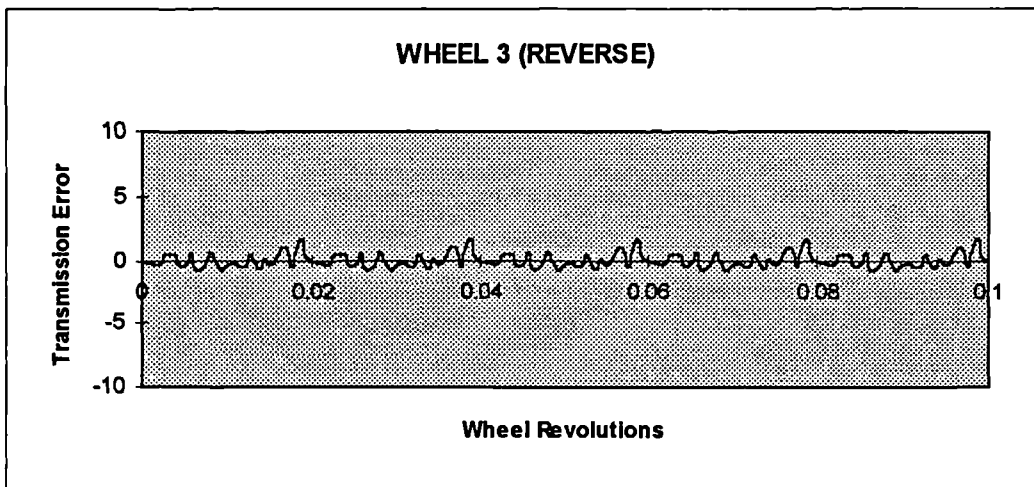
Figure 7.30 :   Synthesised transmission error for Wheel 3.

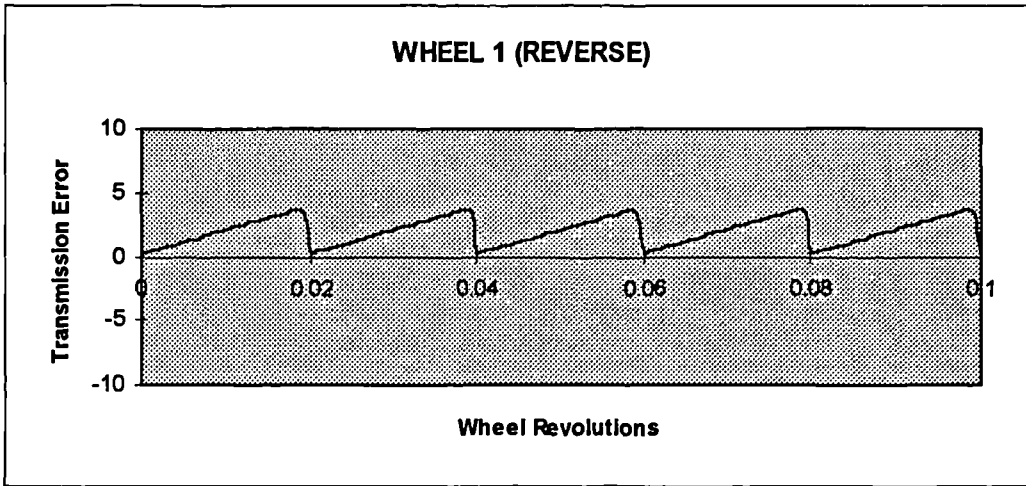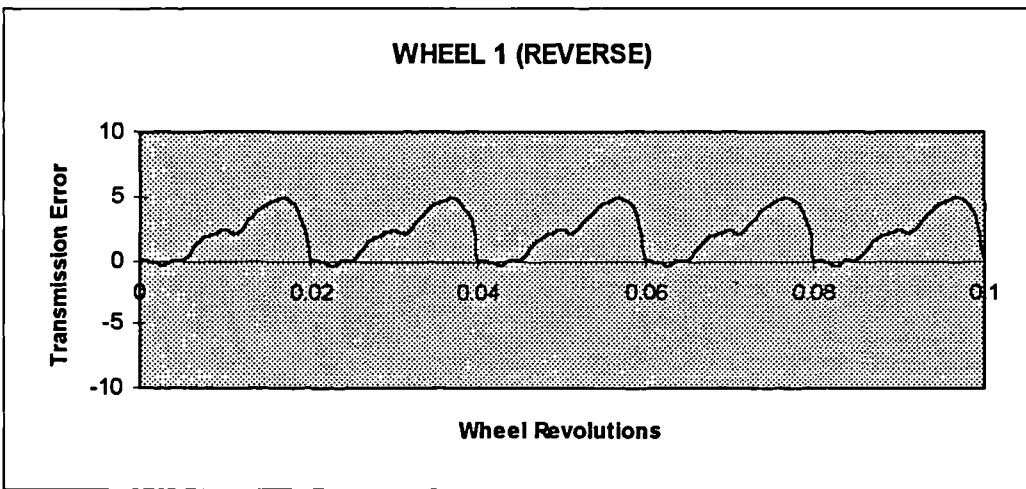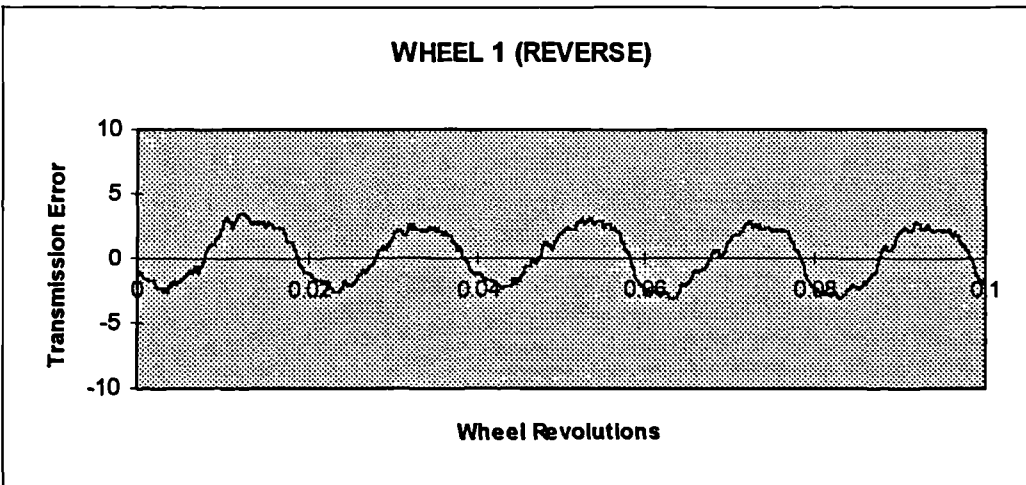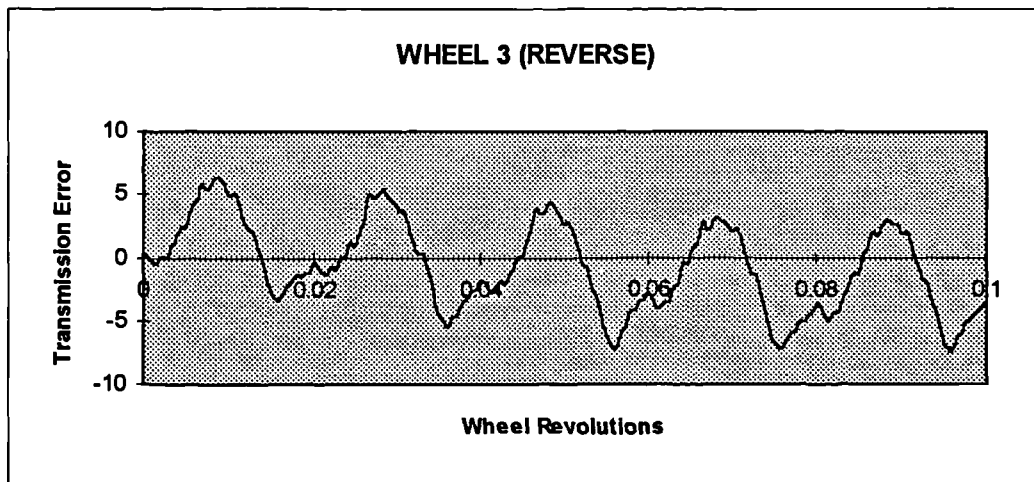Figure 7.31 :   Measured transmission error for Wheel 3.

The synthesised marking patterns for the oversize design are very similar to those expected in the theoretical analysis. They occupy the central band of the tooth almost symmetrically as intended. This shows close agreement with the marking patterns recorded for the gear set.

There is a large variation between the associated synthesised and measured transmission error. It was anticipated that the 1-2μm magnitude graph would be exceeded be a further 1-2μm due to production errors, as demonstrated in the comparison of the theoretical and synthesised graphs. However, the excessive increase in magnitude was unexpected.

An attempt was made to find the cause of this lack of correlation. The theoretical design characteristics were confirmed using other worm gear software sources. Wear in the worm after testing Wheel 1 and 2 was ruled out by comparative measured transmission error results obtained by running the wheel with a new worm produced to the same design. Measurement of the wheel profile in the axial section showed errors of up to 8μm which were not apparent in the cutting tool. These wheel profile errors would be a direct cause of transmission error. This conclusion suggests that the wheel cutter manufacturing technique may influence the achievable machining accuracy since despite very low theoretical magnitudes the measured transmission error in this set was significant. This is especially true when using a fly tool (a single tooth wheel cutter mounted in a bar rotating about the cutting axis) as was used in this case which is susceptible to additional profile shift as described in section 2.4.2.1. due to the manual alignment procedure. A hob is generated by gashing grooves perpendicular to a continuous worm thread form to create a series of cutting profiles. Though the thread form is defined by the same mismatch design parameters as the fly tool, the dimensions and profile of the hob are fixed which encourages a far more dependable outcome for high accuracy applications.

7.3. THE EFFECT OF WHEEL DESIGN TECHNIQUE ON TRANSMISSION ERROR CHARACTERISTICS UNDER LOAD

7.3.1. Transmission error in a gear set under load for a standard industrial gear set design (Wheel 1)

An existing industrial gear specification as described in Section 7.2.1 was used to produce a gear set to assess the behaviour of a standard gear design. The test rig was used to perform a standard series of tests for transmission error on the system using Wheel 1. The results are recorded in Figure 7.32 as a Harris Map. It can be seen from these results that the transmission error wave form and magnitude produced by the gear set while under no load is repeated at each load interval. The wave form remains constant and the magnitude of the wave form does not change by more than 2μm over the 2000 Nm loading cycle.

7.3.2. Transmission error in a gear set under load for a standard industrial gear set design with wheel profile modification (Wheel 2)

The Harris Map in Figure 7.33 shows a standard series of tests for transmission error carried out on a system using Wheel 2 with profile modification described in section 7.2.2. The mean (or DC) transmission error values are consistently 6-8μm larger than those measured for Wheel 1 at each load interval. Unlike the results of Wheel 1, the magnitude of the transmission error changes distinctly with load. The minimising of the wave form magnitude expected in this design occurs on both flanks but at different loads in each case. Also, neither flank produces a minimum magnitude at the intended design load. The magnitude of the recorded error for the forward driven flank containing the linear profile modification is reduced to 1μm magnitude at 1000 Nm which suggests that this load is approximately the optimum design load for this relief. The reverse driven flank, containing the parabolic modification, is reduced to around 2μm magnitude at both the 1500 Nm and 2000 Nm load intervals. This suggests that a design load for the design in this flank would be approximately 1750 Nm, and that the initial estimate of combined tooth stiffness of 10.5N/mm/μm was too large.

7.3.3. Transmission error in a gear set under load for a gear set design using an oversized wheel cutter (Wheel 3)

The results for the Wheel 1 system in Figure 7.32 indicated that for a standard design there was little change in transmission error magnitude due to a load increase over 2000Nm. The Wheel 3 design described in Section 7.2.3 was used to investigate two factors relating to this. The first was whether this behaviour was common to an alternative design method. The second was to investigate to what extent a gear set with minimised transmission error under no load would maintain this characteristic through the loading cycle. The results for this wheel are recorded in Figure 7.34. The correlation of no load synthesised and measured transmission error for this wheel was poor in that the predicted magnitude of 1-2μm could not be obtained, as shown in Section 7.2.3. However, the results of the load tests do show that the characteristic of this set is similar to that of Wheel 1 in that the wave form generated on either flank at no load is not affected by more than 1-2μm in magnitude at each loading interval. Also, the mean transmission error levels are the same as those for Figure 7.32 to within the 5μm repeatability tolerance reported in Chapter 6.

FORWARD   REVERSE
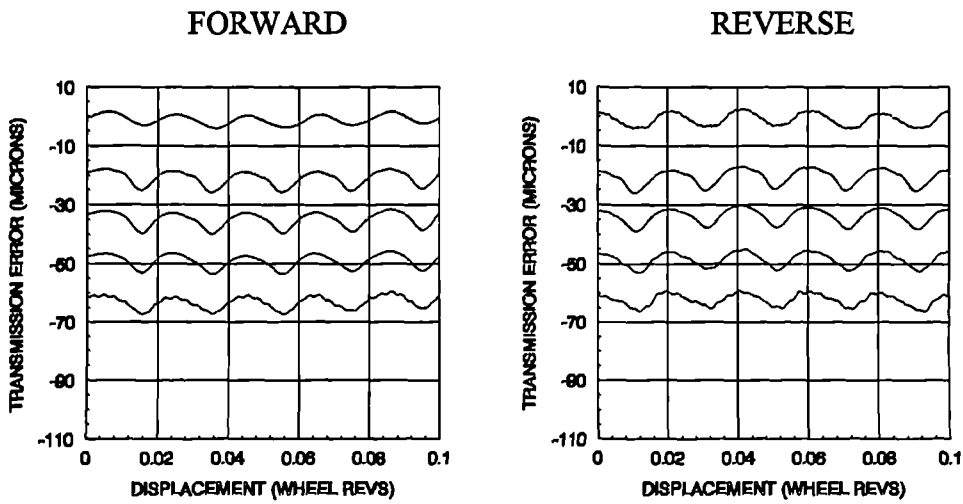
Figure 7.32 : Measured transmission error results from a standard series of tests on
            Wheel 1.
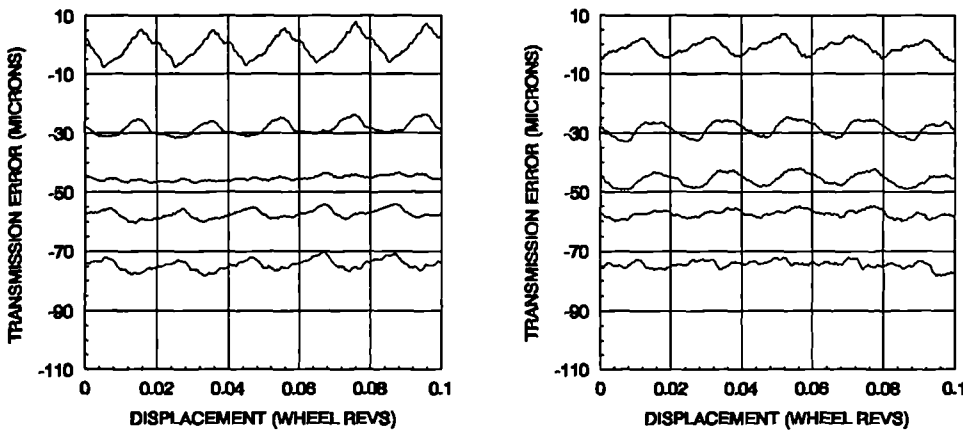
Figure 7.33 : Measured transmission error results from a standard series of tests on
            Wheel 2.
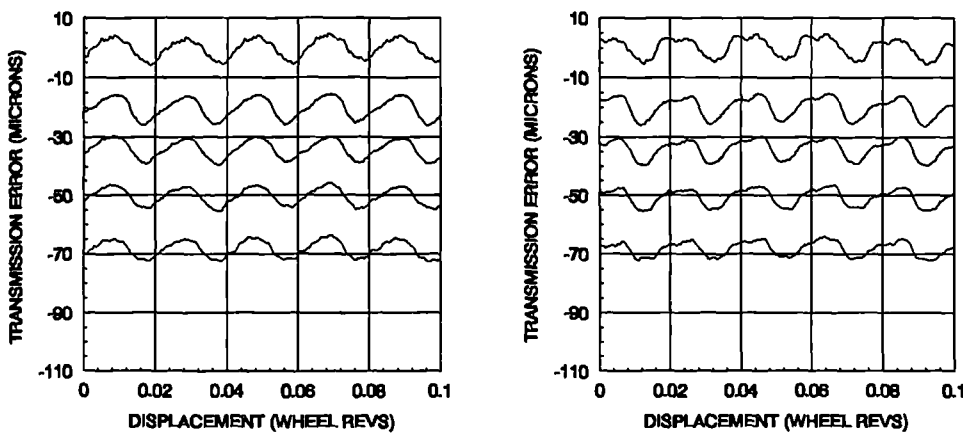
Figure 7.34 : Measured transmission error results from a standard series of tests on
            Wheel 3.

7.4. THE EFFECT OF GEAR SET MISALIGNMENT UNDER LOAD ON TRANSMISSION ERROR CHARACTERISTICS

7.4.1. The effects of centre height variation on transmission error for a standard industrial gear set design (Wheel 1)

A series of tests was performed using the gear set with Wheel 1 to assess the effect on transmission error of offset in centre height position. The worm housing was positioned 0μm, 250μm, and -250μm from the default value for the correct test box assembly. A standard series of test for transmission error under load was carried out, and the results are shown in Figures 7.35/1-3 respectively.

The graphs show that the misalignment induces only a slight change in wave form for the gear set under no load. The exception to this is the reverse flank under a -250μm misalignment in which the no load error curve is increased from 5μm to 10μm magnitude. Also, the transmission error in this plot should resemble that of the 250μm misalignment of the forward driving flank due to the axis-symmetric nature of this gear set design. The difference may have been caused by some inherent offset in the test box assembly.

The system maintains the characteristics of repeating wave form and magnitude during the loading cycle consistent with the results in section 7.3. The mean transmission error level intervals in both the 250μm and -250μm tests are repeated within a 5μm band. These plots are however consistently 12μm greater for each load interval than the equivalent plot in the 0μm misalignment test representing a 15% increase.
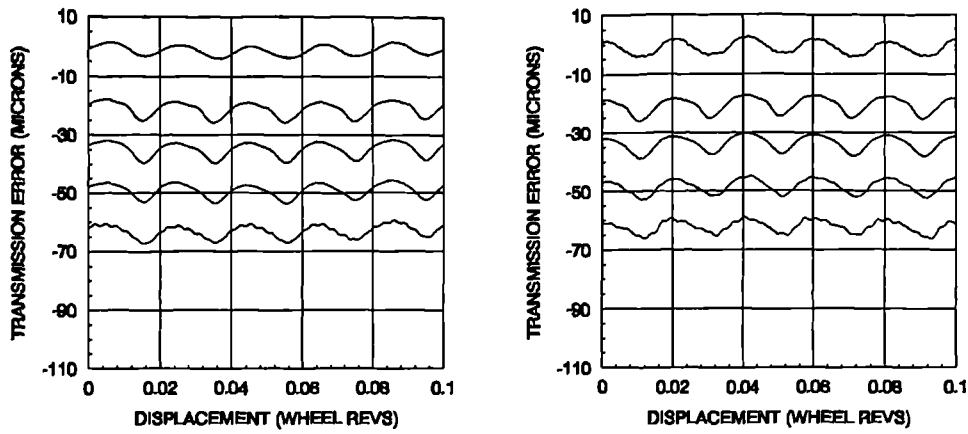
Figure 7.35/1 : Tests performed on Wheel 1 at 0μm misalignment
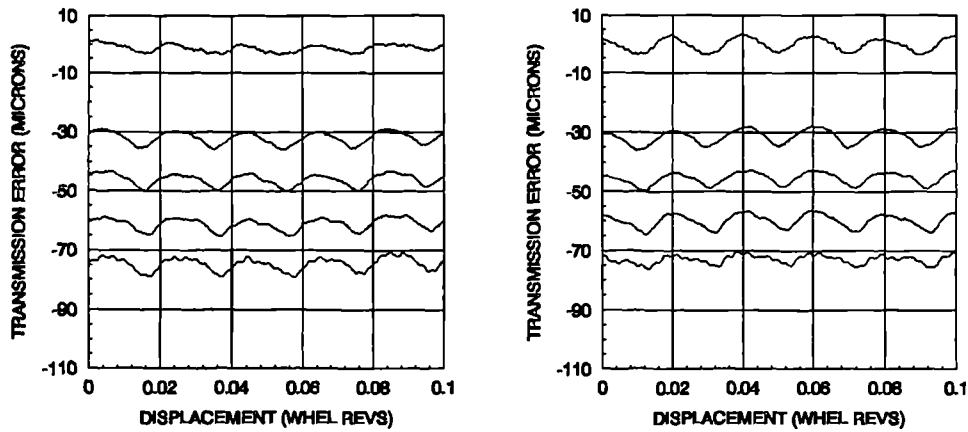
Figure 7.35/2 : Tests performed on Wheel 1 at 250μm misalignment.
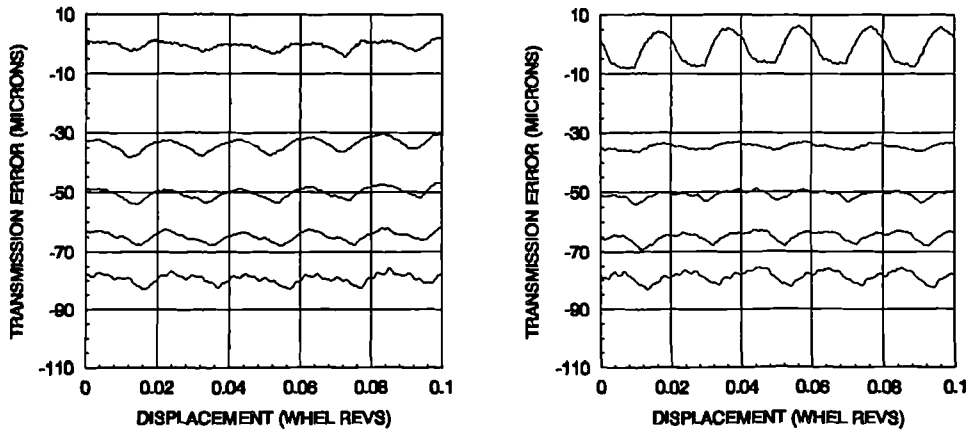
Figure 7.35/3 : Tests performed on Wheel 1 at -250μm misalignment.

Figure 7.35 :   Measured transmission error from a standard series of tests on Wheel 1
while centre height is offset by 0μm, 250μm, and -250μm respectively.

7.4.2. Misalignment effects on transmission error for a standard industrial gear set design with profile modification (Wheel 2)

The tests performed in section 7.4.1 were repeated using the Wheel 2 assembly. The results of this are shown in Figures 7.36/1-3 respectively. As with the standard gear set the misalignment causes a change in transmission error wave form under no load, but in this case the magnitude is dramatically reduced rather than slightly increased. Although the gear set retains the characteristic of producing a minimised magnitude wave form at some point during the load cycle, the results show that this effect occurs at a different load in each case. In the $0\mu m$ misalignment test the optimum load was 1000 Nm for the forward driven flank and 1750 Nm for the reverse driven flank. For the $250\mu m$ test the optimum error signal occurred at around 2000 Nm for both flanks while for the $-250\mu m$ case the optimum was reduced to around 1000 Nm load in both flanks.

As well as this, a difference can be observed in the mean transmission error levels. The tests at $250\mu m$ offset show around $15\mu m$ greater error levels than those for the correctly aligned case, while those in the $-250\mu m$ misalignment tests are generally $5\mu m$ greater. The reason for the distinct differences in the behaviour relative to the Wheel 1 system may be associated with the fact that the gear tooth form is no longer axis-symmetric in this case due to the application of different wheel profile relief in each flank. The offset in this gear set can therefore be expected to produce different results.

FORWARD   REVERSE
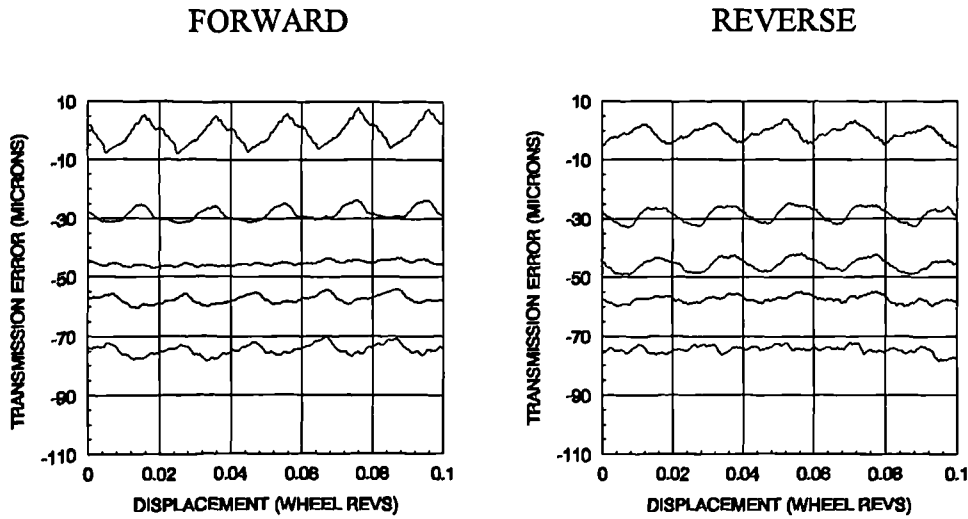
Figure 7.36/1 : Tests performed on Wheel 2 at 0µm misalignment.
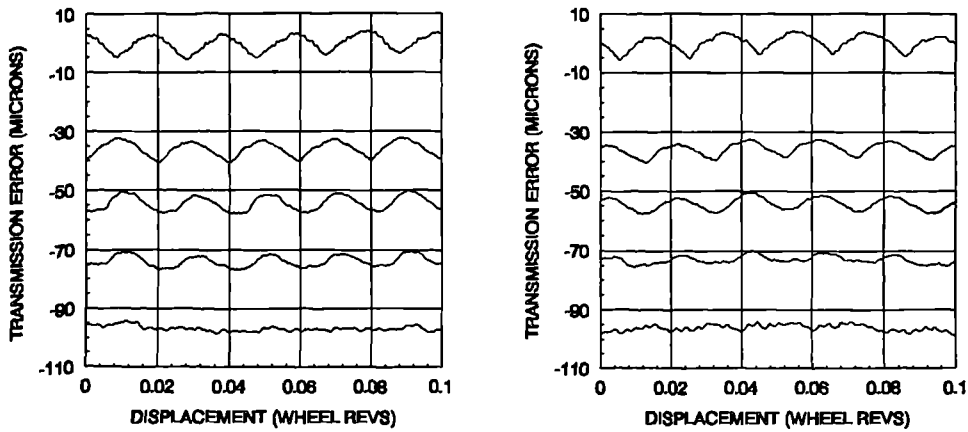
Figure 7.36/2 : Tests performed on Wheel 2 at 250µm misalignment.
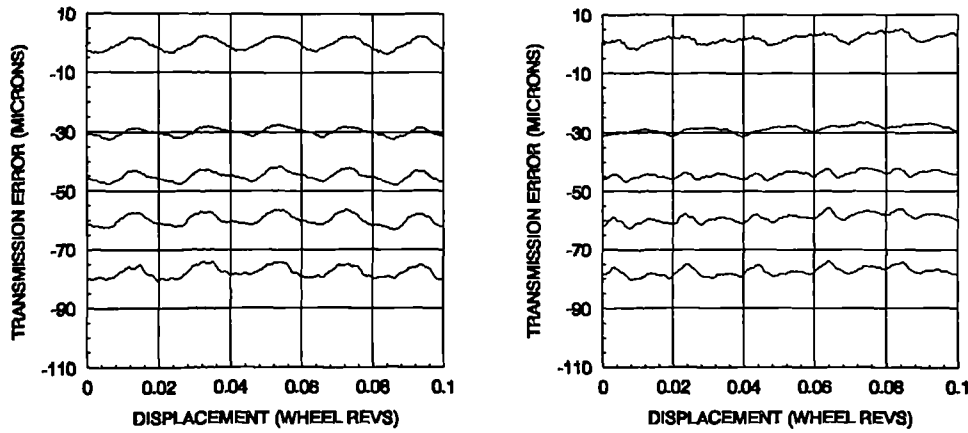
Figure 7.36/3 : Tests performed on Wheel 2 at -250µm misalignment.

Figure 7.36 :   Measured transmission error from a standard series of tests on Wheel 2
while centre height is offset by 0µm, 250µm, and -250µm respectively.

7.5. THE EFFECT OF OPERATING SPEED UNDER LOAD ON TRANSMISSION ERROR CHARACTERISTICS

7.5.1. The effects of shaft speed variation on transmission error for a standard industrial gear set (Wheel 1)

The centre height variation tests for Wheel 1 reported in section 7.4.1 were repeated while operating the test rig at an input speed of 300 rpm. The results for the 0μm, 250μm, and -250μm settings are shown in Figure 7.37/1-3 respectively. These were compared to the results recorded previously at the standard 150 rpm input speed as shown in Figure 7.35.

The results of these tests show a close repeatability in transmission error at the different operating speeds for each alignment. The wave form magnitudes agree to within around 1μm in most cases. The most notable exception to this is in the no load graphs for the 300 rpm tests. In this case there is a distinct noise trace within the underlying signal. This may be caused by the increased inertia within the wheel at this speed overcoming the friction effect of the wheel bearings and allow the gear set to jump out of contact. Applying a load to the system provides a substantial resistance to negate this effect. This is exactly the behaviour observed in all the subsequent loaded traces. The mean transmission error graphs of the 150 rpm and 300 rpm tests show a correlation to within the 5μm repeatability of the load test.
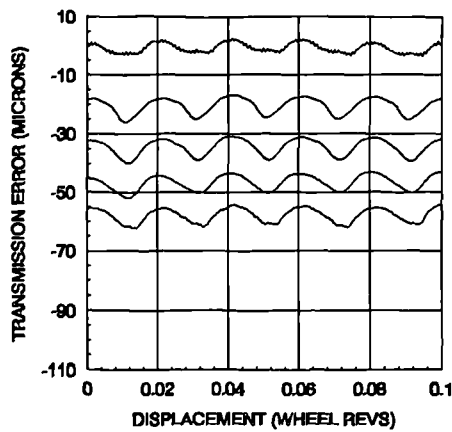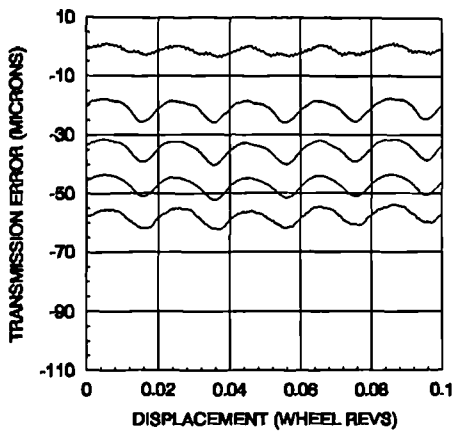
Figure 7.37/1 : Tests performed on Wheel 1 at 0μm misalignment.
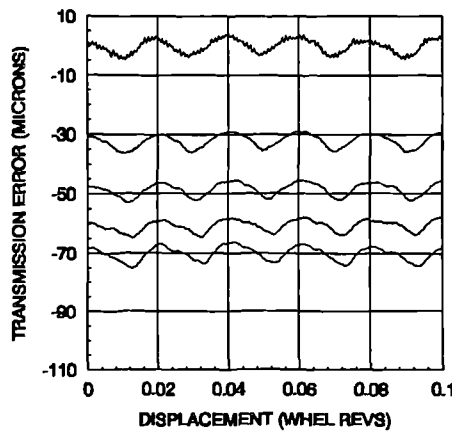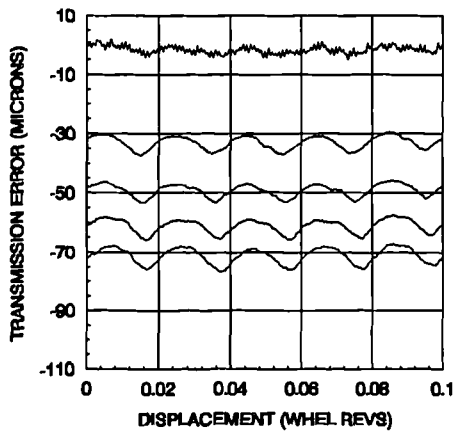
Figure 7.37/2 : Tests performed on Wheel 1 at 250μm misalignment.
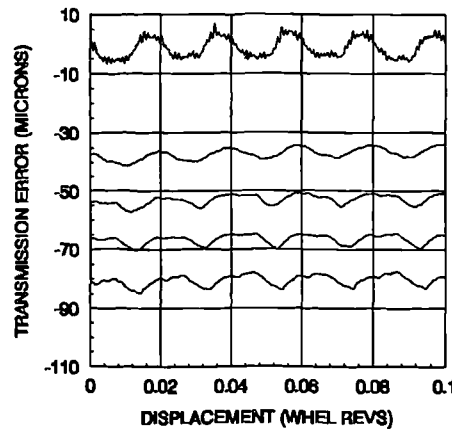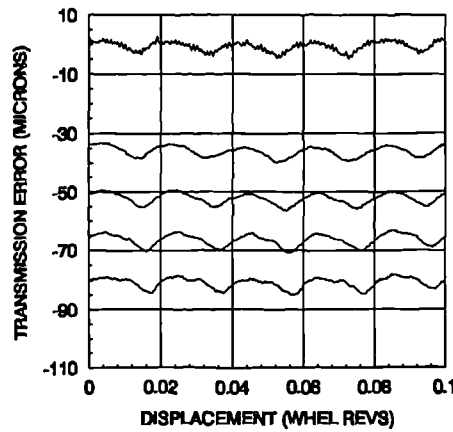
Figure 7.37/3 : Tests performed on Wheel 1 at -250μm misalignment.

Figure 7.37 : Measured transmission error from a series of tests on Wheel 1 with centre height misaligned by 0μm, 250μm, and -250μm respectively while operating at 500 Nm intervals and 300 rpm worm shaft speed.

7.5.2. Shaft speed tests from an industrial gear box operating under a torque load relating transmission error to vibration

Operating speed can be shown to affect the vibration response of the gear system once in operation. The graph in Figure 7.38 shows a single flank transmission error plot for one wheel revolution of a 64:3 ratio gear set. It also shows a table of the FFT analysis for the wave form containing frequencies in cycles per wheel revolution and an associated amplitude. The four dominant frequencies and their ratio to the tooth engagement frequency have been tabulated and are highlighted **A, B, C, and D**. Figure 7.39 shows three dynamic vibration tests from a gear box while operating under load using the same 64:3 gear set. The graphs represent frequency spectra of a signal from a sensor monitoring accelerations of the set of the output shaft at operating speeds of 50, 56, and 64 tooth engagements per second respectively. The graphs show that the dominant frequencies of vibration have ratios which correlate with those of contact recorded under no load.

The amplitudes in the frequency spectrum should behave in a predictable manner with the increase in amplitude being proportional to the square of the frequency for an increase in operating speed. The graphs in Figure 7.39 demonstrate that this is not always the case. There are two main reasons why this should be so. The first is that the torque was not monitored during these tests and therefore the changes in amplitude may be due to small variations in transmission error wave form due to a deformation of the tooth caused by mechanical braking as discussed in section 7.3. Specifically, a higher load may remove ratios above the first harmonic of engagement. This will tend towards a pure wave form at the engagement frequency thus increasing the amplitude while reducing those of others. The second reason is that the complete system must be considered when trying to calculate the output signal. The braking system will influence the characteristic signal in the same way as the interference signal detected in the step up box of the test rig described in section 6.6. Other elements of the system such as couplings, bearings and housing deformation may also contribute to the output signal in industrial installations.

MARKER	FREQUENCY	MESH FREQUENCY RATIO
A	64	1.00
B	84	1.31
C	100	1.56
D	112	1.75

Figure 7.38 : Single flank contact analysis of a 64:3 ratio gear set identifying the major frequencies of rotation in the transmission error signal.
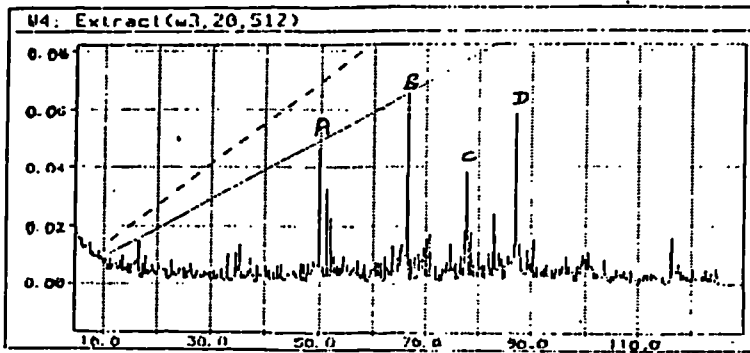
OPERATING FREQUENCY :50 Hz

MARKER	FREQUENCY	MESH FREQUENCY RATIO
A	50	1.00
B	66	1.32
C	77	1.54
D	87	1.74
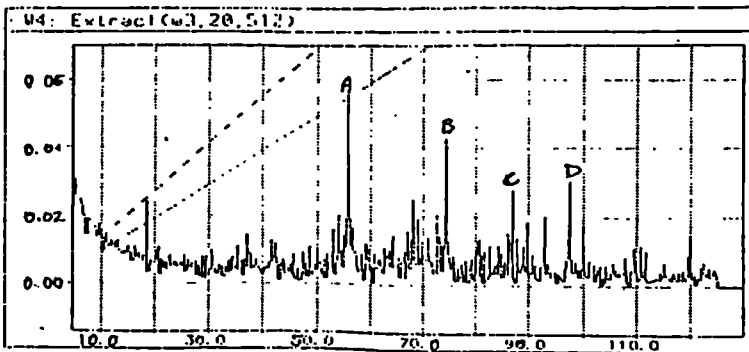
OPERATING FREQUENCY :56 Hz

MARKER	FREQUENCY	MESH FREQUENCY RATIO
A	56	1.00
B	74	1.32
C	87	1.55
D	97	1.73
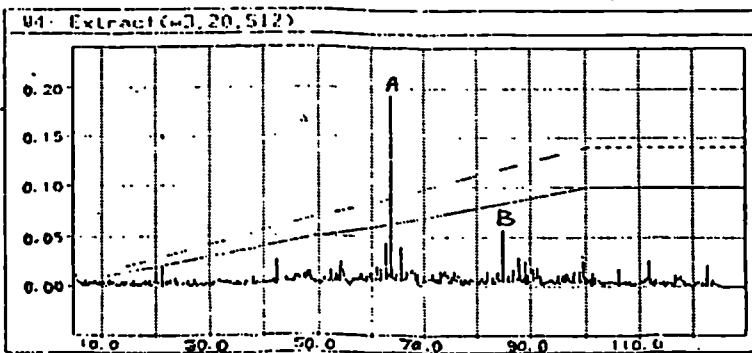
OPERATING FREQUENCY : 64 Hz

MARKER	FREQUENCY	MESH FREQUENCY RATIO
A	64	1.00
B	88	1.32
C	NA	NA
D	NA	NA

Figure 7.39 : Dynamic vibration frequency spectrum analysis of a 64:3 ratio gear set system at operating speeds of 50, 56, and 64 meshing cycles per second.

7.6. SYNTHESIS OF TRANSMISSION ERROR FOR A WORM GEAR SYSTEM OPERATING UNDER LOAD

7.6.1. Synthesis of transmission error under load for a standard industrial worm gear set design (Wheel 1)

The measured data from the test rig was used to model the calculations of transmission error under load using the new software. The results in the Harris Map for Wheel 1 were used as the initial test sample. An equivalent Harris Map was calculated for this wheel system using the theoretical and synthesised contact conditions in turn. An iterative process established 5.9 N/mm/µm as the optimum linear stiffness value for the contact to produce a correlation with the measured results. The theoretical, synthesised and measured results are shown in Figure 7.38/1-3 respectively.

There is only a small detectable difference between the transmission error graphs calculated using the theoretical information and those calculated using the synthesised data in the order of 1-2µm. This correlation is even closer when comparing the curves calculated for the load intervals. This indicates that surface finish does not influence the transmission error calculation under load. The calculations also indicate that the wave form is closely repeated at each load interval. This is also a characteristic consistent with the measured results as evident in the experimental results obtained by the test rig.

The calculated mean transmission error levels agree to within 5µm of the measured value at each load interval. The magnitude of these curves correlate to within 2µm, however the calculated magnitude increase with increasing load while the measured results show a slight decrease. There is a need for a some minor modification to the stiffness function allowing for the effects of local contact conditions between the worm thread and wheel tooth. The characteristics produced by thread and tooth dimensions such as thickness, height and width at the contact point may provide a subtle influence on the stiffness value. This effect has been reported in experimental results on spur and helical gears by Oda et al[35][36].

FORWARD   REVERSE
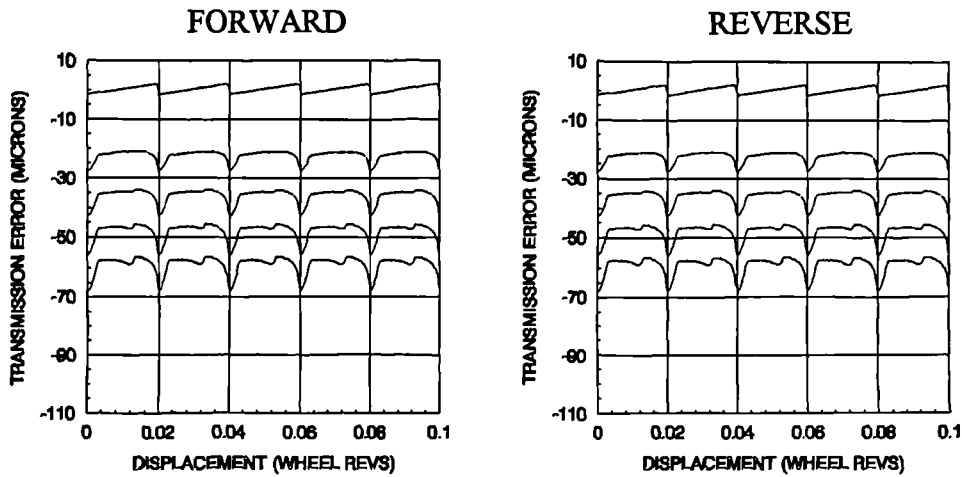
Figure 7.39/1 : Theoretical design transmission error characteristics.
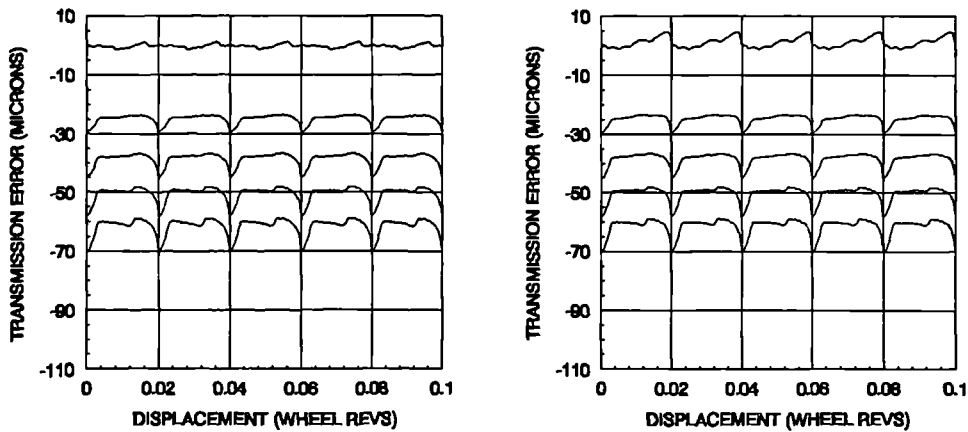
Figure 7.39/2 : Synthesised transmission error characteristics.
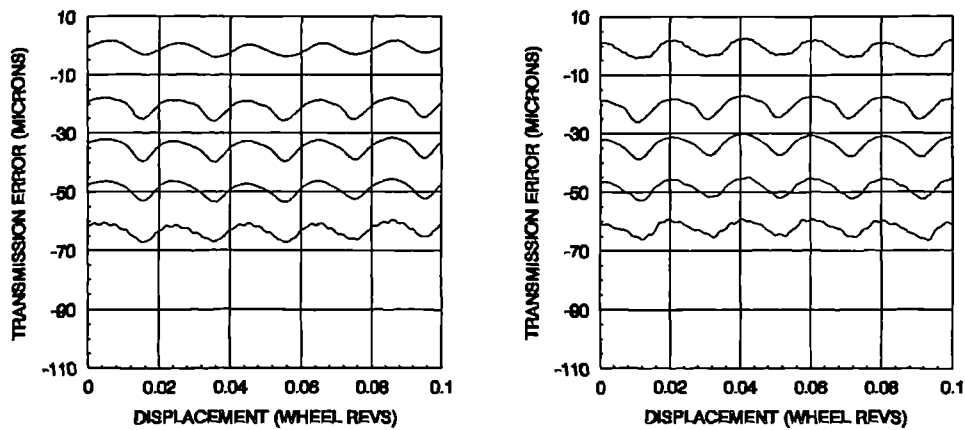
Figure 7.39/3 : Measured transmission error data.

Figure 7.39 : A comparison of theoretical, synthesised and measured Harris Maps of transmission error for Wheel 1 design operating under 0-2000 Nm load in 500 Nm intervals.

7.6.2. Synthesis of transmission error under load for a standard industrial gear set containing profile modification (Wheel 2)

Similar calculations of synthesised transmission error under a torque operating load were made for Wheel 2 using the same linear stiffness model as used for Wheel 1 comparison. The comparison of these synthesised transmission error calculations with the measured data taken from the test rig experiments for this wheel is shown in Figures 7.40/1-2 respectively.

There is an excellent correlation in the forward and reverse flanks for the Wheel 2 comparison. The transmission error wave form and magnitude agree to within 2μm while the mean transmission error level is compatible to within a 5μm tolerance. A noticeable feature of the results is that the predicted transmission error curves maintain the characteristic of a change in magnitude under load. Further, both sets of results indicate an optimum operating level within the same load.

7.6.3. Synthesis of transmission error under load for an oversize design gear set (Wheel 3).

The calculations of transmission error under load were repeated for the Wheel 3 design using the same linear stiffness value as used in the Wheel 1 analysis model. The synthesised and measured results are shown in Figures 7.41/1-2 respectively.

The synthesised results of Wheel 3 show the least correlation with the measured transmission error. They do indicate that the wave form does not change excessively due to load and the magnitude increases by only 3-5μm over the load range. This represents a characteristic common to both these measured results and the Wheel 1 results. This series of results does show a distinct difference in the mean transmission error values representing the vertical spacing of the curves. This is due to the lack of correlation in the initial gear geometry shown in measurements of the wheel tooth profile. This is slightly different from the Wheel 1 system results in which there was little effect in using either the theoretical or synthesised contact due to the close correlation of the geometry.
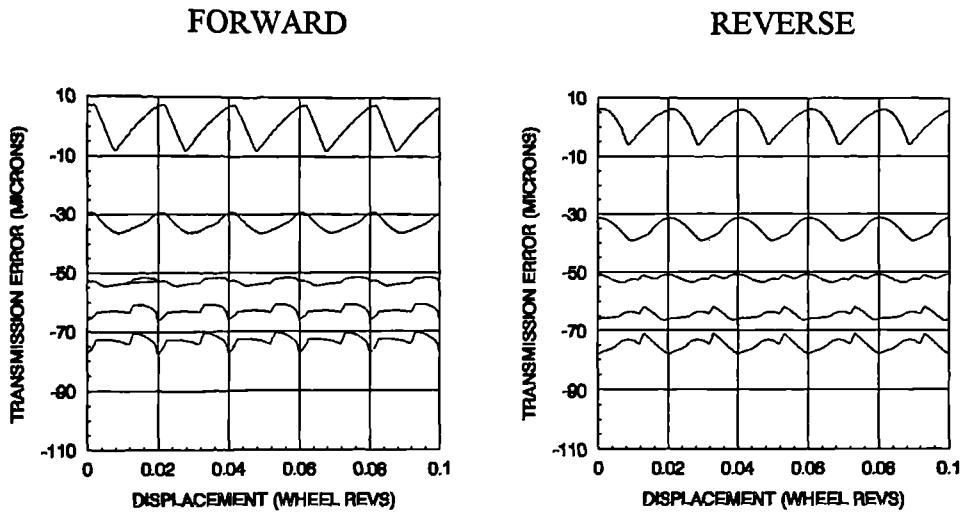
Figure 7.40/1 : Synthesised transmission error characteristics.
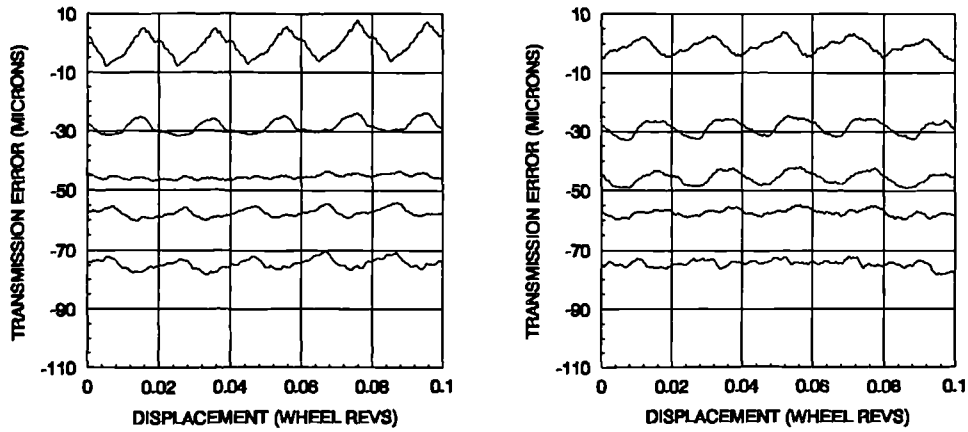
Figure 7.40/2 : Measured transmission error data.

Figure 7.40 : A comparison of synthesised and measured Harris Maps of transmission error for Wheel 2 design operating under 0-2000 Nm load in 500 Nm intervals.

CHAPTER 7

FORWARD   REVERSE
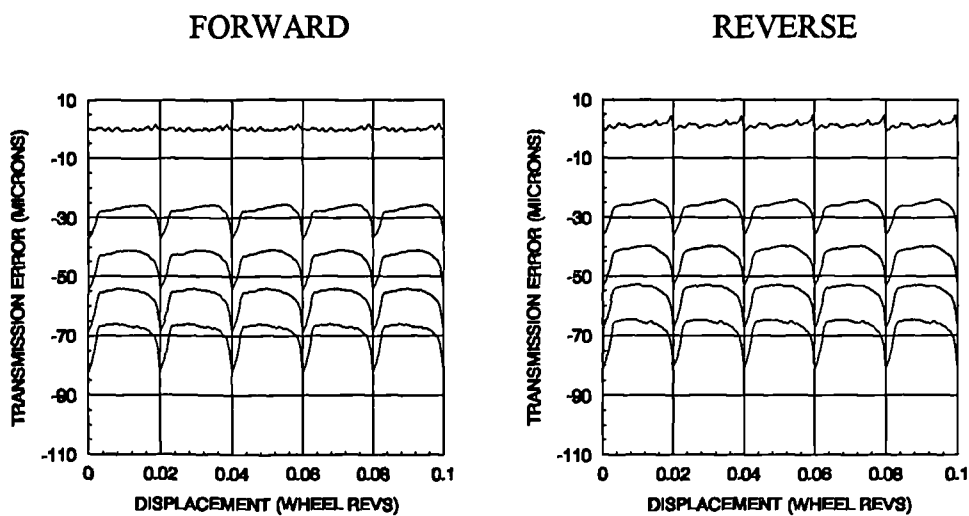
Figure 7.41/1 : Synthesised transmission error characteristics.
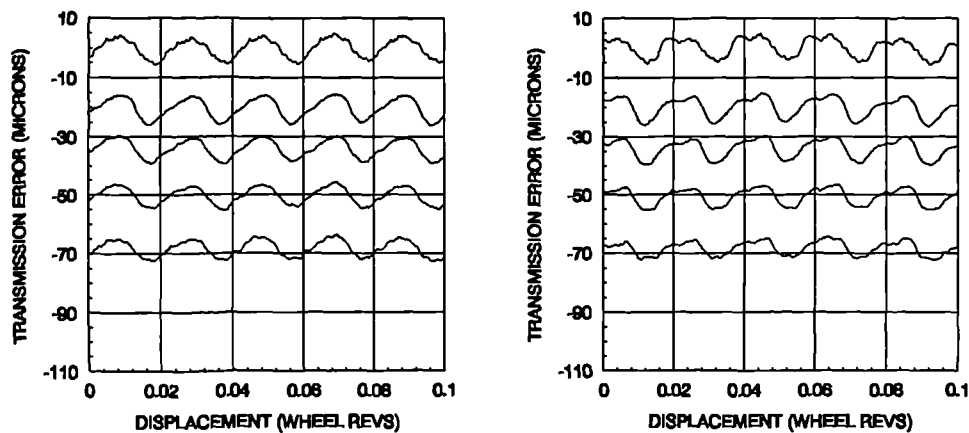
Figure 7.41/2 : Measured transmission error data.

Figure 7.41 : A comparison of synthesised and measured Harris Maps of transmission
               error for Wheel 3 design operating under 0-2000 Nm load in 500 Nm
               intervals.

CHAPTER 7

7.7. SUMMARY

The process used to design the three test wheels demonstrated the capabilities of the new software program. It also provided further validation of the software accuracy through the close correlation of synthesised and measured contact characteristics.

The results of testing gear sets under load showed that mean transmission error for a worm gear set due to load is largely independent of design method. Also, results suggest that if a gear set is produced using a design which creates little or no relief along the path of contact then the set would continue to hold the no load wave form under load. Sets such as these would have minimised transmission error under no load conditions. The effects recorded for Wheel 2 imply that profile modification can be used to influence gear set behaviour and optimise for a specific load.

Tests on operating speed show that there is no great effect on the error signal in either form or magnitude. This combination has significant consequences when linked with the results of operating under load. In applications where vibration in the system is a major factor, it should be possible to calculate whether there will be a problem under specific operating conditions by analysis of the single flank test results for a gear set. The correlation in synthesised results indicates that this is possible through analysis of the transmission error produced by the new software. Further tests recording dynamic behaviour under load have shown that the complete system must be considered when calculating the operating transmission error characteristic of the output shaft.

The alignment of the gear set influences both the transmission error wave magnitude and the mean error values. Although the misalignments were deliberately induced for these tests, this simulates effects occurring in a standard industrial box which uses bearings with lower stiffness values and larger assembly tolerances. In these results, the error wave magnitude has been shown to double, while the changes in mean error value can be in the order of 20% of the original value for a 250μm centre height offset. Tests on Wheel 3 were not considered due to a relative lack of correlation in the calculations of contact characteristics.

A reduction in the stiffness value from 10.5 N/mm/μm, based on spur and helical contact model, to 5.9 N/mm/μm was required to achieve a close correlation between synthesised and measured transmission error curves. This could be attributed to three factors. The first is a variation in normal pressure angle over the contact region. The second is the difference in cross section of thread form for each rack plane in both the worm and wheel. The third is the reduction of face width contact caused by relief from wheel cutter mismatch.

The new computer software now correlates well with the experimental results in predicting transmission error under load though small differences are apparent. These indicate that although the linear stiffness model works well it is crude and will need further development. Other factors such as tooth form, dimension, and load distribution exert a subtle influence on the stiffness function affecting the wave form. Despite this, the constant stiffness model represents a necessary and significant step in establishing a starting point for further work in this area. Any new model will need to be tested on a larger range of worm gear set designations for a more complete validation.

8. THE EFFECTS OF EXTENDED OPERATION UNDER A TORQUE LOAD ON TRANSMISSION ERROR AND MARKING PATTERN

8.1. INTRODUCTION

The test rig was used to investigate the initial wear effects on a standard gear set and assess the impact of wear on contact conditions. The Wheel 1 and 2 gear systems were driven under 2000 Nm load for intervals of 1440 wheel revolutions from 0-7200 wheel revolutions. Signs of wear in the two gear sets were evident, and measurements of the effects were used to investigate the influence of wear when considering the final gear set operating characteristics.

After each wear interval a standard series of transmission error measurements was obtained for Wheel 1, and the contact marking pattern for the gear set was taken to record the contact conditions of the both wheel flanks under no load. This series of tests was repeated for the Wheel 2 system which contained profile modification and 250µm centre height offset misalignment on assembly.

During each wear stage the temperature of the test gear set increased due to operation under load. Further tests were therefore carried out to investigate the effect of temperature variation on transmission error.

8.2. DETECTING INITIAL WEAR DUE TO OPERATING LOAD

8.2.1. Wheel tooth contact marking pattern

The marking patterns for the Wheel 1 and Wheel 2 gear systems while under no load were recorded after each wear operating interval. The results of this analysis over the entire testing period are shown in the Figure 8.1 and Figure 8.2 for Wheel 1 and Wheel 2 respectively.

Marking patterns for Wheel 1 show that the no load contact is restricted to the exit side of the tooth. Contact conditions become stable almost immediately with the only change occurring toward the end of the testing cycle. After 2880 wheel revolutions, clearance develops in the centre of both tooth flanks. The contact conditions for Wheel 2 show far more activity. Over the first three wear intervals the region of contact changes considerably from area contact to almost full face contact. This transitional period is most likely to be associated with the removal of the profile modification applied to the wheel flanks. After the 2880 wheel revolution stage the marking patterns become similar to those for Wheel 1.

8.2.2. Measurements of backlash

At each wear stage the mean backlash value for the gear set under no load was recorded. The relation of change in backlash due to wear after operation over the test period is shown in Figure 8.3 for both wheels. The results show that although the marking patterns in both wheels appear to indicate a stability in contact conditions, large amounts of material are being worn from wheel teeth. The rate of wear leading to the backlash increase remains constant in both wheels with the exception of the initial development in the Wheel 2 series. This is related to the removal of the profile modification from both wheel tooth flanks. These contact areas would be the initial prominent points susceptible to wear. The concentrated contact area implies that relatively small volumes of material wear from the Wheel 2 tooth surface bring about a significant change in tooth profile causing an accelerated wear rate.

The erosion of tooth profile may emanate from three sources. The first is a fault in the filtering of the oil in the lubrication system allowing any metal removed from the gear set by wear to be returned to the contact area causing a grinding action. The second is in the choice of basic materials for the worm and wheel components which would determine hardness and resistance to wear. The third is that the gear set has not reached a satisfactory wear equilibrium, or 'bedded in', state induced by work hardening of the contacting surfaces. Further tests are necessary to identify the cause of this, and establish if this result is unique to these testing conditions.

ENTRY   EXIT   ENTRY   EXIT

0 Wheel Revolutions.

ENTRY   EXIT   ENTRY   EXIT

1440 Wheel Revolutions.

ENTRY   EXIT   ENTRY   EXIT

2880 Wheel Revolutions.

ENTRY   EXIT   ENTRY   EXIT

4320 Wheel Revolutions.

ENTRY   EXIT   ENTRY   EXIT

5760 Wheel Revolutions.

ENTRY   EXIT   ENTRY   EXIT

7200 Wheel Revolutions.

FORWARD FLANK   REVERSE FLANK
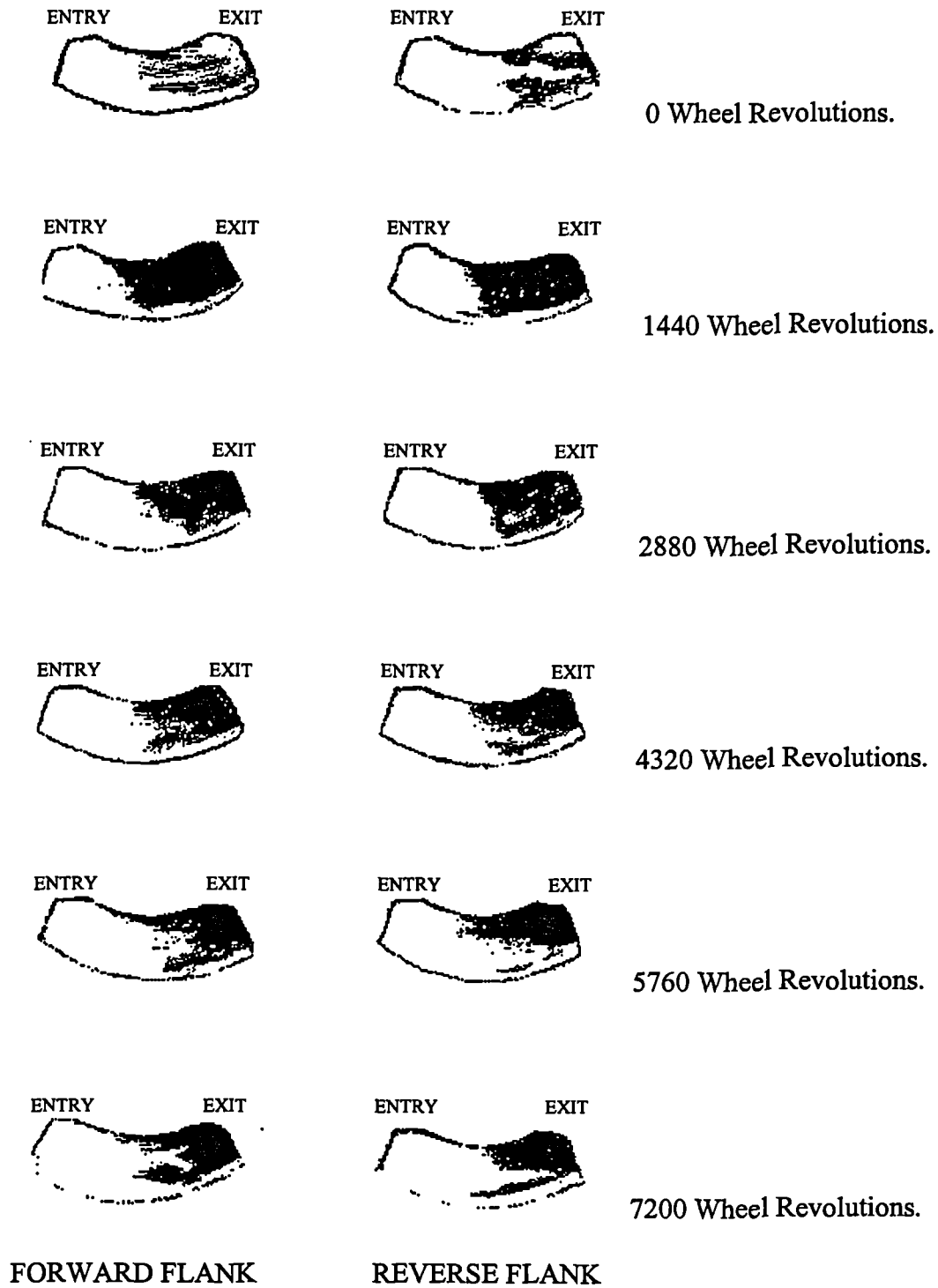
Figure 8.1 :   A series of marking patterns for Wheel 1 at intervals of 1440 wheel revolutions under 2000 Nm load.

ENTRY   EXIT   ENTRY   EXIT

0 Wheel Revolutions.

ENTRY   EXIT   ENTRY   EXIT

1440 Wheel Revolutions.

ENTRY   EXIT   ENTRY   EXIT

2880 Wheel Revolutions.

ENTRY   EXIT   ENTRY   EXIT

4320 Wheel Revolutions.

ENTRY   EXIT   ENTRY   EXIT

5760 Wheel Revolutions.

ENTRY   EXIT   ENTRY   EXIT

7200 Wheel Revolutions.

FORWARD FLANK   REVERSE FLANK
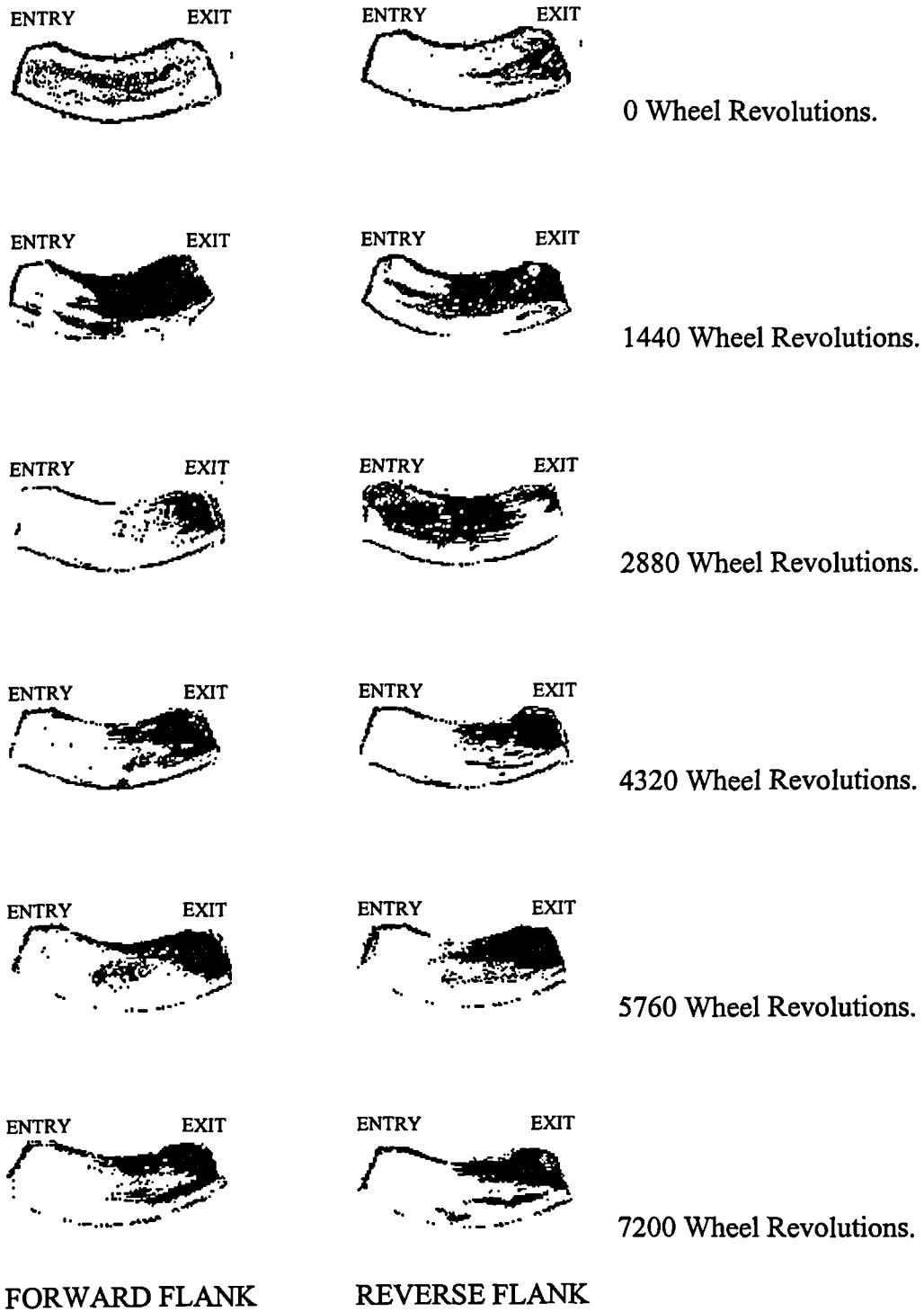
Figure 8.2 :   A series of marking patterns for Wheel 2 at intervals of 1440 wheel revolutions under 2000 Nm load.

Increase In Measured Backlash For Wheel 1 Due To
Wear Under An Operating Load Of 2000Nm

Increase In Measured Backlash For Wheel 2 Due
To Wear Under An Operating Load Of 2000Nm
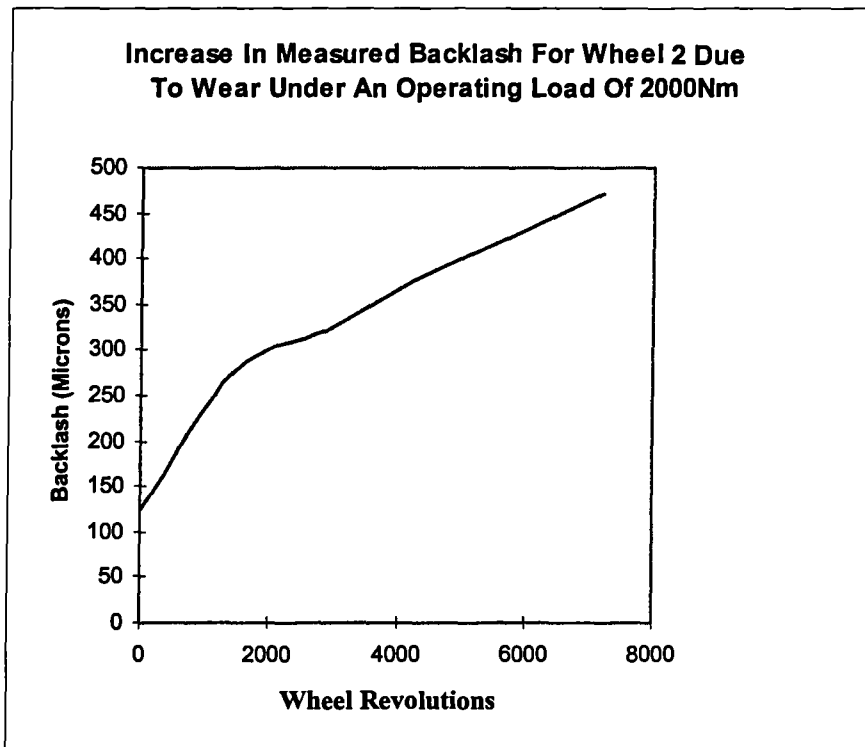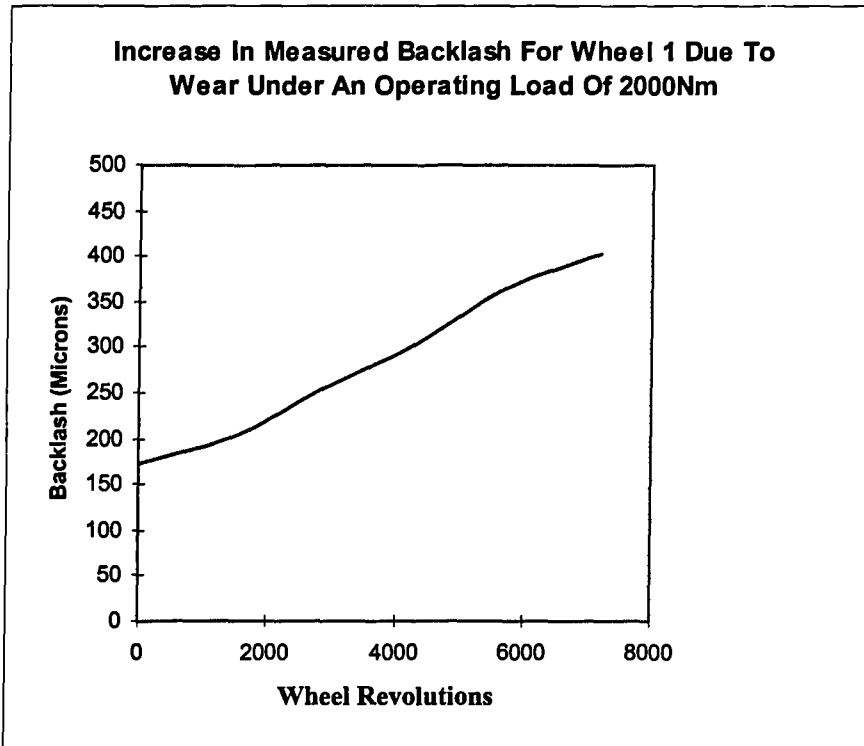
Figure 8.3 :   A graph of the mean backlash for Wheel 1 and Wheel 2 due to wear
after operation under 2000 Nm load up to 7200 wheel revolutions.

8.2.3. Worm thread wear development

Measurements of profile error, as described in section 3.2.2., were taken on both flanks of the worm thread at the beginning of the testing period. A typical sample is shown in Figure 8.4 in which it can be seen that these errors were within 3μm of the involute helicoid form which would have generated a vertical line.
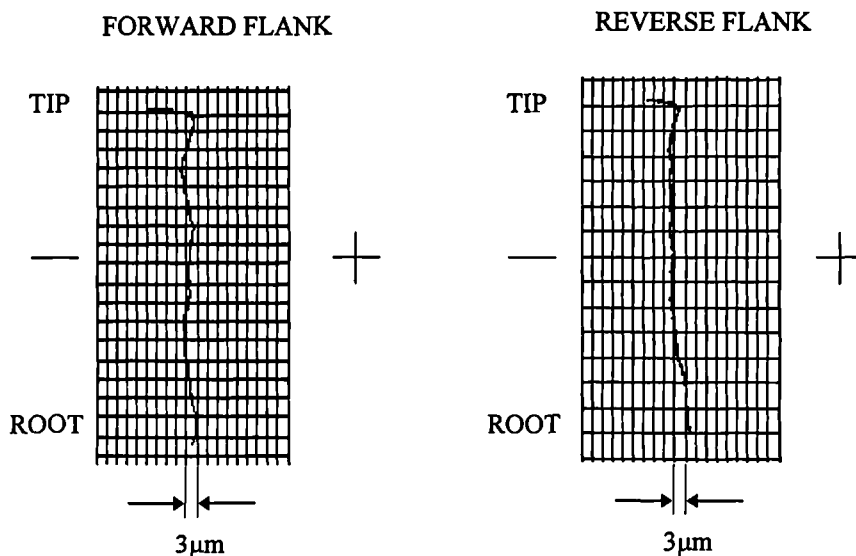
Figure 8.4 : Typical profile production errors in the flanks of the worm.

This worm was then installed in the rig and performed 10^6 revolutions during testing while driving a 2000 Nm load. It was then removed and measured again. The profile errors in both flanks due to wear were recorded at 90° intervals of rotation through the region of engagement. The results for the forward driven flank can be seen in Figure 8.5, while Figure 8.6 shows those of the reverse driven flank.

In both series of traces some profile wear is evident in the root of both flanks at around the 180° position sample. A distinct indent of 15μm appears in the root of the profiles at around the 270° position along the worm thread. The indent in the forward driving flank is concentrated over three vertical areas of the tooth profile while that of the reverse driving flank influences almost the entire profile. This indent progresses from root to tip along the profile, consistent with the contact through mesh, before beginning to dissipate at the 810° position.

Although these errors are small and greatly exaggerated by the relative difference in vertical and horizontal scale of the plots shown, they are of the same order as the transmission errors recorded in the testing. It is reasonable to expect that they have influenced the experimental result which could explain any differences that exist in comparison to the calculated results which assume a conjugate profile.

The errors recorded in these two flanks tend to coincide with the deliberate profile modification on Wheel 2, with linear modification applied to the forward flank and parabolic to the reverse. A possible reason for this worm profile wear may therefore be due to a grinding action caused by this wheel profile modification. However, the worm has also been driven under load while using Wheel 1 and Wheel 3 and hence the errors can not be clearly be attributed to this one source. The source of the errors can not be verified without further research into worm wear.
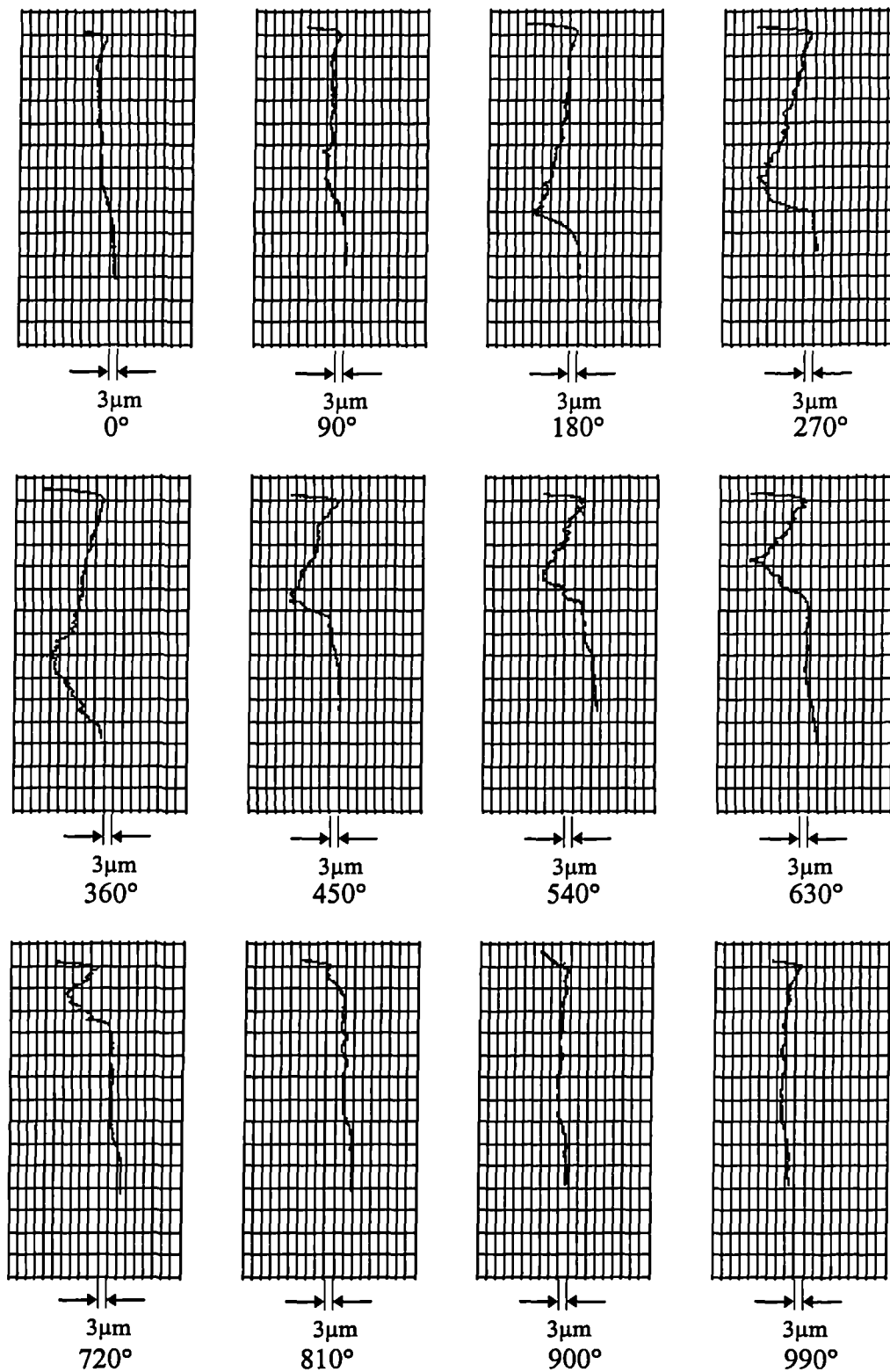
Figure 8.5 : Measured traces of profile error at 90 degree rotation intervals along the thread for the forward driving flank of the test box worm recorded after operating for 1 million engagements under 2000 Nm torque load.
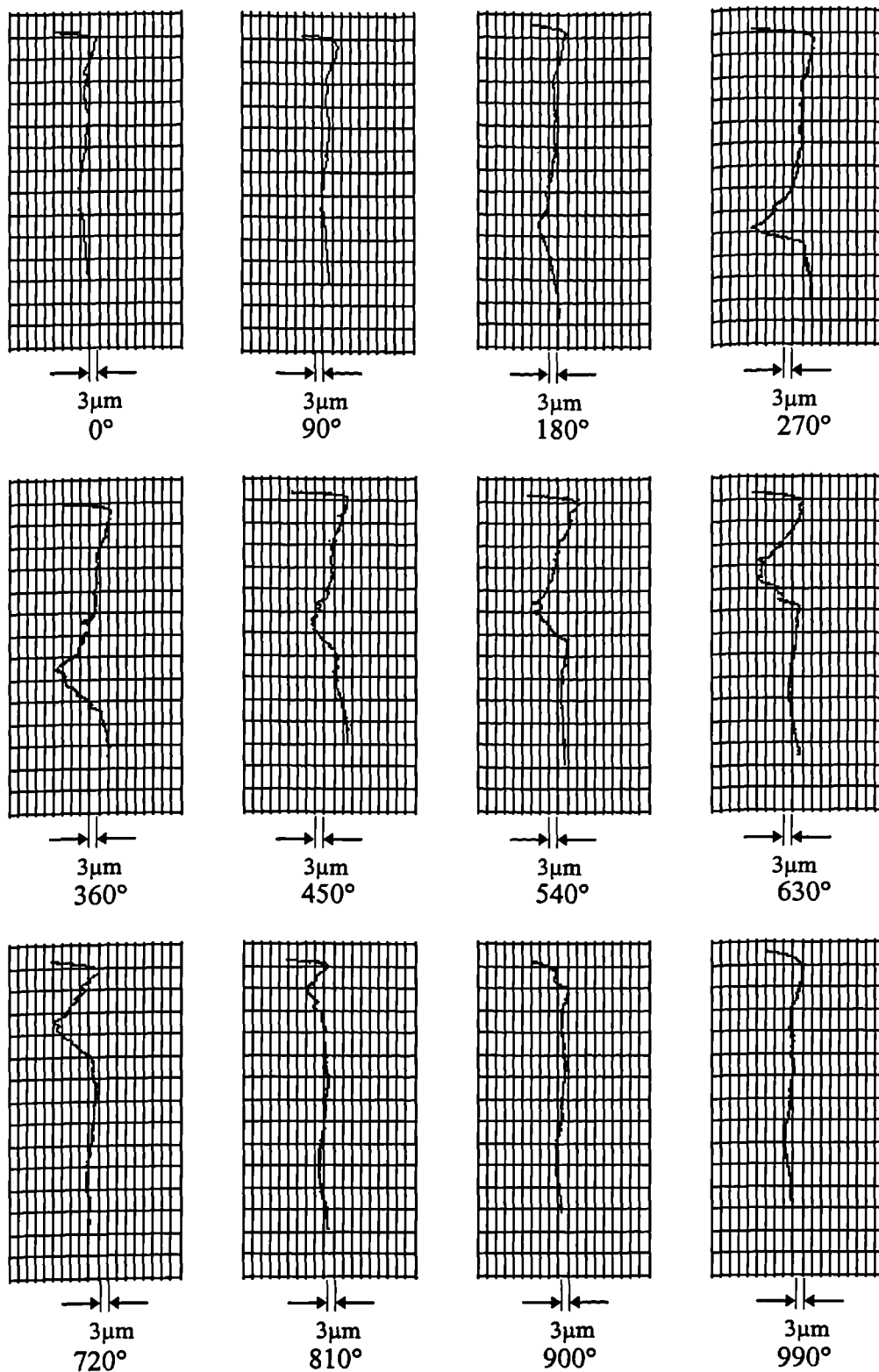
Figure 8.6 : Measured traces of profile error at 90 degree rotation intervals along the thread for the reverse driving flank of the test box worm recorded after operating for 1 million engagements under 2000 Nm torque load.

8.3. THE EFFECT OF WEAR ON TRANSMISSION ERROR CHARACTERISTICS

8.3.1. The effect of wear on transmission error in a standard industrial gear design

The results of standard transmission error tests on Wheel 1 at each wear stage were recorded and are shown in the Harris Maps in Figure 8.7 and Figure 8.8 respectively. The results show that the wave form begins to change within the first test interval of 1440 wheel revolutions on both flanks. A very distinct effect is that the no load trace no longer resembles those recorded under load. A further effect is that the loaded transmission error plots change at each wear stage yet retain the initial characteristic of repeating in form and magnitude to within around 2μm at each load level. Despite the rapid change in transmission error form, the mean level is constant to within 7μm or less for each load interval throughout the wear development. The wave form becomes almost constant from the 4320 wheel revolution stage. This is true for both flanks, however the wave form is different for each.
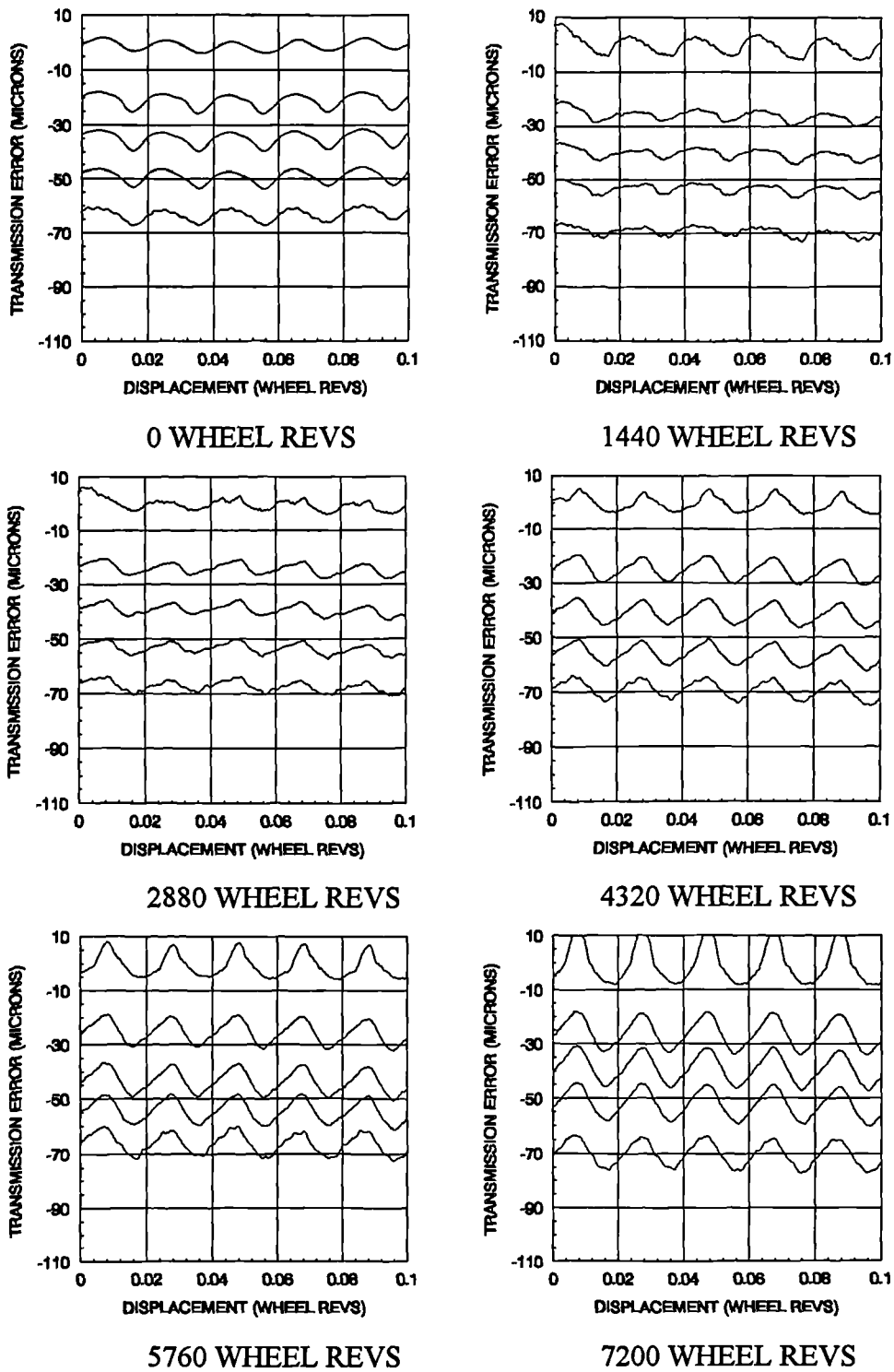
Figure 8.7 : A set of standard transmission error tests from the forward driven flank of Wheel 1 recorded at 500Nm load intervals after 1440 wheel revolution intervals operation under 2000Nm load.
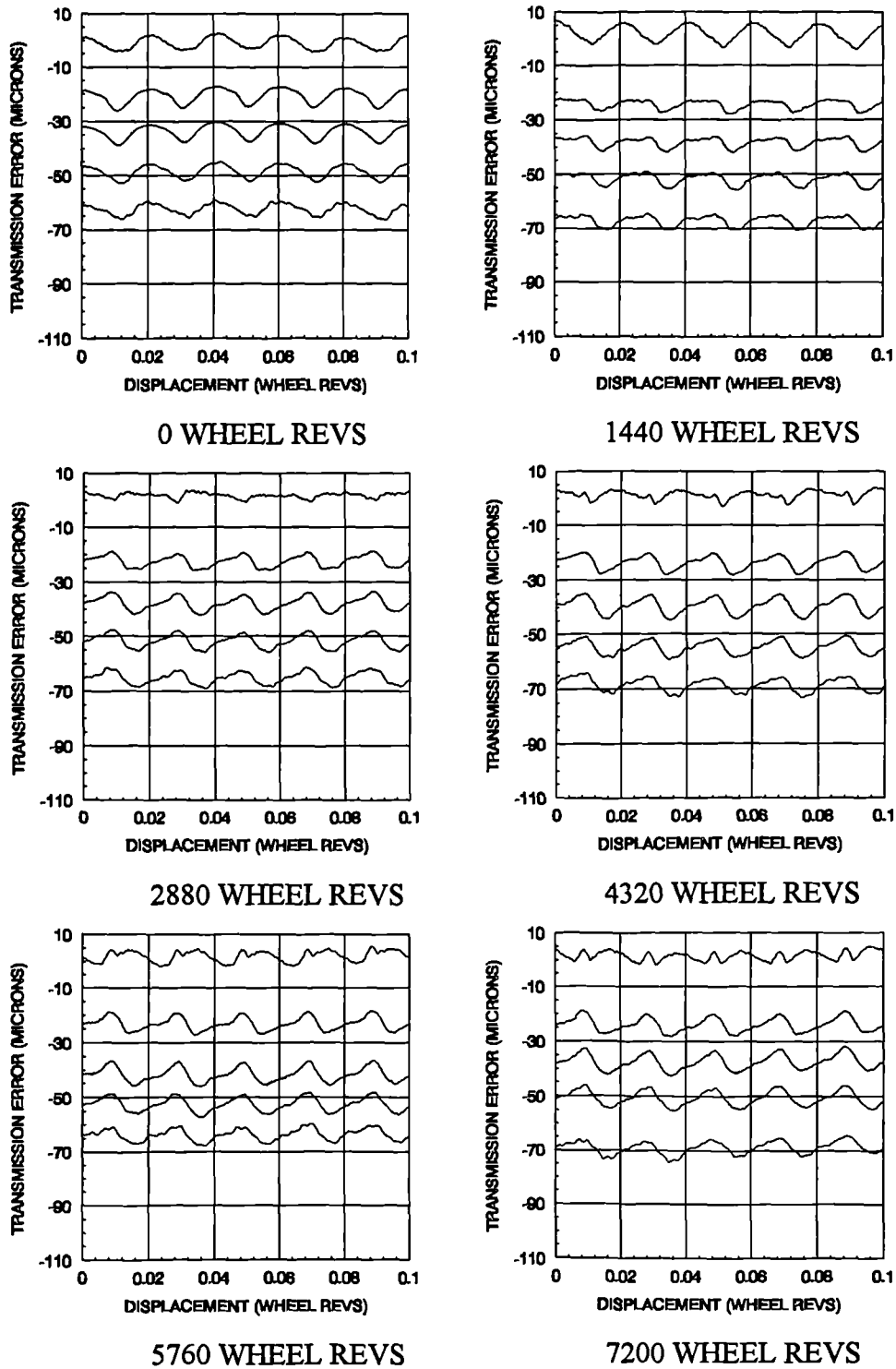
Figure 8.8 :   A set of standard transmission error tests from the reverse driven flank of Wheel 1 recorded at 500Nm load intervals after 1440 wheel revolution intervals operation under 2000Nm load.

8.3.2. The effect of initial contact conditions on wear development and transmission error

Similar tests to those in section 8.3.1 were carried out on Wheel 2, and the results are shown in Figure 8.9 and Figure 8.10 respectively. These results show some idiosyncrasies in the transmission error behaviour due to the initial wear relative to the Wheel 1 case. The first four wear stages show substantial changes in both wave form, magnitude and mean value at each load interval. These may be associated with the changing wheel tooth profile during this period as reported in Section 8.2.1. Changes in magnitude of up to 5μm were evident after the first wear stage while the mean transmission errors were immediately reduced by 50% at each load level. The effect of error magnitude reduction due to load is also lost and the gear set produces graphs which correlate to within 1μm similar to the Wheel 1 behaviour.

After the 4320 wheel revolution stage the Wheel 2 results recorded in both flanks are beginning to resemble the development of transmission error characteristics in the respective flanks of the Wheel 1 system. This effect is clearly shown in Figure 8.11 which compares the graphs of mean transmission error only for Wheel 1 and Wheel 2 at each load interval for the series of wear stages. These show that the Wheel 1 levels remain constant despite the changes in wave form or magnitude, while the Wheel 2 levels fluctuate dramatically before conforming to those shown in the Wheel 1 tests.
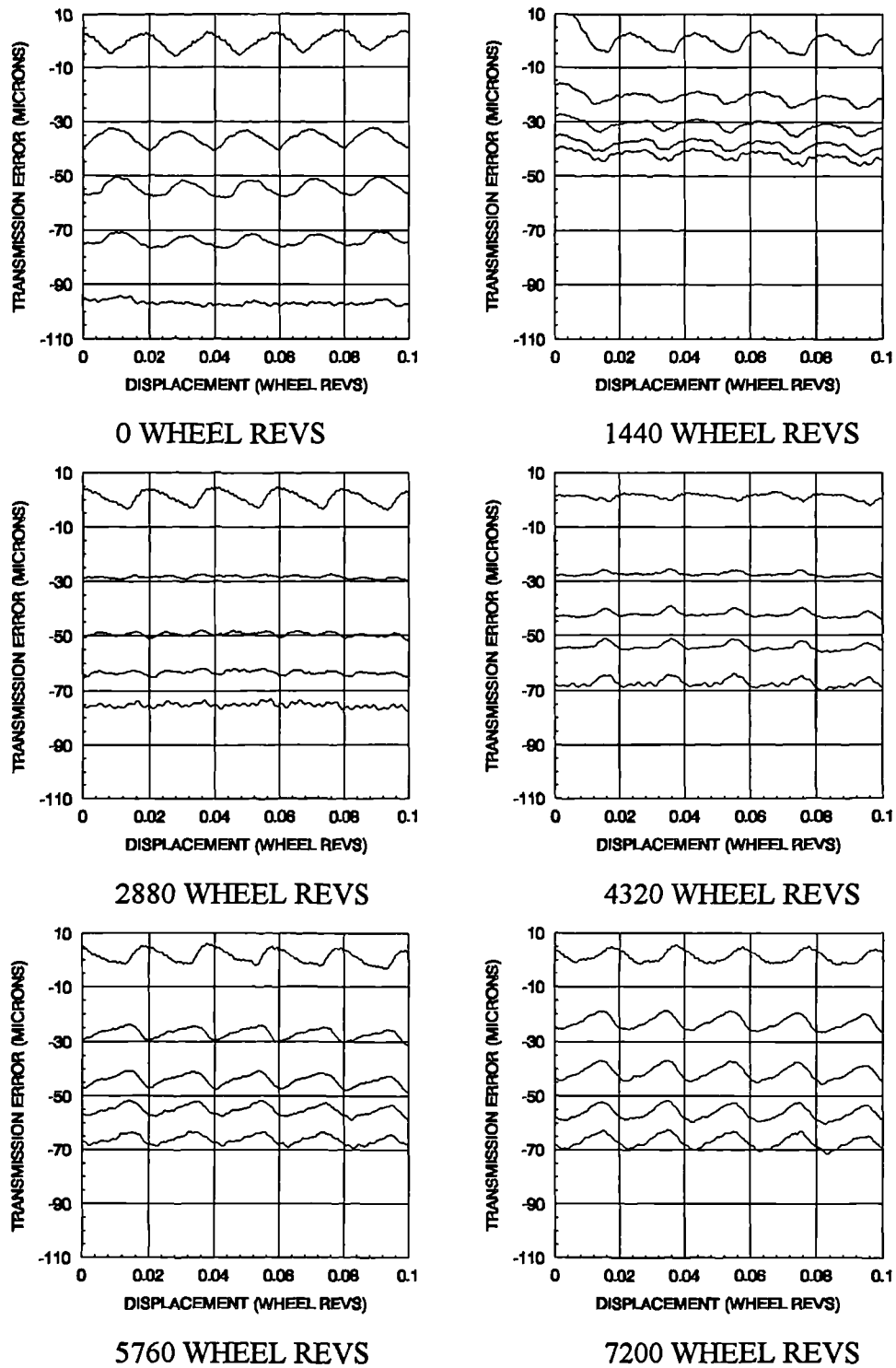
Figure 8.9 : A set of standard transmission error tests from the forward driven flank of Wheel 2 after 1440 wheel revolution intervals operation under 2000Nm load.
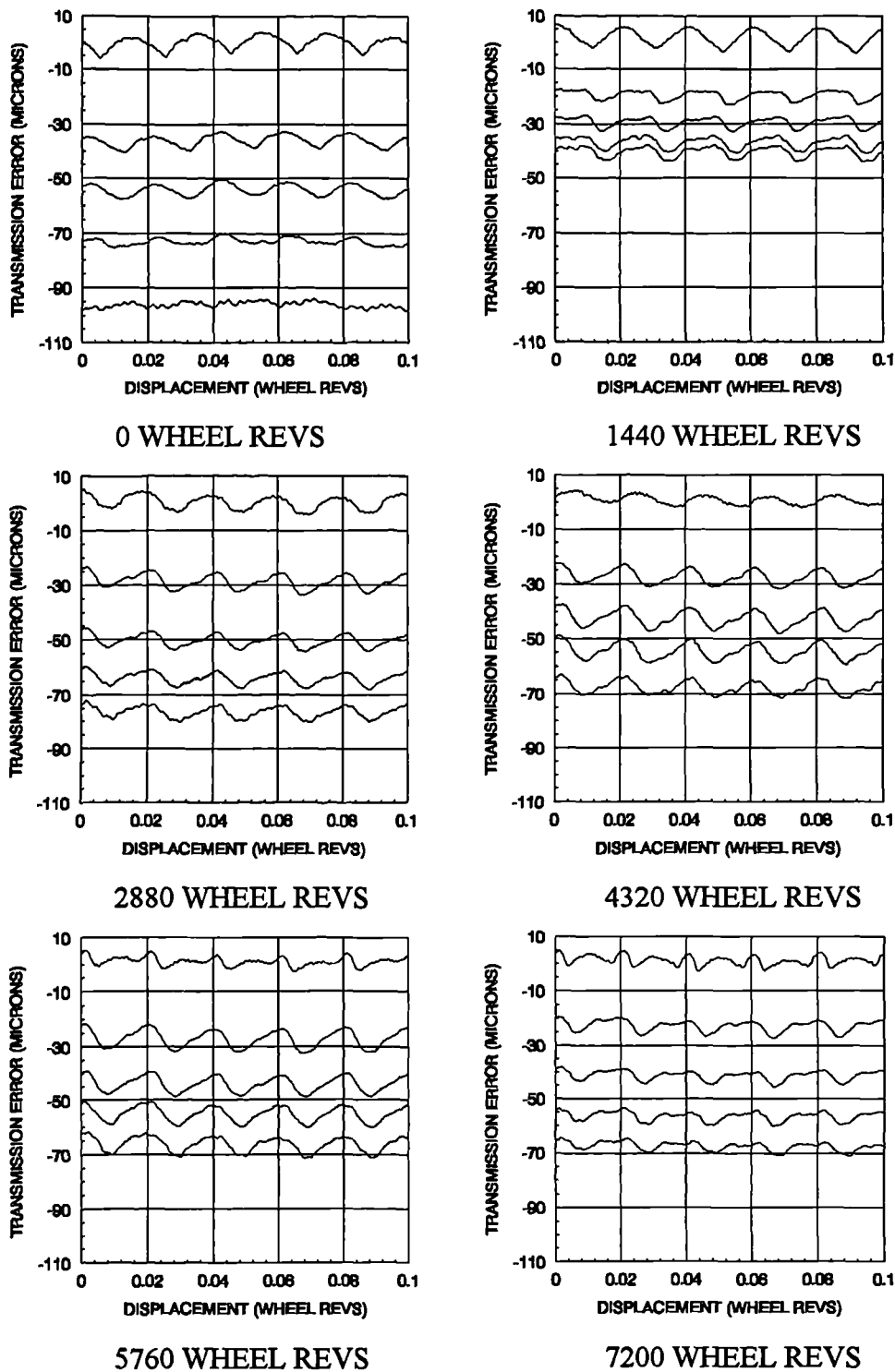
Figure 8.10 : A set of standard transmission error tests from the reverse driven flank of Wheel 2 after 1440 wheel revolution intervals operation under 2000Nm load.
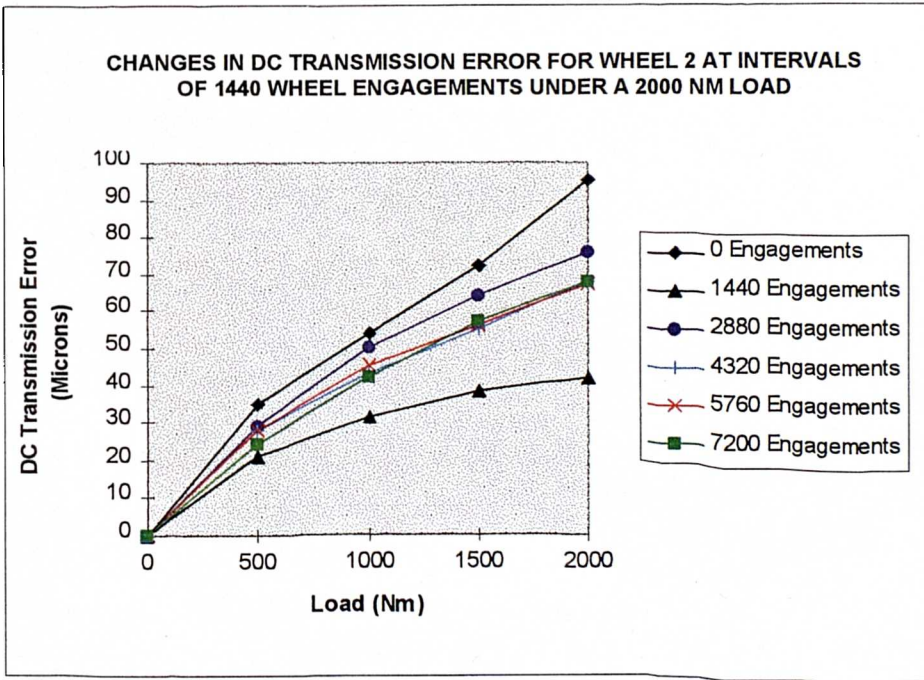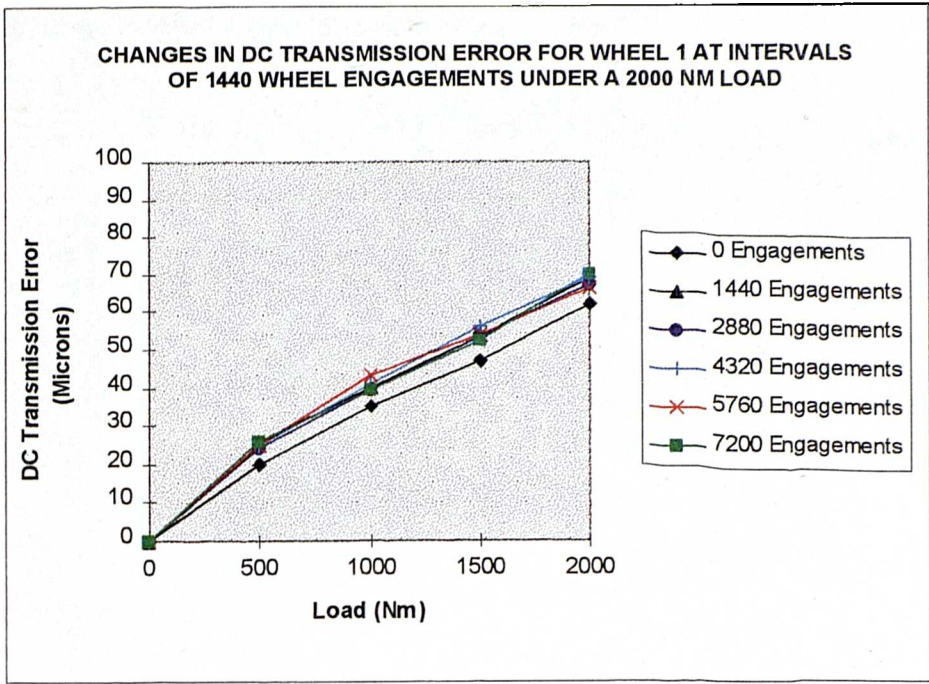
Figure 8.11 : A graph of the measured mean (or DC) transmission error due to tooth deformation under an operating torque load for Wheel 1 and Wheel 2 after running at 2000 Nm in 1440 wheel revolution intervals.

CHAPTER 8

8.3.3. The effect of individual component wear on transmission error

A study was carried out to isolate the effect of individual component wear on contact characteristics using the Wheel 1 gear set in three states of wear. These studies combined a newly produced worm and wheel set, a worn worm with a new wheel, and a set in which the complete system had been in paired operation for 7200 wheel revolutions under a 2000 Nm load. A series of tests were performed over a range of input shaft operating speeds from 100 rpm to 300 rpm under a constant 1500 Nm load. The mean transmission error values were filtered out in each case to isolate the wave form only and allow a better direct comparison. The results over five worm revolutions can be seen in Figure 8.12, 8.13, and 8.14 respectively.

These results show that there is little change in wave magnitude beyond the 1μm level that is expected in a repeatability test. The main exception to conformity of wave form is shown in Figure 8.13 for the case of operating a worn worm and an unworn wheel system. Here there is a distinct change in the transmission error in the forward driven direction with a change in speed. This effect may be due to the gear set being in a state of change due to wear and therefore producing results which are not as stable as the initial unworn or bedded in system.
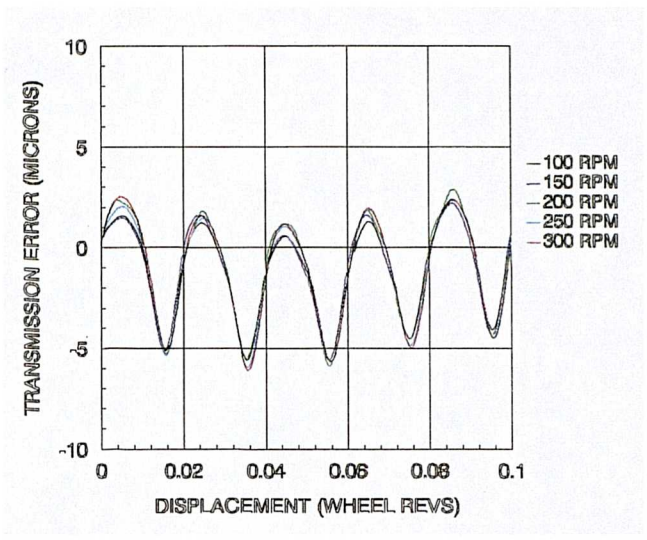
FORWARD
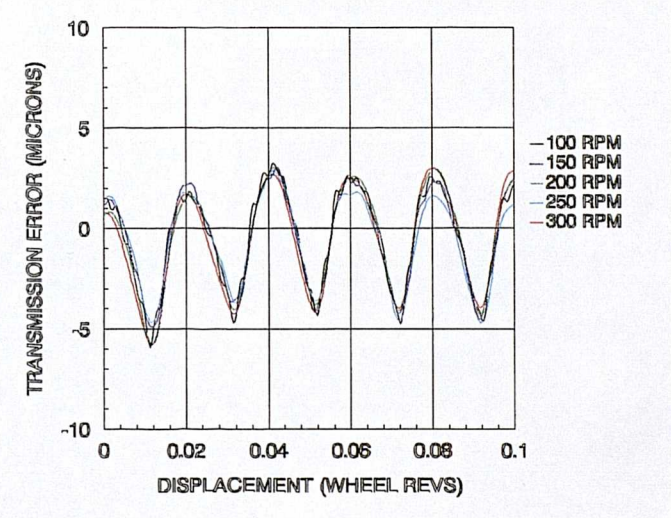
REVERSE

Figure 8.12 : A comparison of change in transmission error due to variation of input shaft speed for an unworn gear set under 1500 Nm load.
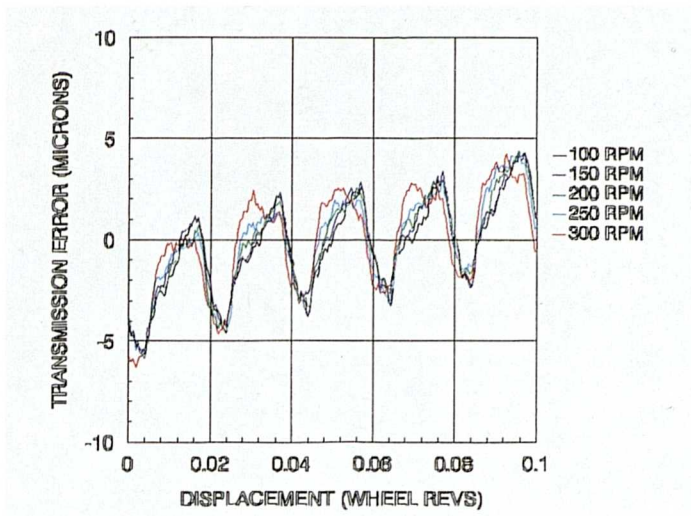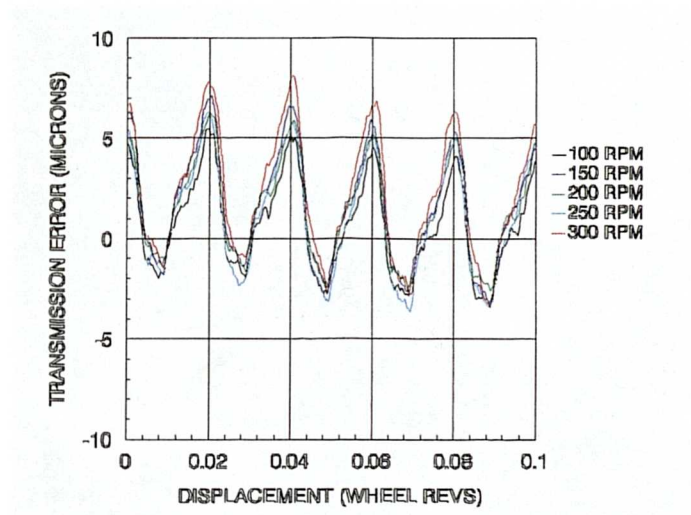
FORWARD

REVERSE

Figure 8.13 : A comparison of change in transmission error due to variation of input shaft speed for a worn worm and unworn wheel under 1500 Nm load.
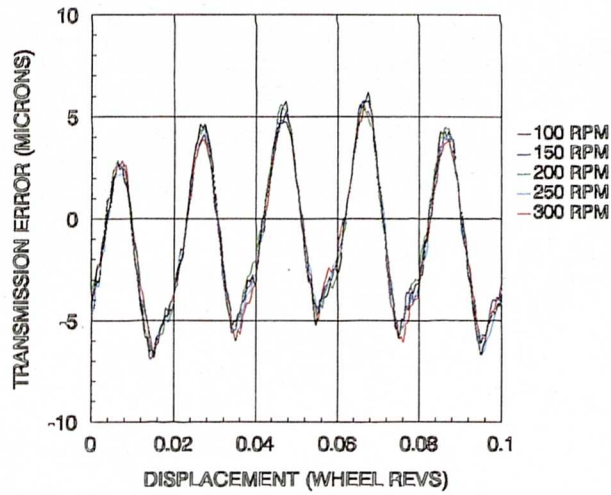
FORWARD
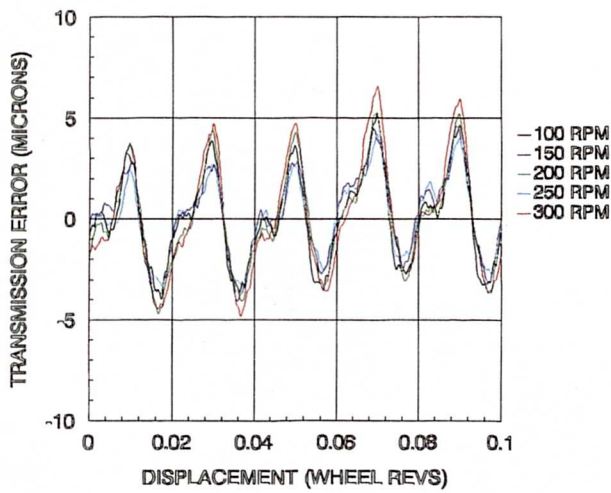
REVERSE

Figure 8.14 : A comparison of change in transmission error due to variation of input shaft speed for a worn worm and wheel under 1500 Nm load.

8.3.4. The effect of temperature variation under load on transmission error characteristics

A series of tests was performed on Wheel 1 to investigate the effect of temperature change on the transmission error of a worm gear system. The test rig was operated under load to induce a temperature rise in the test gear box. A standard series of transmission error measurements was taken after each wear interval while the gear set temperature was 70°C. These measurements were repeated once the gear set had reached 20°C in order to draw a comparison between operating and nominal characteristics. This test was repeated after each wear interval. An example of the test is shown in the Harris Maps in Figure 8.15 representing results taken after the final wear interval.

The results of the tests show that there is no significant change in transmission error wave form or magnitude due to temperature change. There was also less than 4μm difference in mean transmission error levels in the results of each test. It should be noted that despite the parity in both wave form and magnitude, a change in mean backlash was recorded due to temperature change at each wear stage. The backlash reading during the 70°C tests was 20μm lower than that obtained in 20°C tests. This indicated that there was a notable expansion within the system although no measurements were taken to identify the single component, combination of components, or other source which was responsible for this change.
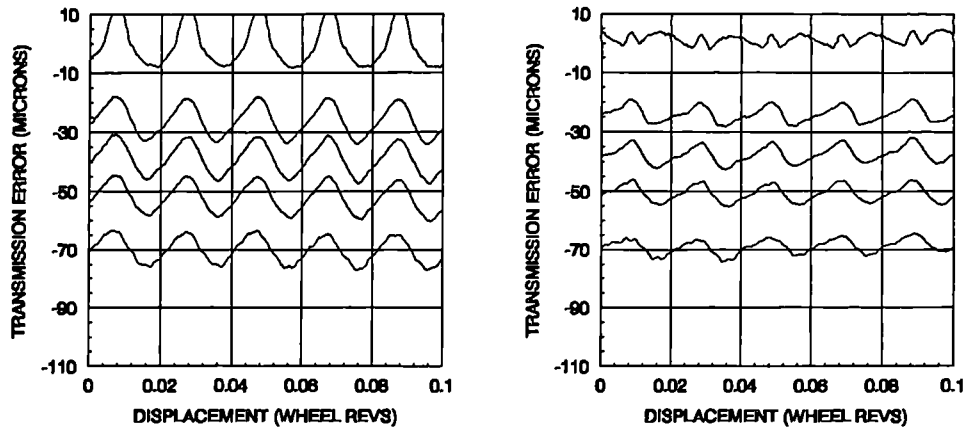
Figure 8.15/1 : Tests Performed On The Gear System While At 20°C.
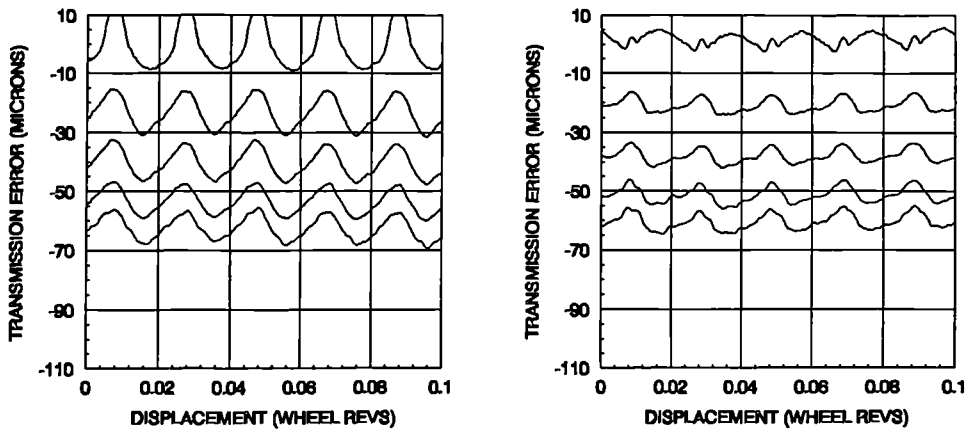
Figure 8.15/2 : Tests Performed On The Gear System While At 70°C.

Figure 8.15 :   A comparison of Harris Maps recorded for the wheel 1 gear system at 20 and 70 degrees Celsius respectively after 7200 wheel revolutions operating at 2000 Nm load.

8.4. SUMMARY

The marking pattern and mean transmission error appeared to achieve equilibrium contact conditions by the end of the wear testing period despite the fact that material was continually being removed as indicated by the increase in backlash. The extreme fluctuations in Wheel 2 results coincide with the changes in marking pattern which suggest that the tooth distortion under load causing changes in mean transmission error level is due to compression of the material rather than a bending effect. This would explain the difference between the associated transmission error in the Harris Maps for these wear intervals. This erosion of wheel profile due to wear had not finished in either gear system by the end of the test period. Further tests are needed to establish the final equilibrium conditions for these gear systems.

In both cases even after large quantities of wheel tooth wear the marking pattern has not become full face as associated with conjugate contact. The no load marking pattern may not however be representative of the contact conditions under load. Wear indicated in the worm profile implies that if a stable geometry exists it will not be conjugate to the original worm design. It will actually be a composite of worm and wheel wear combined with the modified geometry due to tooth distortion while under load.

The similarity between the Wheel 1 and Wheel 2 transmission error and marking pattern characteristics after the wear testing period imply that the gear set behaviour due to wear is independent of initial conditions.

Significant wear is influential on gear set operating characteristics after only a short operating time. This creates problems in modelling and calculating contact conditions which are even more complex than those that exist using only the initial geometry. It brings into question the validity of any mathematical model which does not allow for these changes.

The effects of profile modification imply that this technique can be used to influence transmission error and optimise for a specific load, although the effects are rapidly eliminated through wear. Further research may establish whether this problem could be overcome by use of alternative materials or lubricants.

The tests for temperature indicate that despite a possible change in relative geometry of the gear set, suggested by the change in backlash values, this is not substantial enough to change the transmission error characteristics.

9. · CONCLUSIONS

9.1. INTRODUCTION

The research presented in this thesis has achieved all of the main objectives of the research program. Established theoretical and industrial knowledge has been recorded. Experimental work has outlined several factors which determine the contact characteristics of a worm gear system at the design, manufacture and operating stages. A model of theoretical contact under various conditions has been developed. Theoretical contact analysis calculations produced by new software have been validated by several independent sources using results from similar analysis of existing design specifications in published literature and new design specifications supplied by the collaborating companies. The model has been extended beyond existing contact analysis theory to include manufacturing and operating error sources. The ability of the contact analysis model to fully synthesise the production and operating process has been validated using measurements taken from manufactured gear sets and experimental data obtained from a test rig. Conclusions have been drawn from the comparison of measured and calculated results, and the relevance of the software as a research and development tool has been assessed. The results have led to the identification of several points to be considered for future precision worm gear production. The potential for further development has been identified.

9.2. THE COMPLETION OF PROJECT OBJECTIVES

9.2.1. Design of worm gear set characteristics

After studying the various design techniques and considering the process of controlled relief to influence marking pattern and transmission error characteristics, the following conclusions can be derived :

- Transmission error wave form or magnitude is generated by tooth relief at the point of contact.

- The change in transmission error of a gear set due to centre height and distance misalignment is dependent upon relief along the modified path of contact.

- Iterative use of the software can produce designs with theoretical transmission error magnitudes of approximately $1\mu m$ which still have adequate clearance for oil lubrication.

- The principle of profile modification to minimise transmission error magnitude at a specific operating load can be applied to worm gear systems. This often results in a tooth form which generates a considerable transmission error under no load conditions.

9.2.2. The influence of manufacturing error effects

Measurements of errors in the generated form of the wheel cutting tools and the gear set components have identified the following :

- Including error sources in the calculations significantly improves the accuracy with which contact characteristics can be predicted.

- Due to the small scale of profile errors in the components relative to the thickness of the contact marking indicator ink, accurate machining can influence transmission error in the unloaded worm gear system even when not detected by the marking pattern.

- The wheel cutter tool profile errors are transferred to the wheel tooth with an accuracy of approximately $2\mu m$.

- The CNC machining of wheel cutters is far more accurate than normal tool grinding and can reduce profile error tolerance from around $7\text{-}10\mu m$ to $2\text{-}3\mu m$.

- Errors in the conjugate gear sets produced for this project show that it is not possible to produce transmission error magnitudes of less than $3\mu m$ due to machining tolerances.

- The condition of cutting tools and machinery often necessitates modifications to the theoretical design parameters to compensate for the effective changes in geometry.

9.2.3. Assessment of the new software

The new software developed for this project has been used extensively in conjunction with the research work defined by the objectives. The following facts can be stated with regard to the use of this program at its current stage of development :

- The computer model has successfully calculated the theoretical and synthesised characteristics of several gear sets. Results have been experimentally validated.
- The ability of the computer program to model various error effects allows potential modifications to contact conditions such as assembly error or deformation under load to be assessed and compensated for during the design process.
- A simple linear stiffness model for transmission error under load has been used to develop gear sets using several design techniques.
- After experimentally determining an accurate stiffness value of $5.9N/mm/\mu m$ for the model the calculated transmission error output gives good correlation for the three gear set designs tested.
- The Fourier analysis option has been used to investigate error sources.

Validation of the results has confirmed the software as a practical tool for both academic and industrial institutions. The range of analysis options available permit the software to be used in the following tasks :

- Investigation of new contact geometry.
- Analysis and improvement of existing designs.
- Investigations of production techniques.
- Identifying and correcting problems in existing gear set operation.

This software is already being used for these purposes by the collaborating companies with great effect.

9.2.4. Gear sets operating under a torque load

Results from tests for transmission error on gear systems under load resulted in the following observations :

- It is possible to predict mean transmission error levels at a given load to within a 5μm band.

- Profile modification does not significantly change the mean transmission error level, but does influence the magnitude of the transmission error and can be used to minimise it at a required load.

- The wave form and magnitude of the transmission error in Wheel 1 and Wheel 3 under load did not change by more than 1-2μm over the 2000Nm load range. The changes that do exist may be induced by the small relief present in the tooth form due to the design mismatch parameters.

- Running speed did not significantly affect the transmission error wave form of the gear sets during the experimental tests but is connected to the vibration response of the complete system.

- Centre height misalignment of ±250μm caused increases in mean transmission error level ranging from 40-50% at 500 Nm load, to 10-20% at 2000 Nm load and caused observable changes of 2-3μm magnitude in the wave form.

- The movement of components in the box during operation can upset the alignment by far more than the initial tolerances for assembly. The axial movement of the worm shaft in the bearings is 15 times the magnitude of the transmission error wave and 1.25 times the magnitude of the mean transmission error level.

- Axial deflection of the worm bearings within the housing had a direct effect on recorded backlash, increasing the value by up to 90μm in each driving direction at 2000 Nm load.

Wear tests performed by operating the test rig gear sets under load over a period of several hours showed that :

- Wear was detected almost immediately and continued throughout the testing period. The final equilibrium state for the gear sets was not established despite up to 150μm of surface material being removed from each flank of the wheel.

- The effect of profile modification on transmission error in Wheel 2 was removed after the first wear interval due to wheel tooth wear. Conversely, a gear set manufactured to have a low transmission error may not maintain this for long after operation due to the wear process. An improved bedding in procedure may represent a solution to this problem.

- The contact characteristics recorded for Wheel 1 and Wheel 2 over the wear testing period indicate that equilibrium geometry is independent of initial contact conditions.

- Up to 15μm of profile error was detected in the worm after 10^6 revolutions under a 2000 Nm load. This error is enough to influence the theoretical and synthesised transmission error calculation.

- Wear in the worm indicates that the equilibrium contact state under load will not be conjugate to the original worm design. Even if full face contact is achieved, the final tooth form will be a function of the modified geometry due to this wear and the tooth and thread deformation under specific operating conditions.

- Variation in temperature between 20° and 70° does not result in a significant change in the AC or DC transmission error value.

9.2.5. Applying the conclusions to future worm gear systems

Several points should be considered when developing a worm gear system for the optimisation of accuracy under a given set of operating parameters :

- If significant load variations are expected in a specific application then associated centre height and distance deflections can also be expected. To maintain accuracy the gear set design chosen should take this into account by minimising relief along the path of contact in all of the potential misalignment positions.

- Centre height and distance variation under load can be compensated for by using designs with adequate clearance gap tolerances along the entry and exit edges of the gear tooth form.

- The cutting tool profile accuracy and therefore the wheel tooth form can be improved by 50% by using a CNC machine tool to grind the cutter.

- The condition of the machine used to cut the components should be considered. Any kinematic errors in these machines are transferred to the lead, profile and tooth spacing errors during the machining process.

- In high accuracy applications the worm axial movement under load relative to the wheel contributes far more to the positioning error than any effect caused by radial deflection of the components under load or assembly error. The axial stiffness of the worm bearings should therefore be maximised.

- For high precision applications with torque loads up to 2000Nm, the results indicate that $3.5\mu m$ per 100Nm represents a good guideline for DC level compensation as part of a feed back loop for increased positioning accuracy.

- The fact that the box housing movement did not significantly affect the contact conditions of the gear set components implies that when designing for high load applications bearing deflection is more critical than deformation of the box.

9.3. TOPICS FOR FURTHER INVESTIGATION

The research work has achieved all of the original objectives. The results have revealed the following topics which affect the contact characteristics of a worm gear system and require further research :

- Further validation of contact model for more gear designations

The computer program developed during this research program should be validated using more gear sets of various designations. Appropriate development of the theory and equations defining contact should be made for any inconsistencies found.

- Development of the model of transmission error under load

The results on transmission error for a gear set under load presented in this thesis should be used as a starting point to develop a model with a closer correlation. A stiffness model which has a function to allow for influences from specific tooth characteristics such as height, width, and material would need to be considered. A further effect which should be considered as part of the deformation is compliance of the worm shaft as this would add directly to the DC level. The new stiffness model should be validated using gear sets of varying designations.

- Wear to an equilibrium state

A series of tests should be performed on gear sets using the test rig to run the gear set until an equilibrium condition is reached at which time no further wear occurs. An investigation should be carried out to determine the major influences on wear such as contact geometry and operating conditions. These will establish whether the wear state is repeatable and therefore predictable. It will then be possible to calculate the equilibrium transmission error under load as well as the initial results using measurements of equilibrium geometry in the software model.

- Materials and lubrication

Work to assess the effect of harder bronze alloys such as aluminium bronze to influence wear should be carried out. The appropriate lubrication oil for the operating conditions may influence the wear rate and final equilibrium conditions. A combination which quickly stabilises or prevents wear in a gear set will allow the principle of profile modification to be applied to worm gear sets. This will enable the long term optimisation by design for transmission error at a specific operating load.

- Efficiency

Placing a second torque meter on the input shaft of the test gear box of the test rig will allow the recording of operating efficiency. This will enable an investigation of contact characteristics and efficiency to be carried out. Thermal imaging of the test box or calorimetry of the lubrication oil during operation can also be used to study this characteristic. Criteria for efficiency can then be identified based on design, operating conditions, and wear.

REFERENCES

[1]   Frazer, R.C. & Myers, E.J., 'A Code Of Practice For Interpretation Of Measurements', DUCOP06, BGA Transmission Technology, Issue 1.1, September 1994.

[2]   Walker, H., 'Worm Gear Design', The Engineer, Jul. 1952.

[3]   Loveless, W.G., Barlow, R.J., & Greening, 'Technical Aspects Of Double Enveloping Worm Gear Drives.', Ex-Cell-O Corporation, Cone Drive Operation, 1980.

[4]   Vos, H., 'Design Features Increase The Load Capacity Of Worm Gears', Maschinenmarkt 102, 1996.

[5]   Walker, H 'A Critical Look At The Novikov Gear' The Engineer, 1960.

[6]   Tuplin, W.A., 'Involute Gear Geometry', London, Chatto, Windus, 1962.

[7]   Merritt, H.E., 'Gear Engineering', Halsted Press, 1971.

[8]   Merritt, H.E., 'Worm Gear Performance', Proc. Inst. Mech. Eng., vol 129, 1935, p127.

[9]   BS 721. 'Specification For Worm Gearing, Part 2', BSI, London, 1983.

[10]   Buckingham, E. 'Analytical Mechanics Of Gears.', Dover 1963

[11]   Dudley, D.W. & Poritsky, H., 'On Cutting And Hobbing Gears And Worms', Applied Mechanics, TRANS ASME, 1943, A139-A146, A197-A201, A247-A251.

[12] Octrue, M., 'Etude De La Geometrie Des Roues Et Vis Tangentes', CETIM, Note Technique No. 22, 1992.

[13] Octrue,M., 'Nouvelle Methode De Dimensionnement Des Engrenges A Roue Et Vis Tangentes', AGMA paper FTM 1988.

[14] Wildhaber, E., 'A New Look At Worm Gear Hobbing', AGMA 129.10, Annual Meeting, June 1954.

[15] South, D.W., & Ewert, R.H., 'Encyclopedic Dictionary Of Gearing.', McGraw-Hill Inc., 1995.

[16] Qin, D., Zhang, G., Kato, M., & Zhang, D., 'Study On Hour Glass Worm Gearings With Good Contact State And Insensitivity To Manufacturing Errors', International Gearing Conference, University Of Newcastle Upon Tyne, Technical Paper September 1994.

[17] Chen, N., 'An Investigation Of Globoidal Wormgear Drives.', AGMA Technical Paper, 96FTM12, 1996.

[18] Janninck, W.L., 'Contact Surface Topology Of Worm Gear Teeth', AGMA paper 87FTM14, 1987.

[19] Colbourne, J.R., 'The Geometry Of Involute Gears', Springer-Verlag, 1987.

[20] Colbourne, J.R., 'The Use Of Oversize Hobs To Cut Worm Gears', AGMA paper 89FTM8 1989.

[21] Zhang, F., & Hu, J., 'An Improved Kinematic Method', 5th International Gearing Conference On Computer Aided Production Engineering, Edinburgh, Technical Paper 1989.

[22]   Litvin, F.L., & Kin V., 'Simulation Of Meshing And Bearing Contact For Single Enveloping Worm Gear Drives', AGMA Technical Paper, 90FTM3.

[23]   Litvin, F.L., & Kin V., 'Computerized Simulation Of Meshing And Bearing Contact For Single Enveloping Worm Gear Drives', Journal Of Mechanical Design, USA, 1992, Vol.114, No.2, pp313-316.

[24]   Hu, J., Zhang, F., & Bin, H. Z., 'The Mathematical Model For Helicoid Double Enveloping Worms With An Improved Kinematic Method', Journal Of Mathematics In PracticeAnd Theory, No. 3, China, 1991.

[25]   Munro, R.G., 'A Review Of The Single Flank Method Of Testing Gears,' Annals C.I.R.P., 1979, pp 325-329.

[26]   Harris, S.L., 'Dynamic Loads On The Teeth Of Spur Gears.', Proc. Inst. Mech Eng., 1958, vol 172, pp87-112.

[27]   Gregory, R.W., Harris, S.L. & Munro, R.G., 'Dynamic Behaviour Of Spur Gears.', Proc. Inst. Mech. Eng., Vol. 178 Part 1, 1963 pp 207-218.

[28]   Kohler, H.K., Pratt, A., & Thompson, A.M., 'Dynamics And Noise Of Parallel Axis Gearing', IMechE Conference, Cambridge, Sep. 1970, pp111-121.

[29]   Smith, R.E., 'Identification of Gear Noise with Single Flank Composite Measurement', AGMA 85FTM13, 1985.

[30]   Palmer, D. & Munro, R.G., 'Measurements Of Transmission Error, Vibration And Noise In Spur Gears',B.G.A. Conference Sheffield,Technical Paper, November 1995.

[31]   Walker, H.,'Worm Gear Deflection (A Consideration Of Distortion Effects And Correcting Measures)', Automobile Engineer, 1945.

[32] Weber, C.,'The Deformation Of Loaded Gears And The Effects On Load Carrying Capacity', British Dept Of Science And Industrial Research-Report No. 3, 1949.

[33] Munro, R.G. & Yildrim, N., 'Some Measurements Of Static And Dynamic Transmission Error Of Spur Gears' , International Gearing Conference Paper, University Of Newcastle Upon Tyne, Technical Paper September 1994.

[34] Bagci, C., 'A New Theory For The Design of Helical Gears For Surface Fatigue Using Hertzian Point Contact Stress.', AGMA Technical Paper, 87FTM1, 1987.

[35] Oda, S., Koide, T., Ikeda, T., & Umezawa, K., 'Effects Of Pressure Angle On Tooth Deflection and Root Stress', JSME Bulletin 1986.

[36] Oda, S., Koide, T., & Umezawa, K., 'Root Stresses Of Helical Gears With Higher Pressure Angle', JSME Bulletin 1986.

[37] Umezawa, K., Houjoh, H., Ichikawa, N., & Matsumura, S., 'Simulation On Rotational Vibration Of A Helical Gear Pair Transmitting Light Load', JSME Int. Conf. On Motion And Power Transmissions, 1991.

[38] Smith, J. D. 'Estimation Of The Static Load Distribution Factor For Helical Gears.', Proc. IMechE , 1995, C3 Vol 209 pp193-201.

[39] Smith, J. D. 'Helical Gear Vibration Excitation With Misalignment.' Proc. IMechE , 1994, C2 Vol 208 pp 71-80.

[40] Barnett, D.W. & Yildirim, N., 'Loaded Transmission Error Prediction Using A Computer Model And Its Verification' , International Gearing Conference Paper, University Of Newcastle Upon Tyne, Technical Paper September 1994.

[41]   Li, R., Tang, Q., & Kato, M., 'Deformation Numerical Analysis Of Meshing Gears And Tooth Profile Modification', International Gearing Conference Paper, University Of Newcastle Upon Tyne, Technical Paper September 1994.

[42]   Hiltcher, Y., Guingand, M., & Octrue, M., 'Computed Contact Surface Topology Of Worm Gears (New Approach) And Cutting Parameter Influences', International Gearing Conference, University Of Newcastle Upon Tyne, Technical Paper September 1994.

[43]   Tang, J.S., 'The Hertzian Load Capacity And Lubrication Of A Double Enveloping Worm Gearing With Planar Generating Surface.', PhD Thesis, Mineral University Of China, 1991.

[44]   Hu, J., Pennell, J.A., 'A Practical Method Of Measuring The Worm Wheels Of Cylindrical Worm Gears'., International Gearing Conference (Proceedings), Mechanical Engineering Publication Ltd., 1994.

[45]   Frazer, R.C. & Myers, E.J., 'A Code of Practice for Checking the Reproducibility of Gear Measuring Machines', DUCOP04, BGA Transmission Technology, Issue 1.1, September 1994.

[46]   Frazer, R.C. & Myers, E.J., 'A Code of Practice for Verifying the Accuracy of Gear Measuring Machines', Part 1 DUCOP05/1, BGA Transmission Technology, Issue 1.1, September 1994.

[47]   Frazer, R.C. & Myers, E.J., 'A Code of Practice for Verifying the Accuracy of Gear Measuring Machines', Part 2 DUCOP05/2, BGA Transmission Technology, Issue 1.1, September 1994.

[48]   Frazer, R.C. & Hu, J., 'The Differences Between 3-Axis And 4-Axis Gear Measuring Machines', Proc. of B.G.A. Seminar, Huddersfield, October 1996.

[49]   Frazer, R.C. & Hu, J., 'Verifying The Accuracy Of Involute Gear Measuring Machines.', Proc. of The Third International Conference on Laser Metrology and Machine Performance, Huddersfield, 1997.

[50]   Fish, M. & Munro, R.G., 'Analysis Of Marking Patterns And Transmission Errors In Worm Gears', B.G.A. Technical Paper, November 1995.

[51]   Fish, M. & Munro, R.G., 'Kinematic Errors In Precision Worm Gears', Proc. Lamdamap Conference, Computational Mechanics Publications, 1997.

[52]   Dudley, D.W., 'Gear Handbook.', 1st Ed., McGraw-Hill Book Company, New York, 1962.

[53]   Litvin, F. L., 'Theory Of Gearing', NASA Reference Publication 1212, AVSCOM. Technical Report 88-C-035, 1989 (Translated From The Russian 1968 Edition).

[54]   DIN 3960, 'Concepts And Parameters Associated With Cylindrical Gear Pairs With Involute Teeth', Beuth, July 1980.

[55]   DIN 3962, 'Tolerance For Spur and Helical Gears', Beuth, August 1994.

[56]   DIN 3975, 'Terms And Definitions For Cylindrical Worm Gears With Shaft Angle 90°', Beuth, October 1975.

[57]   ANSI/AGMA 6022-C93, 'Design Manual For Cylindrical Worm Gearing.' ANSI/AGMA, 1993.

[58]   Munro, R.G., & Ling, P.H.K., 'A New Method of Measuring Involute Profile Deviations of Gear Teeth', Proc. Inst. Mech. Eng., Vol 210, 1996.

[59]   Munro, R.G., 'The DC Component of Gear Transmission Error', 5th ASME International Power and Transmission Gearing Conference, 1989, pp 467-470.

[60] Dyson, A., Evans, H.P., & Snidle R.W., 'A Simple, Accurate Method For Calculation Of Stress And Deformations In Elliptical Hertzian Contacts', Proc. Inst. Mech. Eng., Vol 206.

[61] Weimer, R.C., 'Statistics', 2nd Ed, Wm C Brown Publishers, 1993.

[62] Litvin, F.L., Chen, J.-S., Lu, J., & Handschuh, R.F., 'Application Of Finite Element Analysis For Deformation Of Load Share, Real Contact Ratio, Precision of Motion, and Stress Analysis', Journal of Mech. Design, Vol 118, Dec '96.

[63] Narayan, A., (Xerox Corporation), Houser, D, &Vijayakar, 'Study Of The Effect Of Machining Parameters On Performance Of Worm Gears.', AGMA Technical Paper, 95FTM14, 1995.

[64] Shigley, J.E., 'Mechanical Engineering Design.', First Edition, Mcgraw-Hill International Editions.

[65] Ramirez, R. W. 'The FFT Fundamentals And Concepts.' Prentice-Hall International Inc. 1985.

[66] Brigham, E. O. 'The Fast Fourier Transform And Its Applications.' Prentice-Hall International Inc. 1978.

[67] Press, W. H., Vetterling, W. T., Teukolsky, S. A., & Flannery, B. P. 'Numerical Recipes In Pascal.', Cambridge University Press.

[68] Munday,A.J. & Farrar,R.A., 'An Engineering Data Book', Macmillan Education Ltd,1979.

[69] Carvill, J 'Mechanical Engineers Data Handbook', Butterworth-Heinemann,1993.

[70]   Young, W. C., 'Roark's Formulas For Stress And Strain', 6th Ed., McGraw-Hill International Editions.

[71]   Parker, H., & Ambrose, J., 'Simplified Mechanics And Strength Of Materials', 4th Ed, John Wiley & Sons.

[72]   Perry, C., & Lissner, H.R., 'The Strain Gauge Primer', 2nd Ed, McGraw-Hill Book Co., 1962.

APPENDIX A

1995 B.G.A. ANNUAL CONGRESS PAPER

Analysis of marking patterns and transmission errors in worm gears

M Fish & R G Munro, University of Huddersfield

SUMMARY
Good marking patterns and low transmission errors are important for high duty, high precision and low noise worm gears. To meet these requirements has traditionally involved practical experience and trial and error tests. This paper describes a computer program which predicts marking patterns and transmission errors for any type of cutter mismatch, promising to significantly reduce development time. Preliminary comparisons with measurements are encouraging.

Introduction

It is well known that a good marking pattern between a meshing worm and wheel is essential for adequate lubrication and load capacity. An incorrect marking pattern can also lead to excessive transmission error, resulting in positioning errors and sometimes vibration and noise.

The traditional approach to achieving a good marking pattern has been a combination of experience plus trial and error adjustments in manufacture, with little in the way of theoretical guidance. The advent of low cost but powerful digital computers now opens up the possibility of predicting marking patterns at the design and machine setting stage, thus achieving a more optimised design and reducing manufacturing time. The aim of this project is to develop software for this purpose, and to check it experimentally under realistic operating conditions.

Conjugate theory

The starting point for any analysis of worm gears is the conjugate case, where a perfect worm is meshed with a perfect wheel, so that the marking is a full contact of the flanks as the gears go through mesh. This case has been analysed by Buckingham (ref. 1), Merritt (ref. 2) and Tuplin (ref. 3). At any one angular position there is a line of contact across the face of the teeth, and Figure 1(a) shows a series of these lines for different angular positions of mesh.

Theoretical lines of contact   Actual contact pattern
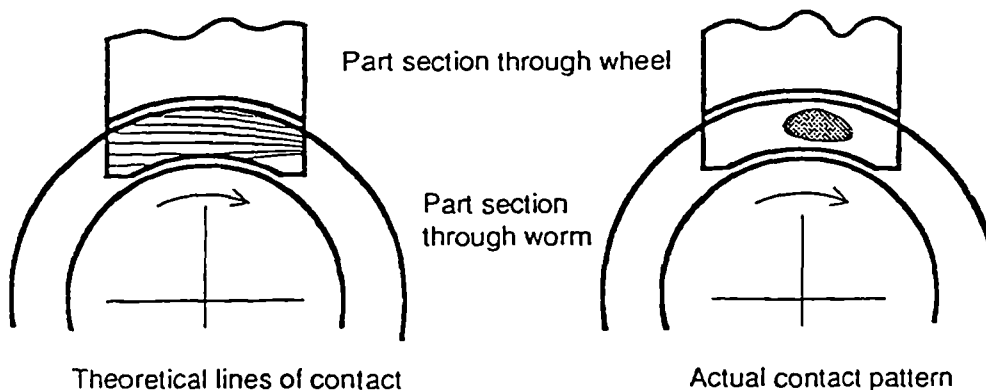
Fig. 1 Contact lines and marking pattern

Mismatch

A conjugate pair would not work in practice, because the lubricating oil has to be entrained in the mesh by a converging gap. In practice there are also gaps at the exit side of mesh and at the tips and roots, to avoid stress-raising edge contacts. These gaps are achieved by having a small mismatch between the geometries of the worm and the hob or fly tool, and they have the effect of producing partial marking as in the pattern of Figure 1(b), rather than full marking as in the conjugate case.

Previous mismatch analyses

The first mismatch analysis was reported by Janninck (ref. 4) in 1987, followed by an elegant three-dimensional vector approach by Colbourne (ref. 5). In both cases the most important outcome was a plot of contour lines of constant relief from the conjugate case, for a given cutter mismatch and cutting centre distance. A typical plot from Colbourne's analysis is given in Figure 2. He used a rather confusing terminology, but it is effectively a two-dimensional plot of relief, which is normally called topological relief. His analysis also gave much other valuable information, such as meshing gaps and single point values for transmission error.
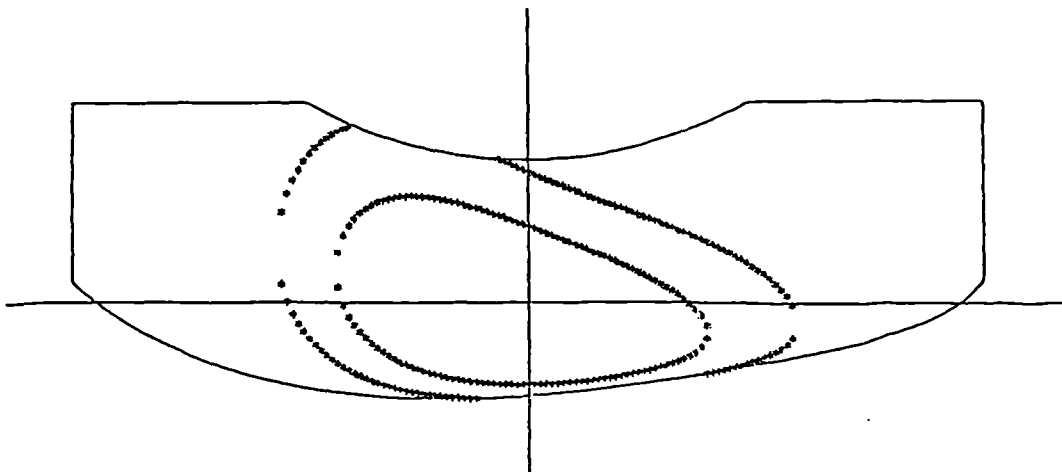
Fig. 2 Topological relief from Colbourne's analysis

Our mismatch analysis

Our analysis is based upon the Colbourne method, but taking advantage of faster modern computers and programs, so that the following plots can be obtained quickly enough for designers to use the program as a design tool:

(a)   Plots of topological relief for any number of chosen contour lines, as in Figure 3(a), which corresponds to the Colbourne example of Figure 2.

(b)   Plots of a succession of constant gap contours between mating flanks at a number of angular positions, see Figure 3(b). A point of zero gap (shown as a dot) is a point of contact of the flanks at each angular

position under no load and with no interference from neighbouring tooth pairs. The locus of these points can then be traced through mesh as the gears rotate.

(c)   If a contour of constant gap as in (b) is selected to correspond to the thickness of the marking paste, then it can be assumed that all points enclosed within this contour will be marked by the paste. If this process is repeated for many angular positions then the superimposed marked areas will simulate the smearing of the marking paste as the gears rotate. Note that the simulated marking pattern Figure 3(c) looks very similar to the topological relief pattern Figure 3(a).

(d)   Plots of transmission error, both for a single tooth pair, see Figure 3(d), and as a continuous curve for a succession of identical pairs, see Figure 3(e).

Effects of manufacturing deviations

Preliminary comparisons of predicted and measured marking patterns and transmission errors showed that it was necessary to extend the analysis to include the effects of some manufacturing deviations. The profiles of a non-mismatched fly tool used for cutting a test wheel were first checked on a Holroyd CNC cutter sharpening machine, with deviations (in the normal plane) from the conjugate profile plotted in Figure 4(a). One concern was whether these deviations were reproduced (in reverse) on the wheel, so the wheel profiles were measured on a specially programmed Gleason CNC gear checker at the National Gear Metrology Laboratory at the University of Newcastle upon Tyne. Figure 4(b) shows that the deviations were reproduced within a few microns.

Fig. 3 Typical program outputs
(a) topological relief
(b) successive constant gap contours
(c) simulated marking pattern
(d) transmission error of single pair
(e) multiple pair transmission error

4
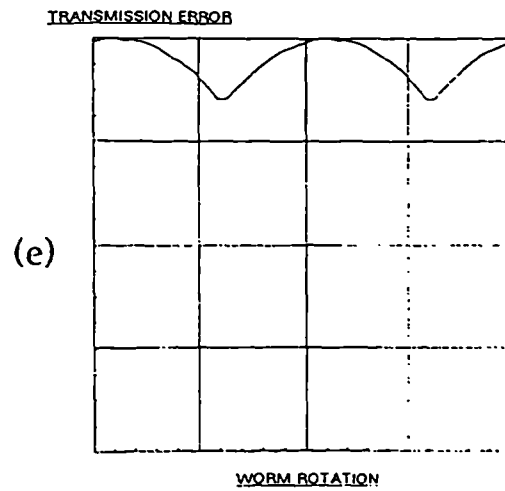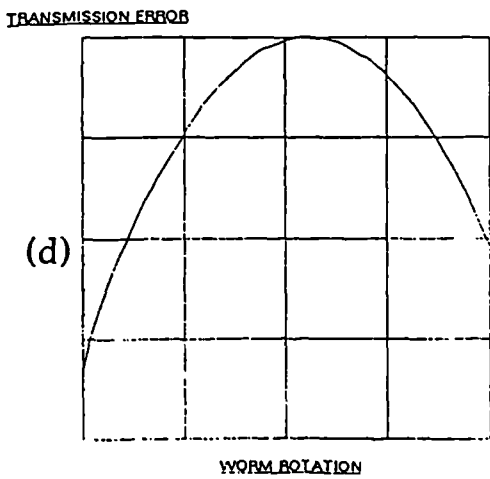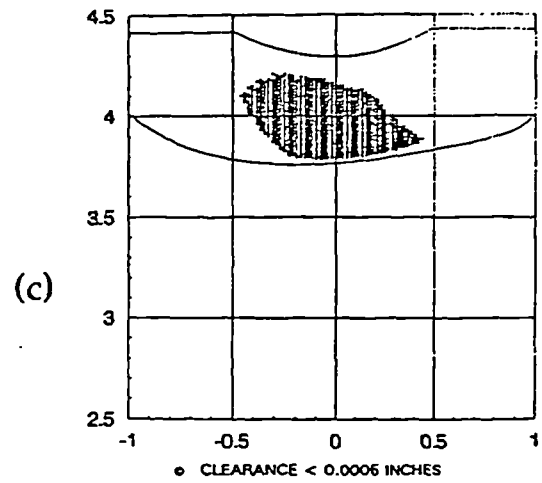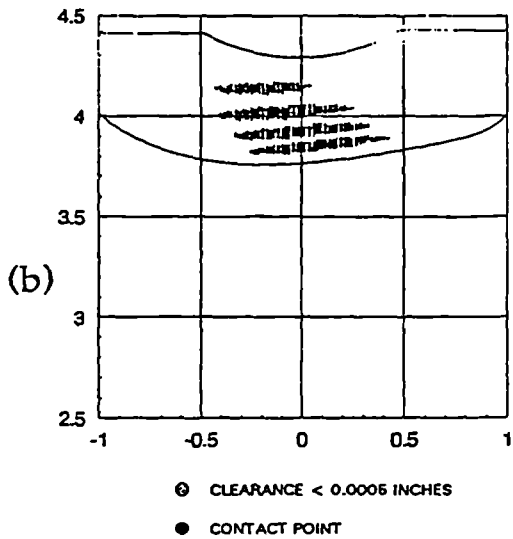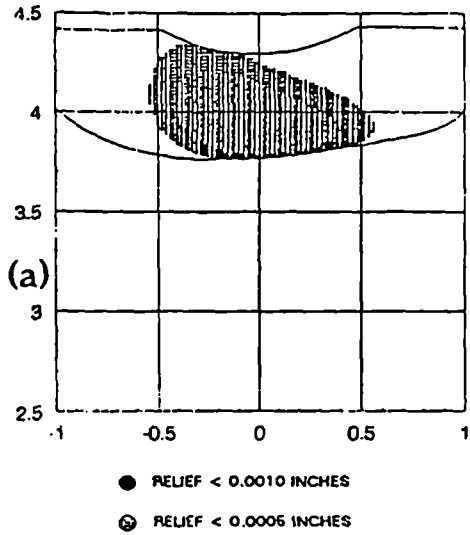
Non Mismatched Flytool Profile Deviations

Fig. 4 Fly tool & corresponding wheel tooth profile deviations

5

Checks were also carried out on worm profile and lead deviations, eccentricity and axis offsets, and with the exception of the lead deviation these deviations were included in the software. Comparisons between predicted and measured marking patterns and transmission errors are shown in Figure 5. The agreement is encouraging at this stage, bearing in mind that not all deviation effects have been included so far.
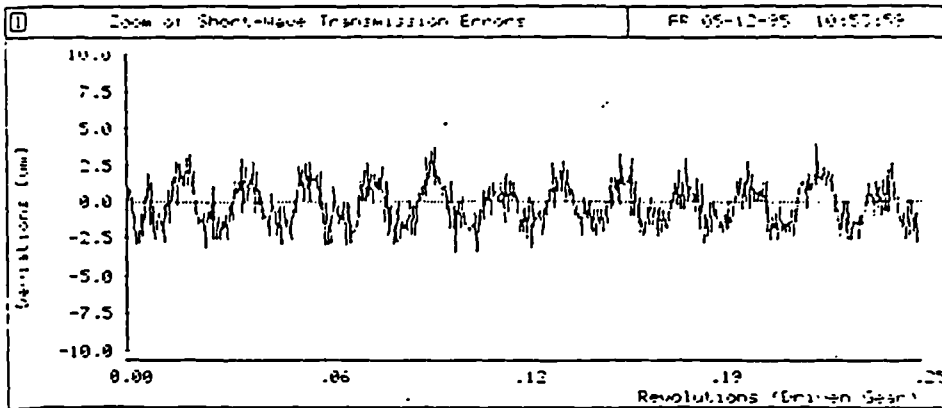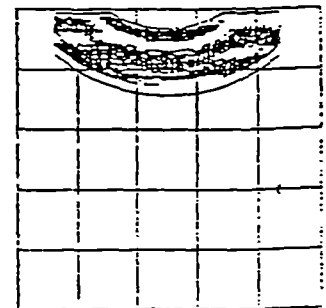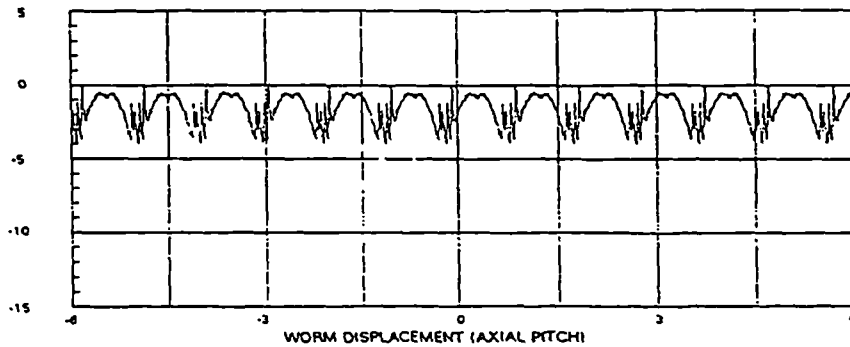
Fig. 5 Measured (upper) & predicted (lower) transmission errors and marking patterns for a non-mismatched pair

A similar comparison was made for a pair cut with deliberate mismatch, and the results are given in Figure 6. Again the comparison is encouraging.
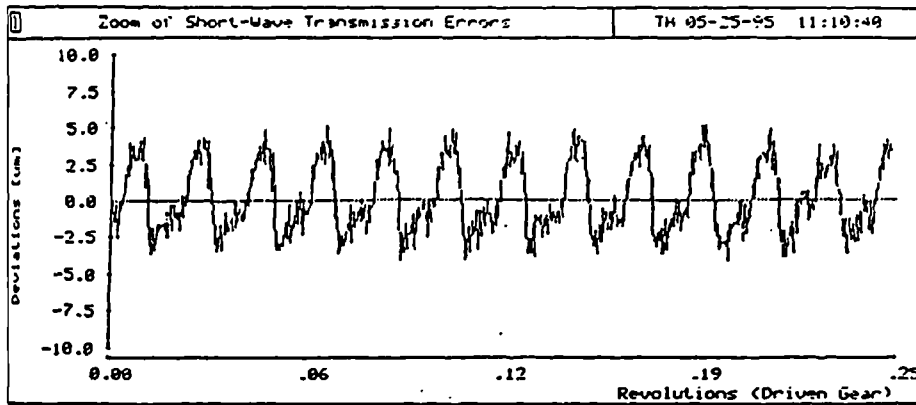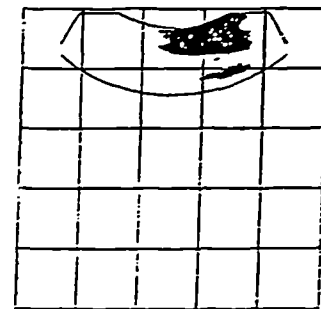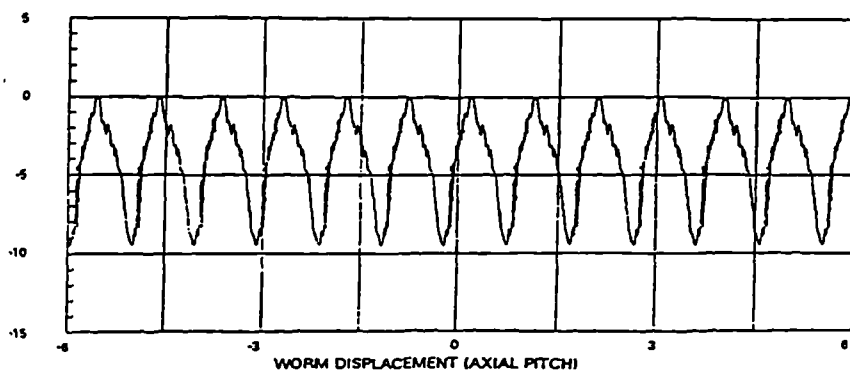
Fig. 6 Measured (upper) & predicted (lower) transmission errors
and marking patterns for a mismatched pair

Further refinements of the analysis

In addition to the geometrical deviations already mentioned, it is planned to incorporate into the software the effects of pitch errors and angular misalignment errors. We also plan to extend the work to the case where the tooth loads are large enough to produce significant tooth and gear body deflections. To check the analysis for the loaded case experimentally a new test rig is being built which will measure transmission errors and gear deflections at working loads. For the loaded case it will be necessary to include deliberate profile deviations, rather like tip and root reliefs in spur and helical gears.

Conclusions

Although the research programme is only at about the half way stage, it is already clear that the software can help in predicting marking patterns and transmission errors for lightly loaded situations. This should help to identify the more critical geometrical error sources and to reduce the amount of time taken by trial and error development work.

The planned work on more heavily loaded gears should take this process further, and should give guidelines on optimum mismatch values and profile reliefs.

References
(1)   BUCKINGHAM, E. Analytical Mechanics of Gears. *Dover Publications*, 1987.

(2)   MERRITT, H.E. Gear Engineering. *Pitman*, 1971.

(3)   TUPLIN, W.A. Involute Gear Geometry. *Chatto and Windus*, 1962.

(4)   JANNINCK, W.L. Contact surface topology of worm gear teeth. *American Gear Manufacturers Association*, paper 87FTM14, 1987.

(5)   COLBOURNE, J.R. The use of oversize hobs to cut worm gears. *American Gear Manufacturers Association*, paper 89FTM8, 1989.

APPENDIX B

1997 LAMDAMAP CONFERENCE PAPER

Kinematic Errors In Precision Worm Gears

M. Fish & R. G. Munro
Department Of Mechanical Engineering,
University Of Huddersfield, Queensgate,
Huddersfield, HD1 2DH.

Abstract

This paper describes the measurement of error sources in a worm gear set and assesses their effects when developing a computer model to synthesise behaviour. To do this several test gears have been made and the process monitored by controlled measurement at several stages using some of the most sensitive and accurate equipment available. A computer program has been written to model the characteristics of these worm and wheel gear pairs under a range of conditions. The predictions have been validated using a test rig measuring rotary accuracy of the input and output shafts under a torque load.

1   Introduction

Precision worm gears are widely used in machine tools, rotary tables and robots. Normal positioning accuracy is around 7-15 arc secs. but this may be influenced by design, production and operating conditions.

The geometry of this type of gearing demands many hundreds of calculations for even a basic analysis. When combined with the sensitivity of the errors relative to working tolerances this has made even subtle changes in design difficult to predict, frequently causing precision worm and wheel sets to be produced as a unique pair. Previous analysis of worm gear design has been carried out in the first half of this century by Merritt[1], Tuplin[2], and Buckingham[3] and more recently by Dudley & Poritsky[4] but performance has been assessed on an empirical basis with results frequently undocumented.

Improvements in computing power and tooling technology within the last decade have allowed a more controlled study to be carried out. A program of research has been established at the University of Huddersfield to take advantage of these developments. The aims are to understand the influence of design on worm gear characteristics, identify and quantify potential error sources, and to create a computer model to predict behaviour under a given set of conditions.

2 Transmission Error

Assessment of a worm gear set is generally made by inspection of the contact marking pattern indicating that entry and exit conditions are sufficient for oil lubrication of the surfaces. For high accuracy applications this method is not sensitive enough since satisfactory conditions can be achieved several ways with different accuracy on each occasion.

The concept and measurement of transmission error was developed by Harris and Munro[5][6] in the 1950's to 1960's for spur gears but can be applied to any form of gearing. It is defined as the error in output position of a gear shaft for a defined position of the input shaft with respect to the gearing ratio. Measurement of this can be achieved by mounting encoder gratings to the input and output shafts of a test gear box and linking these to a computer. A rotary accuracy of 0.3 arc secs. is currently achievable by this method.

Though transmission error is a measure of the positioning accuracy of a gear set research has shown that this positioning inaccuracy can be linked directly to noise and vibration [7]. In order for improvements to be made in any of these areas it is important to establish the contributions from the individual elements of worm gearing.

3 Sources Of Error

3.1 Design

Design is based around modification of the gear wheel cutter known as mismatching. Lead, cutter radius and involute profile relative to the worm dimensions are all parameters which can be changed, while the cutting axis is slightly inclined relative to the operating axis. If no mismatch were to be applied, the cutting tool would be a copy of the worm thread and the contact between worm and wheel defined as conjugate. In practice a controlled design mismatch is essential to allow oil lubrication of the contact surfaces, but in doing this any worm gear design induces transmission error.

For analysis purposes the worm gear set is reduced into several sections of equivalent rack and pinion as shown in Figure 1. For each rack section the difference in conjugate and mismatch thread position along the path of contact can be calculated. This is the relief value and represents the amount of metal which would be removed relative to a conjugate gear tooth as shown in Figure 1 for a typical section for an arbitrary angular position. Calculating relief values in each rack section at a series of angular positions through the cutting cycle a topological relief map can be compiled over the gear tooth as in Figure 2.
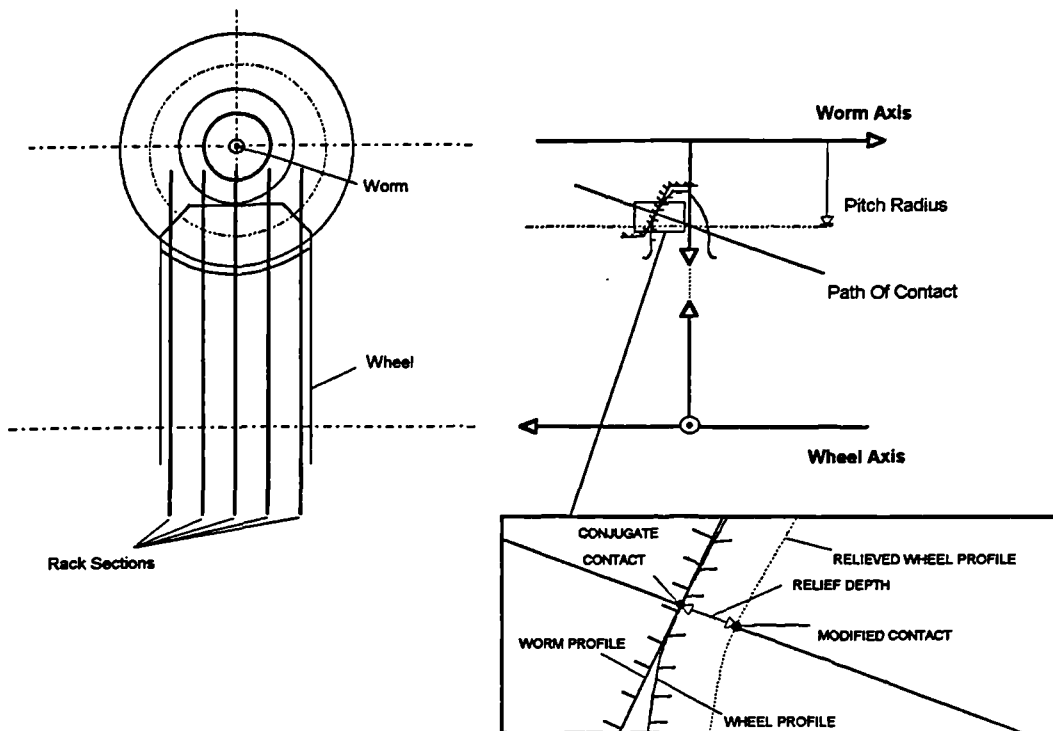
Figure 1 :   A diagram showing typical rack sections through a worm gear set
and the effect of relief in a typical section.
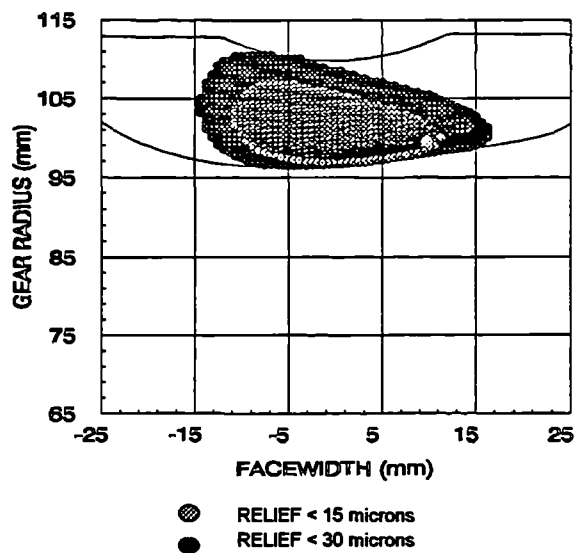
Figure 2 :   An example of a topological relief map with two contour depths for
a specimen gear design.

At each angular position the rack section with the minimum relief will be in contact and the associated modified contact position becomes the transmission error. By calculating this effect at a series of angular positions through the tooth engagement a transmission error curve can be compiled.
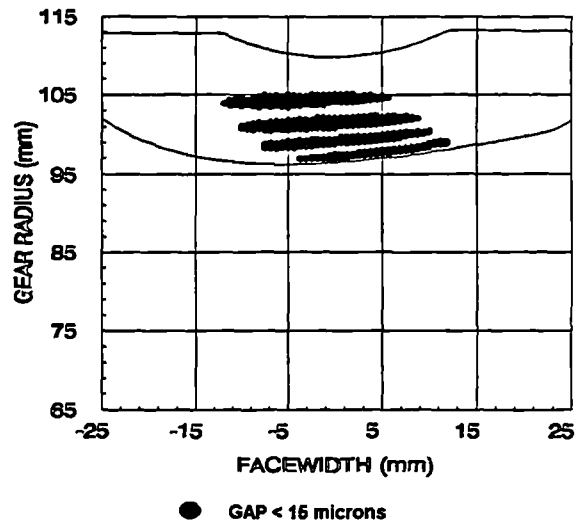
Figure 3 :   An example of worm and gear flank gap calculations in four angular positions for a specimen gear design.
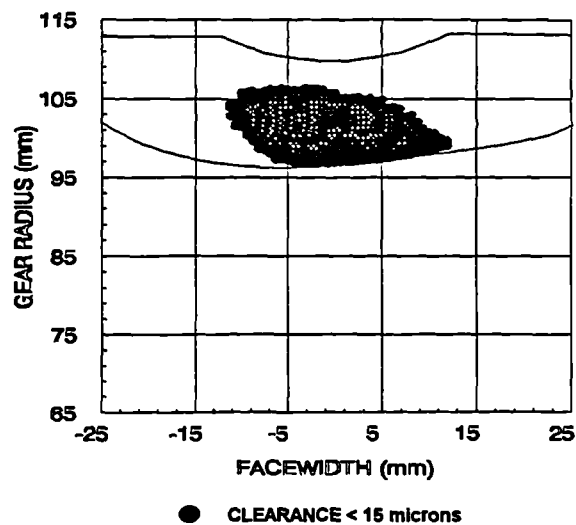
Figure 4 :   An example of a clearance diagram for a specimen gear design.

Once the transmission error has been established the contact conditions can be examined. For any angular position the gap between the mating flanks can be calculated. An example of this is shown in Figure 3 with the gap calculations performed in four angular positions.

By compiling a series of these calculations through the meshing cycle the minimum gap, defined as the clearance, can be found at each point on the gear tooth surface. Clearance diagrams show areas of the gear tooth with a specified value of clearance to assess the lubrication potential. An example is shown in Figure 4. This is the equivalent of performing an accurate contact marking test. Varying the mismatch parameters alters the extent and position of the relief and consequently the contact. The intention is to concentrate contact in a particular area of the gear tooth.

Production of precision worm gear sets is a series of compromises between adequate lubrication conditions and rotary accuracy. Recent work by Janninck[8] and Colbourne[9] has examined the way in which contact can be altered for a particular application. By varying the mismatch parameters theoretical transmission error amplitudes of 1-2 microns can be achieved while still allowing satisfactory contact conditions.

3.2 Manufacturing

The final accuracy of the gear set depends upon the ability of the machine tools to reproduce the theoretical design.
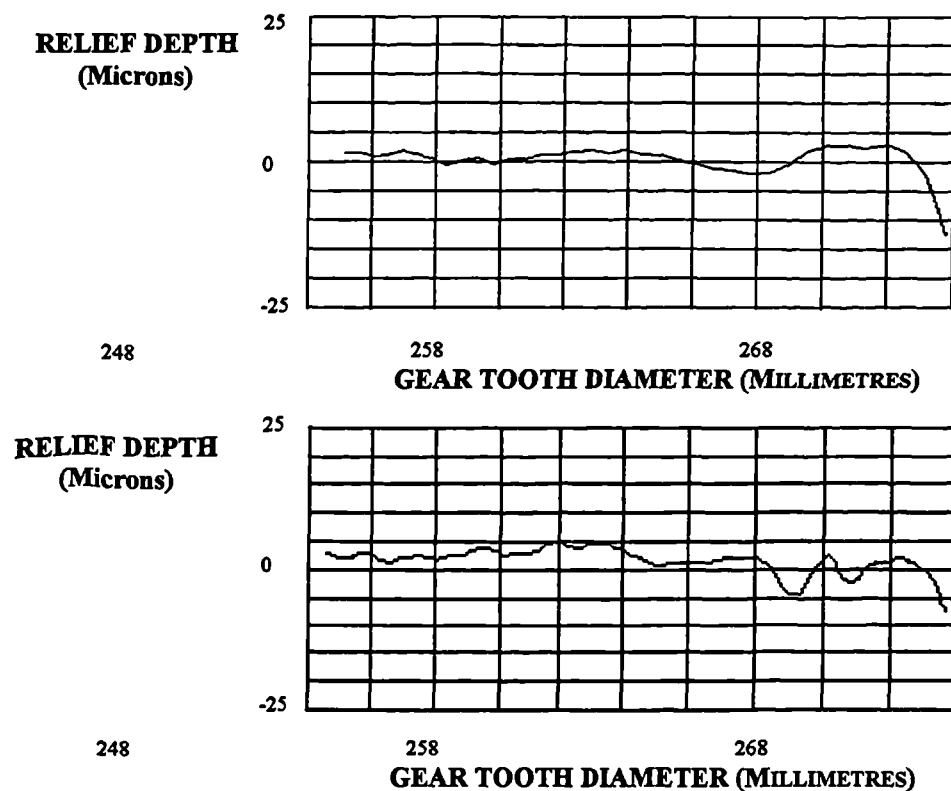
Figure 5 : A comparison of measured and synthesised gear wheel profile errors from a cutting tool produced using a standard cutter grinder machine.

An example of this is the profile error in the gear cutting tool. In Figure 5 synthesised gear tooth profile errors (A), calculated using measured gear cutting tool profiles, are compared with the profile errors from a completed gear wheel cut with this tool (B). This shows that these are transferred directly onto the wheel profile to within 1-2 microns. In extreme cases profile errors can dominate the contact in turn causing transmission error. Clearly a more accurate profile is preferred. A standard cutter grinding machine can produce these profiles to within 10 microns of the original form. CNC machine tools have been able to improve on this producing profile generations to within 2 microns. In Figure 6 examples of profile errors on cutting tools produced using the cutter grinder and a CNC machine are shown.

Other main error sources are in the worm lead which determines the helical shape of the worm, and wheel tooth pitch which defines the angular spacing. These are often caused by errors from the machine tool gearing which determine the feed ratios. The worm form is generally a ground finish allowing high profile accuracy to be achieved with the lead error potentially held to within 4 microns per 100 mm of thread. Pitch errors can be held to within 3 microns between adjacent teeth.
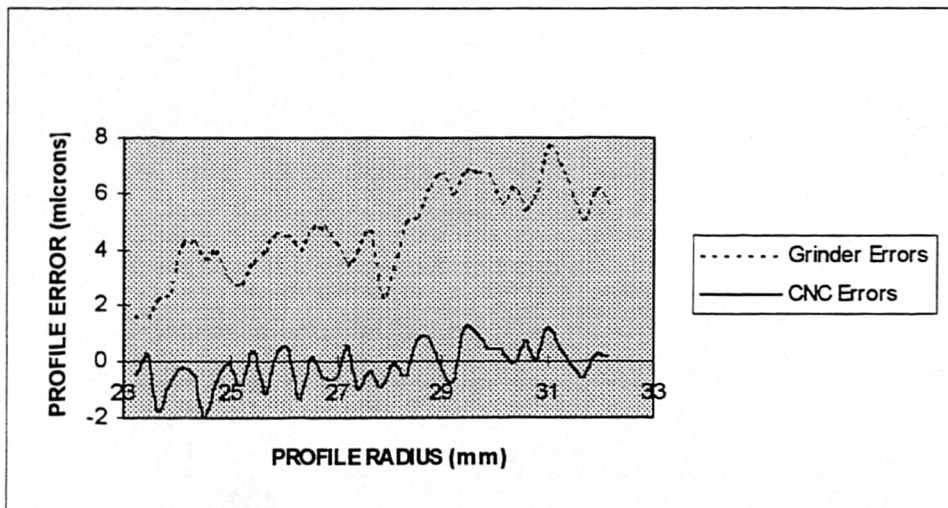
Figure 6 : A plot of profile errors from gear cutting tools produced using a standard cutter grinder machine technique and a CNC machine tool.

3.3 Assembly

The alignment of the gear set in the box can cause small changes in transmission error value, but more critically it is influential over the inlet and outlet contact conditions. Misalignment is caused by machining tolerances in the reference surfaces, or by radial movement in the bearings causing eccentricity in the

machined reference bands of the worm and wheel components. Linear inductive probes can be used to determine this effect. In Figure 7 probes 1 and 2 detect movements in the worm reference bands, probe 3 detects movement in the wheel reference band. A similar bank of probes perpendicular to these monitor lateral shift in the assembly.
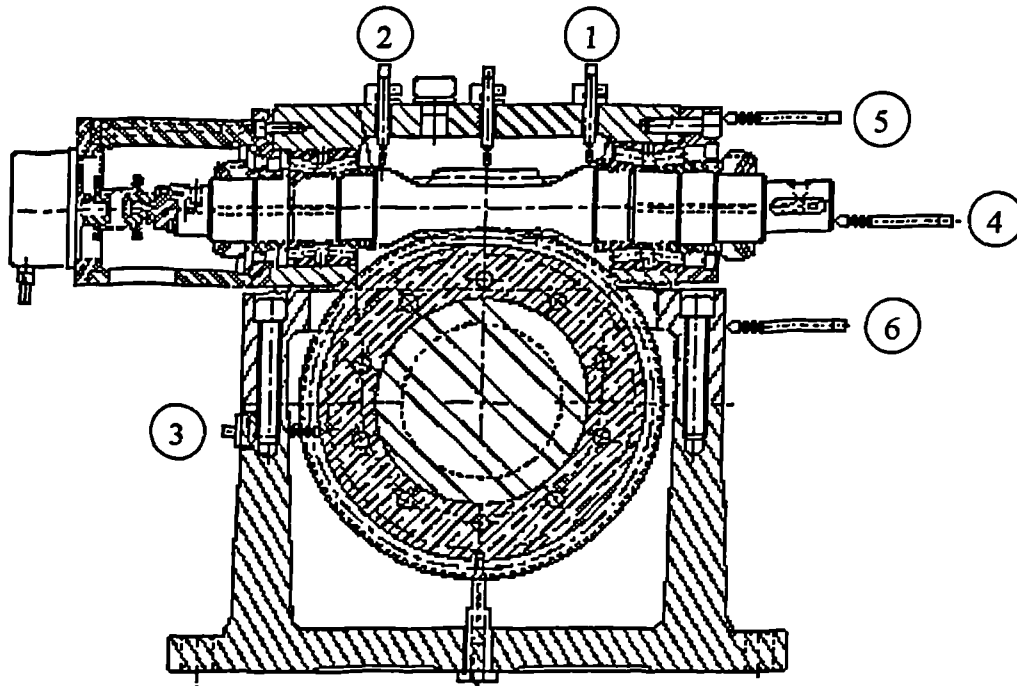
Figure 7 : A diagram of probe points monitoring eccentricity in the assembly and test box movement under load.

3.4 Deflection

Tooth deformation by compression and bending occurs when a torque load is applied to the gear system. This modified tooth form alters the contact point and induces transmission error directly. Movement also occurs axially in the bearings and in the gear box structure. The shift in position of the worm with respect to the wheel contributes directly to the transmission error detected by the measuring encoders, however probe readings can be used to evaluate this effect. In Figure 7, probe 4 monitors the movement in the worm shaft axially, probe 5 indicates the movement of the worm housing while probe 6 monitors the position of the wheel housing. The net worm movement can be calculated from these readings, and when subtracted from the total transmission error isolates the tooth deformation effects.

4   Composite Model

A computer program was developed to calculate the effects of parameter variation on worm gear design. This was then extended to allow analysis including error sources. It was then used to predict the characteristics of several production gear sets all based upon a 152 mm centre and 50:1 ratio design.

The graph shown in Figure 8 is the computer prediction of theoretical transmission error based upon the calculations from one design specification.

TRANSMISSION ERROR (MICRONS)

WHEEL DISPLACEMENT (REVOLUTIONS)
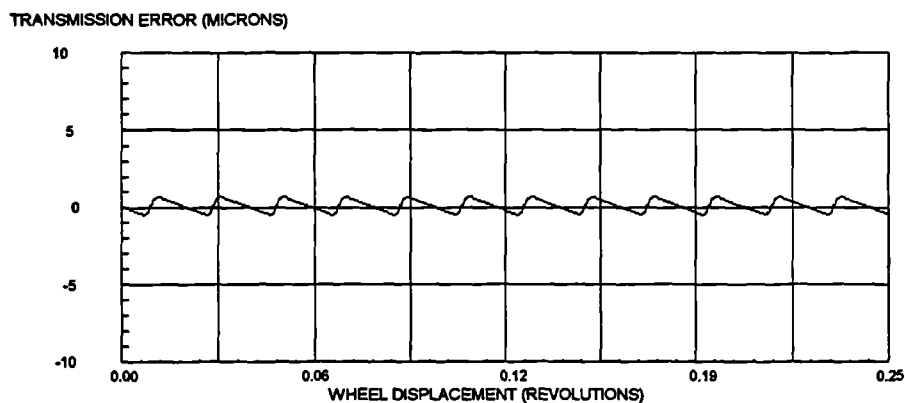
Figure 8 :   Theoretical transmission error for a test worm gear design.

A gear set was then manufactured using this specification. Several error sources such as gear cutting tool profile errors of, 7 microns, eccentricity in the worm and wheel, 5 microns, and misalignment of the operating centre distance, 5 microns, were recorded. These were added to the computer program and a prediction of synthesised transmission error was calculated. The resulting graph is shown in Figure 9.

TRANSMISSION ERROR (MICRONS)

WHEEL DISPLACEMENT (REVOLUTIONS)
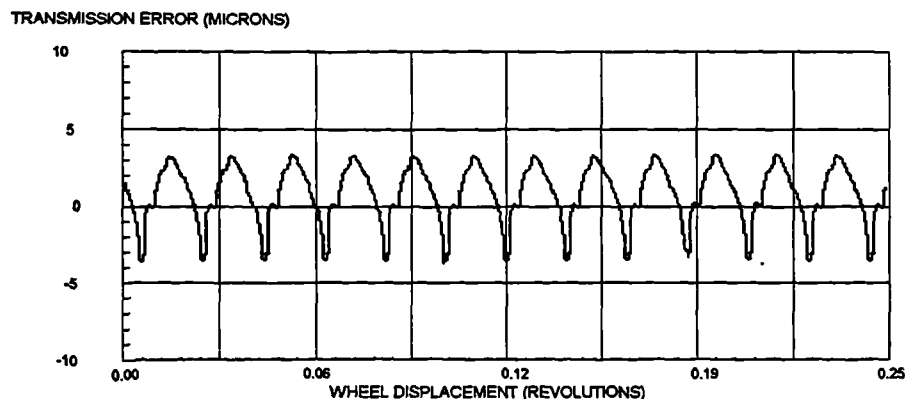
Figure 9 :   Synthesised transmission error for test worm gear set.

A test was then performed on the completed gear set to obtain a measured transmission error plot. The result is shown in Figure 10.
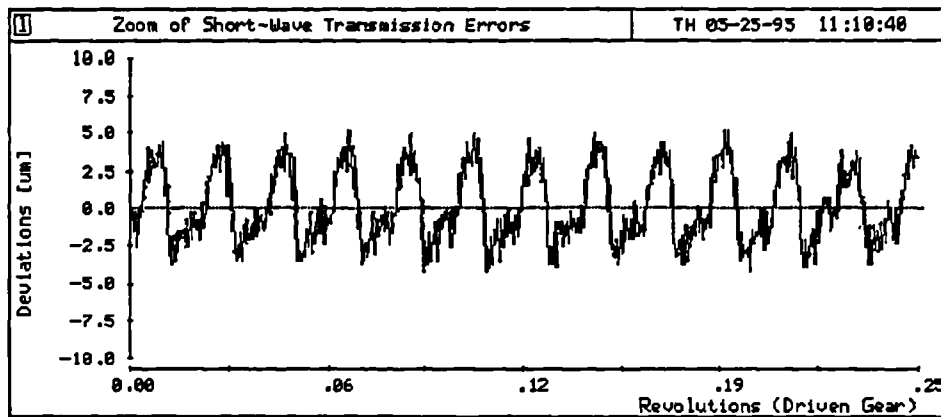
Figure 10 : Measured transmission error from a production worm gear set.

5   Conclusions

From the diagrams shown in section 4 several conclusions can be drawn. The results of Figure 8 show that theoretical designs can be produced with a relatively high accuracy. Comparing this with the synthesised results of Figure 9 indicates that even small inaccuracies can amplify the transmission error. Despite this however, if enough error sources are known then a computer model can be used to synthesise worm gear characteristic errors to within a micron as shown by comparing Figure 9 with Figure 10.

The good correlation in these results allow the computer model to be regarded as a tool. It can be used to investigate the effects of modifying design or isolate which error sources are most influential in determining the error without the need for expensive production costs.

6   Acknowledgements

7   References

1.   Merritt, H.E., *'Gear Engineering.'*, Halsted Press, 1971.
2.   Tuplin, W.A., *'Involute Gear Geometry.'*, London, Chatto, Windus, 1962.
3.   Buckingham, E. *'Analytical Mechanics Of Gears.'*, Dover 1963
4.   Dudley, D.W. & Poritsky, H., *'On Cutting And Hobbing Gears And Worms.'*, Applied Mechanics, TRANS ASME, 1943.+
5.   Harris, S.L., *'Dynamic Loads On The Teeth Of Spur Gears.'*, Proc. Instn. Mech. Eng.,1958,(vol 172), pp87-112.
6.   Gregory, R.W., Harris, S.L., & Munro, R.G. *'A Method Of Measuring Spur Gears Of 1:1 Ratio.'*, Journal Of Scientific Instruments, Jan 1963, (vol 40), pp5-9.
7.   Palmer, D. & Munro, R.G., *'Measurements Of Transmission Error, Vibration And Noise In Spur Gears.'*, British Gear Association Conference Sheffield, Technical Paper, November 1995.
8.   Janninck, W.L., *'Contact Surface Topology Of Worm Gear Teeth.'*, AGMA paper 87 FTM 14, 1987.
9.   Colbourne, J.R., *'The Use Of Oversize Hobs To Cut Worm Gears.'*, AGMA paper 89 FTM 8 1989.

APPENDIX C

SOFTWARE INSTRUCTION BOOKLET

WORM GEAR TRANSMISSION ERROR AND CONTACT ANALYSIS PROGRAM

OPERATING INSTRUCTIONS

(Version 2.1)

Michael Fish
University of Huddersfield

Queensgate
Huddersfield
HD1 3DH

Tel : 01484 422288 (ext. 2406)

CONTENTS

I   EQUIPMENT SPECIFICATION

The program is compatible with IBM type PC computer systems and operates in an MS-DOS environment. It is supplied on a 3.25" diskette which is used in the drive labelled 'A:'. The calculations require a minimum of a 486 processor with a 33Mhz clock speed and 4Mb of RAM. Any compatible machine above this specification will improve the analysis cycle time. Though the program will operate from the diskette, it is recommended that the installation procedure is followed and operation takes place on the main hard drive labelled 'C:' since this will greatly reduce the calculation cycle.

II   INSTALLATION

After switching on the computer the screen should display the DOS prompt :

C:\\>

Insert the program disk in the 'A' drive, type :

a:\\install

This creates a directory on the computers 'C:' drive called 'mfish'. It then copies the executable program and the graphics support file to this directory which will be the working directory. To start the program simply type :

dtiprog

If subsequent installations are necessary to replace a damaged file or updating the version then repeat the installation process. Existing design and calculation data files in the directory from any previous program operation will be unaffected. In order to use the program on further occasions the user must be in the working directory. To do this type :

cd c:\\mfish

Any ASCII files of data created while using the program will be contained within this directory (unless otherwise specified by the user).

It is possible to install this program from inside WINDOWS by choosing the MS_DOS prompt icon from the main group and following the previous instructions, or by selecting 'RUN' from the 'FILE' menu and typing :

a:\\install

It is also possible to set up an icon to drive the program under a *WINDOWS* environment. Follow the instructions on how to use the 'NEW' option from the 'FILE' menu in the user manual supplied with the *WINDOWS* program.

III TERMS AND DEFINITIONS

The majority of expressions used in this document will be familiar to users if they are involved in the gear manufacturing process. Some parameters needed by the program for the analysis are not always used as part of a gear design standard, or form part of the operating input of the program itself. For this reason the following glossary defines some of the more obscure expressions and analysis options used in the course of this program's operation to avoid confusion.

III.A. DURING DESIGN INPUT

Profile Modification
This is maximum amount of additional metal applied to the theoretical profile of the wheel cutting tool defined by the design parameters (see also 'Modification Type').

Modification Type
The profile modification can be applied in a parabolic or linear type. In both cases it is applied symmetrically about the mid point of the tooth in a direction normal to the existing profile in the axial section. The tip and the root will have a value of extra metal added equal to the profile modification. If the modification is linear then an extra parameter is needed. Again, modification is applied symmetrically along the normal to the existing profile, but a further value will have to be entered representing the percentage of the profile to be modified. The distribution of each type of modification is illustrated in the diagrams below.

PROFILE MODIFICATION

PROFILE
MODIFICATION
VALUE

PARABOLIC

PROFILE
RADIUS

ROOT   TIP

PROFILE MODIFICATION

HALF PROFILE
PERCENTAGE

HALF PROFILE
PERCENTAGE

LINEAR

PROFILE
MODIFICATION
VALUE

PROFILE
RADIUS

ROOT   TIP
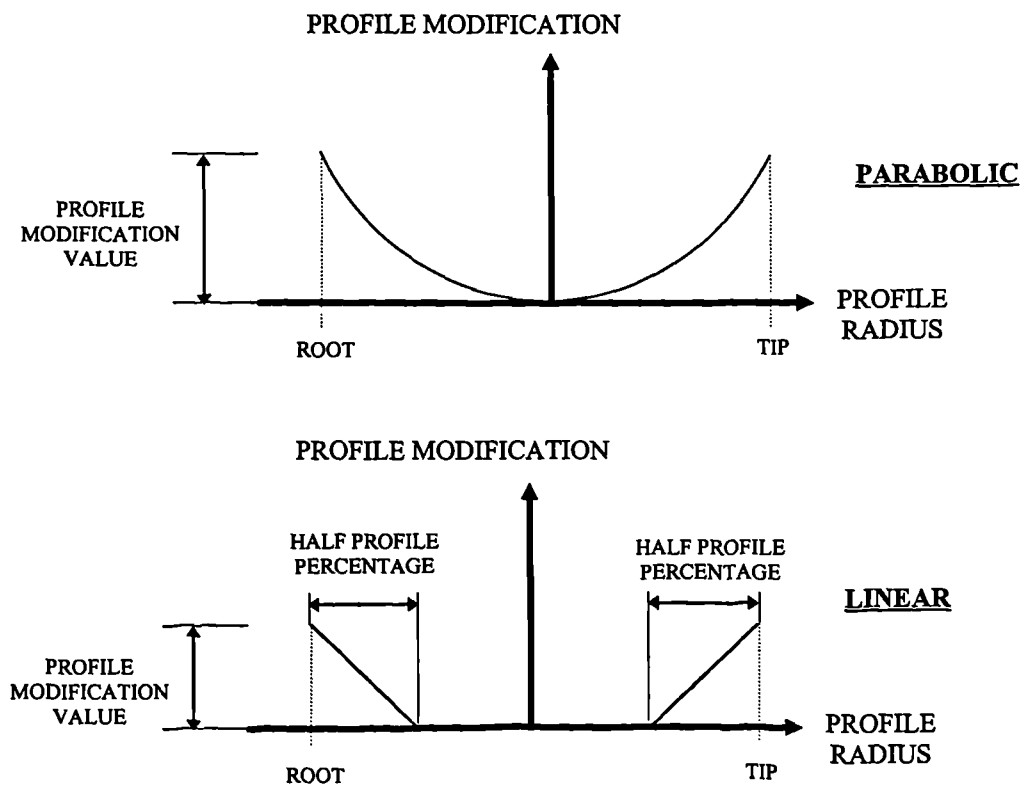
Profile Shift

This option effectively increases the root and outside diameter of the wheel cutting tool but is independent of the design process and any oversize value. It is merely an option to shift the entire calculated profile relative to the cutting tool axis. This is equivalent to lifting or dropping a single tooth wheel cutting tool in a mounting bar. This will alter the calculated tip radius of the cutting tool and thus the overall diameter.

Extension To Centres

This value represents the change in worm mesh centre distance needed to define wheel cutter axis centre distance.

Swivel Angle

Also called 'tilt' or 'tip' angle, this is the angle of inclination of the wheel cutting tool axis in a plane parallel to that of both the worm and the wheel.

Throat Radius

Sometimes called the 'gorge' radius, this is the clearance cut into the wheel tooth to accommodate the worm. The actual value used is that taken from the worm axis and is usually equal to the worm root radius plus any clearance required between the worm and wheel tooth.

NOTE : This value is not that is measured across the wheel diameter. That value is known as the 'throat diameter' and is not necessary once the radius value has been entered.

III.B. DURING OPTIONS FOR ANALYSIS

Number Of Profile Points
This represents the number of points taken from root to tip along the theoretical flank profile of the worm and wheel cutter during the analysis. More points creates a more accurate prediction but increases the time to complete the calculations. This value is automatically defined when using measured profiles.

Rack Sections
This is the number of planes parallel to each side of the axial plane in which the analysis takes place. Like the number of profile points chosen, an increased value here increases the accuracy of the prediction but also increases the time taken to make the calculations.

NOTE : Actual number of rack sections is twice the value entered plus one ensuring symmetry about the axial plane.

Chamfer Settings
There exists an option to include the chamfer on the gear tooth form in the cutting cycle. This requires entering two values, the first is an inset value which represents the distance in from the original tooth edge on the rim of the wheel, while the second is the angle in degrees at which the chamfer develops. The relation of these values to the gear tooth form generation is shown below.
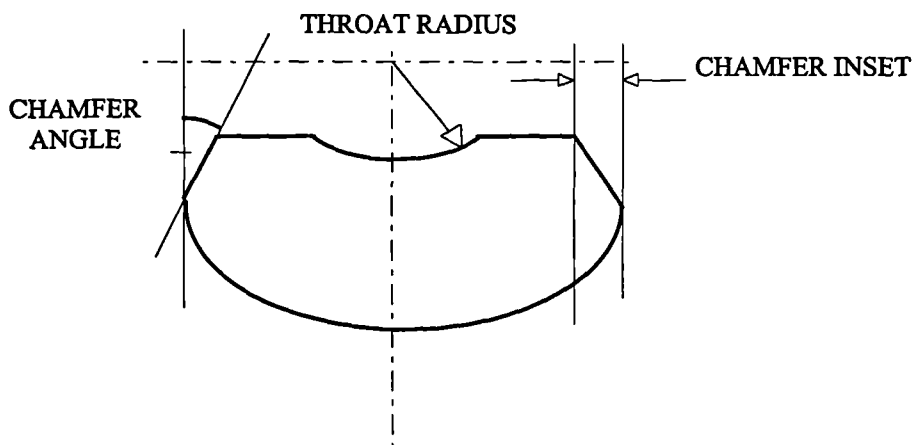
Number Of Mesh Samples
The number of mesh samples represents the number of positions through the wheel displacement interval at which the contact analysis is performed. A displacement equivalent to two worm lead lengths is the minimum interval used, and a minimum of 20 points per tooth pitch is required by the program to generate an accurate representation of contact. Increasing the sample number will be a closer representation of the contact but will take longer to calculate.

Axis Settings

Changing alignment of the gear components allows the user to introduce working errors into the model. The notation for this is as follows :
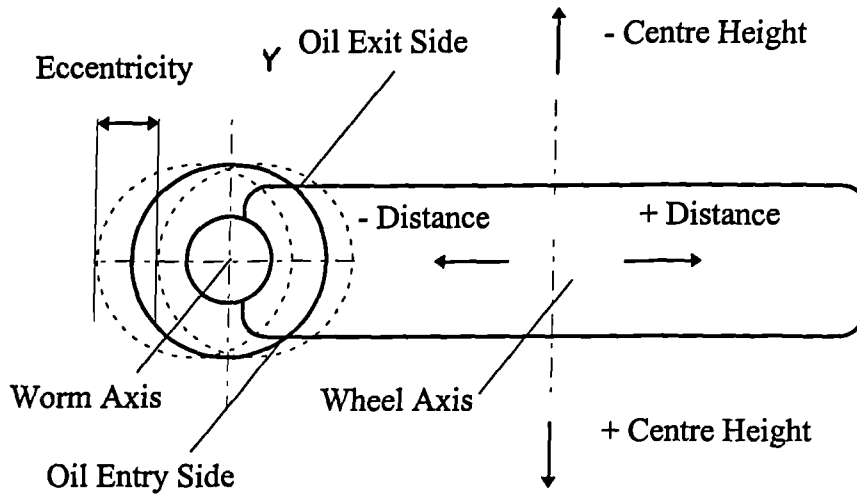
1. INTRODUCTION

The ability to quickly and accurately model the effects of design and operating conditions on the performance characteristics of any gear system is becoming increasingly important. This has proven difficult for a worm gear system due to the complex geometry involved and the large number of variables which determine contact behaviour. Within the last ten years the improvement in computing speed and machine tool technology has overcome this problem to such an extent that a full contact analysis can be calculated within a few seconds, and validated to an accuracy within 1-2μm by direct measurement. Research at the University Of Huddersfield has taken advantage of this principle to develop a computer program to calculate the contact conditions of a gear set given various design parameters and manufacturing conditions.

The worm gear contact analysis software calculates the worm thread and gear tooth form, the clearance between the worm thread and wheel tooth flank, and the resulting positioning accuracy (referred to as transmission error) for a given design specification. Further, it allows an analysis of the factors which directly affect these characteristics such as machining quality, alignment of the components, and deformation of the contacting surfaces under load. The software consequently represents a tool with which to investigate and improve the worm gear design and manufacturing process. It allows an analysis of new or existing designs, and the investigation of manufactured sets which display unacceptable behaviour under specified operating conditions. There is a potential for large savings in time, cost, and resources with the correct application by experienced design and production engineers.

The program will permit a number of functions during operation :

- Entry, modification, and storage of design data.
- Calculation of the gear set component geometry generated by the theoretical settings.
- Modelling of various error sources occurring during production and operation.
- Calculation of the contact characteristics of the gear system under defined conditions.
- Various forms of analysis to permit potential design optimisation.
- Save and recall of analysis files created during previous operation of the program.

This layout represents the general order in which the program is to be operated when conducting an investigation of a given gear set design. These stages will be explained in further detail over the course of this document.

2. PROGRAM OPERATION

2.1. Controlling operation using the menu system

Control of program operation is achieved using a menu system with the required option entered through the keyboard. The display in Figure 1 shows the three menus marked MAIN MENU, DATA MANAGER, and RESULTS MENU which are used to initiate the program functions.

MAIN MENU.	DATA MANAGER.	RESULTS MENU.
1. DATA MANAGER.	1. ENTER NEW GEAR SET	1. PROFILES
2. RUN SIMULATION CYCLE.	2. CHANGE WORM DESIGN	2. TRANSMISSION ERRORS
3. RECALL STORED RESULTS.	3. CHANGE GEAR CUTTER DESIGN	3. RELIEF
4. EXIT PROGRAM.	4. CHANGE GEARING DATA	4. CLEARANCE
	5. IMPORT DESIGN DATA	5. LOADED SYSTEM ANALYSIS
	6. SAVE DESIGN DATA TO FILE	6. FOURIER ANALYSIS
	7. CONVERT TO MILLIMETRES	7 MAIN MENU
	8. UNITS ARE IN INCHES	
	9. MAIN MENU	

Figure 1 :   The three control menus and associated options.

The *MAIN MENU* is used to control the priorities of the user. Choosing *1* will initiate the data manager menu system in order to define a set of design data, *2* will start a new contact analysis simulation for the current gear set specification, while *3* will recall display files from previous analysis calculated for a design specification during a past contact simulation cycle. The exit option defined as *4* on this menu represents the only point at which the program can be terminated. All of the current design data is lost at this point unless saved for later operation by using the data manger menu.

The design specification can be entered using the *DATA MANAGER MENU*. This allows the entry or modification of a design specification. A full set of parameters can be entered or modified from new by choosing *1*, however selecting of *2,3*, or *4* permits the user to review the parameters defining only the worm, wheel cutter, or gearing conditions respectively for more efficient operation. Options *5* and *6* on this menu also allow a completed design specification to be saved or recalled respectively. The program saves both the design and the current analysis parameter settings as a complete file (see section 3 about analysis parameters during analysis options). The user is allowed to view all of the current settings before confirming the file save. On recall, the parameters of the incoming data file are also displayed as verification of the file selection. Option *7* makes it possible to convert an existing set of design data to imperial (inch) or metric (mm) dimensions. It is also possible to toggle between working in these unit systems without altering the design data values using *8*. After a satisfactory design has been entered, choosing *9* returns the user to the main menu.

The *RESULTS MENU* is used to select the analysis of contact characteristics calculated for the current gear set design specification during the gear meshing cycle. Choosing *1* allows the user to view the worm thread or wheel cutting tool profiles in both the axial and normal planes. Option *2* will display the transmission error for the contact over the displacement interval. Number *3* will show the topological relief on the wheel tooth and in each wheel tooth profile (from root to tip) defined by the number of rack sections. Selecting 4 shows the simulated contact marking pattern for the gear set after meshing. Option *5* displays the effect of a torque load on transmission error, while option 6 can calculate the Fourier spectrum for the unloaded or loaded transmission error wave form. Choosing *7* returns the user to the main menu. (See section 4 for further information on the analysis results).

2.2. Data entry and modification

It is frequently necessary to change the gear specification parameters and analysis settings during the research and development of a gear design. The program operates a one key entry system allowing the user to default an entry to the current value. This system improves operating speed by eliminating the need to remember or re-enter every parameter. Changes in the design data can be implemented by options 1-4 in the data manager, while changes in the analysis settings are prompted by command keys indicated on several display screens during the program operation.

Once the entry/modification option is selected the associated parameters are presented individually. In each case the current parameter setting is displayed and the user is prompted to type '*y*' or '*n*' to indicate if modification is necessary. If '*n*' is entered the current setting is kept and the next parameter is shown. If '*y*' is entered then a cursor appears as a prompt to enter a new value. Where limits exist for defining the parameter, such as in the '*Type*' parameter describing the geometrical form to be used, the setting automatically cycles through the possible options. This is repeated until all of the associated parameters have been reviewed.

After any modification of the parameters is requested the associated page of information is displayed to confirm the changes are correct. Changes to the data may be repeated until the user is satisfied that the parameters are correct.

2.3. Viewing the current design data and analysis settings

The current design and analysis settings can be viewed at any time during operation by pressing the "HOME" key on the keyboard. This option is a simple short cut for the user to examine the design at a glance without the data manager or returning to the relevant display of analysis settings. An example of the full gear set specification display is shown in Figure 2. These parameters can be changed using options 1-4 in the data manager menu described in section 2.1. Pressing any key will continue the program and move to the display of analysis settings.

	WORM	WHEEL CUTTER
Type	:Screw	:Screw
Axial Pressure Angle	:20.0000°	:19.9346°
Root Diameter	:47.346	:47.346
Pitch Diameter	:63.500	:63.500
Outside Diameter	:79.654	:79.654
Calliper Depth	:8.077	:8.509
Calliper Thickness	:12.446	:12.620
Lead	:12.446	:50.620
No. of Threads	:2	:2
Profile Modification	:0.000	:0.038
Profile Shift	:0.000	:3.810
Tilt Angle	:0.000°	:0.820°
Gear Centres/Extension	:132.814	:1.905
	WHEEL	
Gear Teeth	:25	
Gear Wheel Outside Diameter	:225.044	
Throat Radius	:23.673	
Gear Face Width	:50.800	
Chamfer Inset	:0.000000	
Chamfer Angle	:0.000°	

Figure 2 :   The full specification of parameters for a sample gear design.

An example of the possible analysis settings is shown in Figure 3. These parameters can be changed during the contact simulation cycle as described in section 3. Pressing any key will return the user to the same status in the program and allow operation to continue.

ANALYSIS SETTINGS.

Number Of Sample Points	:80
Number of Rack Sections	:81
No of profile points	:45
Modification Type	:Parabolic
Cutting Axis Height Offset	:0.000000
Cutting Axis Centre Offset	:0.000000
Cutting Axis Eccentricity	:0.000000
Running Height Offset	:0.000000
Running Centre Offset	:0.000000
Worm Eccentricity	:0.000000

Figure 3 :   The contact analysis parameters stored as part of the complete design data file.

2.4.   Re-calling previously defined design data files

This option recalls design data files saved in previous uses of the program by selecting option 6 from the data manager menu. When the recall function (option 5 in the data manager menu) is selected the program will identify all of the files with a suffix of .DES in the working directory and indicate those found in a screen display such as in Figure 4. File names without this suffix can by saved and recalled but will not be identified by the program in this display.

Directory Listing Of DESIGN (.DES) Files.

DES1.DES	8161.DES	8151-3.DES	8151-5.DES	DES3.DES
8151-6.DES	8151-7.DES	DES4.DES	COL.DES	8073.DES
7634.DES	DES5.DES	DES2A.DES	DES2B.DES	DES6.DES
DES7.DES	DES8.DES	DES9.DES	DES10.DES	DES11.DES
DES12.DES	DES13.DES	DES14.DES	DES15.DES	DES16.DES
DES17.DES	DES18.DES	DES19.DES	DES20.DES	

LOAD FILE (Y/N)
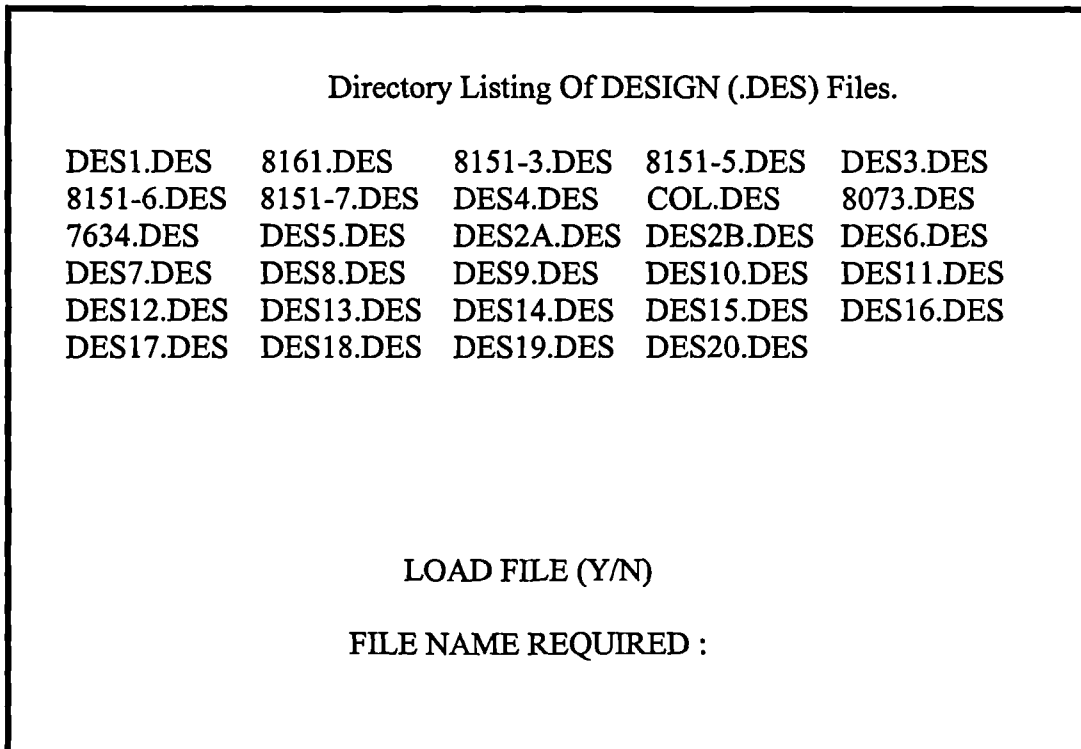
FILE NAME REQUIRED :

Figure 4 :   The catalogue of design data files identified in the working directory.

If the required file is found, type 'y' and enter the required file name at the prompt. Typing 'n' clears the screen and displays further design files detected in the working directory, or returns the user to the main menu when no more can be found.

2.5. Re-calling previously calculated contact analysis data files

This option recalls analysis data saved by the program during previous use. The operating principle is similar to the design data file recall routine described in section 2.4. When this option is selected, the program will identify all of the files with a suffix of .DAT in the working directory and indicate those found in a screen display as in Figure 4. File names without this suffix can by saved and recalled but will not be identified by the program in this display.

The program records gear tooth relief, transmission error, and contact marking pattern information to independent files. Each of these can be given a .DAT suffix as the recall routine will automatically detect the file type and show the appropriate analysis display. (For information on the displays from these files refer to section 4). Pressing the 'HOME' key when viewing an analysis file will display the design and analysis settings used to produce the result. These do not represent the current settings which are restored on return to the main menu

3. THE CONTACT ANALYSIS CALCULATIONS

3.1. Gear tooth form generation

3.1.1. Analysis options

The calculation of gear tooth form for a design is performed by the gear cutting cycle. The screen display in Figure 5 shows the default settings for the routine.

```
GEAR CUTTING CYCLE

    Cutter File Name           :hobtools.dat
    Co-ordinate File Name      :gearform.dat

    Number of Rack Sections    :40
    No of profile points       :50
    Modification Type          :Parabolic

    AXIS SETTINGS.

    Cutting Height Offset      :0.000000
    Cutting Centre Offset      :0.000000
    Cutting Eccentricity       :0.000000


        ENTER - Mesh Settings  Y - Change Current Settings  N - Run Cycle
```

Figure 5 :   The default options page for the gear wheel cutting cycle.

A file containing the profile details of a measured or calculated wheel cutter profile can be selected using this page. The name of the file to which the gear tooth form co-ordinates are written once generated by the routine may be changed here if required. Further details on these files can be found in section 3.1.2. and 3.1.3. respectively.

The number of rack sections and profile points can be changed to vary the point density over the tooth. The type of profile modification applied to the theoretical wheel cutter profile is also defined here.

The axis alignments during the cutting process can be defined using options in this page using centre height, centre distance, and cutter eccentricity values. This is kept independent of the running alignment settings to resemble the production process.

The command keys are identified at the bottom of the display :

ENTER : Moves directly to the meshing cycle settings without calculating a gear tooth form. The existing gear tooth form co-ordinate file is used by the gear set mesh analysis.

Y : Modify the analysis parameters for the gear tooth form generation routine.

N : This selection starts the routine for generating the wheel tooth form.

3.2.2. Using measured tool profiles

The program can calculate geometry analysis of 'Involute' or 'Screw' helicoid worm gear forms. However, by selecting 'Measured' in defining the '*Type*' definition of the wheel cutter it is possible to import a file of alternative pre-determined form or measured cutting tool co-ordinates. The filename given in the Figure 5 is the default used by the program, but this can be changed by the user as required. Files can be created by direct calculation of any arbitrary profile or CNC measurement of an existing cutter profile. The program requires a file containing three columns of floating point data representing the x and y co-ordinates of the tool in the normal plane, and the normal angle, α_{nx}, to the profile relative to the x direction given in radians as in Figure 6.
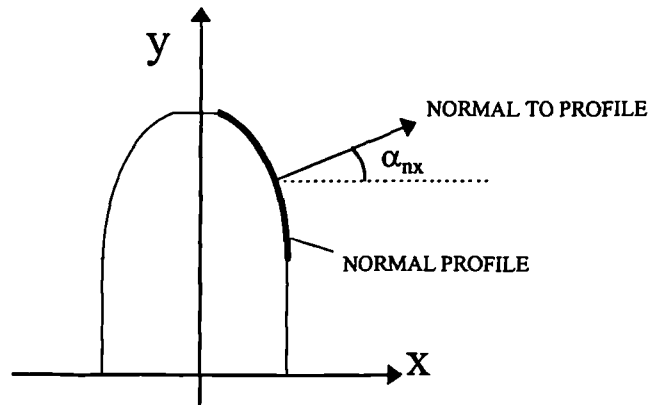
Figure 6 :   The calculated or measured wheel cutting tool notation in the normal plane.

Only the profile from one flank should be included in this file with all dimensions being positive.

3.2.3. The gear tooth co-ordinate file.

The gear tooth co-ordinate file is written during the gear generation routine. This holds a series of points in three columns of floating point numbers representing the x, y, and z co-ordinates respectively as defined by the axis notation shown in Figure 7. The wheel axis is defined as passing through the origin perpendicular to the x-y plane with the centre of the tooth lying in the z = 0 plane. The co-ordinates represent one flank of the gear tooth.
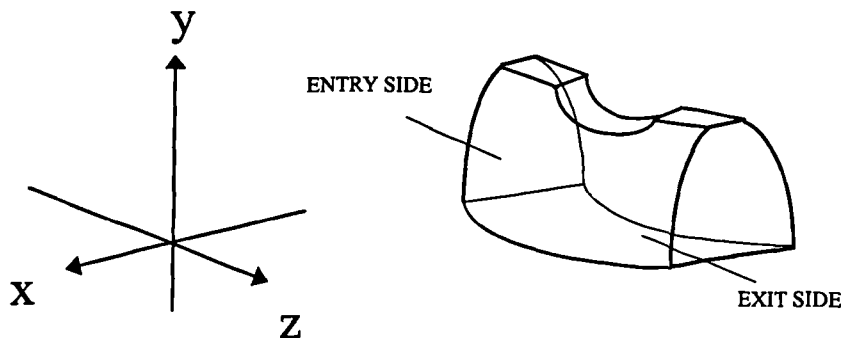
Figure 7 :   The gear tooth co-ordinate file notation.

3.2.   The contact mesh process

3.2.1. Analysis options

The display screen shown in Figure 8 lists the default settings for the worm and wheel meshing cycle.

```
┌──────────────────────────────────────────────────────────────┐
│                                                                │
│     GEAR MESHING CYCLE                                         │
│                                                                │
│                                                                │
│        Long Or Short Analysis   :2                            │
│        Number Of Sample Points :65                            │
│                                                                │
│     AXIS SETTINGS.                                            │
│                                                                │
│        Running Height Offset    :0.000000                     │
│        Running Centre Offset    :0.000000                     │
│        Worm Eccentricity        :0.000000                     │
│        Set Wheel Pitch Errors   :No                           │
│        Set Worm Lead Errors     :No                           │
│                                                                │
│     DATA FILE NAMES.                                          │
│                                                                │
│        Transmission Error File  :teerrors.dat                 │
│        Relief File              :greliefs.dat                 │
│        Clearance File           :markings.dat                 │
│                                                                │
│                                                                │
│        ENTER - Results Menu  Y - Change Current Settings  N - Run Cycle │
│                                                                │
└──────────────────────────────────────────────────────────────┘
```

Figure 8 :   The default options page for the worm gear meshing cycle.

The long analysis, type 1, calculates characteristics over one revolution of the gear wheel. The short analysis, type 2, calculates the contact for the system over a wheel rotation interval equal to two worm lead displacements. The sensitivity of the calculations can be controlled by altering the number of sample positions over the specified interval at which contact is calculated.

The axis alignments of centre height, centre distance, and worm eccentricity during worm wheel engagement are specified here.   Wheel pitch and worm lead errors can be simulated by requesting a change during the modification to the current settings.

The file names which will hold the data from the analysis can be altered as required .

The command keys are identified at the bottom of the display :

ENTER :   Moves directly to the results menu without performing the contact calculations.

Y :   Allows modification of meshing cycle parameters.

N :   Starts the contact analysis calculations.

3.2.2. Including wheel pitch errors.

It is possible to analyse the effect of theoretical or measured adjacent wheel pitch errors on the contact conditions. The display in Figure 9 shows an example of this using the display screen for the entry of arbitrary error values of wheel pitch error for a short analysis engagement cycle. (The short analysis implies that not all of the wheel pitch errors are needed).
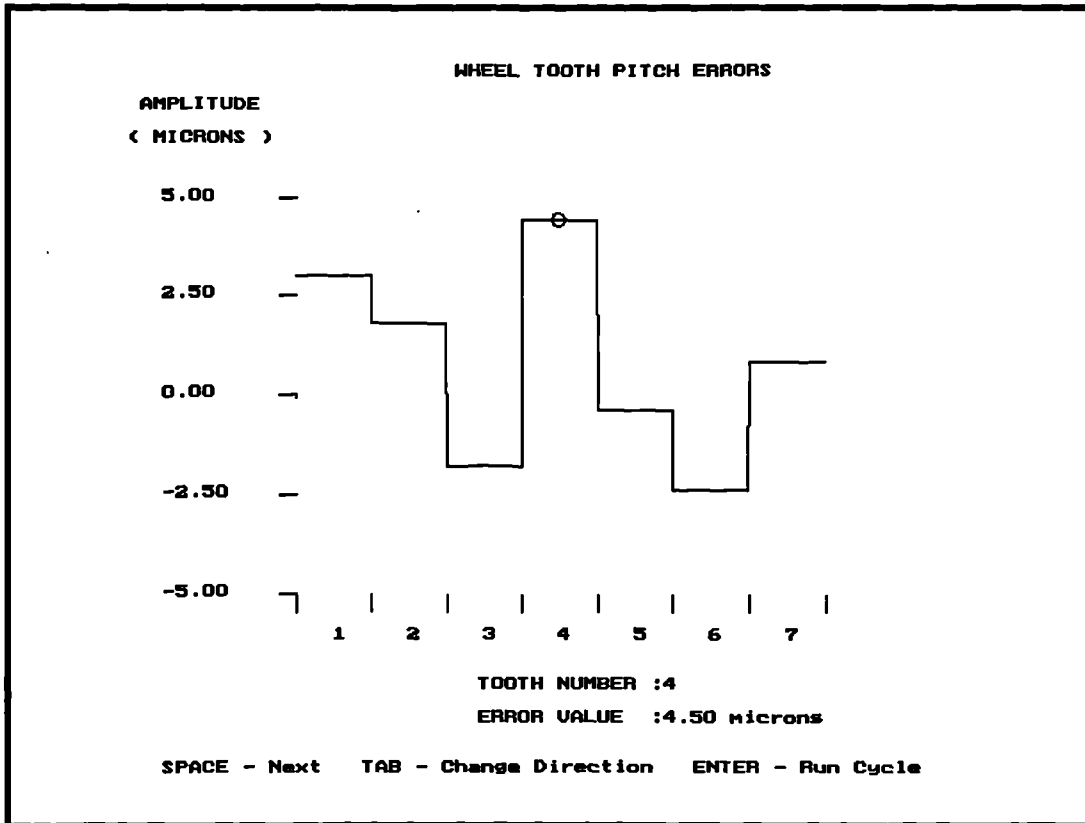
Figure 9 :   The wheel tooth pitch errors input screen used during the program.

In this display it is possible to see that the circle which indicates the error level on the active tooth is assigned to the 4th tooth. The active tooth number and the current error level are reported at the bottom of the screen. The command keys indicated at the bottom of the screen enable the following :

SPACE :   Increment active tooth number.

TAB :   Change direction of active tooth number increment.

Pg Up :   Add a 0.1μm increment to the error level of the active tooth number.

Pg Dn :   Subtract a 0.1μm from the of the active tooth number error level.

ENTER :   Return to the meshing cycle analysis options page.

3.2.3. Including worm lead errors

It is possible to analyse the effect of synthesised or measured worm lead errors on the contact conditions as measured along a helix of a worm thread flank at some reference diameter. The display in Figure 10 shows an example of this using the display screen for the entry of arbitrary error values of worm lead error.
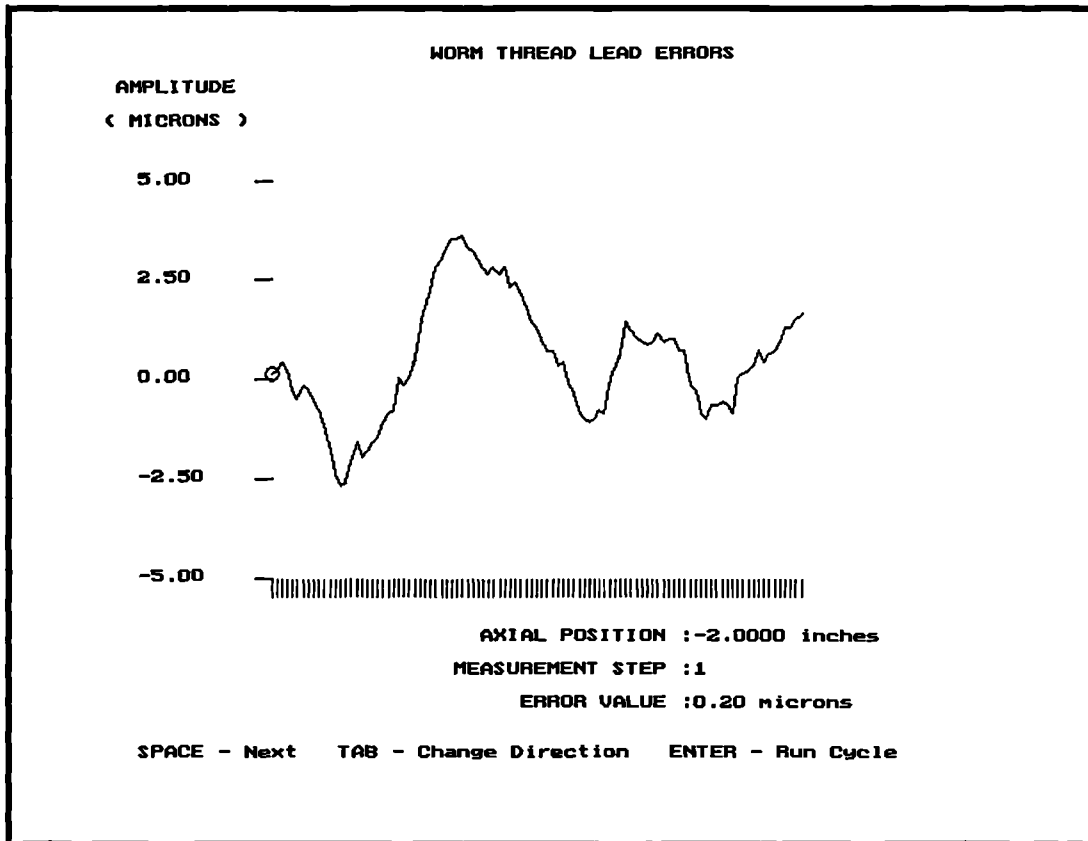
Figure 10 : The worm lead error input screen used during the program.

Error values can be defined at 101 positions over 4 axial thread pitch lengths. In this display it is possible to see a circle which indicates the error level of the active flank position. The active flank position relative to a datum at the centre line, the distance in design units along the flank, and the current error level are reported at the bottom of the screen. The command keys indicated at the bottom of the screen enable the following :

SPACE :   Increment flank position number.

TAB :   Change direction of active flank position increment.

Pg Up :   Add a $0.1\mu m$ increment to the error level.

Pg Dn :   Subtract $0.1\mu m$ from the error value.

ENTER :   Return to the meshing cycle analysis options page.

3.2.4. Calculated data files

The final section of the meshing cycle display screen shows the current names of the calculated data files to be stored by the routine. These are labelled individually for easier analysis and can be recalled in future use of the program using options given in the main menu. These file names can be changed by the operator from the default settings shown. Giving new files a .DAT suffix ensures that the program will find the file in the directory if a recall of these results is required during future operation.

NOTE : The program does not guard against overwriting these files through using identical names during different analysis cycles.

4. RESULTS ANALYSIS

4.1. Worm and wheel cutter profile generation

By choosing option 1 on the results menu the profile of the worm thread or wheel cutting tool can be represented on a graph in the axial or normal section. The plot in Figure 11 shows the axial section through the worm thread for the sample specification as an example.
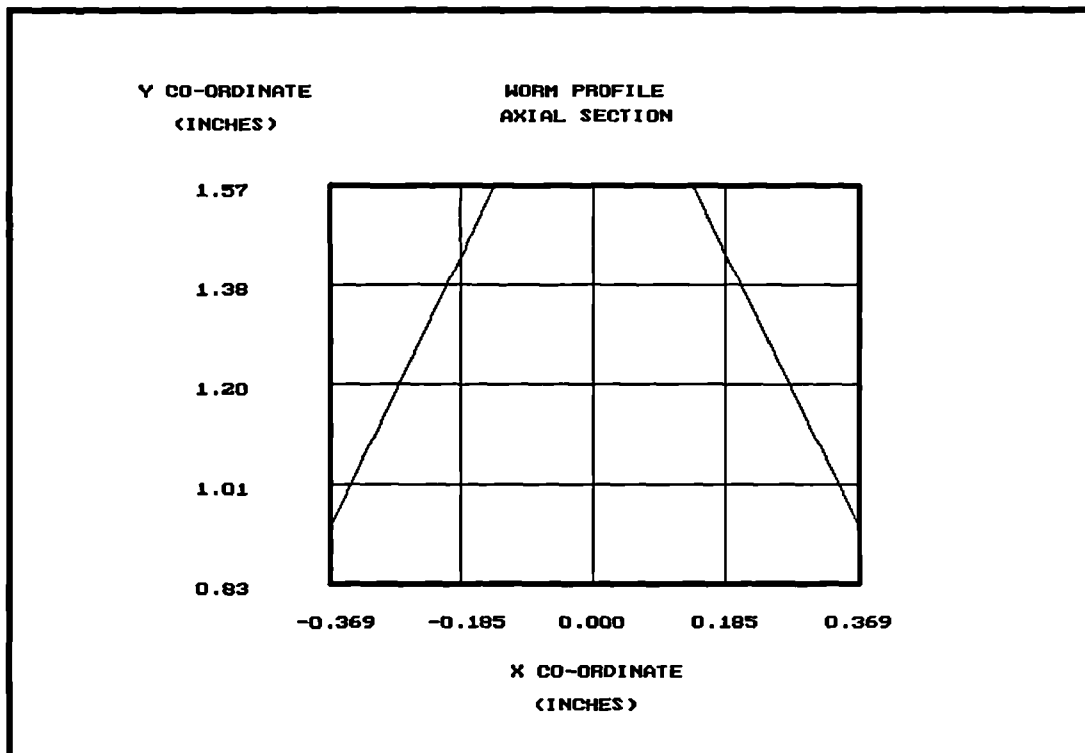
Figure 11 : An example of the profile graph option using the worm thread in the axial section.

Though these graphs are not sensitive enough to be used directly in the manufacturing process, it is possible to write the co-ordinates of the profiles to a computer disk file. The files can be used in conjunction with CNC machine tools as part of a the digital control cutting or measuring program. The files contain three columns defining the x-y co-ordinates and the normal pressure angle in degrees from one flank of the requested profile. The file names are assigned as follows :

PROFILE SELECTION	FILE NAME
1. Worm Axial	: WOAXPROF.DAT
2. Worm Normal	: WONOPROF.DAT
3. Tool Axial	: WHAXPROF.DAT
4. Tool Normal	: WHNOPROF.DAT

4.2.   Transmission error graphs

The graph in Figure 12 illustrates analysis option 2 in the results menu which is the transmission error due to the contact conditions established by the gear cutting and meshing cycle during a short analysis of a 25:2 ratio gear set.
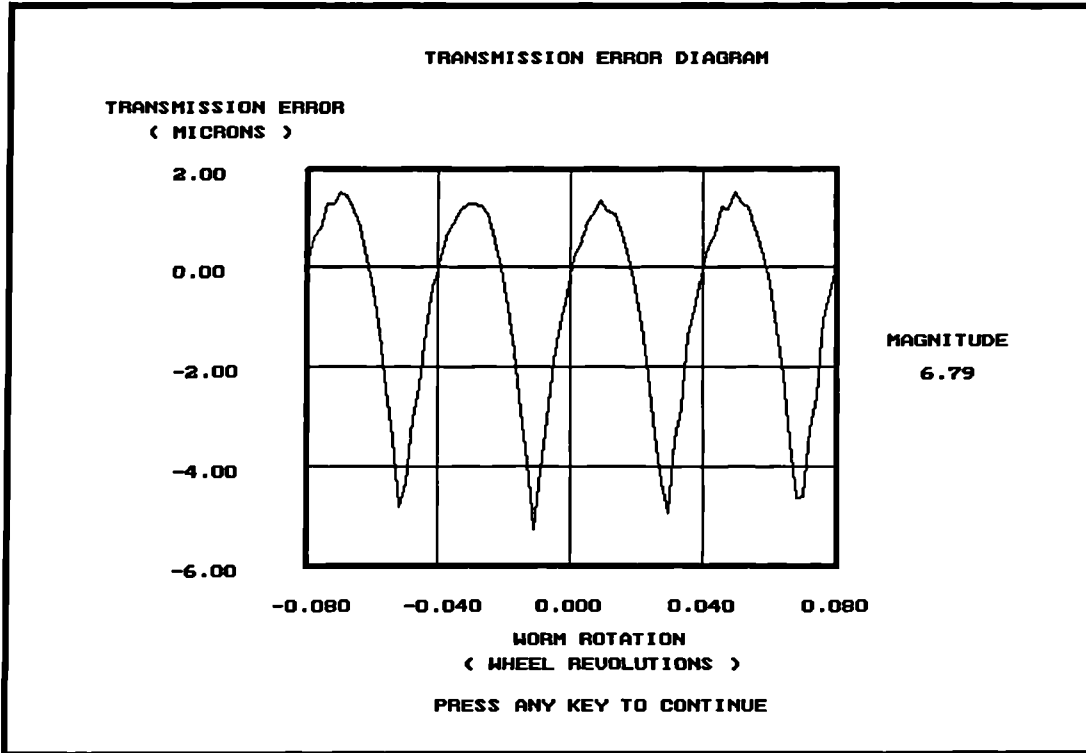
Figure 12 : The 'short' analysis transmission error for the sample gear design.

It shows the dominant trace when considering the engagement of all tooth pairs during the meshing cycle. The absolute value of this wave form, representing the magnitude of the transmission error, is displayed in microns.

4.3. Gear tooth relief

The relief represents the depth of metal on a gear tooth removed by the wheel cutter design relative to the worm thread flank contact. This is calculated by the new software during the meshing cycle. The results can be viewed by the program using option 3 of the results menu The display in Figure 13 shows an example of the default screen for the relief over the gear tooth form derived from a sample specification.

```
                          RELIEF DIAGRAM
        GEAR RADIUS        (10.0 Microns)
       (MILLIMETRES)

         112.52    ┌──────┬──────┬──────┬──────┐
                   │      │      │      │      │
                   │      │      │      │      │
         103.00    ├──────┼──────┼──────┼──────┤
                   │      │  ██  │      │      │
                   │      │ ████ │      │      │
          93.48    ├──────┼──────┼──────┼──────┤
                   │      │      │      │      │
                   │      │      │      │      │
          83.96    ├──────┼──────┼──────┼──────┤
                   │      │      │      │      │
                   │      │      │      │      │
          74.44    └──────┴──────┴──────┴──────┘
              -25.400   -12.700   0.000    12.700    25.400
                              FACEWIDTH
                            (MILLIMETRES)

        SPACE - Next    TAB - Change Direction    ENTER - Relief Profiles
```
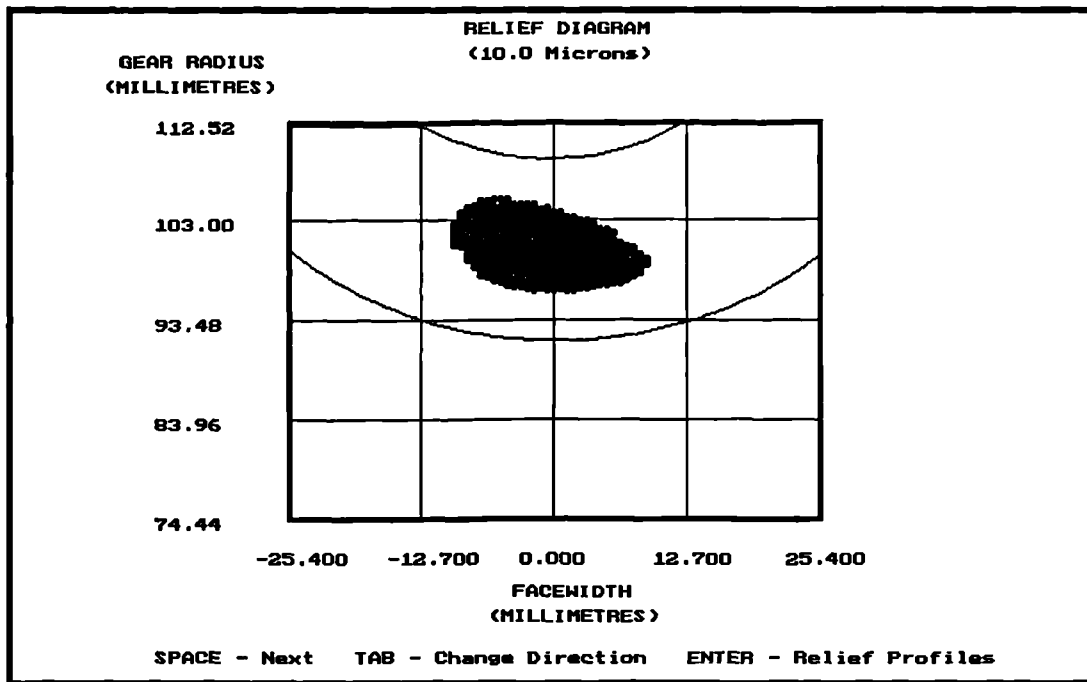
Figure 13 : The default relief diagram for the sample gear design.

Each shaded point represents an area of the gear tooth where the relief is less than the current level. The region indicated in this diagram is at the 10μm default level used by the program. The current level of relief is reported at the top of the screen. It is possible to instantly view the relief region at alternative depths without repeating the mesh analysis by using the command keys :

SPACE :   Increment relief value by 1μm.

TAB   :   Change direction of relief depth increment.

ENTER :   Continue to relief profile plots.

Specific values used to generate the relief diagram can be isolated to show the relief in each profile section of the gear tooth from root to tip. The graph in Figure 14 shows a relief profile which represents results calculated in the axial section of the worm using the same sample gear design as that used in the relief diagram.
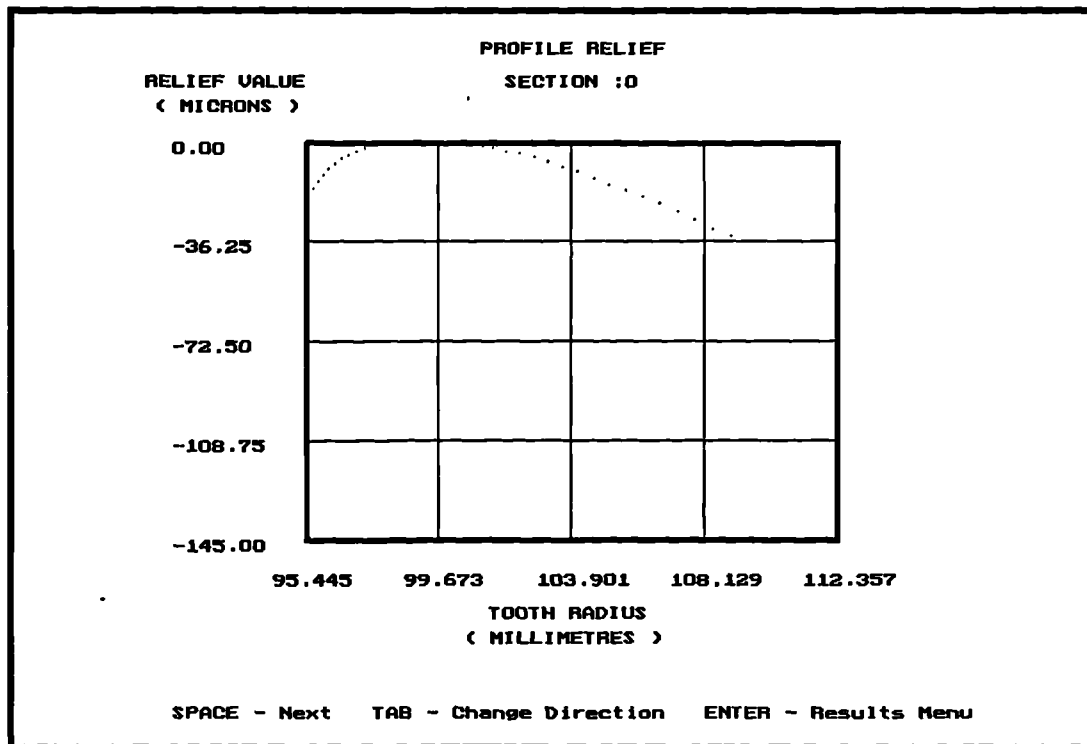
Figure 14 : The profile relief in the axial section (section 0) for a sample gear tooth design.

The scales of the graph are defined by the maximum and minimum relief over the complete tooth face, and its maximum and minimum radius taken regardless of the currently displayed section.

The results in the axial section are shown as a default display. Similar results are calculated on both sides of this axial section in each of the rack sections specified by the user at the gear cutting cycle stage. The current section number is reported at the top of the screen. An example of this is shown in Figure 15 which shows relief diagrams for a selection of five rack sections across the gear tooth form generated by the default settings for the same sample gear design. These can be viewed by using the command keys :

SPACE : Increment section number.

TAB : Change direction of section number increment.

ENTER : Return to the results menu.

(PROFILE SECTION NUMBER)
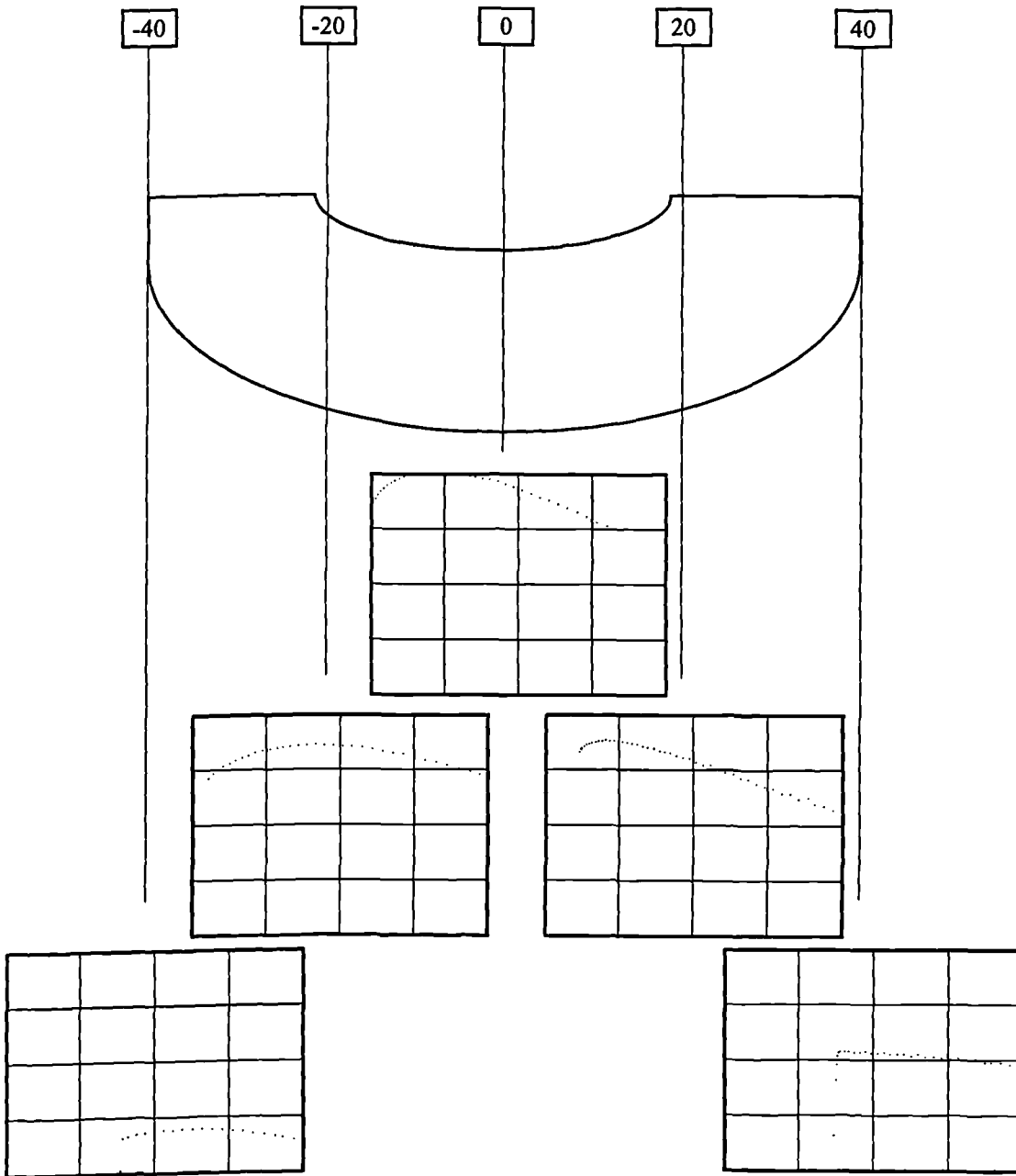
Figure 15 : The change in profile relief across the gear tooth in each tooth profile section for the sample gear design.

4.4. Clearance diagrams

The clearance between each tooth and the worm thread is calculated during the meshing cycle at all meshing positions over the displacement interval. The result can be shown using option 4 in the results menu. The display in Figure 16 shows the composite of all these calculated clearances for the sample specification during the meshing cycle.
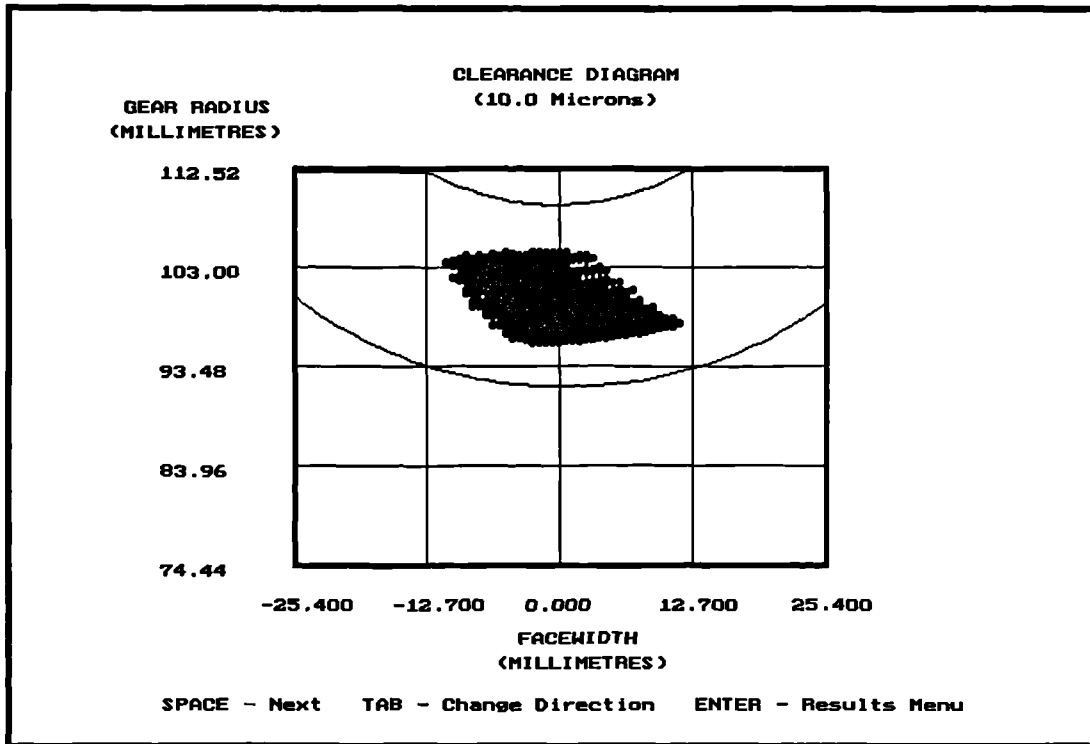
Figure 16 : The default clearance diagram for the sample gear design.

The shaded region on the gear tooth in the clearance diagram represent the those points which have less than a specified gap with the meshing worm flank. The display shown represents the 10μm default level used by the program to approximate ink thickness. The current clearance value for the indicated region is shown by the display at the top of the screen. It is possible to view the clearance region at alternative depths by using the indicated command keys.

SPACE :   Increment clearance depth by 1μm.

TAB   :   Change direction of clearance depth increment.

ENTER :   Return to the results menu.

The calculations displayed take into account the additional clearance due to transmission error from adjacent tooth pair contacts. This is a simulation of the marking, or 'bearing', test performed by industry to validate the contact conditions between the worm thread and wheel flank.

4.5.   Load effects on transmission error

Option 5 on the results menu is the load analysis function and shows the calculated transmission error for a specified load relative to the no load transmission error curve. The user can specify the initial output torque required in the system (the default value is 500Nm), and name a file in which to store the graph of the resulting wave form for use during further program operation (default name 'teloaded.dat'). The file format is the same as that of the contact analysis transmission error file and therefore the results can be recalled by the program during future program operation. The same rules defined as in section 2.5 apply when choosing a file name.

The transmission error at this load is displayed relative to the graph of the no load transmission error in order for the user to gauge mean transmission error effects due to tooth deformation. The graph in Figure 17 shows an example of the display screen for this facility using the sample design specification under a 500 Nm torque load.
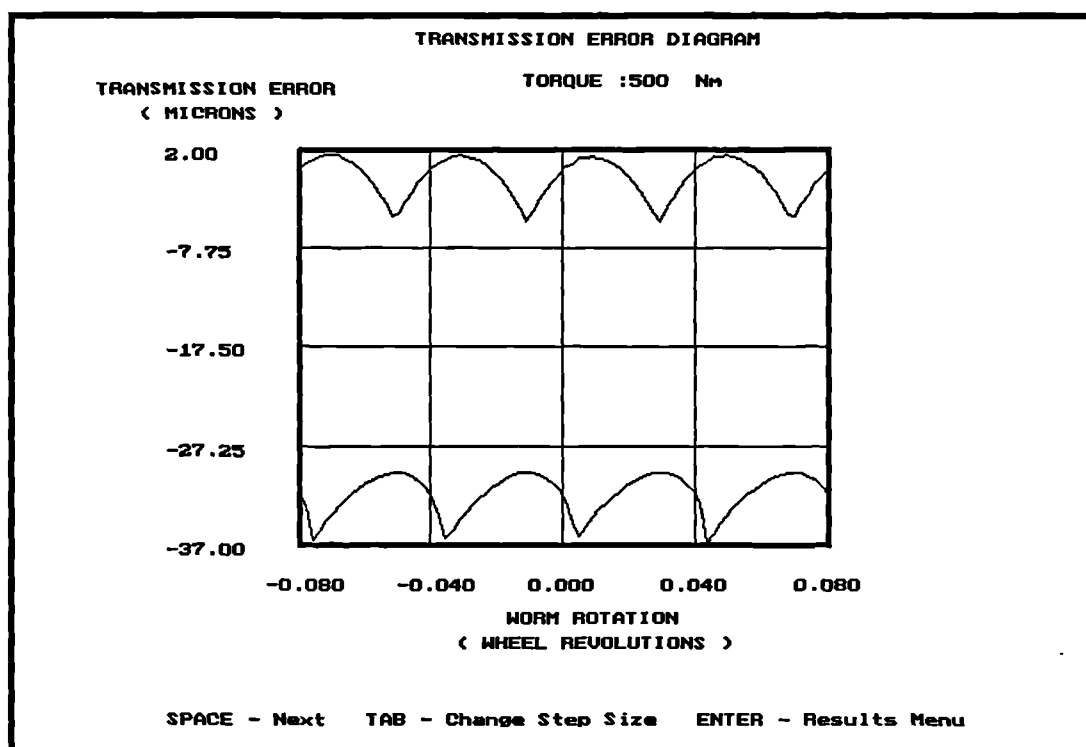
Figure 17 : The graph of the effect on transmission error for the sample gear design under a 500 Nm load.

The current simulated torque value is reported in Nm at the top of the screen. This toque load value can be incremented in steps of 500Nm, 50Nm, or 5Nm. The calculations can be repeated for any load level using the command keys as indicated in the display :

SPACE   :   Increment output torque load by 500/50/5 Nm.

TAB   :   Reduce magnitude of torque load increment.

ENTER   :   Return to the results menu.

4.6. Fast Fourier transform analysis of transmission error graphs

This analysis tool provides a frequency spectrum in cycles per revolution (cyc/wheel rev) for the transmission error wave forms under any load. This is option 6 in the results menu. The display in Figure 18 shows the calculated frequency spectrum from the transmission error wave for the sample gear specification shown in section 4.2.
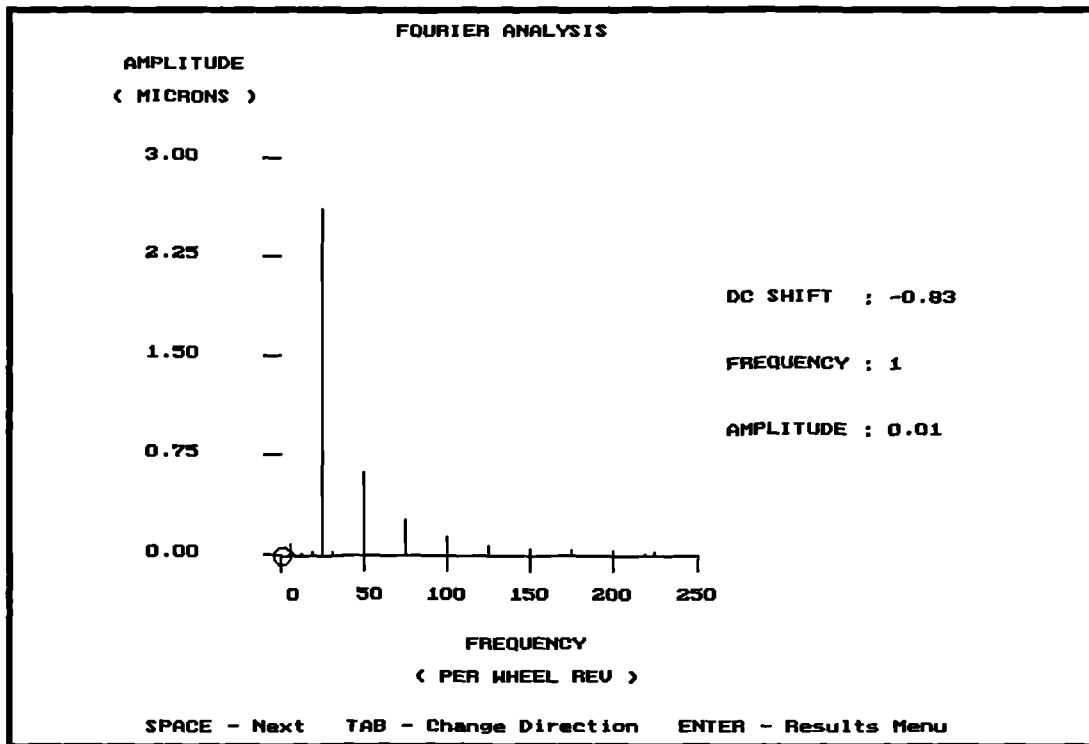
Figure 18 : The Fourier analysis frequency spectrum for the transmission error wave form calculated for the sample gear design.

The display represents the spectrum for the first 250 cyc/rev wave form (or AC) frequencies of revolution. The peaks indicated at 25 cyc/rev and further harmonics in this spectrum reflect the 25:2 ratio of the sample gear specification used. The display also indicates the mean (or DC) transmission error level for the wave. The current selection in the spectrum is indicated on the graph by a circle, and frequency value and the amplitude are reported on the right of the screen. The amplitudes for each of the frequencies over the spectrum range can be viewed by using the command keys indicated :

SPACE   :   Increment frequency by 1 cyc/wheel rev.

TAB   :   Change direction of frequency increment.

ENTER   :   Return to the results menu.

5. ERROR MESSAGES

There are several protective features within the software to prevent mathematical errors during the calculations and assist the user during operation. If an error message is called, a default value is established so that the calculations can continue or the user is prompted to enter required information. The following table contains the possible error messages which may be encountered during operation and a brief explanation of each.

MESSAGE	EXPLANATION
FILE EMPTY (PRESS ANY KEY TO CONTINUE)	The required design or calculated data file has not been found in the working directory or does not exist.
FILE EXISTS (OVERWRITE (Y/N))	The file name chosen to hold design data already exists. The user must choose whether to use the same name as previous design data will be erased.
NO DATA IN FILE (PRESS ANY KEY TO CONTINUE)	Trying to save a design data file with no defined parameters.
DATA INCOMPLETE (PRESS ANY KEY TO CONTINUE)	It is not possible to run a gear cutting cycle or mesh analysis without entering a new design or recalling an existing design data file.
GEAR TOOTH INCOMPLETE (PRESS ANY KEY TO CONTINUE)	It is not possible to run a mesh analysis without a current set of gear tooth form calculations.
NO CURRENT MESH RESULTS (PRESS ANY KEY TO CONTINUE)	It is not possible to view any current results without completing the contact analysis procedure.
!!!!!!!!!! WARNING !!!!!!!!!! UNDER-CUT IN GEAR FORM (PRESS ANY KEY TO CONTINUE)	The program has detected undercut in using the theoretical wheel cutting tool parameters.
RACK SECTION NUMBER MODIFIED	The program uses a minimum of '20' as the entered number of rack sections (creating '41' in all due to symmetry and including axial plane). The value is automatically increased if necessary.

MESSAGE	EXPLANATION
THROAT RADIUS MODIFIED	There was insufficient clearance in the design between the worm and the wheel at the given centre distance. The program compensates by increasing the throat radius as required.
WHEEL CUTTER FILE NOT FOUND (THEORETICAL PROFILE USED)	The user has selected to use a measured profile but has not entered the correct path and name of the co-ordinate file. The program will automatically default to using a theoretical profile.
CHAMFER MODIFIED FOR ANALYSIS	The inset distance of the chamfer from the gear tooth edge has been reduced. This does not affect the contact conditions of the design, but it is necessary to allow the program to continue.
PROFILE POINTS REDUCED	The number of generated gear tooth co-ordinates is limited to 3500 to remain within computer memory limits. If this is exceeded the number of points is reduced in increments of 5. If the number of profile points becomes less than 25 or a measured profile is being used then the number of rack sections is reduced.
NUMBER OF SAMPLE POINTS MODIFIED	The contact analysis considers a displacement interval of 2 lead lengths and uses a minimum of 20 meshing points per tooth pitch. The number is automatically increased to the minimum if necessary.

6. SUMMARY OF POTENTIAL CAPABILITIES AND APPLICATIONS

The completed program offers the following advantages over other existing software programs for worm gear analysis :

- Operating error protection.
- A model of error sources induced during production and operation.
- Prediction of contact meshing conditions considering multiple tooth pairs.
- Continuous transmission error graph for the specified design.
- Full wheel engagement analysis option.
- Transmission error for a gear system operating under a torque load.
- Fourier analysis of transmission error wave forms.

Once a full set of design and analysis data has been entered, the analysis performed by the gear cutting and meshing cycle is completed in approximately 15 seconds using the default settings for the program on a 100 MHz machine with a 16 RAM memory. The software can therefore make savings in time and costs by quickly calculating accurate representations of the final contact conditions. This can provide the following options as part of the worm gear design process :

- Fast analysis of theoretical designs to find optimum contact conditions.
- Compensation for the effects of manufacturing error sources on theoretical contact.
- Assess the tolerance of a design to operating conditions.
- Investigate and remove sources of unacceptable operating errors in existing sets.

APPENDIX D

GEAR DESIGN SPECIFICATIONS

APPENDIX D

1. The screw helicoid design example as analysed in literature from both Janninck[27] and Colbourne[30].

DESIGNATION : 2/25/7.854/8.085

	WORM	WHEEL CUTTER
Type	:Screw	:Screw
Axial Pressure Angle	:20.0000°	:19.9346°
Root Diameter	:47.346	:47.346
Pitch Diameter	:63.500	:63.500
Outside Diameter	:79.654	:79.654
Calliper Depth	:8.077	:8.509
Calliper Thickness	:12.446	:12.700
Lead	:50.800	:50.698
No. of Threads	:2	:2
Profile Modification	:0.000	:0.038
Profile Shift	:0.000	:3.810
Swivel Angle	:0.000°	:0.820°
Gear Centres/Extension	:132.814	:1.905

	WHEEL
Gear Teeth	:25
Gear Wheel Outside Diameter	:225.044
Throat Radius	:23.673
Gear Face Width	:50.800
Chamfer Inset	:0.000
Chamfer Angle	:0.000°

2. A screw helicoid sample specification provided with the Colbourne software used to compare initial calculations from the new software produced during this research program.

DESIGNATION : 2/25/7.854/8.085

	WORM	WHEEL CUTTER
Type	:Screw	:Screw
Axial Pressure Angle	:20.0000°	:19.9082°
Root Diameter	:47.346	:47.346
Pitch Diameter	:63.500	:63.500
Outside Diameter	:79.654	:79.654
Calliper Depth	:8.077	:8.509
Calliper Thickness	:12.446	:12.700
Lead	:50.800	:50.698
No. of Threads	:2	:2
Profile Modification	:0.000	:0.038
Profile Shift	:0.000	:1.270
Swivel Angle	:0.000°	:0.250°
Gear Centres/Extension	:132.814	:0.635

	WHEEL
No. of Gear Teeth	:25
Gear Wheel Outside Diameter	:225.044
Throat Radius	:23.698
Gear Face Width	:50.800
Chamfer Inset	:0.000
Chamfer Angle	:0.000°

GEAR SPECIFICATIONS

3.   An involute helicoid sample specification provided with the Colbourne software.   This was used to compare theoretical calculations of involute contact geometry from the Colbourne software with those of the new software.

DESIGNATION : 3/75/11.394/6.468

	WORM	WHEEL CUTTER
Type	:Involute	:Involute
Base Diameter	:42.862	:43.574
Root Diameter	:63.500	:63.500
Pitch Diameter	:73.696	:75.112
Outside Diameter	:88.900	:88.900
Calliper Depth	:12.700	:12.700
Calliper Thickness	:10.058	:10.287
Lead	:60.960	:60.782
No. of Threads	:3	:3
Profile Modification	:0.000	:0.000
Profile Shift	:0.000	:0.000
Swivel Angle	:0.0000°	:0.0400°
Gear Centres/Extension	:279.400	:0.000

	WHEEL
No. of Gear Teeth	:75
Gear Wheel Outside Diameter	:497.840
Throat Radius	:31.753
Gear Face Width	:50.800
Chamfer Inset	:0.000
Chamfer Angle	:0.000°

‹

4. An industrial design using a 20° normal pressure angle. The theoretical parameters were used to compare the Colbourne calculations with the new software and that produced by the Design Unit at Newcastle University using a known industrial design.

DESIGNATION : 1/70/11.000/6.272

	WORM	WHEEL CUTTER
Type	:Involute	:Involute
Base Diameter	:16.652	:16.975
Root Diameter	:54.049	:56.548
Pitch Diameter	:68.989	:72.149
Outside Diameter	:81.530	:81.530 (Value Not Available)
Calliper Depth	:4.691	:5.941
Calliper Thickness	:8.682	:8.814
Lead	:19.703	:19.651
No. of Threads	:1	:1
Profile Modification	:0.000	:0.000
Profile Shift	:0.000	:0.000
Swivel Angle	:0.0000°	:0.0136°
Gear Centres/Extension	:254.000	:0.000

	WHEEL
No. of Gear Teeth	:70
Gear Wheel Outside Diameter	:457.723
Throat Radius	:28.273
Gear Face Width	:43.452
Chamfer Inset	:0.000
Chamfer Angle	:0.000°

5.   A conjugate design based upon an industrial specification using a 22.5° normal pressure angle. This set was manufactured for the project and used to investigate machining errors. This design is referred to as '*Wheel A*' during the presentation of results in this thesis.

DESIGNATION : 1/50/9.119/5.156

	WORM	WHEEL CUTTER
Type	:Involute	:Involute
Base Diameter	:11.961	:11.961
Root Diameter	:34.773	:36.830
Pitch Diameter	:47.015	:47.015
Outside Diameter	:57.328	:59.385
Calliper Depth	:6.655	:6.655
Calliper Thickness	:8.204	:8.204
Lead	:16.197	:16.197
No. of Threads	:1	:1
Profile Modification	:0.000	:0.000
Profile Shift	:0.000	:0.000
Swivel Angle	:0.000°	:0.000°
Gear Centres/Extension	:152.400	:0.000

	WHEEL
No. of Gear Teeth	:50
Gear Wheel Outside Diameter	:273.050
Throat Radius	:18.415
Gear Face Width	:38.100
Chamfer Inset	:0.000
Chamfer Angle	:0.000°

6.   The complete mismatch industrial design using a 22.5° normal pressure angle associated with Appendix D5. This set was manufactured for the project and, used to validate the software calculations of mismatch geometry and modified machine settings under no load contact conditions. This design is referred to as '*Wheel B*' during the presentation of results in this thesis.

DESIGNATION : 1/50/9.119/5.156

	WORM	WHEEL CUTTER
Type	:Involute	:Involute
Base Diameter	:11.961	:12.136
Root Diameter	:34.773	:36.830
Pitch Diameter	:47.015	:47.015 (Value Not Available)
Outside Diameter	:57.328	:59.385
Calliper Depth	:6.655	:6.655
Calliper Thickness	:8.204	:8.204
Lead	:16.197	:16.157
No. of Threads	:1	:1
Profile Modification	:0.000	:0.000
Profile Shift	:0.000	:0.000
Swivel Angle	:0.000°	:0.067°
Gear Centres/Extension	:152.400	:-0.127

	WHEEL
No. of Gear Teeth	:50
Gear Wheel Outside Diameter	:273.050
Throat Radius	:18.415
Gear Face Width	:38.100
Chamfer Inset	:0.000
Chamfer Angle	:0.000°

7.   An example of a multi-start design with a 22.5° normal pressure angle
      provided by an industrial collaborator.   Marking patterns taken from
      completed gear sets were used to assess the software calculations contact in
      sets with increased lead angle due to more than one thread.

DESIGNATION : 3/56/10.590/8.500

	WORM	WHEEL CUTTER
Type	:Involute	:Involute
Base Diameter	:49.477	:49.985
Root Diameter	:71.029	:75.336
Pitch Diameter	:90.018	:91.034
Outside Diameter	:106.995	:111.303
Calliper Depth	:8.992	:10.617
Calliper Thickness	:12.840	:12.979
Lead	:80.112	:79.898
No. of Threads	:3	:3
Profile Modification	:0.000	:0.000
Profile Shift	:0.000	:0.000
Swivel Angle	:0.000°	:0.267°
Gear Centres/Extension	:283.000	:0.508

	WHEEL
No. of Gear Teeth	:56
Gear Wheel Outside Diameter	:499.999
Throat Radius	:37.160
Gear Face Width	:78.003
Chamfer Inset	:0.000
Chamfer Angle	:0.000°

8. An example of a multi-start design with a 20° normal pressure angle provided by an industrial collaborator. Again, marking patterns taken from completed gear sets were used to assess the software calculations of designs with further increased lead angle.

DESIGNATION : 5/59/10.791/7.576

	WORM	WHEEL CUTTER
Type	:Involute	:Involute
Base Diameter	:61.808	:64.173
Root Diameter	:66.314	:74.332
Pitch Diameter	:81.752	:87.474
Outside Diameter	:96.904	:105.072
Calliper Depth	:7.576	:8.799
Calliper Thickness	:10.798	:10.944
Lead	:119.008	:117.423
No. of Threads	:5	:5
Profile Modification	:0.000	:0.000
Profile Shift	:0.000	:0.000
Swivel Angle	:0.000°	:1.628°
Gear Centres/Extension	:264.376	:2.709

	WHEEL
No. of Gear Teeth	:59
Gear Wheel Outside Diameter	:468.780
Throat Radius	:34.532
Gear Face Width	:55.600
Chamfer Inset	:0.000
Chamfer Angle	:0.000°

GEAR SPECIFICATIONS

9.   A complete mismatch industrial design using a 20° normal pressure angle. This set was manufactured for the project and installed in the test rig to validate the software calculations of mismatch geometry, machine settings, and transmission error under a torque load. This design is referred to as '*Wheel 1*' during the presentation of results in this thesis. This specification was also used as the basis of sets used to investigate the effects of profile modification under load with the modification being applied to the wheel cutting tool before manufacture. This design is referred to as '*Wheel 2*' during the presentation of results in this thesis.

DESIGNATION : 1/50/10.988/4.997

	WORM	WHEEL CUTTER
Type	:Involute	:Involute
Base Diameter	:13.269	:13.523
Root Diameter	:43.053	:45.060
Pitch Diameter	:54.903	:54.903 (Value Not Available)
Outside Diameter	:64.949	:66.954
Calliper Depth	:3.734	:4.724
Calliper Thickness	:6.883	:6.985
Lead	:15.697	:15.657
No. of Threads	:1	:1
Profile Modification	:0.000	:0.000
Profile Shift	:0.000	:0.000
Swivel Angle	:0.000°	:0.083°
Gear Centres/Extension	:152.400	:0.000

	WHEEL
No. of Gear Teeth	:50
Gear Wheel Outside Diameter:	265.000
Throat Radius	:22.525
Gear Face Width	:38.000
Chamfer Inset	:0.000
Chamfer Angle	:0.000°

10. A complete mismatch industrial design using a 20° normal pressure angle. This set was manufactured for the project and was again installed in the test rig to validate the software calculations of mismatch geometry, machine settings, and transmission error under a torque load. The design used the same designation as in Appendix D9 with a different design technique applied to define the wheel cutting tool before manufacture. This design is referred to as '*Wheel 3*' during the presentation of results in this thesis.

DESIGNATION : 1/50/10.988/4.997

	WORM	WHEEL CUTTER
Type	:Involute	:Involute
Base Diameter	:13.269	:13.297
Root Diameter	:43.053	:45.060
Pitch Diameter	:54.903	:57.188
Outside Diameter	:64.948	:66.954
Calliper Depth	:3.734	:4.724
Calliper Thickness	:6.883	:6.985
Lead	:15.697	:15.692
No. of Threads	:1	:1
Profile Modification	:0.000	:0.000
Profile Shift	:0.000	:0.000
Swivel Angle	:0.000°	:0.217°
Gear Centres/Extension	:152.400	:1.143

	WHEEL
No. of Gear Teeth	:50
Gear Wheel Outside Diameter	:265.000
Throat Radius	:22.525
Gear Face Width	:35.560
Chamfer Inset	:0.000
Chamfer Angle	:0.000°